

University of Southampton Research Repository ePrints Soton

Copyright © and Moral Rights for this thesis are retained by the author and/or other copyright owners. A copy can be downloaded for personal non-commercial research or study, without prior permission or charge. This thesis cannot be reproduced or quoted extensively from without first obtaining permission in writing from the copyright holder/s. The content must not be changed in any way or sold commercially in any format or medium without the formal permission of the copyright holders.

When referring to this work, full bibliographic details including the author, title, awarding institution and date of the thesis must be given e.g.

AUTHOR (year of submission) "Full thesis title", University of Southampton, name of the University School or Department, PhD Thesis, pagination

University of Southampton

FACULTY OF NATURAL AND ENVIRONMENTAL SCIENCES

OCEAN AND EARTH SCIENCE

**Modelling and Observational Studies of
Dinoflagellate Bioluminescence within the
Northeast Atlantic**

By

Charlotte L. J. Marcinko

Thesis for the degree of Doctor of Philosophy

May 2012

UNIVERSITY OF SOUTHAMPTON
FACULTY OF NATURAL AND ENVIRONMENTAL SCIENCES
OCEAN AND EARTH SCIENCE

Abstract

Doctor of Philosophy

Modelling and Observational Studies of Dinoflagellate Bioluminescence within the Northeast Atlantic

By Charlotte L. J. Marcinko

Bioluminescence is the emission of light from living organisms and its presence in surface waters is of both ecological and operational interest. However, there is little known about its global spatial and temporal distribution. Forecasting of the bioluminescent field requires representation of the ecological and behavioural dynamics of bioluminescent organisms within models. Bioluminescent dinoflagellates are a major source of light in the surface ocean and their emissions often dominate the stimulated bioluminescent field. Therefore, the modelling of these organisms and their contribution to the bioluminescent field is a priority for forecasting. This thesis aims to address key gaps in the knowledge of dinoflagellates and their bioluminescence needed to improve the forecasting capability of surface ocean bioluminescence within the open ocean North Atlantic.

Observational and modelling studies were conducted that focus upon the waters surrounding the Porcupine Abyssal Plain (49°N 16.3°W) within the northeast Atlantic. In situ observations have indicated that on short time scales of hours to days, forecasting bioluminescent intensity may be heavily dependent upon modelling its relationship with the localised light conditions. Irradiance was seen to control short-term variations in bioluminescent intensity through photo-inhibition, influencing circadian rhythms and photo-enhancement. Insight into the seasonal dynamics of bioluminescent dinoflagellates was gained using Continuous Plankton Recorder (CPR) survey data. A significant positive correlation was present between seasonal changes in bioluminescent dinoflagellate abundance and total dinoflagellate community abundance. Therefore, within the North Atlantic, a first order approximation of the bioluminescent field could be gained by modelling the dinoflagellate community as a whole rather than modelling individual bioluminescent species. Using this information an ecological model was developed which simulated the typical seasonal changes in dinoflagellates within the surface waters of the northeast Atlantic. Several terms representative of the mechanisms by which bioluminescence provides a survival strategy for dinoflagellates were developed utilising current state-of-the-art knowledge regarding its effect upon predators. This is the first modelling study to explore the potential impact of dinoflagellate bioluminescence upon an ecosystem and to investigate whether the explicit consideration of the ecological function of bioluminescence into a mechanistic model can improve its performance. The model developed in this thesis potentially provides a platform for the future forecasting of the bioluminescent field in the North Atlantic.

Contents

Abstract	i
Contents	iii
List of Figures	vii
List of Tables	xiii
Declaration of Authorship	xvii
Acknowledgements	xix
Abbreviations	xxi
Chapter 1: Introduction	1
1.1 General Introduction	1
1.2 Measuring Bioluminescent Emissions In Situ	2
1.3 Field Programmes Investigating Bioluminescence	4
1.3.1 Biowatt – Bioluminescence and Optical Variability of the Sea	5
1.3.2 MLML – Marine Light Mixed Layers	5
1.4 In Situ Observations of Upper Ocean Bioluminescence	6
1.4.1 Identification of Bioluminescent Populations	6
1.4.2 Diurnal Variability in Bioluminescence	7
1.4.3 Global Distributions of Bioluminescence	9
1.4.4 Correlations of Bioluminescence with Other Environmental Variables	10
1.5 Forecasting Upper Ocean Bioluminescence	11
1.6 Bioluminescent Dinoflagellates	13
1.6.1 Mechanical Stimulation of Dinoflagellate Bioluminescence	14
1.6.2 The Effect of Nutrition and Light on Dinoflagellate Bioluminescent Intensity	16
1.6.3 Ecological Function of Dinoflagellate Bioluminescence	17
1.7 Research Objectives	20
Chapter 2: Diurnal Variations of Bioluminescence within the Northeast Atlantic	23
Preamble	23
Abstract	24
2.1 Introduction	24
2.2 Materials and Methods	28
2.2.1 Study Site	28
2.2.2 Instrumentation	29
2.2.3 Experiments	30
2.2.4 Phytoplankton Enumeration	32
2.2.5 Photosynthetically Active Radiation (PAR) Measurements	32
2.3 Results	33
2.3.1 Evidence of Circadian Regulation	33
2.3.2 The Effect of Light	34
2.3.3 Bioluminescent Dinoflagellate Community Composition	37
2.4 Discussion	38
2.4.1 Bioluminescent Dinoflagellate Community Composition	38

2.4.2 Evidence of Circadian Regulation	39
2.4.3 The Effect of light	40

Chapter 3: Seasonal Variations of Bioluminescent Dinoflagellates within the Northeast Atlantic.....43

3.1 Introduction.....	43
3.2 Methods.....	45
3.2.1 CPR Sampling.....	46
3.2.2 CPR Data.....	47
3.2.3 Interannual and Seasonal Variation of the Dinoflagellate Community.....	49
3.2.4 Dinoflagellate Community Composition.....	50
3.2.5 Bioluminescent Dinoflagellate Variability and Composition	50
3.3 Results.....	52
3.3.1 Interannual and Seasonal Variation of the Dinoflagellate Community.....	52
3.3.2 Dinoflagellate Community Composition.....	53
3.3.3 Bioluminescent Dinoflagellate Variability and Composition	55
3.4 Discussion	61
3.4.1 Interannual and Seasonal Variation of the Dinoflagellate Community.....	61
3.4.2 Dinoflagellate Community Composition.....	62
3.4.3 Bioluminescent Dinoflagellate Variability and Composition	63
3.5 Summary	66

Chapter 4: Modelling Dinoflagellates – Model Structure and Data.....69

4.1 Introduction.....	69
4.2 Modelling Dinoflagellates	71
4.3 Model Structure and Equations	73
4.3.1 Mixed Layer Depth	75
4.3.2 Phytoplankton Equations	76
4.3.3 Zooplankton	78
4.3.4 Nitrate	80
4.3.5 Silicate.....	80
4.3.6 Model Parameters	81
4.4 Physical Forcing Data	82
4.4.1 Mixed Layer Depth	82
4.4.2 Photosynthetically Active Radiation.....	83
4.4.3 Below Mixed Layer Nutrient Concentrations	84
4.5 Data for Model Assessment	84
4.5.1 Phytoplankton Seasonal Variability	85
4.5.2 Chlorophyll	88
4.5.3 Nutrients	92
4.5.4 Estimating Missing Variance	94
4.5.4.1 CPR Phytoplankton Data.....	94
4.5.4.2 World Ocean Atlas Nutrient Data	96
4.6 Summary	98

Chapter 5: Modelling Dinoflagellates – Model Parameterisation and Assessment99

5.1 Introduction	99
5.2 Methods.....	99
5.2.1 Model Simulations	99
5.2.2 Cost Function	100
5.2.3 Micro-Genetic Algorithm	101
5.2.4 Parameter Optimisation	103
5.2.5 Twin Experiment	106
5.2.6 Model Calibration	107
5.2.7 Sensitivity Analysis	109
5.3 Results	110
5.3.1 Twin Experiment	110
5.3.2 Model Calibration	112

5.3.3 Model Sensitivity.....	113
5.3.4 Model Assessment	115
5.3.4.1 Nutrients	115
5.3.4.2 Phytoplankton	116
5.3.4.3 Chlorophyll.....	117
5.3.5 Model System Dynamics.....	118
5.4 Discussion.....	122
5.5 Summary	127

Chapter 6: Modelling the Ecological Function of Dinoflagellate Bioluminescence129

6.1 Introduction	129
6.2 Development of Bioluminescent Terms	132
6.2.1 Determining Parameters To Represent Bioluminescence Effect	132
6.2.1.1 Startle Response.....	132
6.2.1.2 Burglar Alarm.....	133
6.2.2 Formulation of Bioluminescent Terms	134
6.2.2.1 Startle Response.....	134
6.2.2.2 Burglar Alarm.....	137
6.3 Preliminary Analysis	140
6.3.1 Parameterisation	140
6.3.2 Sensitivity analysis.....	141
6.3.3 Effects on Baseline Model Output.....	142
6.4 Methods for Detailed Analysis.....	144
6.4.1 Assessment of Model Parameterisation	145
6.4.2 Assessment of Model Performance	145
6.4.3 Assessment of Model Ecosystem Dynamics	147
6.5 Results.....	147
6.5.1 Assessment of Model Parameterisation	148
6.5.2 Assessment of Model Performance	149
6.5.3 Assessment of Model Ecosystem Dynamics	151
6.6 Discussion	158
6.6.1 Impact upon Parameterisation and Performance.....	159
6.6.2 Impact upon Ecosystem Dynamics	160
6.6.3 Limitations.....	161
6.6.4 Future Work	163
6.7 Summary.....	164

Chapter 7: Discussion165

7.1 Summary of Research Findings	166
7.1.1 Objective 1.....	166
7.1.2 Objective 2.....	167
7.1.3 Objective 3.....	167
7.1.4 Objective 4.....	168
7.2 Forecasting Bioluminescence in the North Atlantic	169
7.2.1 Correlations between Bioluminescence and Dinoflagellate Abundance.....	169
7.2.2 Modelling Dinoflagellates	170
7.2.2.1 Further Validation.....	170
7.2.2.2 Model Structure.....	171
7.2.2.3 Mixotrophy	171
7.2.2.4 Physical Limitations.....	172
7.2.2.5 Data Limitations	173
7.2.3 What it is Feasible to Forecast?	173
7.2.4 Future Work for Forecasting Bioluminescence	174
7.3 Conclusion.....	175

Appendix A: Bioluminescent Dinoflagellate Species177

Appendix B: Dinoflagellate Nutritional Strategy181

Appendix C: Model Code	185
Appendix D: Derivation of z-score Uncertainty	189
Appendix E: Model Sensitivity to Forcing.....	191
References	195

List of Figures

Figure 1.1: Schematic of scintillon structure and location within a cell and mechanism for bioluminescence emission (reproduced from Fritz et al., 1990).....	14
Figure 1.2: Schematic of the relative intensities of bioluminescent flashes of several well-known bioluminescent dinoflagellate genera (Painter et al. 2011).	15
Figure 1.3: Schematic of the startle response (top image) and burglar alarm response (bottom image) hypothesised to take place when predators prey upon bioluminescent dinoflagellate cells (Haddock et al., 2010).	17
Figure 2.1: Location of Porcupine Abyssal Plain (PAP) observatory 49° N, 16 30' W with bathymetry contours overlaid.....	28
Figure 2.2: Diagram of laboratory rig for the measurement of bioluminescence from discrete 2 L samples. A 1 mm excitation grid induces turbulence and stimulates bioluminescence of organisms within the sample which is recorded by a GLOWtracka bathyphotometer at a frequency of 1 kHz. A flow meter provides a method for determining the start and stop time of the sample flow through the instrument.	29
Figure 2.3: Example of primary data from GLOWtracka bench top instrument. a) Two litre sample containing mixed bioluminescent dinoflagellate community measured at 23:00 GMT during experiment 1. b) Two litre sample containing mixed bioluminescent dinoflagellate community measured at 08:00 GMT during experiment 1.....	30
Figure 2.4: Variations in bioluminescence measured in a) Experiment 1, all samples deprived of light (solid line shows 7 point running average, 'x' represent individual values). b. Experiment 2, repeat of experiment 1 with the addition of 10 litres of water exposed to natural day-night cycle (solid line shows 7 point running average, 'x' represent individual values from samples kept in continuous darkness, '●' show individual values from samples exposed to daytime irradiance). c) Experiment 3, parallel measurements of samples exposed to a natural day-night cycle (individual values shown as '●', running average shown as dashed line) and samples kept in continuous darkness (solid line shows 7 point running average, 'x' represent individual values).....	35
Figure 2.5: Relationship between integrated daytime photosynthetically active radiation (PAR) and log maximum night-time bioluminescence. Closed circles are from experiment 1, open circles are from experiment 2 and closed triangles are from experiment 3.....	36
Figure 3.1: Continuous Plankton Recorder schematic (courtesy of David Johns at SAHFOS).	46
Figure 3.2: Map of CPR standard areas across the North Atlantic	47
Figure 3.3: Location of CPR tows and abundance samples taken within the E5 region between January 2001 and December 2007.....	48

Figure 3.4: Interpolated monthly abundance of total dinoflagellates sampled between January 2001 and December 2007.....	52
Figure 3.5: Month of seasonal peak dinoflagellate abundance in 2001 through to 2007. Solid line indicates regression through data indicating there is no significant change in timing over the 7 year period.....	53
Figure 3.6: Monthly climatological averages of total dinoflagellates sampled, indicating the typical seasonal variation in dinoflagellate abundance between 2001 and 2007...	53
Figure 3.7: Relative contributions of individual dinoflagellate genus or species to the total dinoflagellate community sampled for the averaged typical year between 2001 and 2007.	54
Figure 3.8: The seasonal variations of dinoflagellates with different nutritional strategies compared to the seasonal variation of the total dinoflagellate community within a typical year (2001 – 2007). Solid black line at zero indicates the annual average abundance.....	55
Figure 3.9: Percentage contribution of bioluminescent dinoflagellates to the total dinoflagellate community within a typical year (2001– 2007).	56
Figure 3.10: Comparison of the seasonal variation of bioluminescent dinoflagellates and that of the total dinoflagellate community within a typical year (2001 – 2007). Solid black line at zero indicates the annual average abundance.....	57
Figure 3.11: Correlation between abundance of bioluminescent dinoflagellates and total dinoflagellates over the 7 year time series between 2001 and 2007.	57
Figure 3.12: Percentage contribution of genera or species to the total bioluminescent community over a typical year (2001 – 2007).....	58
Figure 3.13: Inter-comparison of the seasonal variation of bioluminescent species and genera within a typical year (2001 –2007). Solid black line at zero indicates the annual average abundance.....	59
Figure 3.14: Percentage contribution of genera or species to the estimated bioluminescent field over a typical year (2001 – 2007).....	60
Figure 3.15: Intercomparison of the seasonal variability of bioluminescent intensity with total dinoflagellate abundance within a typical year (2001 – 2007). Solid line at zero indicates the annual average value.....	61
Figure 4.1: Model schematic stating major coupling processes between state variables. Solid arrows indicate flows of nitrogen between model components within the mixed layer. Dashed arrows indicate input and output from the mixed layer.....	74
Figure 4.2: Mixed layer depth used for physical forcing of model. Red closed circles show calculated monthly averaged MLD within the E5 region from 2001 to 2007, error bars indicate +/- 1 standard deviation from the monthly mean calculated from temporal and spatial variability across the E5 region, dashed line shows interpolated daily changes in MLD using temperature data from Argo profiles.	82
Figure 4.3: Photosynthetically active radiation data used for physical forcing of model. Red closed circles show calculated monthly averaged PAR within the E5 region from 2001 to 2007, error bars show +/-1 standard deviation from the monthly mean calculated from temporal and spatial variability across the E5 region, dashed line shows interpolated daily changes in PAR.....	83

Figure 4.4: Below mixed layer nutrient concentrations. Red closed circles show calculated monthly nitrate and silicate within the E5 region averaged over 2001 to 2007, dashed lines show spline interpolated daily changes in nitrate and silicate.	84
Figure 4.5: Diatom and dinoflagellate z-scores calculated from climatologically averaged CPR abundances within the E5 region from 2001 to 2007 and their associated uncertainties.	88
Figure 4.6: Q-Q plots indicating averaged \log_{10} transformed monthly chlorophyll data approximates to a normal distribution, red line indicates perfect normal distribution.	89
Figure 4.7: Monthly climatologically averaged chlorophyll data within the E5 region from 2001 to 2007 and their associated uncertainties.....	91
Figure 4.8: Q-Q plots indicating that $\log_{10}(x+1)$ transformed nitrate data approximates to a normal distribution, red line indicates perfect normal distribution.	92
Figure 4.9: Q-Q plots indicating that $\log_{10}(x+1)$ transformed silicate data approximates to a normal distribution, red line indicates perfect normal distribution.	93
Figure 4.10: Nitrate and silicate monthly climatologically averaged values within the E5 region from 2001 to 2007 and their associated uncertainties.....	94
Figure 4.11: Comparison of uncertainties in nutrient data from the WOA09 (black) without temporal variance estimation to that from CAVASSOO (red), BODC (blue) and the PAP mooring (green) for nitrate and silicate.....	96
Figure 4.12: Comparison of nutrient data from the WOA09 (black) with temporal variance estimation to that from CAVASSOO (red), BODC (blue) and the PAP mooring (green) for nitrate and silicate.....	97
Figure 5.1: Flow diagram illustrating the general optimisation process of a μ GA. 'Individuals' are representative of a parameter vector made up of a set of parameter values.....	102
Figure 5.2: Parameter optimisation procedure to increase confidence in solutions gained using the μ GA.	105
Figure 5.3: Example of averaged synthetic dinoflagellate abundance data (red x) in comparison to averaged true observational data (black o) and associated uncertainty.	108
Figure 5.4: Model twin experiment: comparison of monthly averaged model output created by optimised parameter set (dashed line) and assimilated data (triangles) created by a known set of parameters. Error bars indicate uncertainties in assimilated data used in the cost function. Data has been \log_{10} transformed in order to approximate a normal distribution for use in the cost function which assumes data have Gaussian uncertainty distributions.	111
Figure 5.5: Model Cost sensitivity to perturbations in individual parameters for each of the parameter vectors obtained through optimisation. Parameters were varied individually whilst all others were held at their optimised values. Red dot indicates optimised parameter value for the best performing parameter vector, solid lines shows changes in cost between model output and real observations as the parameter varied. A cost value over 50 indicates no co-existence of phytoplankton groups.....	114
Figure 5.6: Comparison of model simulated nitrate and silicate (red dashed lines) against observations taken from the WOA09 dataset (black triangles). Data has been	

log transformed in order to approximate to a normal distribution for use in the cost function which assumes Gaussian uncertainty estimates.	116
Figure 5.7: Comparison of model simulated z-scores of diatoms and dinoflagellates (red dashed lines) against observations taken from the CPR (black triangles). See Chapter 4 for details of calculation of z-score and associated uncertainties.	117
Figure 5.8: Comparison of model simulated chlorophyll (red dashed lines) against SeaWiFS satellite remotely sensed data (black triangles). Data has been log transformed in order to approximate to a normal distribution for use in the cost function which assumes Gaussian uncertainty estimates.....	117
Figure 5.9: Model simulations of seasonal changes in nitrate, silicate, diatom and dinoflagellate biomass, zooplankton biomass and total phytoplankton biomass are shown (reading left to right) for a typical year (2001–2007) in the waters surrounding the Porcupine Abyssal Plain observatory. The bottom right plot shows mixed layer depth (blue dashed line) and photosynthetically active radiation (black solid line) used to force seasonal changes.	118
Figure 5.10: Top plot shows nutrient limitation terms for diatoms indicating silicate regulates diatom nutrient limited growth in all months except August. Bottom plot shows that diatom light limited growth (defined in Equation 4.6) is greater than dinoflagellate light limited growth.	119
Figure 5.11: Seasonal changes of phytoplankton specific growth rates (Phytoplankton growth rates are defined in Equation 4.4 and 4.5).	120
Figure 5.12: Fluxes for diatom and dinoflagellate state variables indicating zooplankton grazing is the dominant source of loss to phytoplankton.	120
Figure 5.13: Top plot shows seasonal changes in zooplankton specific grazing rate indicating the total grazing rate on phytoplankton (solid line) and individual grazing rates on diatom (dashed line) and dinoflagellates (dotted line). Bottom plot shows seasonal changes in specific zooplankton mortality rate.	121
Figure 6.1: Illustration of changes to the zooplankton grazing term when varying the grazing half saturation constant (k_z).	132
Figure 6.2: Illustration of changes to the zooplankton grazing term when varying the maximum grazing parameter (g).	133
Figure 6.3: Illustration of the relationship between zooplankton maximum grazing rate (g) and bioluminescent dinoflagellates (P_{BL}) given by Equation 6.3	136
Figure 6.4: Illustration of the relationship between zooplankton maximum mortality rate (ϵ) and bioluminescent dinoflagellates (P_{BL}) given by Equation 6.8	138
Figure 6.5: Model sensitivity to perturbations in (from left to right) k_g in SR1 scenario λ in the SR2 scenario, k_ϵ in the BA1 scenario and λ in the BA2 scenario. Plots indicate changes in cost between model output and real observations.	142
Figure 6.6: Comparison of model output with the inclusion of SR1, SR2, BA1 and BA2 bioluminescent terms (solid lines) with baseline model output without a bioluminescent term (dashed line).	143
Figure 6.7: Variations in maximum zooplankton grazing rate g (shown in black) and maximum zooplankton mortality rate ϵ (shown in red) caused by the bioluminescent terms in models run using the best performing parameter vector.....	151

Figure 6.8: Comparison of output from models including SR1, SR2, BA1, BA2, SR1 and BA1 and SR2 and BA2 bioluminescent terms with that from the baseline model without a bioluminescent term. Models were run with their respective best performing parameter vectors.....	153
Figure 6.9: Comparisons of zooplankton specific ingestion rates for models including bioluminescent terms and the baseline model without a bioluminescent term.	154
Figure 6.10: Comparisons of phytoplankton specific growth rates for models including bioluminescent terms and the baseline model without a bioluminescent term.	155
Figure 6.11: Comparison of phytoplankton and zooplankton fluxes for models including bioluminescent terms (solid lines) and the baseline model without a bioluminescent term (dashed lines).....	157
Figure 6.12: Comparisons of zooplankton specific mortality rates for models including bioluminescent terms and the baseline model without a bioluminescent term.	158
Figure E.1: (a) Interannual variations in MLD and PAR between January 2001 and December 2007. Comparison between interannual model simulations and observational data for (b) nitrate, (c) silicate. (d) chlorophyll, (e) relative seasonal variations in diatoms, (f) relative seasonal variations in dinoflagellates).	194

List of Tables

Table 1.1: List of bathyphotometer instruments for the measurement of bioluminescence.....	3
Table 2.1: List of photosynthetic and heterotrophic dinoflagellates where photo-inhibition or circadian regulation of their bioluminescence has been investigated in laboratory studies.....	26
Table 2.2: Details of experiments carried out to investigate diurnal variations of bioluminescent intensity from natural population of dinoflagellates in the north-east Atlantic in summer 2009.	31
Table 2.3: Minimums and maximums of observed cycles in measured flow stimulated bioluminescent intensity over each experiment.	33
Table 2.4: Results of microscopy analysis showing the median cell abundance and range for bioluminescent genera or species. Note that cell numbers are rounded to the nearest 20 due to a multiplication factor of 20 when converting from per 50ml to per 1 litre.	37
Table 2.5: Results of Spearman rank-order correlation analyses. Results show no negative correlations at the $p < .05$ significance level between abundance (cells L^{-1}) of bioluminescent genera or species and time elapsed into an experiment. r_s : correlation coefficient; p : significance level. ** denotes a significant result at the $p < .05$ level.	37
Table 2.6: Percentage contribution of bioluminescent taxa to estimated total light budget (see text for details).	39
Table 3.1: Results of spearman rank-order correlation analyses and Pearson correlation analyses between individual bioluminescent genus or species and the total dinoflagellate community respectively. Correlation coefficients are shown. ** denotes a significant result at the $p < .05$ level.....	59
Table 4.1: List of parameters used in model containing dinoflagellates for the waters surrounding the PAP observatory for a typical year within the period 2001 to 2007... ..	81
Table 4.2: Monthly average dinoflagellate and diatom abundance, $\log(x+1)$ transformed, for the E5 region from 2001 to 2007 and their corresponding standard deviations.....	86
Table 4.3: Monthly averaged chlorophyll data within the E5 region from 2001 to 2007 and their corresponding standard deviations.....	91
Table 4.4: z-scores for averaged diatom and dinoflagellate abundance within the E5 region between 2001 and 2007 together with originally calculated temporal uncertainties and revised estimated uncertainties including a spatial variance.	95
Table 4.5: Monthly averaged nutrient concentrations within the E5 region from 2001 to 2007 and original spatial uncertainties and revised estimated uncertainties including temporal variance.....	97

Table 5.1: Parameter ranges defined from the literature for use within the parameter optimisation process. A description of model parameters is given in Table 4.1 (p.77).	104
Table 5.2: Parameter values which created the model generated data used in the twin experiment.....	106
Table 5.3: Idealised dataset generated by the model for use in the twin experiment.	107
Table 5.4: Model twin experiment: comparison of parameter vector used to generate assimilated data and parameter vector gained through optimisation.	110
Table 5.5: Parameter vectors obtained from model optimisation to the four synthetic data sets. Parameter vector 1 is the optimal set of parameters found through the calibration process.	112
Table 5.6: Matrix of model costs gained through calibration of model parameters across four synthetic datasets. Diagonal values shown in bold indicate that assimilated data was used in the optimisation process to find the respective parameter vector..	113
Table 5.7: Breakdown of calculated misfit between model output and observations.	115
Table 6.1: List of parameters used in bioluminescent terms representative of the startle response and the burglar alarm hypothesis.....	139
Table 6.2: Summary of models including bioluminescent terms and additional parameters required for optimisation within the calibration process.....	144
Table 6.3: Results of student t-tests are shown comparing the parameter vectors from models incorporating bioluminescent terms and the baseline model (n=4). Average parameter values over the four parameter vectors gained through calibration to synthetic datasets are given. ** indicates a significantly difference at the $p < .05$ confidence interval and * denotes significant difference at $p < .10$ confidence interval.	148
Table 6.4: Results of Student t-tests are shown comparing the cost functions for models incorporating bioluminescent terms with those from the baseline model (n=4). Average model costs, indicating the misfit of model simulations to observational data, across the four parameter vectors gained through calibration to synthetic data are given. . ** indicates a significantly difference at the $p < .05$ confidence interval and * denotes significant difference at $p < .10$ confidence interval.....	150
Table 6.5: Comparison of the best performing parameter vector gained through calibration to synthetic data of the baseline model and models including bioluminescent terms.....	152
Table A.1: List of 68 dinoflagellate species identified as bioluminescent within the literature reviewed throughout the thesis.....	177
Table B.1: Classification of dinoflagellate types into representative nutritional strategies. P = Photoautotrophy; M = Mixotrophy and H = Heterotrophy.....	181
Table E.1: Breakdown of calculated misfit between model output and observational data using interannual MLD and PAR forcing between 2001 and 2007 for the four parameter vectors found through model optimisation.....	191
Table E.2: Recalculation of misfit between model output and observational data for the four optimised parameter vectors with the comparisons between model diatom and dinoflagellate relative seasonal variations and observational data in September 2004	

and diatom relative seasonal variation to observational data in July 2007 removed.	
.....	192

Declaration of Authorship

I, Charlotte Marcinko declare that the thesis entitled '**Modelling and Observational Studies of Dinoflagellate Bioluminescence within the Northeast Atlantic**' and the work presented in the thesis are both my own, and have been generated by me as the result of my own original research. I confirm that:

- this work was done wholly or mainly while in candidature for a research degree at this University;
- where any part of this thesis has previously been submitted for a degree or any other qualification at this University or any other institution, this has been clearly stated;
- where I have consulted the published work of others, this is always clearly attributed;
- where I have quoted from the work of others, the source is always given. With the exception of such quotations, this thesis is entirely my own work;
- I have acknowledged all main sources of help;
- where the thesis is based on work done by myself jointly with others, I have made clear exactly what was done by others and what I have contributed myself;
- Part of this work have been published as:
 - Material in Chapter 1 is based on a review article: Marcinko C.L., Painter S.C., Martin A.P., and Allen J.T. "*A review of the measurement and modelling of dinoflagellate bioluminescence.*" Progress in Oceanography (in prep for resubmission).
 - Material in Chapter 2 is based on a research article: of Marcinko CL., Allen J.T., Poulton A.J., Painter S.C., and Martin A.P. "*Diurnal variations of dinoflagellate bioluminescence within the open ocean north-east Atlantic.*" Journal of Plankton Research (in review).

Signed:

Date:

Acknowledgements

Firstly, I would like to thank my supervisors, Adrian Martin, John Allen and Stuart Painter for all their knowledge, experience and guidance throughout this project. Thanks also goes to my panel chair Tom Anderson for his insightful advice and making sure the project kept on track.

Further acknowledgements go to David Johns and Darren Stevens at SAHFOS for providing data from the CPR survey and much more information besides, Maureen Pagnani for providing the code to calculate mixed layer depths from ARGO float data, Alex Poulton for counting the phytoplankton samples as well as lots of other advice, Sue Hartman for providing nutrient data from CAVASSOO, Thanos Gkritzalis for providing nutrient data from the PAP mooring and Graham Quartly for initial help tracking down the SeaWiFS chlorophyll data and introducing me to the GADGET archive.

A huge amount of thanks also has to go to my family and friends. A special thanks to all my office mates: Jen Riley, who I have constantly bounced ideas off and had many thoughtful and interesting discussions with, ranging from statistics to Doctor Who; Martha Valiadi, who provided many interesting discussions about dinoflagellate bioluminescence and many shared references and; Chris Marsey, who never complained about how much Jen and I talked in the office. Thanks to my Mum, Dad, Nana and Sister, they have always provided me with support and advice whenever I needed it. Finally, but most importantly, I would not have come this far in science without the support of Gary. His continual encouragement and reassurance pushes me to achieve things I don't believe possible and his work ethic is something I can only try and match. He has been a constant source of inspiration and laughter. This thesis is dedicated to him.

Abbreviations

ADR	Advective Diffusion Reaction
BODC	British Oceanographic Data Centre
BP	Bathypotometer
CAVASSOO	CARbon VARIability Studies by Ships Of Opportunity
Chl:C	Chlorophyll <i>a</i> :Carbon
CPR	Continuous Plankton Recorder
CTD	Conductivity Temperature and Depth
CZCS	Coastal Zone Color Scanner
(μ)GA	(micro) Genetic Algorithm
HAB	Harmful Algal Bloom
HTC	High Throughput Computing
LBP	Luciferin Binding Protein
MLD	Mixed Layer Depth
MLML	Marine Light Mixed Layers
NPZ	Nutrients Phytoplankton Zooplankton
NPZD	Nutrients Phytoplankton Zooplankton Detritus
PAP	Porcupine Abyssal Plain
PAR	Photosynthetically Active Radiation
PFT	Phytoplankton Functional Type
SeaWiFS	Sea-viewing Wide Field-of-view Sensor
SAHFOS	Sir Alister Foundation of Ocean Science
WOA09	World Ocean Atlas 2009

Chapter 1: Introduction

1.1 General Introduction

Bioluminescence is the emission of visible light by living organisms. Predominantly a feature of marine species, bioluminescence occurs in over 14 marine phyla ranging from single celled organisms, such as bacteria, to large vertebrates including sharks and angler fish (Herring and Widder, 2001). Bioluminescence can be found in all marine habitats, both pelagic and benthic and at all depths. However, it is most commonly found in the upper 1000 m of the pelagic environment (Herring and Widder, 2001). The reasons for the wide distribution of bioluminescence within marine organisms are varied and include strategies for predator avoidance, prey attraction and intra-species communication (Haddock et al., 2010).

There are at least 30 physiologically different systems of bioluminescence in existence and bioluminescent organisms may differ in their cell biologies and in the regulation of their bioluminescence (Wilson and Hastings, 1998). It is thought that many systems of bioluminescence evolved independently. However, at a molecular level all systems produce bioluminescence through luciferase-catalysed reactions of molecular oxygen with luciferin (Wilson and Hastings, 1998). Different biochemical families of luciferase and luciferin exist and different organisms have distinct reactions associated with their bioluminescence. Due to the diverse chemistries, the bioluminescence associated with organisms has varying optical properties. The majority of pelagic and deep sea organisms emit light with a wavelength between 450 – 490 nm, corresponding to blue light which has optimal transmission through oceanic water (Hastings, 1996). Coastal and some bottom living organisms emit a greener light with emission wavelengths between 490 – 520 nm (Herring, 1983; Latz and Rohr, 2005).

Displays of bioluminescence visible at the surface of the ocean have been reported for centuries (reviewed in Harvey, 1957). There are several planktonic organisms that are responsible, which include; bacteria, dinoflagellates, radiolarians, copepods, ostracod crustaceans and cnidarians. For most of these organisms, mechanical stimulation via turbulence within the water (e.g. breaking waves or the movement of ships or larger organisms) triggers a bioluminescent response. This stimulation can lead to displays of light being produced which are easily visible to the naked eye.

Upper ocean bioluminescence is of great interest ecologically, physically and for operational purposes. Ecological studies have shown that bioluminescent intensity in surface waters can act as a sensitive indicator for distributions of plankton biomass in relation to physical processes, toxicity in the marine environment and the functional state of planktonic ecosystems (Lapota et al., 1993; Kushnir et al., 1997; Piontkovski et al., 2003; Kim et al., 2006). There has been a high level of military interest in upper ocean bioluminescence (e.g. Lynch 1978, 1981) as the emitted light could potentially be used to identify surface and subsurface vessels (Moline et al., 2007). The United States Naval Oceanographic Office has monitored bioluminescence activity for more than 20 years (NAVOCEANO, 2009). Other environmental parameters have also been collected to explore their correlations with bioluminescence and to identify characteristics of areas where vessels were potentially at risk of detection (Latz and Rohr, 2005).

The primary aim of this thesis is to undertake research which can improve the capability to forecast the bioluminescent field in open ocean surface waters (<300 m depth). The focus here is on the North Atlantic although the work conducted will also be relevant to other regions. Over the past five decades there have been many measurements and studies into this ubiquitous phenomenon. These studies have shown dinoflagellates to be the most prolific light emitters in the surface ocean and a major source of observed bioluminescence. Consequently, this thesis will specifically investigate these organisms and their bioluminescent behaviour.

This chapter provides an extensive review of previous in situ studies of surface ocean bioluminescence and attempts to predict its temporal and spatial distributions. This is followed by an overview of what is currently known regarding bioluminescent emissions from dinoflagellates. Finally, the specific objectives of the thesis are set out in the context of the information gained from the review.

1.2 Measuring Bioluminescent Emissions In Situ

Bioluminescence is widespread over all ocean basins and is frequently reported by mariners (Staples, 1966; Lynch, 1981; Watson and Herring, 1992). However, scientific observations and measurements are spatially limited and little is known explicitly about the distribution of bioluminescence throughout the oceans. There are several reasons for this relative lack of information including the short duration and variable intensity of bioluminescent events, and the complex nature of interactions between bioluminescent organisms and their environment which make the prediction of the time and location of an event difficult (Marra, 1995).

A variety of instruments have been developed since the 1950's that have been used to measure mechanically stimulated bioluminescence in situ within the water column (**Table 1.1**). These instruments are generically known as bathyphotometers (BP) and typically measure the amount of light produced in a certain volume of water following stimulation. A light sensor (photodiode or photomultiplier tube) is generally contained within a light-tight chamber into which water is drawn directly after being "stimulated". Methods of stimulation typically involve creating turbulent motion in the water, usually via an impeller or inlet grid, although this can also be achieved through the construction of the water intake apparatus (McDuffy and Bird, 2002).

Table 1.1: List of bathyphotometer instruments for the measurement of bioluminescence

Instrument	Reference
Biolite	McDuffy and Bird (2002)
Glowtracka	Aiken and Kelly (1984); www.chelsea.co.uk (viewed 03/03/2011)
Hidex	Widder et al. (2003)
MBBP	Herren et al. (2005)
Moordex	Neilson et al. (1992); Case et al. (1993); Lapota et al. (1994)
SALPA	Bivens et al. (2002); Tokarev et al. (2008)
SPLAT CAM	Widder (2002a)
Towdex	Naval Oceanographic Office Bioluminescence Survey System (undated)
UBAT	www.WETLabs.com (viewed 03/03/2011)

Mechanical stimulation and measurement geometry are not standardised across bioluminescence sensors because no common method or quantification of excitation exists. This makes inter-comparison of measurements between different studies and instruments problematic (Bivens et al., 2001, 2002; Herren et al., 2005). For example, measured bioluminescent intensity often depends on factors such as the detection chamber volume, the flow rate through the chamber, the efficiency of stimulation and the effectiveness of the light baffling which influences the base noise of the signal (Widder et al., 2003). Many past instruments have been restricted to prototypes and therefore comparisons between historical observations are problematic due to a lack of standardised units (Bivens et al., 2001, 2002). Furthermore, instruments often varied in their approach to measurement rate and calibration protocols. More recently,

instruments such as the GLOWtracka, produced by Chelsea Technologies Group (www.chelsea.co.uk), and the Underwater Bioluminescence Assessment Tool (UBAT), produced by WET Labs (www.wetlabs.com), have become commercially available. This may lead to an increase in the number of studies which can be directly compared as several research groups begin to use the same 'off the shelf' instrumentation.

Instrument design can easily fail to consider variability in flash duration between organisms. The number and duration of flashes given off by a particular organism depends on the amount of intracellular luminescent material and the manner and rate of the luciferase based reaction. For example, one organism might respond to stimulation with a single bright flash whereas another organism may produce numerous flashes until their excitation pathways are fatigued or their chemical stores are completely depleted (Herring and Widder, 2001). Historically, BP instruments have been used with the assumption that they produce sufficient turbulence to stimulate the maximum amount of light possible from the organisms within the water sample. However, this is difficult to verify as organisms may have been stimulated to fatigue before reaching the BP or the excitation method may not stimulate a particular organism to emit its maximum light intensity. Thus, it is entirely possible that application of two instruments with different methods for excitation could measure two very different values of stimulated bioluminescence for the same organism and water sample. There is no such thing as a standardised BP measurement, measurements are instrument dependent. For a more detailed overview of bioluminescent instrumentation the reader is directed to Herren et al. (2005) and Bivens et al. (2002).

1.3 Field Programmes Investigating Bioluminescence

Early reports on surface bioluminescence spanned all major seas and oceans and describe various qualitative aspects of bioluminescence including likely responsible organisms, seasonality and geographic location (Staples, 1966; Lynch, 1978, 1981). However, they do not provide a quantitative measure of the bioluminescence observed or any corresponding environmental measurements or biological samples. It was not until the 1980's that dedicated programmes, funded through the U.S. Office of Naval Research, specifically investigated and made quantitative measurements of upper ocean bioluminescence.

1.3.1 Biowatt – Bioluminescence and Optical Variability of the Sea

Biowatt, conducted in the Sargasso Sea between Bermuda and Cape Hatteras in the late 1980's, was the first dedicated attempt to investigate bioluminescence, as part of a larger objective to examine ocean bio-optical properties (Dickey et al., 1991, 1993; Smith et al., 1989). As part of the programme an instrumented mooring was deployed for several months in 1987 which measured bioluminescence as one of a variety of other bio-optical properties. In addition to the mooring, a number of research cruises were conducted from which bioluminescence sensors were also deployed (Dickey et al., 1991). These studies enabled the temporal and spatial variability of bioluminescence to be measured (Batchelder et al., 1990, 1992) and resulted in the identification of potential causes for observed day to night variations in bioluminescent intensity. Detailed information regarding the spectral properties of bioluminescent organisms, including light emission intensity and flash kinetics, was also obtained (Latz et al., 1988). Findings from the Biowatt programme are discussed in greater detail in **Section 1.4.**

1.3.2 MLML – Marine Light Mixed Layers

The Marine Light Mixed Layers (MLML) programme was undertaken in the sub-Arctic North Atlantic, south of western Iceland (59.5°N 21°W) between 1989 and 1993. MLML aimed to improve the understanding of processes within the mixed layer to allow better predictions of the spatial and temporal variability of bioluminescence (Marra, 1995). The programme investigated which organisms exhibited a bioluminescence response and how seasonal changes in the upper layer physics, including mixed layer depth, and the succession of plankton populations influenced measured bioluminescence. The MLML study included observations of bio-optical properties and the variability in the physical environment and plankton population during the spring stratification and the summer months on a seasonal time-scale. Ship based measurements were made of physical processes and plankton ecology in 1990 and 1991. This was combined with moored sensor observations over a 106 day period between May and August 1991 to provide a seasonal context (Marra, 1995).

Results from the MLML programme revealed several important seasonal trends in bioluminescence that short term measurements would not have observed. For example, it was found that bioluminescent intensity peaked in the summer months and that dinoflagellates were primarily responsible for mixed layer bioluminescence. However, the relative contribution from photosynthetic and heterotrophic dinoflagellates (as characterised then) varied seasonally. The contribution from photosynthetic species was found to be larger in late summer and early autumn. Heterotrophic dinoflagellates appeared to produce the bulk of bioluminescence

throughout spring, early summer and late autumn (Neilson et al., 1995; Swift et al., 1995). On shorter timescales it was noted that large differences (10–100 fold) could be observed between daytime and night-time bioluminescence intensity (Ondercin et al., 1995; Swift et al., 1995).

It is not clear how typical the results from MLML are for the North Atlantic on account of the unusually intense seasonal stratification observed during the summer of 1991, when the majority of measurements were made (Plueddemann et al., 1995). Time series data from 1989 and 1991 showed large inter-annual variability in the timing and magnitude of the spring bloom at the MLML site (Stramska et al., 1995). The intense stratification observed in 1991 was linked to anomalously high short wave radiation levels (Plueddemann et al., 1995). The conditions led to the onset of the spring bloom to be both earlier and more intense (i.e. higher chlorophyll concentration) than recorded in 1989 (Stramska et al., 1995) and consequently may have favoured dinoflagellates as the dominant bioluminescent organism.

1.4 In Situ Observations of Upper Ocean Bioluminescence

1.4.1 Identification of Bioluminescent Populations

Identifying the organisms responsible for upper ocean light emission is not straightforward. Planktonic populations are often complex in composition and the organisms dominating a bioluminescent signal may differ depending upon seasonal, inter-annual and spatial variability of the plankton community or the application of different sampling strategies.

Many in situ measurements have indicated that dinoflagellates are significant contributors in terms of their light emissions, to the upper ocean bioluminescent field in many oceanic and coastal regions. For example, bioluminescent *Ceratium* and *Protoperidinium* species of dinoflagellate were found to be responsible for over 90% of the bioluminescent intensity measured within the surface waters of the North Atlantic by Swift et al. (1995). Lapota et al. (1988) found that over 50% of the bioluminescence signal observed in the Arabian sea was due to dinoflagellates, with *Protoperidinium* and *Pyrocystis* species being significant contributors. Metazoan zooplankton (euphausiids and copepods) were responsible for the remainder of the bioluminescent signal. Within Vestfjord, Norway, approximately 96% of bioluminescence measured in surface waters was attributed to dinoflagellate species of *Ceratium* and *Protoperidinium* (Lapota et al., 1989). Bioluminescent dinoflagellate species have also

been identified as responsible for the 'bioluminescent bays' of Jamaica (Soli, 1966) and Puerto Rico (Margalef, 1957) and as the major source of bioluminescence in coastal waters around the United Kingdom (Tett, 1971).

It is now widely recognised that dinoflagellates are responsible for much of the stimulated bioluminescence observed within surface waters across the world's oceans. However, zooplankton, such as bioluminescent copepods and euphausiids, can also contribute significantly to the bioluminescent field. For example, Moline et al. (2009), used differences in zooplankton and dinoflagellates flash intensities to show that zooplankton were responsible for 34% of the bioluminescent field measured within Monterey Bay, California. Swift et al. (1985) compared bioluminescent intensity measured using a BP with biological samples collected from the BP outflow and concluded that zooplankton were responsible for the majority of upper ocean bioluminescence in the Sargasso Sea. However, this was later contradicted by Batchelder and Swift (1989), who estimated that approximately 64% of the bioluminescent field in the warm waters of the Sargasso Sea and Gulf Stream was due to the large dinoflagellate *Pyrocystis noctiluca*, while only 36% was explained by the presence of bioluminescent zooplankton.

The contrasting results in Swift et al. (1985) and Batchelder and Swift (1989) may have been due to seasonal changes in the planktonic community structure. However, the contrasting results may also be explained by differences in sampling strategy and assumptions regarding the bioluminescent intensity of the organisms. The methodologies of the two studies were both likely to underestimate the contribution of dinoflagellates to the bioluminescent field of the Sargasso Sea. Batchelder and Swift (1989) used a 202 μm mesh net to collect plankton samples. Thus, organisms smaller than 202 μm were not captured fully, including small bioluminescent dinoflagellates. Swift et al (1985) potentially biased their findings by assuming flashes with intensity $>0.5 \times 10^{11}$ photons, could only be produced by zooplankton. Thus, even though dinoflagellates were in high abundance they were not considered to contribute significantly to the total bioluminescent field. Subsequent studies have since shown several dinoflagellate species with maximum flash intensities above this threshold. For instance, *Protoperidinium curtipes* and *Pyrocystis fusiformis* have a maximum flash intensity of 4.0×10^{11} photons and 6.9×10^{11} photons respectively (Lapota et al., 1989; Latz et al., 2004a).

1.4.2 Diurnal Variability in Bioluminescence

Significant differences in the intensity of bioluminescence measured during the day and night have been observed in several in situ studies (Swift et al., 1983; Batchelder

et al., 1992; Ondercin et al., 1995; Utyushev et al., 1999; Cussatlegras et al., 2001). Several explanations for this variability have been proposed, which include; changes in the composition of bioluminescent organisms being measured (Greenblatt et al., 1984; Lapota et al. 1984), vertical migration of organisms through the water column (Seliger et al., 1962), and the effect of diurnal variations in dinoflagellate bioluminescent intensity which has been observed in several species (Sadovskaya and Filimonov 1985; Filimonov and Sadovskaya 1986; Buskey et al., 1994). Lapota et al. (1992) showed *Ceratium fusus* and *Protoperidinium curtipes* have diurnally varying bioluminescent intensities in both laboratory and field experiments. In the laboratory both *P. curtipes* and *C. fusus* increased their night-time stimulated bioluminescence by 137 and 29 times respectively relative to daytime values.

Variations associated with a reduction in daytime dinoflagellate bioluminescence can be caused by endogenous circadian regulation or the inhibition of bioluminescence by daytime irradiance (photo-inhibition). Studies have indicated that both of these processes may play a role. Kelly and Katona (1966) showed that flash rates from natural coastal dinoflagellate populations kept in darkness varied on a near 24 hour cycle, indicating an endogenous control of their bioluminescence. These results are supported by a study of natural *Pyrodinium bahamense* populations within Oyster Bay, Jamaica (Biggley et al., 1969) and several laboratory studies (Sweeney 1981a; Knaust et al., 1998; Seo and Fritz, 2000).

Exposure to light has also been shown to inhibit dinoflagellate bioluminescence (Hamman and Seliger 1981; Sadovskaya and Filimonov, 1985; Li et al., 1996) and several in situ studies have attributed the diurnal changes in observed bioluminescence to photo-inhibition, rather than endogenous regulation or vertical migration of organisms. Batchelder et al. (1992) concluded that photo-inhibition was the principal mechanism for the diurnal changes in bioluminescence within the Sargasso Sea. Their results showed a 34% increase in the number of flashes recorded and a 50% increase in bioluminescence during the transitional period of day to night (dusk) that could not be accounted for by changes in organism distribution (i.e. vertical migration). Similarly within the Mediterranean Sea, Cussatlegras et al. (2001) found that, although there were significant increases in bioluminescent intensity from day to night, the vertical distribution of bioluminescence did not change. These findings were again attributed to the effects of photo-inhibition on dinoflagellate bioluminescence. It must be noted that, the influence of the endogenous circadian regulation of bioluminescent organisms upon the diurnal changes in bioluminescent intensity were not considered by Batchelder et al. (1992) or Cussatlegras et al. (2001). Therefore, circadian regulation by bioluminescent dinoflagellates cannot be excluded as a mechanism controlling the diurnal changes in stimulated bioluminescent intensity.

Although diurnal variability in bioluminescent intensity has been observed for many bioluminescent dinoflagellate species, not all species exhibit similar rhythms. For example, there is no endogenous rhythm or photo-inhibition of the bioluminescence produced by *Noctiluca scintillans* (Sweeney 1971; Buskey et al., 1992). The diurnal rhythms of many bioluminescent dinoflagellates and other planktonic organisms not in culture are not well known, and there are still few cultured species, particularly for oceanic waters. Differences in diurnal rhythms between species make variations in bioluminescence within multi-species plankton communities, such as those in regions of open ocean, complex and dependent on community structure (Utyushev et al., 1999). For example, during 20 months of measuring bioluminescence at Woods Hole, Yentsch and Laird (1968) found that daytime bioluminescence intensity was higher than night-time intensity for a small number of days in winter. This was potentially due to a low abundance of dinoflagellates during this time of year leaving zooplankton bioluminescence, which is not photo-inhibited, to dominate the bioluminescent field.

1.4.3 Global Distributions of Bioluminescence

Attempts to map bioluminescent intensity quantitatively on a basin and global scale have been made by Piontkovski et al. (1997) and Piontkovski et al. (2006) respectively. Both studies used a dataset comprising over 24,000 vertical profiles of bioluminescence, collected over a 20 year period (1970–1990). Piontkovski et al. (1997) produced contour maps of bioluminescence across the tropical and sub-tropical Atlantic that reveal some well-defined spatial patterns. High bioluminescent intensity coincided with areas of upwelling, specifically along the West African coast (Figure 3 of Piontkovski et al., 1997). Intensity declined significantly in central sub-tropical oligotrophic waters and results indicated a general trend of decreasing bioluminescence from east to west across the entire basin. However, this pattern of decreasing bioluminescence may have been an artefact of the data distribution as there were far fewer profiles near coastlines on the western side of the basin than on the eastern side.

Piontkovski et al. (2006) used an extended global dataset which included data used by Piontkovski et al. (1997) to create a 2D bioluminescence field on a global scale across all major ocean basins. Bioluminescence data were averaged for the months of November to April over the upper 50 m of the water column. This global map was then compared with Coastal Zone Color Scanner (CZCS) chlorophyll data, seasonally averaged from January 1978 through March 1986. Results were varied, but some similarities between bioluminescence and chlorophyll distributions were observed. Other areas showed notable disagreement, with high chlorophyll concentrations not

accompanied by high bioluminescent intensities. The varying results between different regions might be unsurprising as the relationship between bioluminescence and chlorophyll is dependent upon organisms dominating the photosynthetic plankton assemblages coinciding with increased presence of bioluminescent organisms. More recently, Haddock et al. (2010) compared the North Atlantic bioluminescent dataset used in Piontkovski et al. (1997) with a longer ocean colour climatology combining SeaWiFS and MODIS (1997 – 2009) data and found strong qualitative similarities between the two distributions. High bioluminescent intensities were found to coincide with high chlorophyll regions in the north-west African upwelling system (as in Piontkovski et al., 2006). This suggests that increased bioluminescence may be related to areas of high productivity on basin scales.

1.4.4 Correlations of Bioluminescence with Other Environmental Variables

Attempts to quantitatively determine relationships between field observations of bioluminescence and coincident environmental variables have found varying correlations which are not consistent across different study regions or over different spatial scales (Lieberman et al., 1987; Losee et al., 1989; Cussatleguas et al., 2001). Within the Gulf of California, Lieberman et al. (1987) demonstrated that spatial variability of stimulated planktonic bioluminescence was not random. On a spatial scale of less than 10 km bioluminescence correlated with patches of enhanced chlorophyll and low surface temperatures at frontal zones. Although bioluminescence was not correlated with chlorophyll on a spatial scale over 10 km, a strong negative relationship with sea surface temperature remained. Weak correlations have also been found between bioluminescence, chlorophyll and temperature on spatial scales of the order of 10s km within the North Atlantic (Losee et al., 1989). However, no significant correlations between bioluminescence and other environmental variables were found at greater spatial scales of the order of 100s km.

Measurements made in three different water masses (Mediterranean, Frontal and Atlantic) found near the Almeria – Oran front in the Mediterranean Sea indicated that each water mass had a distinct bioluminescent profile associated with it (Cussatleguas et al., 2001). Frontal zone waters exhibited high bioluminescence emissions from the surface down to 130 m. In contrast, Mediterranean waters were characterised by intense bioluminescence in the upper 50 m of the water column with maximum bioluminescence located just above the thermocline (ca. 30 m). In Atlantic waters, bioluminescence was more evenly vertically distributed with no strong maxima. Although broad hydrographic patterns were observed, no correlations were found between temperature or salinity and bioluminescence. However, as found by Lieberman et al. (1987), high bioluminescence in frontal zone waters correlated with

chlorophyll. Cussatlegras et al. (2001) concluded that bioluminescence in frontal waters was due to organisms containing chlorophyll-*a*, which were assumed to be photosynthetic dinoflagellates. Mediterranean waters, on the other hand, were argued to contain more zooplankton and heterotrophic dinoflagellate species as chlorophyll did not coincide with bioluminescence in this region. However, there were no plankton samples collected to definitively test this hypothesis.

The intermittent correlations discovered by Cussatlegras et al. (2001) reflect those found within a Norwegian Fjord by Lapota et al. (1989), in the sense that correlations between bioluminescence and other environmental variables depended upon the complex plankton community structure and upon which organisms dominated the bioluminescent field. The complex spatial heterogeneity observed in the bioluminescent field may indicate that although patterns and correlations with environmental parameters can be present at particular locations, they may not be present across wider geographic regions. For example, water masses in different geographical locations experience different ranges in temperature, nutrient concentration and irradiance which in turn influence the plankton community within them and thus their bioluminescent signal.

1.5 Forecasting Upper Ocean Bioluminescence

As part of the MLML programme, Ondercin et al. (1995) developed a model of plankton bio-optical properties including bioluminescence for the North Atlantic. Given an initial set of oceanographic conditions including surface chlorophyll, surface temperature and mixed layer depth, the model simulated the vertical and horizontal distribution of an all-inclusive 'portmanteau' population of phytoplankton, its growth rate and its optical properties. An algorithm, which included a description of photo-inhibition, was then used to yield estimates of stimulated bioluminescence as a function of chlorophyll concentration, and scalar irradiance. The model was tested by comparing output to observed profiles of chlorophyll, beam attenuation coefficient, and stimulated bioluminescence obtained from two transects using a towed instrument. Transects were approximately 1000 km and 2000 km in length and located near the North Atlantic MLML mooring, south of western Iceland.

The model created by Ondercin et al. (1995) achieved good replication of the relative diurnal variability of bioluminescence within the mixed layer, most likely due to the inclusion of a photo-inhibition term. However, predicted daytime intensities below the mixed layer were substantially higher than observed. Night-time bioluminescence within the mixed layer was also 2–3 times higher than measured. The model was

unable to recreate some of the more complex chlorophyll distributions, particularly increases in chlorophyll at depth. Where this was the case, comparisons between modelled and measured bioluminescence distributions were poor. An advantage of the model was that data for initialisation could be obtained from satellite and climatology data alone, potentially enabling the calculation of a predicted bioluminescence profile for any region. Unfortunately, however, the model was unable to predict the intensity or spatial distribution of stimulated bioluminescence accurately.

Several short term bioluminescence forecasting studies have been conducted within Monterey Bay, California (Shulman et al., 2003; 2005; 2011). Shulman et al. (2003; 2005; 2011) investigated a simple advective–diffusive reaction (ADR) model to forecast the intensity, depth and location of bioluminescence over periods of 24–72 hours across 25–35 km transects within Monterey Bay. The model contained no biological processes. However, observations of bioluminescent intensity from a transect within the bay were required for model initialisation. Early results indicated the distribution of bioluminescent intensity was strongly dependent on flow conditions and that good agreement between predicted and observed distributions could be achieved from consideration of hydrodynamic transport processes alone (Shulman et al., 2003). However, the location and timing of the initial bioluminescence observations assimilated into the model were critical for the success of the short-term bioluminescence predictability (Shulman et al., 2005).

Shulman et al. (2003) highlight that no knowledge of the interactions characterising the life cycles of bioluminescent organisms is required if accurate short-term predictions of bioluminescence, over 24–72 hours, can be achieved by modelling advective–diffusive processes alone. This forecasting approach relies upon the assumption that the short term spatial distribution of bioluminescent organisms over time–scales of hours to days will be primarily influenced by physical advection rather than biological processes. If successful the approach has several advantages. Forecasting the distribution of organisms such as plankton from dynamical biological models is known to be problematic. For example, models themselves may not accurately reproduce a system and large uncertainties in the parameterisation of processes can often lead to difficulties interpreting or understanding predictions.

Shulman et al. (2011) found the ADR model gave generally good agreement between the predicted and observed inshore bioluminescence distribution. However, further offshore at the entrance to Monterey bay, the model predicted areas of high bioluminescence that were not observed. The difference between the predicted and observed distributions was due to a southward flow of water, correctly predicted within the physical model, but in reality bioluminescent organisms appeared not to be

advected. Shulman et al. (2011) thus concluded that the modelling of advective–diffusive processes on their own was not sufficient to fully explain the temporal and spatial variability of bioluminescence. Their results indicate that even on short time scales of the order of days there could be a strong biological forcing upon the distribution of bioluminescence.

Overall, there have been very few attempts to forecast the distribution or occurrence of upper ocean bioluminescence. Previous models have been limited in their success, either providing inconsistent results on very short timescales of 24–72 hours, or failing to simulate the distribution of bioluminescence over relatively large spatial scales (1000 – 2000 km). Successful modelling of bioluminescence requires the consideration of the ecological and potentially also the behavioural dynamics of bioluminescent organisms. As field measurements reveal that dinoflagellates are responsible for the majority of bioluminescence observed (Seliger et al., 1962; Batchelder and Swift 1989; Lapota et al., 1992; Neilson et al., 1995; Latz and Rohr, 2005), modelling these organisms and their contribution to the total bioluminescent field explicitly, may provide a feasible approach to identify where and when high intensities of stimulated bioluminescence might occur.

1.6 Bioluminescent Dinoflagellates

Dinoflagellates are abundant throughout the ocean and are both important primary producers and heterotrophic consumers (Sherr and Sherr, 2007). Estimates suggest there to be approximately 1600 free living species in the marine environment. The most recent study of free living marine dinoflagellates lists a total of 1555 species categorised into 117 genera (Gomez, 2005). However, much uncertainty exists over the exact number due, in part, to the large number of synonyms given to species (Elbrächter pers comms, 2008). The uncertainty in species numbers is understandable considering, for example, that between 2000 and 2007 three new dinoflagellate families, more than 20 new genera and over 80 new dinoflagellate species were described (CEDiT, 2008). Dinoflagellate species can be tremendously diverse. However, many dinoflagellates share certain physiological and structural characteristics. Species can be split into two subgroups: thecate species which have thick cellulose cell walls (called theca); and naked forms lacking theca.

Dinoflagellates include the only members of the phytoplankton community with the ability to emit visible light. However, only a small number of dinoflagellate species are known to be bioluminescent. Poupin et al. (1999) lists 81 bioluminescent species. However, this list may contain several inaccuracies, including the omission of

Alexandrium affine (Liu et al., 2004) and *Pyrophacus steinii* (Lapota et al., 2007) and the inclusion of non-bioluminescent species such as *Prorocentrum micans* (Sweeney, 1963). Identifying bioluminescent species is often difficult. Firstly, it requires the isolation of a single species or individual cells. Secondly, several factors (including diurnal variations and a cellular nutritional state) could lead to bioluminescence not being seen. Thirdly, there are bioluminescent and non-bioluminescent strains of the same species (Shmidt et al., 1978; Buskey, 1995) which can add identification difficulties. Cultures of dinoflagellates formed from a single isolated cell can be misclassified as non-bioluminescent due to inherent cell to cell variability in bioluminescent capacity. Those species which have been identified as bioluminescent are known to be prominent members of the dinoflagellate community in both open-ocean and coastal environments. **Appendix A, Table A.1** lists 68 dinoflagellate species which have been identified as bioluminescent in laboratory and in situ studies.

1.6.1 Mechanical Stimulation of Dinoflagellate Bioluminescence

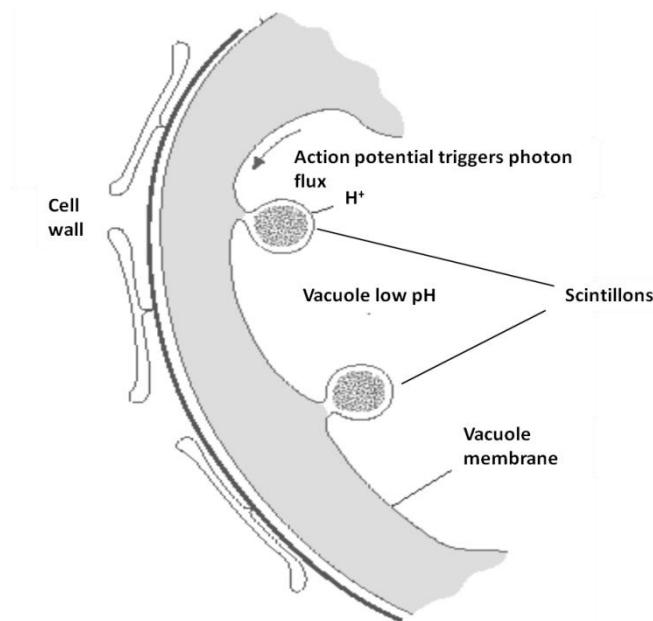


Figure 1.1: Schematic of scintillon structure and location within a cell and mechanism for bioluminescence emission (reproduced from Fritz et al., 1990).

Within a dinoflagellate cell, bioluminescence originates from within scintillons, cytoplasmic organelles that project into the main vacuole (Nicolas et al., 1987). Scintillons contain the substrate luciferin, the enzyme luciferase and, depending on species, luciferin-binding protein (LBP) is also present. Bioluminescence is produced by physical deformation of the cell wall which creates an action potential across the

vacuole membrane. The action potential causes a shift in pH in the scintillons, which in turn causes the luciferase to become active (**Figure 1.1**). Once active the luciferase acts as a catalyst and allows oxygen to bind with luciferin. It is the oxidation of luciferin which brings about a brief flash of light with a wavelength in the range of 474 – 476 nm (Wilson and Hastings 1998; Baker et al., 2008).

Flash duration for dinoflagellate bioluminescence is generally of the order of 100 ms (Latz and Rohr, 2005). However, it is known to vary between species. For example, *Noctiluca scintillans* has a relatively short flash lasting approximately 80 ms whilst bioluminescent flashes from *Pyrocystis* spp. can last over 5 times longer, ~500 ms (Widder, 2002b). The intensity of the emitted light also varies between species and can range from approximately 10^7 photons s^{-1} to 10^{11} photons s^{-1} (Lapota et al., 1989; Swift et al., 1995). A schematic of the relative flash intensities of several well-known bioluminescent genera is shown in **Figure 1.2**. Intensity of bioluminescent flashes released by a cell are also affected by the cell's previous stimulus history, with the intensity of flashes decreasing as luciferin stores become depleted due to previous flashes (Latz and Rohr, 2005).

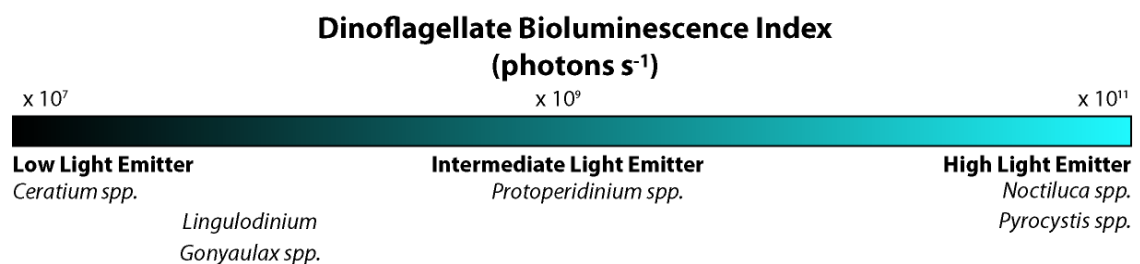


Figure 1.2: Schematic of the relative intensities of bioluminescent flashes of several well-known bioluminescent dinoflagellate genera (Painter et al. 2011).

The emission of bioluminescence by dinoflagellates is known to be a response to fluid shear, which produces deformation of the cell (Latz et al., 2004b). However, the level of shear stress required to stimulate bioluminescence can differ significantly between dinoflagellate species. Latz et al. (2004a) compared the shear stress threshold necessary, in laminar flow, to stimulate bioluminescence from four different dinoflagellate species and found thresholds varied between 0.02 and 0.3 Nm^{-2} . Oceanic species were observed to have lower thresholds than their coastal counterparts, potentially indicating that shear-stress thresholds are tuned to species' typical environmental conditions (e.g. turbulent coastal regions or less turbulent open ocean regions) to prevent excessive or needless stimulation of bioluminescence. The magnitude of shear required for the stimulation of bioluminescence is found to be

much larger than any typically occurring ambient flows, with the exception of a few coastal processes. Latz et al. (2004a) concluded that feeding currents produced by zooplankton were unlikely to be sufficient to induce a bioluminescent response and that this would only occur upon predator contact.

Latz and Rohr (1999) found increases of shear above threshold values to be positively correlated with the number of bioluminescent flashes recorded (indicative of the number of individual organisms being stimulated). Maldonado and Latz, (2007) showed bioluminescent intensity and flash decay rate are shear dependent. Since turbulent flows produce higher shear this suggests that turbulent flows, rather than laminar flows, will be associated with a higher bioluminescent intensity (Latz et al 2004a). Cussatlegras and Gal (2004) support this hypothesis, with findings that showed turbulent flows triggered a much more pronounced bioluminescent response in comparison to stationary–laminar flow using cultures of *Pyrocystis noctiluca*.

It has also been found that bioluminescence in the species *Lingulodinium polyedrum* is strongly dependent not only on the magnitude of the shear but also on the rate at which it increases. Bioluminescence in this species was seen to have a preferential response to rapidly increasing shear and became desensitised to slowly increasing shear (Von Dassow et al., 2005). The findings by Von Dassow et al. (2005) support those of Latz et al. (2004a) but also suggest that desensitisation of cells may influence which naturally occurring flows stimulate bioluminescence. This suggests that the stimulation of dinoflagellate bioluminescence may be avoided when organisms are within slow changing flows or become entrained in large scale flows containing significant shear.

1.6.2 The Effect of Nutrition and Light on Dinoflagellate Bioluminescent Intensity

The nutritional state of dinoflagellates has been found to affect the intensity of their bioluminescence. For example, bioluminescence from the heterotrophic species *Protoperidinium huberi* has been shown to vary with cell nutritional condition and population growth rate (Buskey et al., 1994). Under growth limiting conditions, cells were observed to have lower levels of bioluminescence. Held without food, cultures lost their bioluminescent capacity within a matter of days suggesting that cells could no longer afford the energy required for bioluminescence. The bioluminescent capacities of other heterotrophic species, *Protoperidinium cf. divergens* and *Protoperidinium crassipes*, have also been shown to be significantly affected by diet (Latz and Jeong 1996). Bioluminescence in *P. cf. divergens* was significantly correlated with feeding frequency. Unlike *P. huberi*, the bioluminescent capacity of *P. cf. divergens* reduced but did not completely disappear when cultures were held without

food. It was suggested that bioluminescent ability was retained due to nutrients being gained through cannibalism. These results led Latz and Jeong (1996) to suggest that dinoflagellates invest heavily in bioluminescence and prioritise it higher than reproduction in terms of energy utilisation.

In contrast to the studies on heterotrophs, the bioluminescent capacity of the photosynthetic species *Lingulodinium polyedrum* is not known to vary significantly under nutrient depletion even when it leads to reduced growth rates (Sweeney, 1981b). However, night-time bioluminescence of photosynthetic species such as *L. polyedrum* and *Ceratium fusus*, has been found to be positively correlated with preceding daytime irradiance levels. This indicates photo-enhancement of bioluminescence and demonstrates that the light history of organisms can affect the magnitude of night-time bioluminescent intensity (Sweeney, 1981b; Sullivan and Swift, 1995).

1.6.3 Ecological Function of Dinoflagellate Bioluminescence

There is much uncertainty about the ecological function of dinoflagellate bioluminescence. It is widely thought to be a survival strategy, though it is unclear if the flashes of light themselves deter predators, due to a startle response, or whether the flashes act as a “burglar alarm” (Figure 1.3). The “burglar alarm” hypothesis (Burkenroad, 1943) asserts that the flash emitted by a dinoflagellate due to herbivore grazing activity would enable a carnivore to perceive and capture the herbivore, thereby benefiting the dinoflagellate population as a whole.

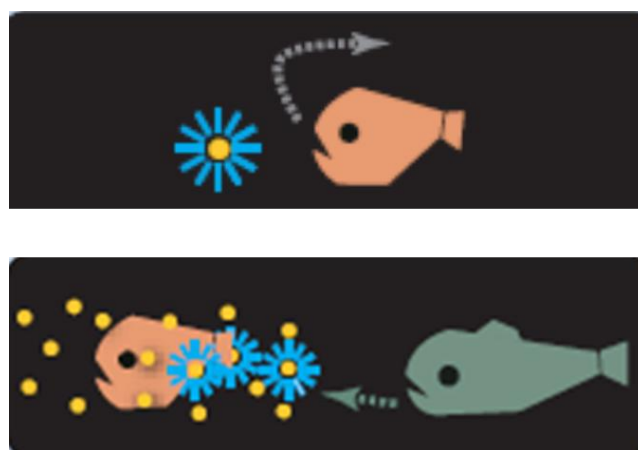


Figure 1.3: Schematic of the startle response (top image) and burglar alarm response (bottom image) hypothesised to take place when predators prey upon bioluminescent dinoflagellate cells (Haddock et al., 2010).

Studies have tested the “burglar alarm” hypothesis directly, with bioluminescence shown to increase predation efficiency of several organisms upon grazers. Abrahams and Townsend (1993) found increased mortality of copepods grazing upon bioluminescent dinoflagellates in the presence of sticklebacks, with copepod deaths at a rate of 33.4 ± 10.3 per hour in the presence of a bioluminescent culture compared to 19.6 ± 5.4 deaths per hour in the presence of the non-bioluminescent culture. This study concluded that increased mortality of copepods should increase the survival of dinoflagellates. However, the authors were unable to obtain cell count densities of the surviving dinoflagellates to support their conclusion.

The predation efficiency of higher trophic organisms has also been observed under bioluminescent conditions. For example, Fleisher and Case (1995) found that, for two species of squid, 85% and 90% of strikes on mysids, grass shrimp and mosquito fish occurred in the presence of bioluminescence and strikes under non-bioluminescent conditions were rare. Mensinger and Case (1992) found improved strike success rate of teleost predation upon mysids from 53.3% to 76.1% in the presence of low concentrations (< 12.5 cells mL^{-1}) of bioluminescent dinoflagellates. However, concentrations of bioluminescent organisms greater than 17.5 cells mL^{-1} were found to decrease predation efficiency. This was thought to be due to increased flash frequencies creating substantial photic background noise and making targets more diffuse (Mensinger and Case, 1992).

Although studies indicate that higher trophic level species may be able to take advantage of bioluminescence to detect prey, they do not directly indicate any advantage to dinoflagellate survival (Mensinger and Case, 1992; Abrahams and Townsend, 1993; Fleisher and Case, 1995). For example, experimental results did not explicitly measure dinoflagellate survival rates and only inferred increased survival from their findings. It is also worth noting that these studies used dinoflagellate species that do not naturally occur in the same environments as the grazers or the secondary predators, creating somewhat artificial predator prey interactions.

Several experimental studies have also been conducted to determine the direct influence of bioluminescence upon grazers of dinoflagellates, to examine the startle response hypothesis. Buskey and Swift (1983) and Buskey et al. (1983) demonstrated that in the presence of pulses of artificial light or flashes of bioluminescence the copepod *Acartia hudsonica* made an increased number of high speed swimming bursts than when no flashes were present. These findings were interpreted as representing a startle response by the copepods responding to the bioluminescent flash. It was further suggested that, as no feeding occurred during these high speed swimming

bursts, grazing in the presence of bioluminescence would be decreased (Buskey et al., 1983).

Esaias and Curl, (1972) investigated the effect of bioluminescence on the ingestion rates of the copepod *Calanus pacificus* when grazing upon three bioluminescent *Gonyaulax* species and one non-bioluminescent *Gynodinium* species of dinoflagellate. The study indicated lower ingestion rates of dinoflagellates which had a higher potential for bioluminescence. A similar result was found for *Acartia tonsa* grazing upon *Gonyaulax excavata*, though only when concentrations of dinoflagellates were $> 500 \text{ cells ml}^{-1}$ (White, 1979). These results were taken to demonstrate that bioluminescence in dinoflagellates has value as a defence against copepods by reducing their grazing efficiency. However, in both studies the cell concentrations at which lowered ingestion rates were found are rare in nature and only likely to occur under coastal bloom conditions. White (1979) also found that the movement of *Pseudocalanus minutes* and copepod nauplii did not stimulate bioluminescence within cultures, indicating that bioluminescence may not act to reduce grazing from all predators.

Bioluminescence is a complex process that is found in dinoflagellates throughout the world's oceans. It is also likely to be very energy expensive, with the emission of light with wavelength $\sim 470 \text{ nm}$ corresponding to approximately 255 J mol^{-1} equivalent to eight times the energy released by the hydrolysis of ATP to ADP which is 30.5 J mol^{-1} (Rees et al., 1998; Wilson and Hastings, 1998). Therefore, it is reasonable to propose that it provides some benefit to the individual or to the community as a whole. The experimental work discussed above has failed to identify whether the ability of dinoflagellates to emit light is of individual or community benefit. It could be argued that if the function of bioluminescence involves the death of the bioluminescent individual then there can be no selective pressure for preserving the response (Buck, 1978). However, it has been suggested that as bioluminescent dinoflagellates reproduce asexually that such an altruistic behaviour could continue through kin selection (Smith, 1964). Tett and Kelly, (1973) and Buskey et al. (1983) hypothesise it is likely that genetically identical or sibling clones would reside in the same vicinity of the consumed individual and benefit from the decreased grazing pressure brought about by the bioluminescent flashes of the consumed individual. Thus, genes for bioluminescence continue to survive in the dinoflagellate population.

It is perhaps logical to reason that as well as a benefit there must also be some additional cost or trade-off associated with the ability to emit light, particularly if it is such an energetic process. One hypothesis might be that the additional cellular machinery and energy required for bioluminescence may impact upon the growth rate

of bioluminescent individuals. However, there is very little, if any, discussion of such a cost within the current literature and at present the cost of bioluminescence to an individual remains unclear. Further work is required to confirm and quantify the costs and benefits of dinoflagellate bioluminescence and the mechanisms responsible.

1.7 Research Objectives

The reviewed literature has revealed that dinoflagellates are responsible for the majority of bioluminescence observed in the surface waters of the world's oceans (Seliger et al., 1962; Batchelder and Swift 1989; Lapota et al., 1992; Neilson et al., 1995; Latz and Rohr, 2005). Previous attempts to forecast the distribution of bioluminescence over short time scales (1–3 days) or large spatial scales (1000s km) using direct empirical relationships with chlorophyll or purely considering advective physical processes have been limited in their success (Ondercin et al. 2005; Shulman et al., 2003, 2011). The consideration of the ecological and behavioural dynamics of these bioluminescent organisms within models has the potential to improve forecasting of the bioluminescent field. However, the literature also indicates that there is still much to learn about bioluminescent dinoflagellates and their ability to emit light. The impact of these organisms upon the diurnal variability of the in situ bioluminescent field and its causes are unclear with many in situ studies coming to conflicting conclusions (Seliger et al., 1962; Greenblatt et al., 1984; Lapota et al. 1984; Sadovskaya and Filimonov 1985; Buskey et al., 1994). Seasonal variations of these organisms and their bioluminescent emissions have also been rarely studied. It is not clear how, or even if, their ability to luminesce affects their temporal and spatial distribution compared to non-bioluminescent organisms particularly those of non-bioluminescent dinoflagellates. There is also uncertainty surrounding the ecological purpose of dinoflagellate bioluminescence with studies suggesting multiple hypotheses regarding how it acts as a defence/survival strategy (Burkenroad, 1943; Esaias and Curl, 1972; Buskey et al., 1983). It is unclear at present how the ecological function of bioluminescence might be incorporated into future forecast models and its potential impact upon ecosystem dynamics has largely been ignored. This lack of knowledge regarding the ecology of these organisms and their ability to luminesce may hinder their representation in models and therefore hold back the capability to forecast the bioluminescent field within the surface ocean.

The research presented over the next five chapters looks to advance our knowledge of dinoflagellate bioluminescence using a multidisciplinary approach combining in situ observations, time-series analysis and ecological modelling. The thesis specifically aims to address key gaps in the knowledge of dinoflagellates and their

bioluminescence needed to operationally forecast surface ocean bioluminescence within the open ocean North Atlantic. All of the studies within the thesis are focused upon the open ocean region surrounding the Porcupine Abyssal Plain (PAP) sustained observatory within the northeast Atlantic (49° N 16.3° W). The objectives of the thesis are to:

Objective 1: Investigate controls upon diurnal changes in bioluminescent intensity within northeast Atlantic dinoflagellate communities (**Chapter 2**).

Objective 2: Explore the seasonal dynamics of bioluminescent dinoflagellates, their inferred bioluminescent signal and relationship with the dinoflagellate community as a whole within the northeast Atlantic (**Chapter 3**).

Objective 3: Develop a simple biological model which allows the investigation of the ecological function of dinoflagellate bioluminescence (**Chapter 4 and 5**).

Objective 4: Explore how the ecological function of dinoflagellate bioluminescence could be modelled using current understanding of the mechanisms by which it is hypothesised to occur and examine its potential affects upon an ecosystem (**Chapter 6**).

These research objectives form the basis of the **Chapters 2 to 6**. The introduction of each chapter gives more specific background material relevant to the research objectives which are being addressed. The results of the analysis being carried out are discussed at the end of each analysis chapter, with the exception of **Chapter 4** which leads directly on to **Chapter 5**. **Chapter 7** brings together the results of **Chapters 2 to 6** to summarise and synthesise key findings and relates them back to the overall aim of the thesis. Given the findings of the thesis, a discussion is then presented on how forecasting the surface ocean bioluminescent field can progress.

Chapter 2: Diurnal Variations of Bioluminescence within the Northeast Atlantic.

Preamble

This chapter is based broadly on a research article entitled "*Diurnal variations of dinoflagellate bioluminescence within the open ocean north-east Atlantic*" submitted to the Journal of Plankton Research 2nd April 2011 by Marcinko CL., Allen JT., Poulton AJ., Painter SC., and Martin AP.

All of the analysis was carried out by Charlotte Marcinko, using data collected by Charlotte Marcinko, John Allen, Stuart Painter and Adrian Martin. Alex Poulton provided count data for the collected phytoplankton samples. The work was written up entirely by Charlotte Marcinko with intellectual input from John Allen, Stuart Painter, Adrian Martin and Alex Poulton.

Abstract

Diurnal variations of bioluminescence in mixed dinoflagellate communities within the open ocean north-east Atlantic were examined during summer 2009. Bioluminescent intensity at night was over 23 times greater than daytime levels for the same populations. Experiments explored the influence of circadian regulation and light exposure upon diurnal variations of bioluminescence within natural dinoflagellate communities. Results indicate that under continual darkness diurnal variability of bioluminescence was retained over a 48 hour period, demonstrating a degree of circadian control. This circadian signal is thought to relate to the presence of photosynthetic bioluminescent species *Gonyaulax* and *Pyrocystis*. Results show that light strongly influenced the diurnal variation of bioluminescence. The observed circadian rhythms were photo-entrained to the phase of the natural photoperiod and light further inhibited daytime bioluminescence. Exposure to daytime irradiance was required to maintain night-time bioluminescence; without exposure night-time intensities were damped up to 75%. Maximum night-time bioluminescence was found to increase monotonically with the intensity of previous daytime irradiance, indicative of photo-enhancement. These findings highlight how taxonomic, cellular and environmental factors influence diurnal variations of bioluminescent intensity in summer dinoflagellate communities within the open ocean north-east Atlantic. Furthermore, these results emphasize the importance of considering the light history of bioluminescent communities when analysing in situ datasets of bioluminescence.

2.1 Introduction

Bioluminescence is the emission of light by a living organism. Displays of bioluminescence visible at the surface of the ocean have been reported for centuries and bioluminescent emissions in the upper ocean are of great interest to the scientific community. For example, bioluminescent intensity in surface waters can act as an indicator of the distribution of plankton biomass in relation to physical processes, the presence of toxicity in the marine environment, and for the functional state of the planktonic ecosystem (Lapota et al., 1993; Kushnir et al., 1997; Piontkovski et al., 2003; Kim et al., 2006).

Bathypotometer measurements of flow stimulated bioluminescence from surface waters have revealed diurnal patterns in bioluminescent intensity (Batchelder et al., 1992; Swift et al., 1995; Moline et al., 2001). Increases of several orders of magnitude between day and night have been recorded in many regions including the Southern California Bight, Black Sea, Vestfjord (Norway) and Mediterranean Sea (Greenblatt et al., 1984; Tokarev et al., 1999b; Lapota et al., 1992; Cussatlegras et al., 2001).

Measurements compiled across several regions of the world's oceans show night-time bioluminescent intensity in surface waters is typically 1 – 3 orders of magnitude greater than corresponding daytime intensities (Utyushev et al., 1999).

Bioluminescent dinoflagellates are responsible for much of the bioluminescence detected in the surface waters of the world's oceans (Batchelder and Swift 1989; Neilson et al., 1995; Tokarev et al., 1999a; Latz and Rohr 2005). This group of unicellular organisms, with cell dimensions between 5 μm and 2 mm, contain the only members of the phytoplankton community with the ability to emit visible light. Their bioluminescence is generally thought to deter or decrease predation by zooplankton (Esaías and Curl, 1972; Buskey et al., 1983).

Several hypotheses have been proposed to explain *in situ* diurnal variations in bioluminescent intensity where dinoflagellates have contributed significantly to the bioluminescent field. Some have pointed to the influence of exogenous (external) behaviour or environmental factors such as the diurnal migration of dinoflagellates through the water column (Seliger et al., 1962) or the (photo-)inhibition of bioluminescence by light (Yentsch et al., 1964; Sadovskaya and Filimonov, 1985; Batchelder et al., 1992).

Photo-inhibition of flow stimulated dinoflagellate bioluminescence has been proposed as an energy saving mechanism that stops the emission of light when daytime irradiance would prevent it from being effective as a defence mechanism (Esaías et al., 1973). Photo-inhibition has been demonstrated in laboratory studies for a number of photosynthetic and heterotrophic species (**Table 2.1**). However, bioluminescence is not believed to be photo-inhibited in all species, for example *Noctiluca scintillans* (Sweeney, 1971). Studies of both natural populations and single species have shown that photo-inhibition of mechanically stimulated bioluminescence can be rapid, occurring approximately 1 minute after exposure to light (Esaías et al., 1973; Filimonov and Sadovskaya, 1986).

Studies have also shown that several dinoflagellate characteristics, including bioluminescence, exhibit variability which is under endogenous (internal) circadian control (Prezelin et al., 1977; Vicker et al., 1988; Roenneberg and Mittag, 1996). Diurnal rhythms in bioluminescence which persist under controlled conditions of constant temperature and light for several days have been recorded within laboratory studies for several species of photosynthetic dinoflagellate (**Table 2.1**). These persistent diurnal variations are controlled at a cellular level, rather than by external factors such as photo-inhibition, and demonstrate a circadian regulation of bioluminescence (Roenneberg and Mittag, 1996). Circadian systems within organisms

exist to regulate the time at which biological events occur in relation to a diurnal cycle (Roenneberg and Foster, 1997). Changes in light intensity during dawn and dusk are known to be the most reliable indicators of phase of day and it is common that the phase of circadian rhythms within organisms can be adjusted to daily changes in light through a process known as photo-entrainment (Roenneberg and Foster, 1997).

Table 2.1: List of photosynthetic and heterotrophic dinoflagellates where photo-inhibition or circadian regulation of their bioluminescence has been investigated in laboratory studies

Species	Photo-inhibition of Bioluminescence	Circadian Regulation of Bioluminescence	References
<i>Photosynthetic</i>			
<i>Lingulodinium polyedrum</i>	✓	✓	Hastings and Sweeney (1958); Sweeney et al. (1959)
<i>Alexandrium catenella</i>	✓	-	Esaias et al. (1973)
<i>Alexandrium acatenella</i>	✓	-	Esaias et al. (1973)
<i>Alexandrium tamerensis</i>	✓	-	Esaias et al. (1973)
<i>Alexandrium monilatum</i>	-	✓	Hastings (1959)
<i>Pyrocystis lunula</i>	✓	✓	Hamman et al. (1981a); Sweeney (1987)
<i>Pyrocystis noctiluca</i>	-	✓	Knaust et al. (1998)
<i>Pyrocystis fusiformis</i>	-	✓	Sweeney (1981a)
<i>Ceratium fusus</i>	✓	-	Sullivan and Swift (1994)
<i>Heterotrophic</i>			
<i>Protoperidinium</i> spp.	✓	-	Buskey et al. (1992); Li et al. (1996)
<i>Protoperidinium divergens</i>	-	✗	Buskey et al. (1992)
<i>Protoperidinium huberi</i>	-	✓	Buskey et al. (1994)
<i>Noctiluca scintillans</i>	✗	✗	Nicol (1958); Sweeney (1971)

Circadian regulation of bioluminescence is not thought to be common among heterotrophic dinoflagellates. There is only one example, with circadian regulation exhibited by heterotrophic *Protoperidinium huberi* (Buskey et al., 1994). However, laboratory studies have focused upon a relatively small number of individual bioluminescent dinoflagellate species due to the difficulty of isolating and keeping species in culture. Thus, it is uncertain whether the majority of other bioluminescent dinoflagellates, particularly heterotrophs, exhibit circadian control of their bioluminescence.

Only a small number of field studies have detected circadian regulation of bioluminescence within natural dinoflagellate communities. These studies specifically examined diurnal variations of bioluminescence in single species or mixed populations in coastal regions. Circadian rhythms in bioluminescence were found in natural populations of *Pyrodinium bahamense* within Oyster Bay, Jamaica (Soli, 1966; Biggley et al., 1969). Dinoflagellate populations containing multiple bioluminescent species, collected from a coastal salt pond at Woods Hole in August 1965, were also found to demonstrate a circadian rhythm in stimulated flash rates when kept in complete darkness (Kelly and Katona, 1966). However, these rhythms did not persist throughout the year and were associated with the seasonal presence of *Gonyaulax* spp. (Kelly, 1968). Similarly, Yentsch and Laid (1968) found that circadian rhythms of bioluminescence in natural dinoflagellate populations in coastal waters surrounding Woods Hole were not present year round. Circadian regulation was only observed in October. However, photo-inhibition of bioluminescence was observed throughout the year (Yentsch and Laid, 1968).

The north-east Atlantic is an open ocean region with a history of bioluminescent research and observations (e.g. Neilson et al., 1995; Swift et al., 1995). Ecological processes within open ocean regions like this are somewhat different to those found in shelf and coastal waters, where previous *in situ* studies of bioluminescent dinoflagellate communities and their diurnal variations have been focused. For example, coastal regions are highly eutrophic and the bioluminescent field can often be dominated by a singular species (such as *Lingulodinium polyedrum* or *Noctiluca scintillans*). In comparison, open ocean regions are less nutrient rich and multiple bioluminescent species will often contribute to the bioluminescent field. Thus, it is important that the diurnal variability of surface ocean bioluminescence in natural open ocean populations are examined and quantified in their own right and not just extrapolated from previous coastal studies.

This study presents an examination of the diurnal variations of bioluminescence in mixed dinoflagellate communities from an open ocean region of the north-east Atlantic during summer. Measurements of flow stimulated bioluminescence allowed the influence of circadian regulation and light exposure upon diurnal variations of bioluminescence to be explored. The study assesses whether circadian regulation of bioluminescence can be detected in summer dinoflagellate communities within the open ocean north-east Atlantic and determines how bioluminescent intensity observed *in situ* is influenced by light. The diurnal variations of bioluminescent intensity observed *in situ* are then related to the composition of the summer dinoflagellate communities and to previous observations from laboratory studies on species in culture.

2.2 Materials and Methods

2.2.1 Study Site

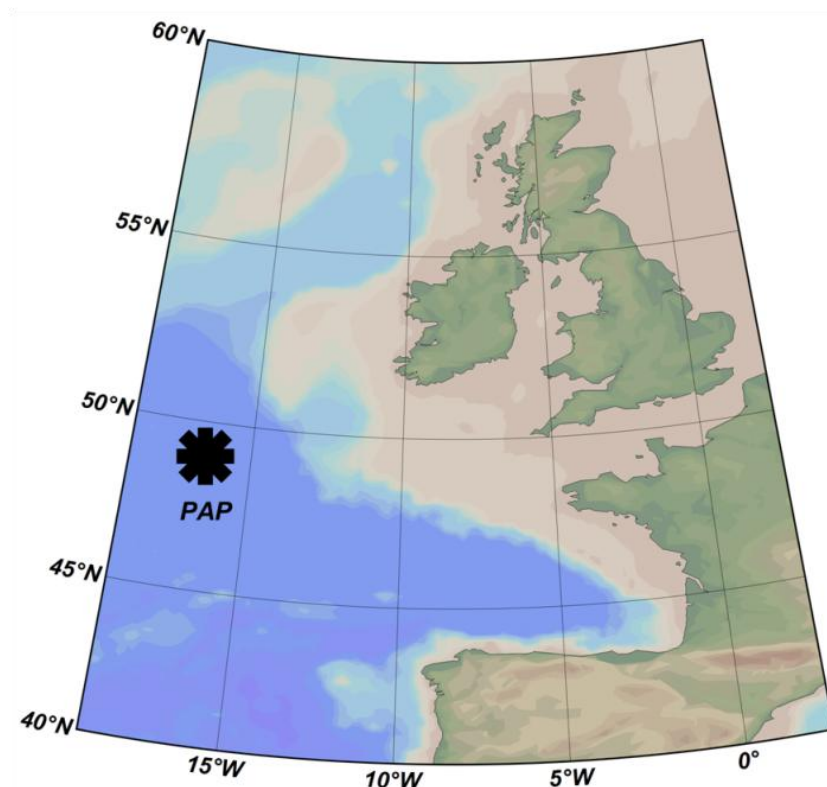


Figure 2.1: Location of Porcupine Abyssal Plain (PAP) observatory 49° N, 16 30' W with bathymetry contours overlaid.

Experiments were carried out around the Porcupine Abyssal Plain (PAP) observatory, located at 49°N 16°30' W, between 28th July and 9th August 2009 (**Figure 2.1**) aboard the *RRS Discovery*. The PAP site and the surrounding area has been the focus for sustained biogeochemical measurements since 1989 and is characterised by a large spring phytoplankton bloom (Ducklow and Harris, 1993). The spring bloom is dominated by diatoms, with dinoflagellates contributing significantly to the phytoplankton population during the summer months (Dodge, 1993; Leterme et al., 2005; Smythe-Wright et al., 2010).

2.2.2 Instrumentation

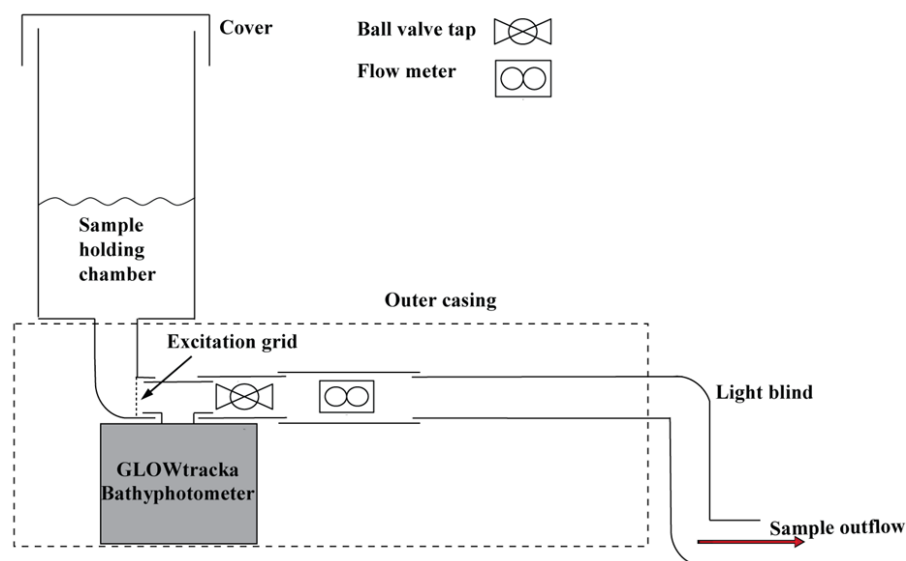


Figure 2.2: Diagram of laboratory rig for the measurement of bioluminescence from discrete 2 L samples. A 1 mm excitation grid induces turbulence and stimulates bioluminescence of organisms within the sample which is recorded by a GLOWtracka bathyphotometer at a frequency of 1 kHz. A flow meter provides a method for determining the start and stop time of the sample flow through the instrument.

Measurements of stimulated bioluminescence were made using a GLOWtracka bathyphotometer (Chelsea Technologies Group Ltd) which is based on the design described in Aiken and Kelly (1984). The GLOWtracka bathyphotometer was set up for bench-top use by combining it with a flow meter and data logging unit to produce a system which allowed measurements to be made from discrete water samples (**Figure 2.2**). The bench top system provided measurements of stimulated bioluminescence at a frequency of 1 kHz from a controlled flow of water. Two litres of water were used for each discrete measurement. A sample was placed into a light-tight holding chamber and left to rest for a period of five minutes for any disturbance induced through transfer into the chamber to subside. After resting the sample was allowed to pass through the instrument under gravity. A 1 mm mesh excitation grid induced turbulence and stimulated the organisms within the sample to flash as they passed a photodiode sensor. Emissions of light are converted to a voltage by the photodiode and data were recorded using Agilent VEE release 8.5 software. An example of the raw bioluminescent data is given in **Figure. 2.3**. Measurements in Volts were converted to units of photons $\text{cm}^{-2} \text{sec}^{-1}$ using the manufacturer's calibration coefficients. The integrated bioluminescent signal for each sample was then calculated over the period of sample flow, which was determined from the output of the flow meter. This method provided a quantitative measure of bioluminescent intensity that can be compared between samples. A value integrated over a period of time is susceptible to less error

and variability than an estimate of the single peak value. However, it must be noted that this measurement is not equivalent to the maximum stimulated bioluminescent intensity of the water sample. Typically the integrated value will be lower because of the steady decrease in the head of water and therefore the flow rate through the bathyphotometer.

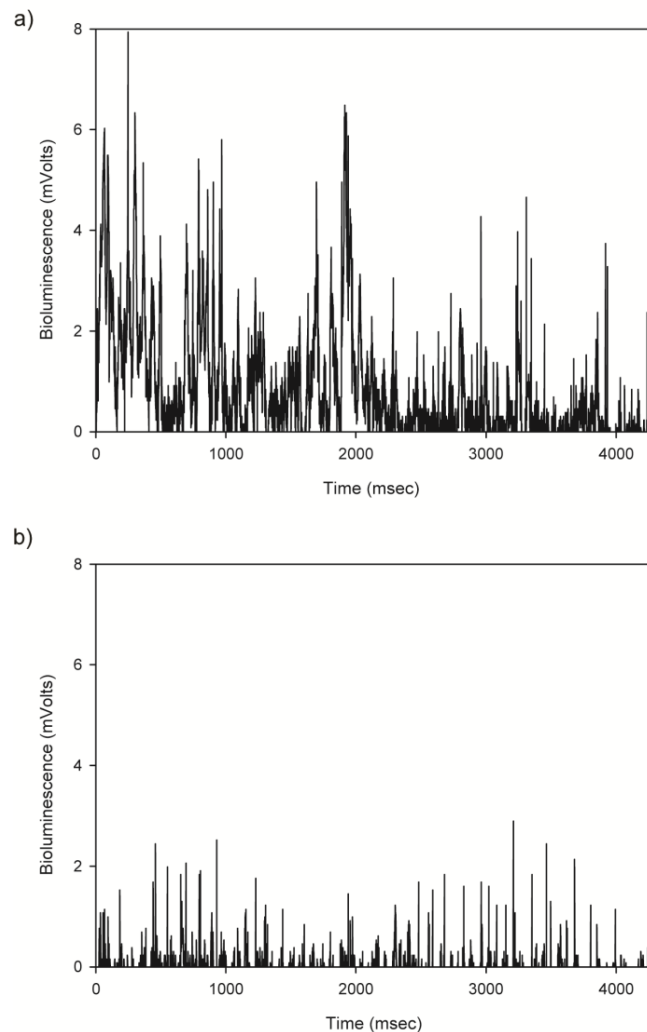


Figure 2.3: Example of primary data from GLOWtracka bench top instrument. a) Two litre sample containing mixed bioluminescent dinoflagellate community measured at 23:00 GMT during experiment 1. b) Two litre sample containing mixed bioluminescent dinoflagellate community measured at 08:00 GMT during experiment 1.

2.2.3 Experiments

The bench top set up of the GLOWtracka bathyphotometer was used to conduct three experiments. Water for each experiment was collected using a set of 20 L niskin bottles attached to a CTD Rosette. Details of the location, time and volume of water collected for each experiment are presented in **Table 2.2**. Each experiment was carried

out over a time period which encapsulated two night-time phases (44–48 hrs). Sunrise and sunset during the cruise period occurred at approximately 05:00 and 20:00 GMT respectively.

Experiment one simply investigated whether circadian regulation of bioluminescence could be detected in summer dinoflagellate communities within the open ocean north-east Atlantic (**Table 2.2**). To test whether diurnal variations of bioluminescent intensity persisted in the absence of a natural photoperiod, 100 L of sea water were collected from a single CTD deployment and stored in complete darkness at a constant temperature of 16°C to match surface water temperature. A 2 L sub-sample was taken hourly and measured for bioluminescence.

Table 2.2: Details of experiments carried out to investigate diurnal variations of bioluminescent intensity from natural population of dinoflagellates in the north-east Atlantic in summer 2009.

Experiment	Location	DOY (2009)	Volume of Water (L)	Water Collection Time(GMT)	Water Collection Depth (m)	Start Time (GMT)	Experiment Length (Hours)
Experiment 1	48° 59' N, 16° 41' W	209	100	14:56	5	16:00	48
Experiment 2	48° 53' N, 16° 32' W	219	110	17:14	5	17:30	48
Experiment 3	48° 44' N, 16° 31' W	221	240	20:08	5	21:00	44

Experiment two, in addition to providing a replicate of experiment one, further examined the bioluminescent response after re-exposure to a natural photoperiod (**Table 2.2**). As in experiment one, 100 L of water were stored in darkness at a constant temperature of 16°C and bioluminescence was measured from 2 L sub-samples every hour. An additional 10 L of sea water was re-exposed to the natural photoperiod 12 hours after initial water collection. The 10 L of water were transferred into a sealed polycarbonate container and placed within an *in situ* incubator in full sunlight on deck. Screens to reduce the natural light level were not used, however the polycarbonate container reduced the level of photosynthetically active radiation (PAR) by 43 %. The temperature within the incubator was kept at ~16°C by a continually renewed surface sea water supply. Bioluminescent intensity was measured using 2 L

subsamples from this container every 3 hours between 19:00 and 07:00 GMT during the second night phase of the experiment.

Experiment three investigated how bioluminescent intensity observed *in situ* is influenced by light. Comparisons were made between diurnal variations in bioluminescent intensity with and without the influence of a natural photoperiod. The methodology followed that of experiment two but with improved resolution of the light exposed measurements. One hundred and twenty litres of sea water were stored in clear polycarbonate containers in *in situ* incubators, at a constant temperature of ~16°C, and exposed to the natural photoperiod. Another 120 L of sea water were kept in continuous darkness at 16°C. Bioluminescence was measured hourly from both sets of water.

2.2.4 Phytoplankton Enumeration

Water samples for phytoplankton enumeration by light microscopy were taken every 4 to 6 hours throughout the sampling period of each experiment for the purposes of monitoring the plankton community composition. Samples were preserved in 100 ml brown bottles with 2 % acidic Lugol's solution. After the cruise, the following samples were analysed: experiment one, samples from 0, 8, 24, 36 and 44 hrs; experiment two, samples from 0, 8, 24, 32 and 44 hrs; experiment three, samples from 0, 18, 30 and 42 hrs. Sub-samples from each sample were settled in 50 ml settling chambers for approximately 10 – 12 hours and the full chamber was examined using an SP-95-I inverted microscope under a magnification of x100 or x200 depending on cell size and density of the sample (Brunel microscopes Ltd). Dinoflagellates were identified to genus or species level following Tomas (1997).

To investigate whether there were any significant correlations between the abundance of bioluminescent genera/species and the time elapsed in the experiments, Spearman rank-order correlation analyses, for use on non-parametric data, were conducted. Mann-Whitney U tests, for use on non-parametric data, were also carried out to determine whether there were significant differences in the median abundance of bioluminescent genera/species within light deprived and light exposed samples from experiment three. All statistical tests were carried out using PASW Statistics 18.0 and statistical significance was considered at $p < 0.05$.

2.2.5 Photosynthetically Active Radiation (PAR) Measurements

Photosynthetically active radiation (400 – 700 nm, PAR) at the sea surface was measured continually by two Skye Instruments photosynthetically active radiation

SKE510 sensors located port and starboard of the foremast platform on the *RRS Discovery*. Integrated daytime PAR was calculated for the day of water collection and for the second daytime period in each experiment. Second daytime PAR levels for light exposed samples in experiments two and three have been corrected for light attenuation due to the incubation method which was found to decrease PAR levels by 43%, no further screening of PAR levels occurred.

2.3 Results

Diurnal changes in flow stimulated bioluminescent intensity for the three experiments are shown in **Figure 2.4** and **Table 2.3**. A seven point running average was calculated using the 1 hour data points in each experiment to provide a clearer visual indication of the time when peaks in bioluminescent intensity occurred and to reduce measurement noise.

Table 2.3: Minimums and maximums of observed cycles in measured flow stimulated bioluminescent intensity over each experiment.

Experiment	1st Minimum	1st Maximum	2nd Minimum	2nd Maximum
Bioluminescent Intensity (Photons cm ⁻²)				
<i>Experiment 1</i>	0.57 x10 ¹¹	4.1 x10 ¹¹	0.25 x10 ¹¹	1.1 x10 ¹¹
<i>Experiment 2 Light Deprived</i>	0.10 x10 ¹¹	2.3 x10 ¹¹	0.24 x10 ¹¹	0.62 x10 ¹¹
<i>Experiment 2 Light Exposed</i>	–	–	–	1.7 x10 ¹¹
<i>Experiment 3 Light Deprived</i>	–	1.8 x10 ¹¹	0.21 x10 ¹¹	0.63 x10 ¹¹
<i>Experiment 3 Light Exposed</i>	–	1.7 x10 ¹¹	0.07 x10 ¹¹	1.2 x10 ¹¹

2.3.1 Evidence of Circadian Regulation

Results of experiments one and two show bioluminescent intensity increased by approximately 10 and 23 fold, respectively, during first night-time phases compared to the first daytime phases (**Table 2.3**). Running averaged time-series indicate that peaks in bioluminescent intensity occurred at approximately 23:00 GMT during the first night phases in both experiments, three hours after local sunset (**Figure 2.4a and 2.4b**). As experiment three did not commence until 21:00 GMT it was not possible to compare the first night peak in bioluminescent intensity in this experiment to the intensities measured the previous day. The running average time-series indicate that

peak bioluminescent intensity in this experiment occurred slightly earlier at 22:00 GMT (**Figure 2.4c**). However, it must be noted that the first night peak shown by the running averaged time-series in this experiment may be biased towards earlier times by the lack of data prior to 21:00 GMT.

Results from all experiments indicate that diurnal variations in flow stimulated bioluminescent intensity persisted in the absence of a natural photoperiod. Second and third day intensities were decreased compared to second night phase intensities in the light deprived samples in all experiments (**Figure 2.4**). Maximum second night intensities were 4.4, 2.6 and 3.0 times greater than preceding day phase intensities for experiment one, two and three, respectively (**Table 2.3**). However, second night maximum intensities for light deprived samples in all experiments were decreased by approximately 75% compared to their respective first night peak intensities (**Table 2.3**). Running averaged time-series in all experiments indicate that second night peaks in bioluminescent intensity occurred later than first night peak intensities. Second night peaks in intensity occurred approximately 7 (06:00 GMT), 5 (04:30 GMT) and 10 (08:00 GMT) hours later than in first night phases for experiments one, two and three, respectively (**Figure 2.4**).

2.3.2 The Effect of Light

Diurnal variations in flow stimulated bioluminescent intensity were also detected in the presence of a natural photoperiod (**Figure 2.4c**). Results from experiments two and three show that peak bioluminescence in second night phases was much higher in intensity when samples had been exposed to light in the previous day phase (**Figure 2.4b and 2.4b**). Maximum bioluminescent intensities were approximately triple and double those reached by the light deprived samples in experiment two and three, respectively (**Table 2.3**). Results from experiment three also indicate that daytime bioluminescent intensities were consistently lower in the samples exposed to light compared to those kept in darkness (**Figure 2.4c**). The running averaged time-series for the light exposed samples in experiment three also indicates that the second night phase bioluminescence peak occurred only two hours later (00:00 GMT) than that observed the previous night (22:00 GMT). Unfortunately, a running average could not be calculated for the light exposed samples in experiment two due to the sparseness of the measurements. However, the data suggests that maximum bioluminescent intensity in the second night phase occurred at approximately 01:00 GMT, also only 2 hours later than the peak in light deprived samples in the previous night phase.

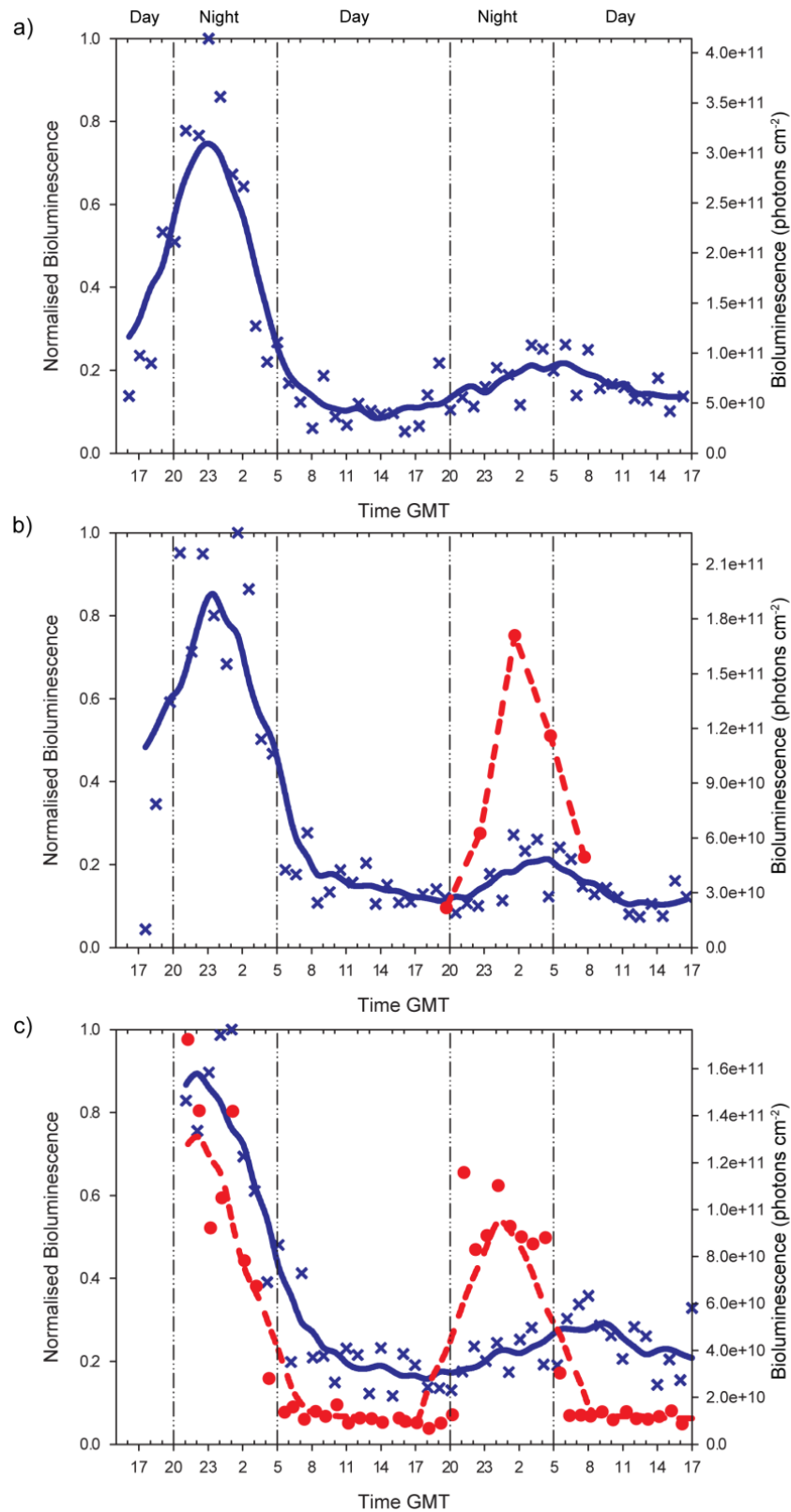


Figure 2.4: Variations in bioluminescence measured in a) Experiment 1, all samples deprived of light (solid line shows 7 point running average, 'x' represent individual values). b. Experiment 2, repeat of experiment 1 with the addition of 10 litres of water exposed to natural day-night cycle (solid line shows 7 point running average, 'x' represent individual values from samples kept in continuous darkness, '•' show individual values from samples exposed to daytime irradiance). c) Experiment 3, parallel measurements of samples exposed to a natural day-night cycle (individual values shown as '•', running average shown as dashed line) and samples kept in continuous darkness (solid line shows 7 point running average, 'x' represent individual values).

Results from samples exposed to a natural photoperiod in experiment three show the running averaged time-series peak bioluminescence to be lower than that calculated from samples kept in darkness during the first night phase (**Figure 2.4c**). It was noted that, prior to 23:20 GMT on the first night of the experiment, incubator covers used during the night to prevent the ship's deck lights penetrating into the incubators had come loose and therefore samples were potentially exposed to a small amount of light. Covers were subsequently amended. Consequently, given that our results show that daylight had a substantial inhibitory effect upon bioluminescence, this difference in magnitude can be explained by the effect of the ship's lights on incubated samples taken before incubator covers were made fully light-tight.

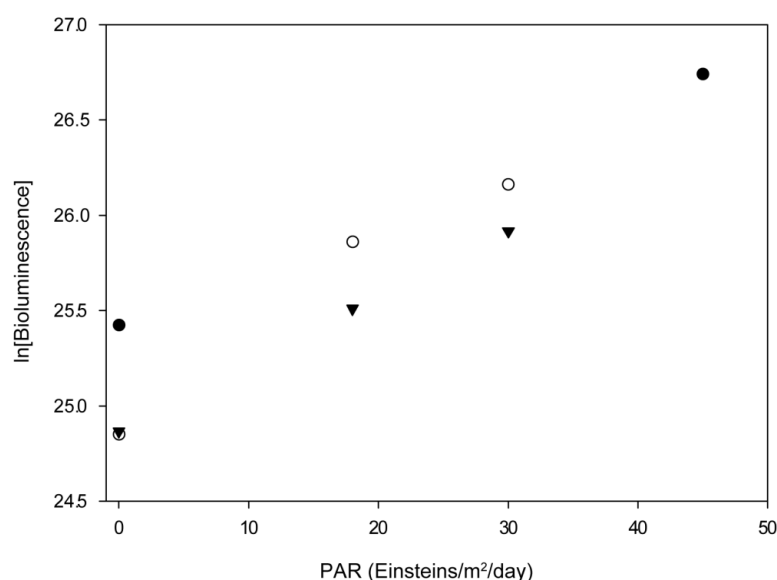


Figure 2.5: Relationship between integrated daytime photosynthetically active radiation (PAR) and log maximum night-time bioluminescence. Closed circles are from experiment 1, open circles are from experiment 2 and closed triangles are from experiment 3.

Levels of PAR on the day of water collection varied between experiments. Integrated PAR on the day of water collection for experiment one was calculated as 45 Einsteins $\text{m}^{-2} \text{day}^{-1}$ in comparison to 30 Einsteins $\text{m}^{-2} \text{day}^{-1}$ in experiment two and experiment three. Corrected for light attenuation, the second day phase integrated PAR for incubated light exposed samples in experiments two and three was calculated as 18 Einsteins $\text{m}^{-2} \text{day}^{-1}$. In each of the three experiments, the log of maximum night phase bioluminescent intensity was consistent with a proportional relationship to the preceding day phase integrated PAR (**Figure 2.5**).

2.3.3 Bioluminescent Dinoflagellate Community Composition

Table 2.4: Results of microscopy analysis showing the median cell abundance and range for bioluminescent genera or species. Note that cell numbers are rounded to the nearest 20 due to a multiplication factor of 20 when converting from per 50ml to per 1 litre.

Genus	Experiment 1	Experiment 2 light deprived	Experiment 3 light deprived	Experiment 3 light exposed
	cells L ⁻¹			
Photosynthetic				
<i>Gonyaulax</i> spp.	1260 (780 – 1580)	1740 (1140 – 4360)	1460 (880 – 2440)	1860(1480 – 2720)
<i>Alexandrium</i> spp.	100 (0 – 180)	80 (0 – 220)	160 (120 – 320)	20 (0 – 120)
<i>Pyrocystis</i> spp.	20 (0 – 40)	0 (0 – 20)	0 (0 – 40)	0 (0 – 40)
<i>Ceratium fusus</i>	160 (120 – 280)	160 (120 – 280)	180 (120 – 200)	260 (160 – 400)
Heterotrophic				
<i>Protoperidinium</i> spp.	160 (100 – 340)	160 (80 – 220)	60 (0 – 120)	120 (80 – 160)

All samples from each experiment contained bioluminescent dinoflagellate genera or species, both heterotrophic and photosynthetic. These were the photosynthetic *Gonyaulax* spp., *Alexandrium* spp., *Ceratium fusus* and *Pyrocystis* spp., and the heterotrophic *Protoperidinium* spp.. Counts indicated that *Gonyaulax* spp. numerically dominated all three experiments and that *C. fusus* and *Protoperidinium* spp. contributed considerably to the remaining fraction (Table 2.4).

Table 2.5: Results of Spearman rank-order correlation analyses. Results show no negative correlations at the $p < .05$ significance level between abundance (cells L⁻¹) of bioluminescent genera or species and time elapsed into an experiment. r_s : correlation coefficient; p : significance level. ** denotes a significant result at the $p < .05$ level.

Genus	Experiment 1		Experiment 2 light deprived		Experiment 3 light deprived		Experiment 3 light exposed	
	r_s	p	r_s	p	r_s	p	r_s	p
<i>Photosynthetic</i>								
<i>Gonyaulax</i> spp.	.700	.188	1.00	<0.05**	0	1	.200	.800
<i>Alexandrium</i> spp.	.000	1	-.564	.322	.632	.386	-.738	.262
<i>Pyrocystis</i> spp.	.053	.933	-.707	.182	.775	.225	.775	.225
<i>Ceratium fusus</i>	-.500	.391	-.462	.434	.400	.600	-.400	.600
<i>Heterotrophic</i>								
<i>Protoperidinium</i> spp.	-.872	.054	.700	.188	-.316	.684	-.400	.600

Correlation analyses of the microscopy results for each experiment indicated no significant negative correlations between the abundance of individual bioluminescent genera or species and the time elapsed into an experiment (**Table 2.5**). There was no evidence that the increased bioluminescence measured from the light exposed samples during the second night phase in experiment three was related to an increased bioluminescent population due to growth over the incubation period. Cell abundance results from experiment three showed no significant differences (Mann Whitney U-test, $p > .05$) between the abundance of bioluminescent genera or species in light exposed compared to light deprived samples.

2.4 Discussion

A detailed examination of the diurnal variations in bioluminescence for mixed dinoflagellate communities within the north-east Atlantic during summer has been carried out. Flow stimulated bioluminescence was observed to vary by at least an order of magnitude over a diurnal cycle. This level of variability compares well with that observed in mixed layer bioluminescence from other *in situ* observations (Utyushev et al. 1999). Peak bioluminescent intensity during first night phases occurred approximately three hours after local sunset between 23:00 and 00:00 GMT.

2.4.1 Bioluminescent Dinoflagellate Community Composition

Bioluminescent intensities throughout experiment one were almost two times (~46% on average) higher than those observed in experiments two and three (**Table 2.3**). This difference, in part, may be due to differences in the species composition between experiments. Flash intensity between bioluminescent species can vary by several orders of magnitude. For example, individual cells of *Pyrocystis* spp. have a flash intensity of the order 1×10^{10} photons s^{-1} (Cussatlegras and Le Gal, 2004), while flashes from cells of *Protoperidinium* spp. are of the order of 1×10^9 photons s^{-1} (Swift et al., 1995), and flashes from cells of *Gonyaulax* spp., *Alexandrium* spp. and *Ceratium fusus* are of the order of 1×10^8 photons s^{-1} (Swift et al., 1995). This means that one cell of *Pyrocystis* will emit the same amount of light as ~100 *Gonyaulax* cells. Although, abundance data showed only a small decline (of ~ 20 cells/L) in the median number of *Pyrocystis* spp. between experiments, these differences may, to some extent, be responsible for explaining the higher bioluminescent intensities recorded in experiment one compared to that in experiments two and three.

Table 2.6: Percentage contribution of bioluminescent taxa to estimated total light budget (see text for details).

Genus	<i>Experiment 1 light deprived</i>	<i>Experiment 2 light deprived</i>	<i>Experiment 3 light deprived</i>
<i>Photosynthetic</i>			
<i>Gonyaulax</i> spp.	25%	49%	61%
<i>Alexandrium</i> spp.	2%	2%	7%
<i>Pyrocystis</i> spp.	39%	–	–
<i>Ceratium fusus</i>	3%	4%	8%
<i>Heterotrophic</i>			
<i>Protoperidinium</i> spp.	31%	45%	25%

The literature values for flash intensities quoted above were combined with the median cell counts to construct an approximate light budget (as in Swift et al., 1995) and give an indication of the potential percentage contribution of photosynthetic and heterotrophic dinoflagellates to the bioluminescence signal observed (**Table 2.6**). This approach demonstrates that photosynthetic dinoflagellates had the potential to emit 69%, 55% and 75% of the total calculated light budget for experiments one, two and three respectively. This can be compared to 31%, 45% and 25% of the total calculated light budget for heterotrophic dinoflagellates. These rough calculations indicate that the majority of the observed bioluminescence signal may have been due to photosynthetic dinoflagellates, specifically *Pyrocystis* and *Gonyaulax* in experiment one and *Gonyaulax* in experiments two and three. However, it must be noted that the calculation of such light budgets are based on several assumptions, most notably that all cells counted luminesced and that the cells were all physiologically fit.

2.4.2 Evidence of Circadian Regulation

Measurements from light deprived samples kept under controlled conditions show the persistence of diurnal variations in bioluminescence over a 48 hour period without the need of exogenous cues (i.e. exposure to a photoperiod). These results demonstrate circadian regulation of bioluminescence for mixed bioluminescent populations sampled in oceanic conditions. The detection of such circadian regulation can be related to the dominant contribution that photosynthetic dinoflagellates made to the bioluminescent signal. Specifically, it can be related to the large abundance of *Gonyaulax* spp., as well as the presence of *Pyrocystis* spp. and *Alexandrium* spp., genera which are all known to demonstrate circadian regulation of their bioluminescence (Hasting, 1959; Kelly 1968; Sweeney, 1981a; Knaust et al., 1998). It is currently unknown if photosynthetic *Ceratium fusus* or heterotrophic *Protoperidinium* spp. also demonstrate circadian regulation.

Detection of circadian regulation in this study should be extrapolated cautiously to other regions or seasons within the North Atlantic. As circadian regulation of bioluminescence is dependent upon the bioluminescent community composition it influence on the diurnal variations of bioluminescent intensity may vary seasonally or spatially. Furthermore, circadian rhythms in bioluminescence have been shown to be disrupted by both low temperatures and nitrate concentration, which may also lead to spatial and temporal variations (Hastings and Sweeney, 1957; Roenneberg and Rehman, 1996).

2.4.3 The Effect of light

The periodicity of the diurnal variation in bioluminescence was seen to drift from 24 hours, when samples were exposed to the natural light/dark photoperiod, to between 29 and 34 hours, under light deprived conditions during purely circadian regulation. These changes in periodicity indicate that the circadian rhythms were photo-entrained to the phase of the natural photoperiod (i.e. day length). Circadian regulation of bioluminescence therefore used light as an exogenous cue for synchronising endogenous time keeping.

Second night maximum bioluminescent intensities for light deprived samples were dampened by as much as 75% compared to those observed during the first night peak. The statistical analyses indicated no significant reduction of individual bioluminescent taxa within subsamples over the course of the individual experiments. Therefore, population losses cannot account for the decreased bioluminescent intensities observed. As bioluminescent intensities increased to levels similar to those observed in the first night phases when re-exposed to light (**Figure 2.4b and 2.4c**) it would appear that the decreases were a consequence of the darkened conditions the water samples were subject to.

The physiological health of the cells preserved for microscopy cannot be fully assessed. Therefore, it is difficult to gauge accurately whether organisms had become stressed due to light deprivation or bottle enclosure. Previous studies have shown that bioluminescence of heterotrophic dinoflagellates can be affected by nutritional state (Buskey et al., 1994; Latz and Jeong, 1996). Photosynthetic dinoflagellates have also been shown to lose some of their bioluminescent capacity when deprived of light. For example, in culture conditions, *Lingulodinium polyedrum* held in darkness lost between 33 and 50% of their bioluminescent capacity per day (Sweeney et al., 1959), whilst *Pyrocystis noctiluca*, *P. lunula*, and *P. fusiformis* lost between 40 and 95% of their bioluminescent capacity over 2 days in darkened conditions (Swift et al. 1981).

Thus, the lack of light could have potentially caused photosynthetic dinoflagellates in our experiments to become sufficiently stressed that their bioluminescent capacity was reduced. It is notable, however, that the extent to which bioluminescence was decreased after only one day without light was much greater than that usually seen within laboratory studies of circadian rhythms for single species. This result may indicate that daytime light exposure is more important in maintaining night-time bioluminescent capacity for *in situ* bioluminescent populations, where light can vary considerably in intensity from day-to-day, compared to those in culture where light levels are well regulated.

The diurnal variations observed in samples exposed to light indicate daytime bioluminescent intensities were lower than those from light deprived samples. This demonstrates that under natural daytime light conditions, bioluminescent intensity in the mixed populations was further decreased by photo-inhibition.

Observations indicated night phase bioluminescent intensity and previous day phase PAR intensities increased monotonically in each of the three experiments (**Figure 5**). These results indicate photo-enhancement and suggest that the daytime irradiance intensity received by the mixed bioluminescent populations has a direct influence upon the stimulated night-time bioluminescent intensity observed. Previous laboratory studies using cultures of *Lingulodinium polyedrum* and *Ceratium fusus* have found similar relationships between organisms' bioluminescent capacity and previous daytime irradiance which supports this conclusion (Sweeney 1981b; Sullivan and Swift 1995). Unfortunately there are insufficient field data to properly quantify the relationship indicated.

Collectively, the results of this study relate the diurnal variations of open ocean bioluminescence to the composition of the dinoflagellate community and to their endogenous and exogenous controls. This study provides the first example of the circadian regulation of bioluminescence in natural dinoflagellate populations in an open ocean environment. Results also highlight the important influence of light upon the diurnal variation of stimulated bioluminescence in natural bioluminescent dinoflagellate communities dominated by photosynthetic species. This influence includes a control upon the phase of the variation observed, the inhibition of daytime bioluminescence when not suppressed by circadian regulation and also an influence upon the intensity of night-time bioluminescence. These findings emphasize the importance of considering previous light history as well as community composition when analysing or predicting bioluminescence *in situ*.

Chapter 3: Seasonal Variations of Bioluminescent Dinoflagellates within the Northeast Atlantic.

3.1 Introduction

The analysis in **Chapter 2** indicated the important effects of both environmental and cellular processes upon the short term variability in bioluminescent intensity within the dinoflagellate communities surrounding the Porcupine Abyssal Plain (PAP) sustained observatory. Within this chapter the focus broadens to examine how the bioluminescent dinoflagellate population within the same region varies on longer seasonal timescales and how such variations are related to those of the wider dinoflagellate community.

Relatively little is known about seasonal variations of mechanically stimulated bioluminescence¹ as most in situ studies of bioluminescence are rarely conducted over long enough periods for seasonal changes to be evaluated (Marra, 1995). The few studies carried out on seasonal timescales have indicated strong correlations between the number of spontaneous or stimulated bioluminescent flashes and the abundance of bioluminescent dinoflagellates (Kelly, 1968; Tett, 1971). These results unsurprisingly suggest a link between the abundance of luminescent organisms and potentially stimulated bioluminescent intensity. It has also been shown that bioluminescent intensity is correlated more generally with the abundance of the wider phytoplankton community with stimulated bioluminescent intensity following the known seasonal cycle of phytoplankton abundance (Yentsch and Laird, 1968).

More specifically, increases in stimulated bioluminescent intensity have been found to coincide with increases in the abundance of the dinoflagellate community as a whole, including both bioluminescent and non-bioluminescent species, within the Southern Sea of Korea (Kim et al., 2006). Similar associations have been found within the Mediterranean and Black Sea. Here, a compilation of over 3500 bioluminescent

¹ From this point forward within the chapter any reference to stimulated bioluminescence or stimulated bioluminescent intensity refers to bioluminescence which is mechanically stimulated by turbulence in the water unless stated otherwise.

measurements and 1000 phytoplankton samples between 1970 and 1995 showed extremely strong positive relationships ($r^2 > 0.8$; $p < .05$) between stimulated bioluminescent intensity and dinoflagellate abundance in non-polluted waters across several locations (Tokarev et al., 1999a). This is surprising as it may be taken to suggest that the ecology of bioluminescent dinoflagellates is not that different from their non-bioluminescent counterparts or that bioluminescence is an altruistic behaviour that can equally benefit nearby non-luminescent phytoplankton.

More practically, the correlations observed between stimulated bioluminescent intensity and dinoflagellate abundance suggest that seasonal variations in dinoflagellate abundance could be used as a proxy for seasonal variations in stimulated bioluminescence intensity. It is not clear whether such an association between stimulated bioluminescent intensity and dinoflagellate abundance is present in the open ocean region surrounding the PAP observatory. Unsurprisingly, many of the long term measurements of bioluminescence have been carried out in coastal waters at accessible locations. An exception to this was the MLML programme which conducted several cruises in the open ocean North Atlantic between April 1989 and August 1991 (Marra, 1995). In the waters of the Iceland Basin (59° N, 21° W) the potential for bioluminescence, as calculated from stimulated light budgets, was found to increase by 2 orders of magnitude between early April and after the onset of the spring bloom in May (Swift et al., 1995). From May onwards the potential bioluminescent intensity stayed approximately constant through to September. Dinoflagellates were the dominant bioluminescent organisms throughout spring, summer and autumn, responsible for $>90\%$ of the calculated light budgets. These findings suggest that the seasonal variation in stimutable bioluminescent intensity in the North Atlantic may follow that of bioluminescent dinoflagellates. However, they do not indicate whether increased bioluminescent intensity will be associated with increased abundance of all dinoflagellates as observed in the Mediterranean and elsewhere (Tokarev et al., 1999a; Kim et al., 2006).

Dinoflagellates are a tremendously diverse and complex group of organisms with behaviours that differ considerably between species. Despite the interspecies diversity, dinoflagellates as a group are widely observed to bloom between late spring and late summer (Gayoso 2001; McQuatters-Gollop et al. 2007) as they are thought to prefer calm stratified waters (Margalef, 1978). Many physiological and behavioural reasons have been put forward to explain why dinoflagellates succeed in stratified waters where inorganic nutrients are often depleted, but are out competed in more turbulent conditions when nutrients are more abundant. For example, several laboratory studies have suggested that small scale turbulence negatively influences dinoflagellate cell growth and physiology (Thomas and Gibson, 1990; 1992; Juhl and Latz, 2002).

However, there is no clear evidence to support this hypothesis in field studies and more recent laboratory studies give contradictory results (Sullivan and Swift, 2003; Havskum et al., 2005). In general, dinoflagellate ecology is still relatively poorly understood and judgements have often been made about the group as a whole based on the study of just a few well studied "model" species (e.g. *Lingulodinium polyedrum*).

Long time series data providing information on the temporal variability of phytoplankton are sparse, especially regarding dinoflagellates in non-coastal regions. However, the Continuous Plankton Recorder (CPR) survey is able to provide such data for many plankton throughout the North Atlantic and North Sea, dating back to its inception in 1931 (Hardy, 1939). As well as providing vital long term (i.e. decadal) measurements, it is also one of very few datasets available to the scientific community that allows the annual cycles of plankton to be resolved due to its consistent sampling throughout the year.

The CPR survey records data on over 400 plankton taxa within the North Atlantic providing semi-quantitative information on several major plankton functional types (Richardson et al., 2006). Abundance information regarding dinoflagellates as a functional group, specific dinoflagellate genera and in some cases even individual dinoflagellate species are available. CPR dinoflagellate data has previously been used to assess the frequency of Harmful Algal Blooms (HABs) in the North Sea (Edwards et al., 2006), to show evidence of climate warming signals throughout plankton communities (Edwards and Richardson, 2004) and in the parameterisation of ecological models (Allen et al., 2001).

This chapter uses data from the CPR survey to analyse the composition and relative seasonal variation of the dinoflagellate community in the waters surrounding the PAP observatory. Analysis is focused on examining seasonal changes in the abundance of bioluminescent dinoflagellates and how these changes are related to those observed in the total dinoflagellate community. The study aims to gain a clearer understanding of how bioluminescent dinoflagellates, and thus stimutable bioluminescent intensity itself, may vary over a typical seasonal cycle. The analysis also aims to explore whether the association found between stimulated bioluminescent intensity and dinoflagellate abundance in the Mediterranean and elsewhere may also apply to the oceanic waters surrounding the PAP observatory.

3.2 Methods

3.2.1 CPR Sampling

Continuous Plankton Recorders are towed behind a large number of ships of opportunity along a number of standard routes on a monthly basis (Richardson et al., 2006). Each ship has a set length of wire which has been specifically calculated to ensure that the CPR is towed at a depth of ~ 7 m. During a tow, water enters the CPR through a 1.27 cm aperture at the front of the instrument (**Figure 3.1**). The water is then filtered through a strip of 270 μm mesh silk and exits through the rear of the instrument. Movement of the CPR through the water causes a propeller on the outside to rotate, which in turn, rotates a gear system that pulls the silk across the width of the inlet at a known rate. At the far side of the opening the filter silk meets a second strip of silk that lies on top of, and sandwiches, the filtered plankton. Both silks are then wound on to a single spool and stored in a tank containing a 4% formaldehyde solution for preservation. Full details on the sampling mechanisms and analytical procedures of CPR's are given in Warner and Hays (1994) and Batten et al. (2003).

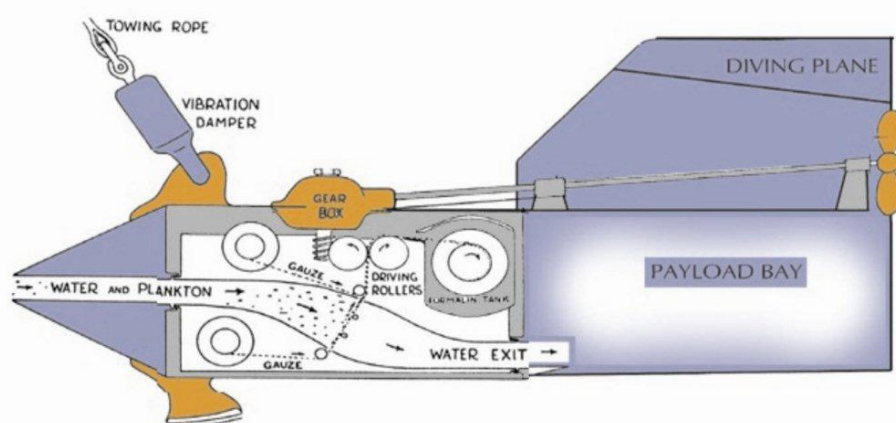


Figure 3.1: Continuous Plankton Recorder schematic (courtesy of David Johns at SAHFOS).

Once a tow is complete the CPR is sent back to the Sir Alister Hardy Foundation for Ocean Science (SAHFOS), Plymouth, where the silk samples are removed and undergo analysis. The samples are cut into segments representative of 10 nautical miles of tow (approximately 3 m³ of filtered sea water) and the mid-point position and local time is calculated for each sample. Phytoplankton counts are then made through the analysis of each sample under $\times 450$ magnification. Twenty fields of view (10 running across each diagonal of each silk segment), corresponding to 0.001% of the total area of the silk, are counted. The taxa present in each field of view are recorded in a manner similar to a present-absence classification. Depending on how many fields of view taxa have been recorded within, they are given a pre-defined value which is calculated to be representative of their total abundance on the filtering silk. The accepted abundance values are derived from a Poisson distribution as set out in Colebrook (1960). A full

description of the CPR survey sample processing methodology can be found in Richardson et al. (2006).

Although the mesh size of the filtering silk, at 270 μm , is relatively large, in comparison to the size of many phytoplankton species, phytoplankton as small as 10 μm are regularly retained. However, it is likely that all phytoplankton, particularly very small organisms such as coccolithophores, are under sampled (Hays et al., 1995; Richardson et al., 2006). Despite this, the CPR captures a consistent fraction of the in situ population of each taxon and the proportion of the population retained is known to reflect the major changes in abundance, distribution and composition even for very small-celled species (Robinson, 1970). Therefore, the CPR survey provides robust semi-quantitative data which can be used to investigate relative temporal or spatial changes (rather than absolute changes) in abundance or composition on seasonal or longer time scales.

The CPR survey counts 189 species of dinoflagellates with cell sizes ranging from 20 – 1200 μm , all of which are thought to be captured equally well by the silk mesh (Johns, pers comms). The range of cell sizes captured by the CPR compares well with the typical size range of dinoflagellate species which is between 10 and 100 μm , although extreme ranges can be between 2 and 2000 μm . Unfortunately, the survey is unable to count many dinoflagellate cells without a theca (unarmoured; **Section 1.6**) as these cells do not stay intact throughout the sampling and preservation process.

3.2.2 CPR Data

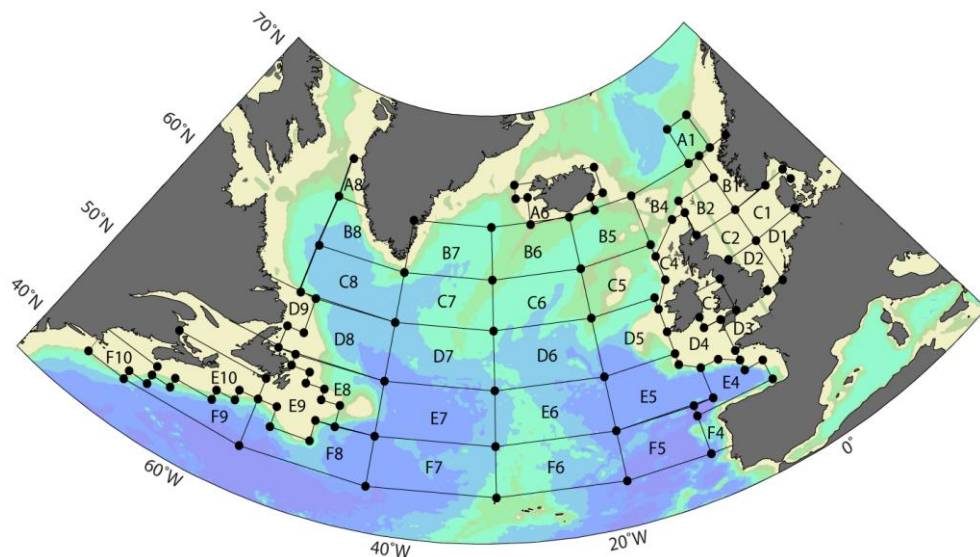


Figure 3.2: Map of CPR standard areas across the North Atlantic

Due to changes in shipping routes over time and space it is commonplace to average CPR phytoplankton abundances temporally into monthly values and spatially across a predefined area of interest (Richardson et al., 2006). The CPR survey divides its coverage of the North Atlantic into a number of standard areas (**Figure 3.2**). These areas are chosen to ensure areas are well sampled and to minimise the number of hydrodynamic regimes crossed (Richardson et al., 2006).

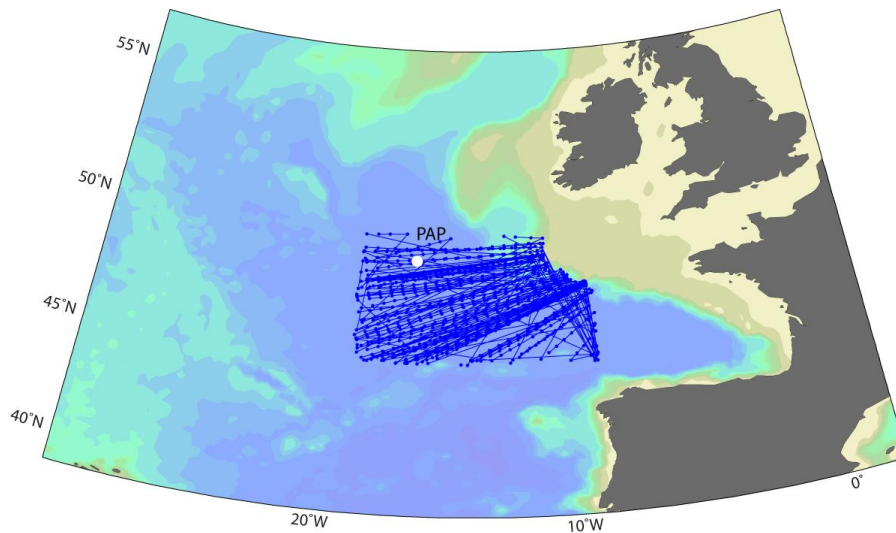


Figure 3.3: Location of CPR tows and abundance samples taken within the E5 region between January 2001 and December 2007.

Data from CPR standard area E5 were chosen for analysis as this includes the PAP observatory and surrounding waters. The E5 region is bounded by the coordinates 50°N, 19°W; 50°N, 11°W; 49°N, 11°W; 48°N, 9°W; 45°N, 9°W; 45°N, 19°W (**Figure 3.2**). For this study dinoflagellate data for the E5 region between the years 2001 and 2007 were obtained from SAHFOS. Data extracted comprised 1239 silk segments taken on over 100 tows (**Figure 3.3**). The number of silks available in each of the seven years ranged between 138 and 212. Data from this time period were chosen for analysis for several reasons. Each of these years was sampled in eight or more months and no month was systematically unsampled. CPR data prior to 2000 contains a signal of environmental regime shift that occurred in the North Atlantic during the late 1980's and late 1990's (Reid et al., 2001). The influence of these events could complicate the interpretation of this study's results and consequently the data is restricted in time to avoid this issue.

3.2.3 Interannual and Seasonal Variation of the Dinoflagellate Community

Although many unarmoured dinoflagellates are not sampled by the CPR (**Section 3.2.1**), for the purpose of simplicity any reference to the total number of dinoflagellates sampled will be termed "total dinoflagellate" abundance or community from here on. The limitations of the CPR dataset will be discussed in **Section 3.4**. For analysis of the total dinoflagellate community, all dinoflagellate genera or species identified by the CPR (excluding dinoflagellate cysts) were summed to provide a total abundance of dinoflagellates per sample. Data were then $\log_{10}(x+1)$ transformed to ensure an approximate normal distribution and averaged for each month of each year following the methodology set out in Head and Pepin (2010).

Interannual changes in the timing of the seasonal peak in dinoflagellate abundance were estimated as in Edwards and Richardson (2004). The seasonal peak throughout an entire growing period (the central tendency, T) was calculated as

$$T = \frac{\sum_{j=1}^{12} M_j \cdot x_{ij}}{\sum_{j=1}^{12} x_{ij}} \quad \text{Eq. 3.1}$$

where x_{ij} is the average abundance in month j in year i , M is equal to the number of month j where January = 1, ..., December = 12 and T is the decimal month of the seasonal peak. Regression analysis was used to test whether there was a statistically significant trend in the timing of the seasonal peak over the 2001 to 2007 period.

To investigate the seasonal cycle over a typical year between 2001 and 2007, climatological monthly averages were calculated using **Equation 3.2** (Cochran, 1977).

$$\bar{x}_j = \frac{\sum_{i=1}^n w_{ij} x_{ij}}{\sum_{i=1}^n w_{ij}} \quad \text{Eq. 3.2}$$

where x_{ij} is the average abundance for month j for year i and w_{ij} is the number of samples used to calculate x_{ij} .

A weighted average, using the number of samples in each month as weights, was calculated to better represent the seasonal pattern over the seven year period. The weightings ensured that years with a high sampling frequency were given a larger influence on the average than those with a low sampling frequency.

3.2.4 Dinoflagellate Community Composition

To study the dinoflagellate community composition the same transformation and averaging procedures to produce monthly climatologies, as previously described in **Section 3.2.3**, were applied to individual genus or species data. The typical percentage contribution of each genus or species to the dinoflagellate community in each month over the 2001 to 2007 period was then analysed.

The nutritional strategies of different genera or species were identified from the literature. For analysis of the seasonal variation in dinoflagellate groups with different nutritional strategies, species or genera of the same nutritional preference (photoautotrophic, mixotrophic or heterotrophic) were summed for each sample. These summed data were transformed and averaged as described in **Section 3.2.3** to produce monthly climatologies which showed the seasonal pattern of each nutritional strategy over a typical year.

To examine how the seasonal pattern of the different nutritional strategies compared to one another and to that of the total dinoflagellates sampled, monthly climatologies were normalised to a zero mean z-score following **Equation 3.3** (Cheadel et al., 2003).

$$Z_j = \frac{\bar{x}_j - \mu}{\sigma_\mu} \quad \text{Eq. 3.3}$$

where \bar{x}_j is the average value for month j , μ is the average of all months over the year and σ_μ is the standard deviation associated with μ . The standardisation of monthly climatological averages to z-scores allows for the relative temporal changes in abundance, rather than absolute changes, to be focused upon and thus permits the differences in seasonal pattern between groups to be seen more clearly. A z-score which has a positive value indicates a monthly abundance that is greater than the annual average whereas, a negative z-score indicates a monthly abundance that is less than the annual average. A z-score value of ± 1 is equivalent to a change in abundance which is ± 1 standard deviation from the annual average. Uncertainty estimates related to the CPR monthly climatology data and their corresponding z-scores is looked at in detail in **Chapter 4**.

3.2.5 Bioluminescent Dinoflagellate Variability and Composition

For analysis of the bioluminescent dinoflagellate community, bioluminescent genera or species were identified as in **Chapter 2**. Bioluminescent genera and species were summed to produce a total number of bioluminescent cells per sample. These data

were then transformed and averaged following the methodology described in **Section 3.2.3**. The relative seasonal variation of the summed bioluminescent dinoflagellates was compared to that of the total dinoflagellate community. This was done through the standardisation of data as z-scores following **Equation 3.3**. The variations over a typical seasonal cycle were analysed.

To investigate whether there was a significant relationship between the monthly abundance of bioluminescent dinoflagellates and the abundance of the total dinoflagellate community, a Spearman rank analysis, for use on non-parametric data, was carried out. The same analysis was also performed on the climatologically averaged data. However, the climatological data were found to be normally distributed, thus instead of a Spearman rank correlation a Pearsons correlation, for use on normally distributed data, was used. Correlation analyses were also conducted to investigate whether any correlations between the total dinoflagellate community and the summed bioluminescent community held true for each individual bioluminescent dinoflagellate type.

Approximate light budgets were calculated as in **Section 2.4** to give an indication of the potential percentage contribution of each bioluminescent genera or species to the bioluminescent field over the typical year. *Gonyaulax* spp. and *Ceratium fusus* were, as in **Chapter 2**, assumed to have flash intensities of 1×10^8 photons s^{-1} whilst *Protoperdinium* spp. were assumed to flash at an intensity of 1×10^9 photons s^{-1} (Swift et al., 1995). An estimation of the total potential bioluminescent intensity per m^{-3} in each month was calculated by summing the bioluminescent potential for each bioluminescent genera and species. The relative seasonal variation of the potential bioluminescent intensity was compared to that of the seasonal variation in the total dinoflagellate community by standardising the data as z-scores.

All statistical analyses within this chapter were performed in Sigma Plot 11.0 and statistical significance was considered at the $p < .05$ level. Figures illustrating 7 year time series data and typical seasonal cycles from monthly climatological averages show monthly data points linked by a spline interpolated line. A spline interpolated line was used to visualise the smoothed interannual and seasonal changes in abundance but these interpolations were not used in any quantitative analyses.

3.3 Results

3.3.1 Interannual and Seasonal Variation of the Dinoflagellate Community

Monthly total dinoflagellate abundances, between 2001 and 2007, show that there are interannual variations in the magnitude of peak abundance (**Figure 3.4**). However, there is no evidence to suggest an increasing or decreasing trend in the abundance of dinoflagellates over that period. The year 2001 was a particularly successful one for dinoflagellates as this year has the seasonal peak with the largest magnitude in abundance.

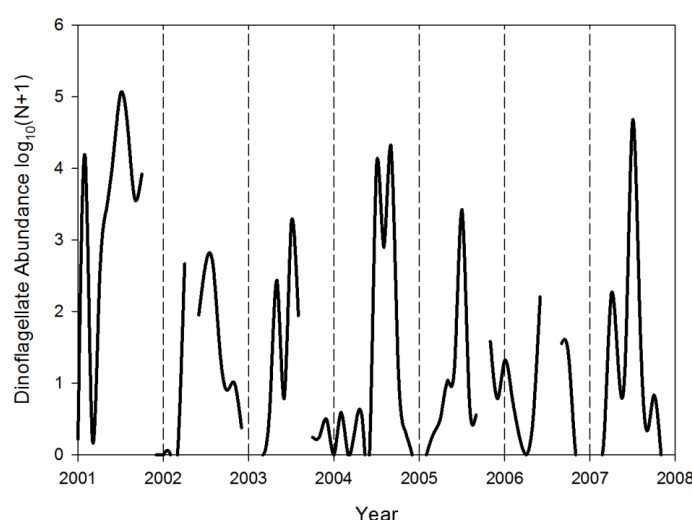


Figure 3.4: Interpolated monthly abundance of total dinoflagellates sampled between January 2001 and December 2007.

The seasonal peak in dinoflagellate abundance in the years 2001 to 2007 is shown to consistently occur from late June to July (**Figure 3.5**). Regression analysis indicates that there is no significant increase or decrease in the timing of peak dinoflagellate abundance throughout the 2001 to 2007 period ($r^2 = 0.01$, $p > 0.82$).

The results presented in **Figures 3.4** and **3.5** indicate that averaging data over the 7 year period (2001 – 2007) does not produce climatologies that are substantially biased by any large anomalies or trends within the multi-year data. The monthly climatological averages and the smoothed seasonal pattern in dinoflagellate abundance over the 2001 to 2007 period are shown in **Figure 3.6**. Monthly climatologies indicate that the abundance of dinoflagellates surrounding the PAP observatory is elevated between early spring to late autumn. The results also show that although abundance initially increases in April, there is only a marginal increase in May. It is not until July that dinoflagellates substantially increase in abundance and a

prominent peak is observed. This peak in abundance is short lived, declining during August and returning to pre-July levels by September/October before declining further over winter (November to March).

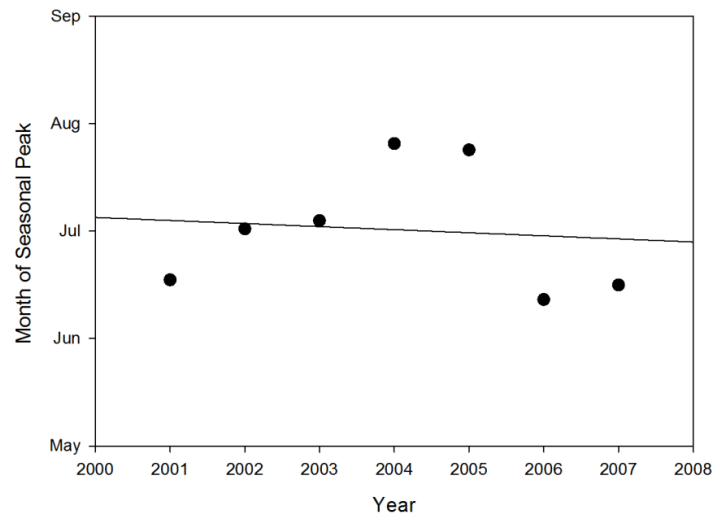


Figure 3.5: Month of seasonal peak dinoflagellate abundance in 2001 through to 2007. Solid line indicates regression through data indicating there is no significant change in timing over the 7 year period.

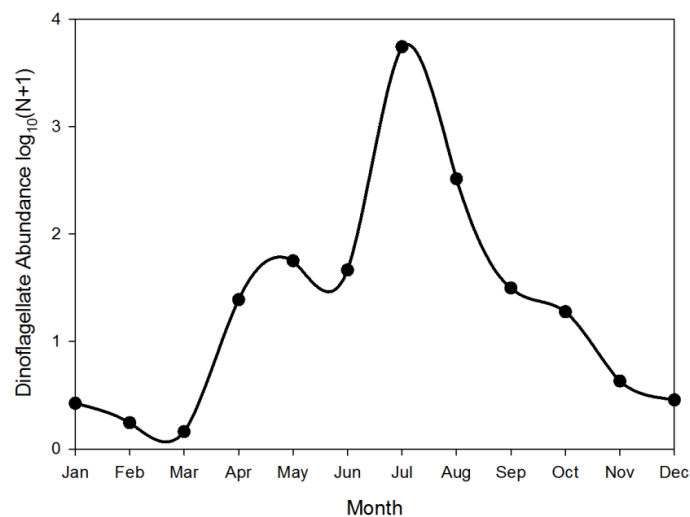


Figure 3.6: Monthly climatological averages of total dinoflagellates sampled, indicating the typical seasonal variation in dinoflagellate abundance between 2001 and 2007.

3.3.2 Dinoflagellate Community Composition

The relative contribution of each of the sampled dinoflagellate genus or species to the dinoflagellate community in a typical year between 2001 and 2007 is shown in **Figure**

3.7. Dinoflagellates from the genus *Ceratium* are seen to be extremely prevalent in the dataset. This genus dominates the CPR dinoflagellate record in all months and accounts for all cells sampled in both February and December. *Ceratium* spp., as a percentage of total dinoflagellates decrease in the summer months of June, July and August to just over 50%. Diversity in the number of genera and species within the data increases over the summer months and reaches a maximum in September. Other notable members of the dinoflagellate community during the summer months are *Prorocentrum* spp. ('*Exuviaella*' type), *Gonyaulax* spp., *Proto-peridinium* spp. and *Oxytoxum* spp.

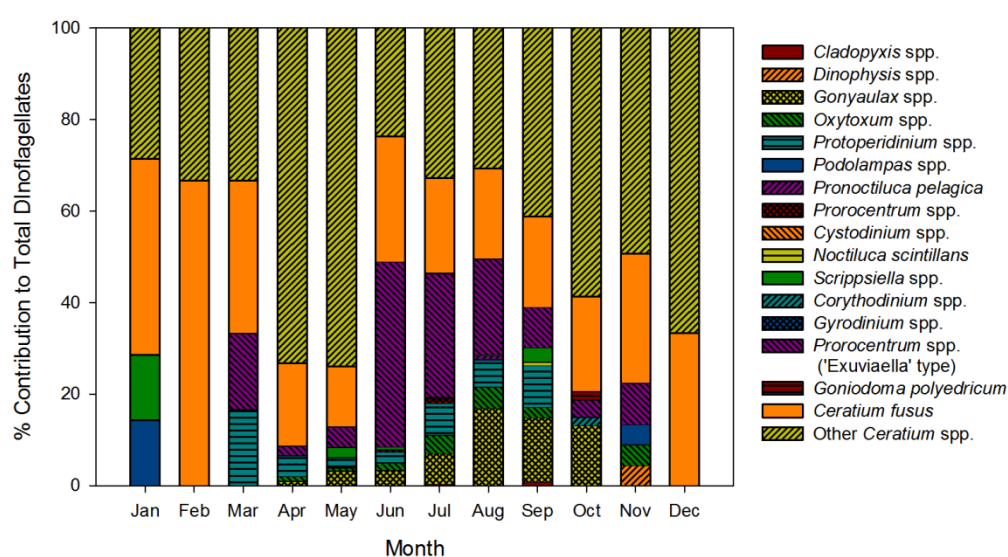


Figure 3.7: Relative contributions of individual dinoflagellate genus or species to the total dinoflagellate community sampled for the averaged typical year between 2001 and 2007.

All dinoflagellate genera were classified into a nutritional strategy grouping (photoautotroph, mixotroph or heterotroph) using information from the literature (**Appendix B, Table B.1**). Of the 15 dinoflagellate genera or species within the data, five are classified as photoautotrophs, 3 are classified as heterotrophs and 7 are classed as mixotrophs. On average, over a typical year, 93% of the dinoflagellate population by number are mixotrophic. Photoautotrophs and heterotrophs each make up less than 5% of the total dinoflagellate abundance. Within the monthly climatologies, between 85 and 100% of the mixotrophic grouping is comprised of genera whose species are considered primarily photosynthetic or known to contain permanent chloroplasts; these are *Ceratium* spp., *Prorocentrum* spp., *Scrippsiella* spp. and *Gonyaulax* spp.. These results indicate that over a typical year >85% of the dinoflagellates sampled were primarily photoautotrophic.

The seasonal pattern of photoautotrophs, mixotrophs, heterotrophs, and the total dinoflagellate community are presented in **Figure 3.8**. All nutritional strategies are found to peak in abundance in July. The seasonal variation in mixotrophs shows that organisms with this nutritional strategy increase their abundance above the annual average earlier in the year (April) than those of the solely heterotrophic or photoautotrophic dinoflagellates (June). The relative increase in photoautotrophic dinoflagellates into the peak month of July is marginally greater than that of mixotrophs and heterotrophs. The data show that heterotrophic dinoflagellates decrease in abundance more slowly than that of photoautotrophs and mixotrophs from August to September. Overall, however, all three nutritional strategies are extremely similar in their seasonal variations. The seasonal variation in mixotrophs very closely follows that of the dinoflagellate community as a whole, which is unsurprising given the large proportion of mixotrophs within the data. The seasonal patterns of autotrophs and heterotrophs do not vary considerably from each other and both broadly follow the same seasonal pattern, in terms of when peak abundance occurs, as the total dinoflagellate community.

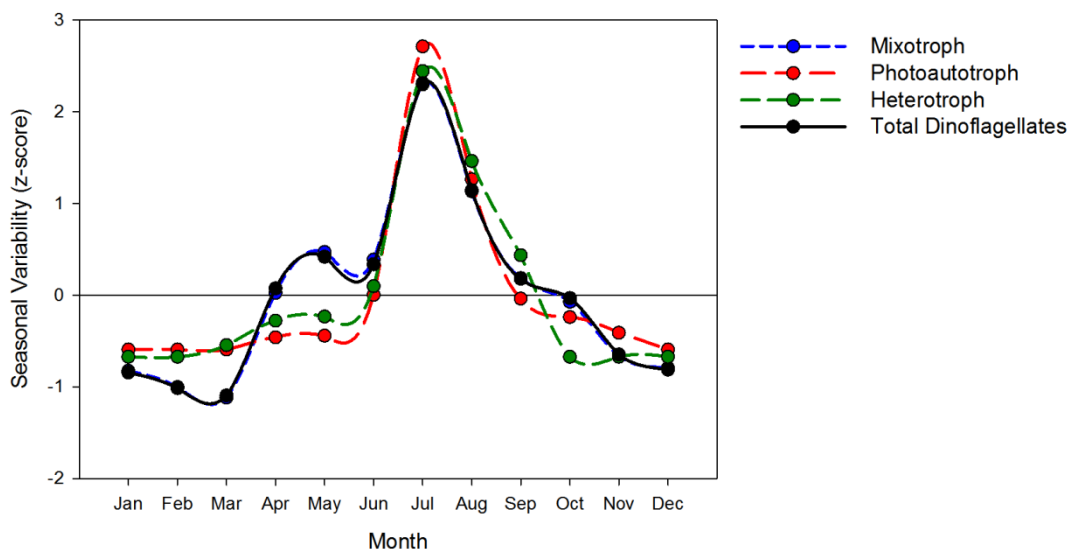


Figure 3.8: The seasonal variations of dinoflagellates with different nutritional strategies compared to the seasonal variation of the total dinoflagellate community within a typical year (2001 – 2007). Solid black line at zero indicates the annual average abundance.

3.3.3 Bioluminescent Dinoflagellate Variability and Composition

Several dinoflagellate genera and species which are known to be bioluminescent are present in the data. These are *Ceratium fusus*, *Noctiluca scintillans*, *Gonyaulax* spp., and *Protoperdinium* spp.. *Noctiluca scintillans* were not taken forward for analysis as it was found these cells were only present in one of the 1239 samples from the seven

year CPR time series. Thus, it was judged that their presence in the data was anomalous and could not be taken into account in the analysis.

Climatologically averaged data show that bioluminescent dinoflagellates represent between 19% (May) and 67% (February) of the dinoflagellate population throughout a typical year (**Figure 3.9**). On average 37% of the dinoflagellate community is made up of cells from bioluminescent species or genera. Bioluminescent dinoflagellates decrease as a percentage of the dinoflagellate community in spring (April and May) before their percentage contribution increases and stays relatively constant (a variation of <15%) over the summer, autumn and into the winter months (June to January). The months of February and March are notable for an increased percentage contribution of bioluminescent dinoflagellates to the dinoflagellate community.

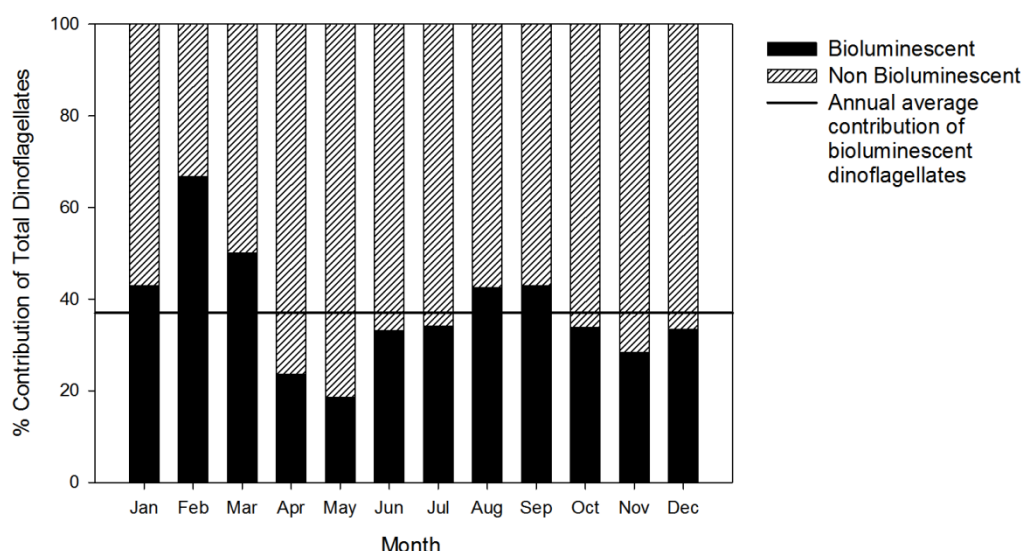


Figure 3.9: Percentage contribution of bioluminescent dinoflagellates to the total dinoflagellate community within a typical year (2001– 2007).

The seasonal variation in abundance of bioluminescent dinoflagellates over a typical year broadly mirrors that of the total dinoflagellate community (**Figure 3.10**). The seasonal changes in the two groups are particularly close from June to December. The greatest difference between the two seasonal patterns occurs in spring (April and May) where data indicates that the bioluminescent dinoflagellate community increases its abundance above the annual average slower than the total dinoflagellate community.

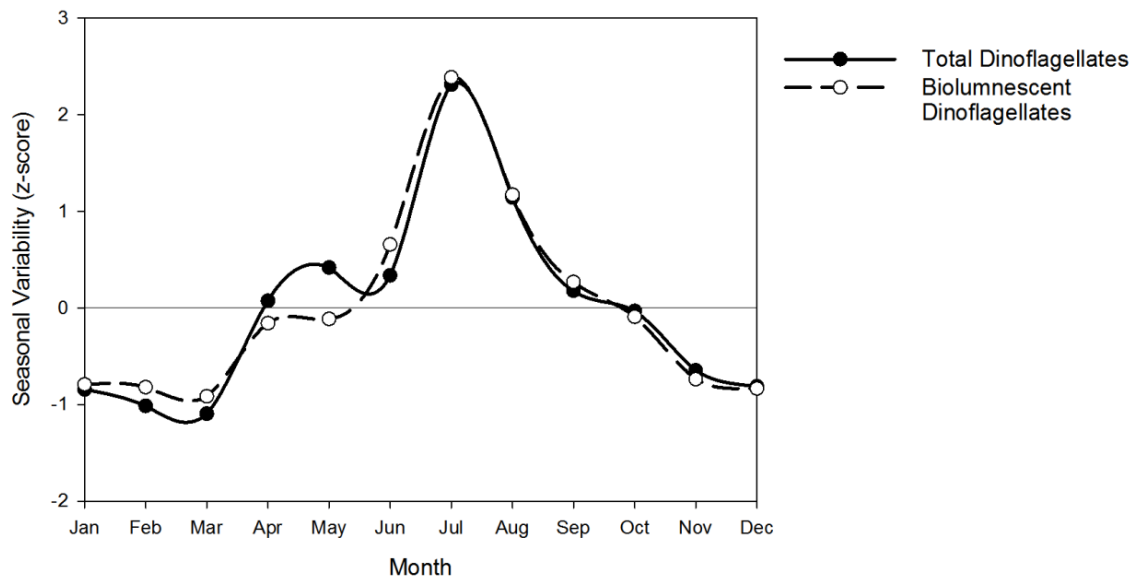


Figure 3.10: Comparison of the seasonal variation of bioluminescent dinoflagellates and that of the total dinoflagellate community within a typical year (2001 – 2007). Solid black line at zero indicates the annual average abundance.

Statistical analysis reveals a significant correlation ($r_p = .976$; $p < .0001$; $n = 12$) between summed bioluminescent dinoflagellates and the total dinoflagellate community in the monthly climatological data. A significant correlation was also present over the 7 year time series (Figure 3.11) ($r_s = .848$; $p < .0001$; $n = 75$).

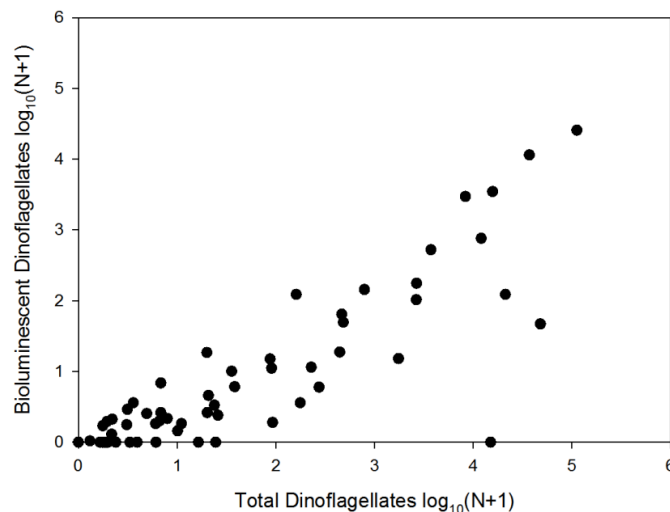


Figure 3.11: Correlation between abundance of bioluminescent dinoflagellates and total dinoflagellates over the 7 year time series between 2001 and 2007.

A more detailed analysis of the bioluminescent community shows that *Ceratium fusus* tends to dominate the bioluminescent community particularly in winter months

(November – February) where it accounts for 100% of the bioluminescent cells captured by the CPR (**Figure 3.12**). *C. fusus* is seen to have the lowest relative contribution to the bioluminescent community in August and September. In these months *Gonyaulax* and *Protoperidinium* species make up over 50% of bioluminescent cells. It is also noteworthy that *Protoperidinium* spp. account for approximately one third of the bioluminescent cells in March when *Gonyaulax* spp. are not present. This pattern is reversed in October when approximately 40% of the bioluminescent community are *Gonyaulax* spp. and there are no *Protoperidinium* cells.

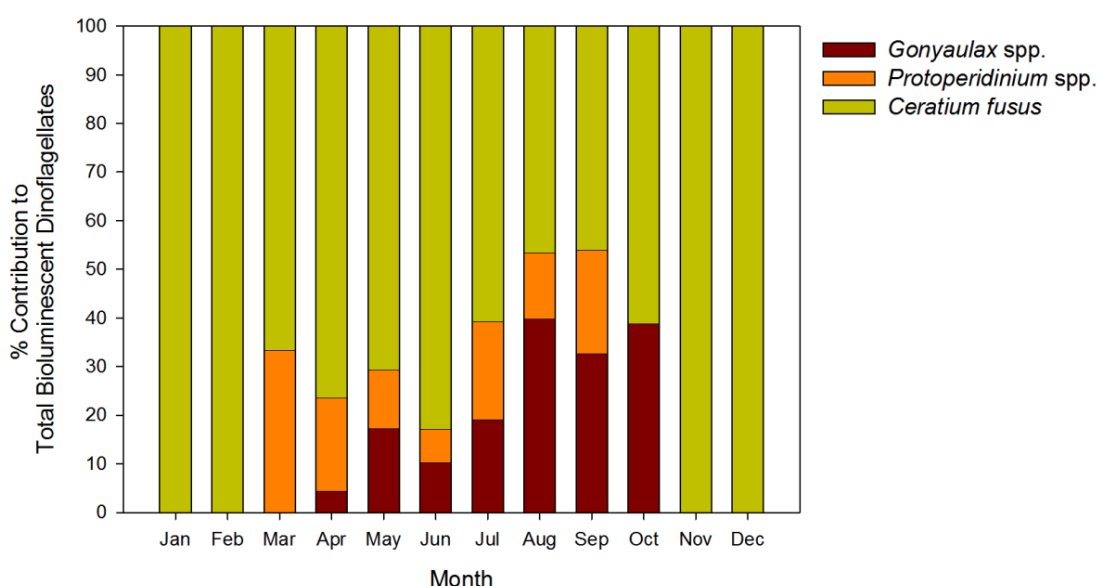


Figure 3.12: Percentage contribution of genera or species to the total bioluminescent community over a typical year (2001 – 2007).

Comparing seasonal variations in abundance indicates that *C. fusus* and *Protoperidinium* spp. have very similar seasonal patterns over the typical year (**Figure 3.13**). The seasonal pattern of the genus *Gonyaulax* stands out from that of *C. fusus* and *Protoperidinium* spp. as peak abundance occurs in August rather than July. *Gonyaulax* spp. are also shown to have a relatively smaller increase in abundance over the summer months but that they maintain a higher than annual average abundance until October, longer than *C. fusus* and *Protoperidinium* spp. whose abundance drops below the annual mean in September.

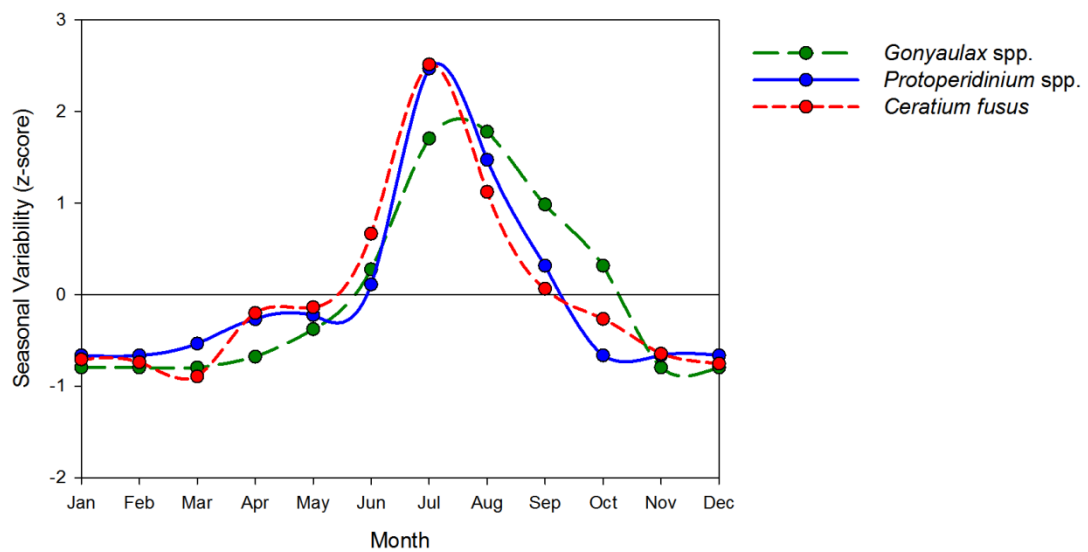


Figure 3.13: Inter-comparison of the seasonal variation of bioluminescent species and genera within a typical year (2001–2007). Solid black line at zero indicates the annual average abundance.

Significant correlations were found between each bioluminescent genus or species and the total dinoflagellate community within the full 7 year time series and the monthly climatological data (**Table 3.1**). This indicates that the association between bioluminescent dinoflagellates and the total dinoflagellate abundance holds for each individual bioluminescent genus or species in the data. This also confirms that the correlation shown in **Figure 3.11** is not being driven by the presence of only one bioluminescent genus or species.

Table 3.1: Results of spearman rank-order correlation analyses and Pearson correlation analyses between individual bioluminescent genus or species and the total dinoflagellate community respectively. Correlation coefficients are shown. ** denotes a significant result at the $p < .05$ level.

Genus/Species	Monthly Averages	Monthly Climatological Averages
	$n = 75$	$n = 12$
<i>Gonyaulax</i> spp.	.603**	.868**
<i>Ceratium fusus</i>	.819**	.966**
<i>Protoperidinium</i> spp.	.524**	.926**

Calculation of light budgets for individual bioluminescent genera or species indicates that *Protoperidinium* spp. are responsible for between 42% and 83% of the potentially stimulated bioluminescence from March through to September (**Figure 3.14**). This result is despite *Ceratium fusus* being the most abundant bioluminescent species in these months (**Figure 3.12**). *Ceratium fusus* is seen to dominate the dinoflagellate potentially stimulated bioluminescence in November to February since no other

bioluminescent genera were captured by the CPR survey. *Gonyaulax* spp. are seen to contribute between 2% and 39% to the dinoflagellate potentially stimulated bioluminescence between April and October when they were present.

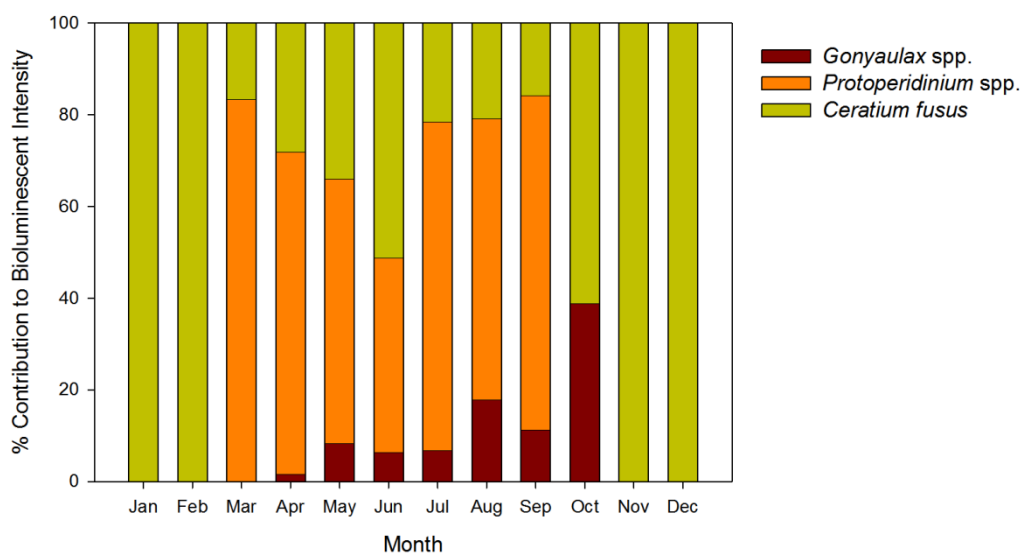


Figure 3.14: Percentage contribution of genera or species to the estimated bioluminescent field over a typical year (2001 – 2007).

An estimate of the potential bioluminescent intensity associated with the dinoflagellate population in each month was calculated to indicate how the potential for stimulated bioluminescent intensity varied seasonally. This seasonal variation was compared to the seasonal variations in total dinoflagellate abundance (**Figure 3.15**). Peak potential bioluminescent intensity coincides with peak total dinoflagellate abundance. As with the seasonal pattern in bioluminescent dinoflagellates, the potential bioluminescent intensity deviates from the seasonal pattern of the total dinoflagellate community in spring (April and May). **Figure 3.15** also indicates that although dinoflagellate abundance remains at a level approximately equal to the annual average from September to October, potential bioluminescent intensity decreases in October to a level below its annual average. This is in contrast to the seasonal variation of bioluminescent dinoflagellate abundance which follows the seasonal variation in total dinoflagellates abundance closely (**Figure 3.10**). In general, the seasonal pattern of potential bioluminescent intensity lies close to that of the total dinoflagellate abundance.

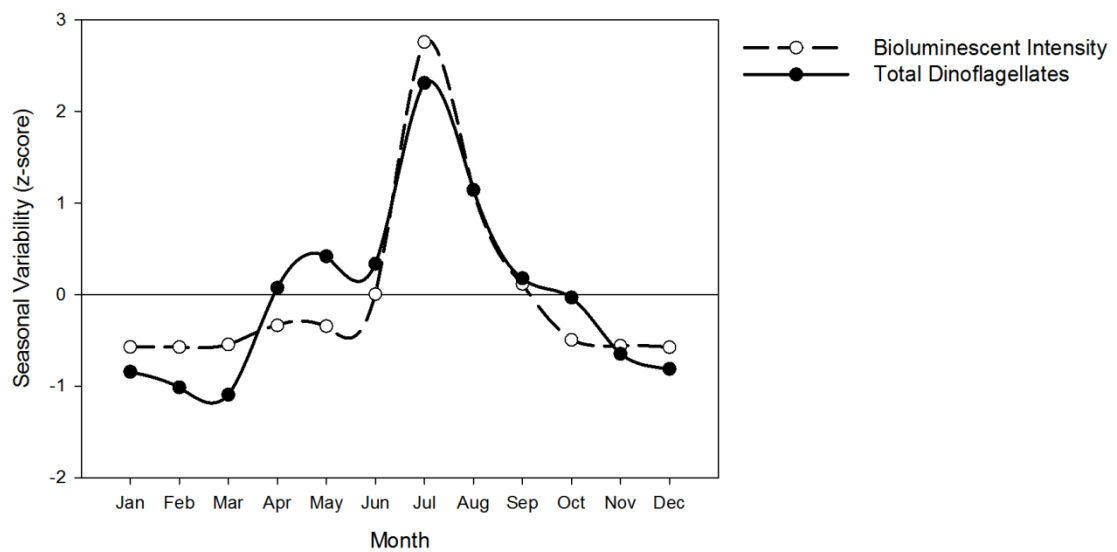


Figure 3.15: Intercomparison of the seasonal variability of bioluminescent intensity with total dinoflagellate abundance within a typical year (2001 – 2007). Solid line at zero indicates the annual average value.

3.4 Discussion

3.4.1 Interannual and Seasonal Variation of the Dinoflagellate Community

The dinoflagellate community within the waters surrounding the PAP observatory has been examined using data collected by the CPR survey between 2001 and 2007. The year 2001 was found to be particularly successful for dinoflagellates, showing the largest peak in abundance over the seven year time series. Lampitt et al. (2010) found that this year at the PAP observatory was characterised by an early shoaling of the mixed layer (mid February), the highest spring (April) peak in chlorophyll ever recorded for the site and high particle flux during late summer. It is beyond the focus of this study to investigate the linkages between these findings. However, taken together they indicate that 2001 may have been a somewhat unusually productive year for this region.

Despite the indication that 2001 was an unusually productive year, no significant trend in abundance was found over the seven year time series or in the timing of peak abundance. Therefore, there was no evidence to suggest that the data from 2001 biased the calculated climatological averages used to analyse the typical seasonal variations in the dinoflagellate community and the data from this year was retained in the analysis.

Examination of the average seasonal pattern between 2001 and 2007 indicates that peak dinoflagellate community abundance occurs in July, supporting the hypothesis that dinoflagellates succeed in the stratified waters of summer and agreeing with findings from previous studies in the region (Leterme et al., 2005; Smythe-Wright et al., 2010). The genus *Ceratium* was found to dominate the sampled dinoflagellate community, particularly in the winter months when many other genera were not present in the samples. This is in accord with studies of the armoured dinoflagellate community, independent of the CPR, which have also shown *Ceratium* spp. to be the dominant dinoflagellate genus within the region (Dodge, 1993).

3.4.2 Dinoflagellate Community Composition

Seven out of the 15 dinoflagellate taxonomic groupings present in the CPR data were identified as mixotrophic, and mixotrophs made up 93% of dinoflagellates on average over a typical year in the 2001 to 2007 period by number. Of the dinoflagellates classified as mixotrophic the majority are known to demonstrate Type II mixotrophy (Stoecker, 1998), in that they are primarily photosynthetic with the ability to use phagotrophy (feeding by ingesting prey) (**Table B.1**). The data indicates only slight differences between the seasonal patterns of the three nutritional strategies (mixotrophy, photoautotrophy and heterotrophy) and all reached peak abundance in July. Interestingly, heterotrophs did not increase above their annual average abundance until June. This may suggest that the success of heterotrophic dinoflagellates is not coupled with the diatom spring bloom, as zooplankton are thought to be, but instead with the occurrence of other dinoflagellates that occur post spring diatom bloom. It is known that heterotrophic dinoflagellates can survive by feeding upon other dinoflagellate species and under some circumstances turn to cannibalism (Nakamura et al., 1995; Jeong et al., 1997; Jeong, 1999).

A limitation of the CPR data that must be addressed is that unarmoured dinoflagellates are either significantly under-represented or not counted, because cells do not stay intact within the formaldehyde solution used to preserve samples. Therefore, it must be kept in mind that results are biased towards the armoured dinoflagellate population. Despite this bias, the CPR survey is unparalleled in its spatial and temporal coverage and has been used by many to give great insight into the variability of the dinoflagellate community across the North Atlantic (Edwards and Richardson, 2004; Leterme et al., 2005; A&mus et al., 2008).

3.4.3 Bioluminescent Dinoflagellate Variability and Composition

The primary aim of this chapter was to investigate the composition and seasonal variation of the bioluminescent dinoflagellate community and to examine how these changes are related to changes observed in the total dinoflagellate community. Data indicated that bioluminescent dinoflagellates represented, on average, 37% of the total dinoflagellate community over a typical year and that from June through to January the bioluminescent fraction of the dinoflagellate community stayed relatively constant. The typical seasonal pattern of the bioluminescent dinoflagellate community was found to broadly mirror that of the total dinoflagellate community and a strong positive correlation was found between their abundances. This positive correlation was seen to hold even if viewed as a 7 year time series. These results imply that for the waters surrounding the PAP observatory, the seasonal variations of the total dinoflagellate community can be used as a proxy for those of the bioluminescent dinoflagellate population. Since previous studies have shown strong correlations between the abundance of bioluminescent dinoflagellates and the number of stimulated flashes (Kelly, 1968; Tett, 1971), it might also be assumed that total dinoflagellate abundance can be an indicator for the number of bioluminescent flashes potentially stimulated in the environment.

A breakdown of the bioluminescent community indicated that *Ceratium fusus* dominated abundance in all months but August and September. *Protoperidinium* spp. were found to have their largest contribution to the bioluminescent population in spring (March – April) whereas *Gonyaulax* spp. had their largest contribution in late summer and autumn (August – October). These results are in contrast to those found at the PAP site in late July and early August 2009 (**Chapter 2**) where cells of *C. fusus* accounted for ~10% of the bioluminescent community and *Gonyaulax* spp. dominated in terms of cell abundance. However, the results from the CPR data are in agreement with those found in **Chapter 2** in that they indicate primarily photosynthetic species dominate the summer bioluminescent community, in terms of abundance. The abundance of each of the bioluminescent genus and species individually was significantly correlated with that of the total dinoflagellate community over both the average year and the entire 7 year time series. Although the correlation between some individual bioluminescent genera or species and the total dinoflagellate abundance were weaker than others, this result nevertheless increases confidence in the correlation observed for the total bioluminescent dinoflagellate population as it suggests that it was not solely due to one dominant genus or species.

The calculation of light budgets for the individual bioluminescent genera or species indicated that, although *Ceratium fusus* was the most abundant, *Protoperidinium* spp.

were responsible for the majority of the potentially stimulated bioluminescence (42% to 83%) within the PAP region from March to September. These findings are in agreement with those of Swift et al. (1995) which showed that, within the North Atlantic at 59° N, 21° W, heterotrophic *Protoperdinium* spp. typically accounted for the majority of bioluminescent potential throughout spring, summer and autumn. Swift et al. (1995) also found that photosynthetic *Ceratium fusus* and *Gonyaulax* spp. increased their contribution to the bioluminescent field during late summer and autumn due to increased abundance. However, the CPR data indicate that surrounding the PAP observatory, photosynthetic species increase their contribution to the bioluminescent field in mid-summer (May and June) and autumn (post September). *Ceratium fusus* were shown to contribute 100% to the bioluminescent field from November to February due to no other bioluminescent species being recorded. However, it should be remembered that zero abundance in the CPR survey does not indicate other species were not present, only that their abundance was not high enough for them to show up in the survey. Thus, it is likely that other bioluminescent genera also contribute to the bioluminescent field in these months. This is particularly true for smaller or unarmoured species which are not retained intact on the CPR mesh. It should be noted however, that the majority of species listed as bioluminescent in **Table A.1** are relatively large armoured cells and therefore are likely to be seen in the CPR data.

The light budgets calculated using the CPR data for the months of July and August are in contrast to those calculated using microscopy count data in **Chapter 2** at the end of July and beginning of August 2009. *Gonyaulax* spp. were found to contribute between 25% and 61% to the bioluminescent field in the waters surrounding the PAP observatory. This is in contrast to the CPR data which showed *Gonyaulax* spp. contributed between just 7% and 18% to the average bioluminescent field in the same months. The contribution made by *Ceratium fusus* to the bioluminescent field calculated using the CPR data was also found to be more than double (~ 20%) the percentage calculated in the 2009 data (~7%). The contrast in the percentage contribution to the bioluminescent field is unsurprising considering the large disparity between the percentage contributions to abundance, noted earlier. These differences could result from a variety of causes including large spatial and temporal averaging of the CPR data for the purpose of examining broad scale trends. This contrasts with the data in **Chapter 2** which investigates one specific time and location.

This chapter also aimed to explore whether an association between stimulated bioluminescent intensity and dinoflagellate abundance may exist in the region surrounding the PAP observatory. The analysis indicates that the seasonal variability of estimated potential bioluminescent intensity for the sampled population broadly followed the same pattern as the total dinoflagellate abundance (**Figure 3.15**).

Therefore, assuming dinoflagellates dominate the bioluminescent field, the data may indicate that a correlation between stimulated bioluminescent intensity and dinoflagellate abundance exists in the waters surrounding the PAP observatory. This is a result which has also been found in the Mediterranean and Black Sea (Tokarev et al., 1999a) and may suggest that total dinoflagellate abundance could be used as a proxy for stimulated bioluminescent intensity. However there are several considerations, described below, that need to be taken into account before coming to such a conclusion.

As discussed in **Section 2.4**, in the process of classification it is assumed that all cells within a bioluminescent genera or species will luminesce. This is not necessarily accurate. Bioluminescent and non-bioluminescent strains of the same species can exist and it is not possible to know which species are bioluminescent at any particular location without individually isolating and testing them (**Section 1.6**). Thus, there remains a possibility that an increase in abundance of a genera or species classified as bioluminescent will not necessarily increase potentially stimulated bioluminescence.

Different flash intensities are associated with different bioluminescent species. As demonstrated in **Chapter 2**, a small abundance of very bright bioluminescent species, such as *Pyrocystis* spp., can produce more light than a high abundance of comparatively dim species such as *Ceratium fusus*. In this analysis the seasonal pattern of unarmoured *Pyrocystis* spp. could not be confirmed because they are not sampled in the CPR survey. However, if *Pyrocystis* spp. have a different seasonal pattern to the armoured bioluminescent dinoflagellates, a situation could arise where maximum bioluminescent dinoflagellate abundance does not correspond with maximum bioluminescent intensity.

The physiological state of the bioluminescent cells can influence the relationship between bioluminescent intensity and bioluminescent dinoflagellate abundance. Stimulated bioluminescent intensity can be affected by the nutritional state of a cell, particularly in heterotrophic species (Buskey et al., 1994; Latz and Jeong, 1996). Thus, bioluminescent intensity may be considerably reduced towards the end of a bloom when cells become nutritionally stressed even though cell abundance remains high.

The total amount light that can be emitted from a cell under continuous stimulation until exhaustion is known as the cells bioluminescent capacity. In dinoflagellates bioluminescent capacity is approximately proportional to cell size (Buskey et al., 2002). Thus, it could be assumed that a highly significant positive correlation may exist between dinoflagellate biomass and measured stimulated bioluminescent intensity. However, flash intensity itself is not proportional to cell size (Latz et al., 2004a). For

example, under the same level of stimulation the flash intensity of *Gonyaulax* spp. can be twice that of *Ceratium fusus* yet *Gonyaulax* spp. are only half the size (Latz et al., 2004a). This suggests that the correlation between dinoflagellate biomass and stimulated bioluminescent intensity may not be any stronger than that between dinoflagellate abundance and stimulated bioluminescent intensity, unless each cell was being stimulated to exhaustion.

Using the current dataset it is not possible to fully assess the issues raised above. It is only possible to say, at present, that the CPR data indicate a significant association between dinoflagellate abundance and stimulated bioluminescent intensity for the waters surrounding the PAP observatory. However, this relationship could be affected by the composition and physiological state of the bioluminescent community. In future, analysis should be carried out to examine if the relationships between total and bioluminescent dinoflagellate abundance and potentially stimulated bioluminescence found in E5 are consistent with those across other areas of the North Atlantic. This could be achieved through analysing similar CPR data for adjacent standard areas such as E6.

3.5 Summary

Data from the CPR survey have indicated that for the period 2001 to 2007 dinoflagellates in the waters surrounding the PAP observatory are most abundant in the month of July. During a typical year the community was dominated by species from the genus *Ceratium*. Dinoflagellate species which exhibited mixotrophy, heterotrophy and photoautotrophy were all present and closely co-varied over the course of a typical year. Mixotrophs which gained nutrition primarily through photosynthesis dominated the population. The CPR data have also been used to gain insights into the seasonal dynamics of bioluminescent dinoflagellates. A strong correlation exists between the abundance of bioluminescent dinoflagellates and the total dinoflagellate community. These results indicate that the total dinoflagellate abundance can be used as a proxy for the abundance of bioluminescent dinoflagellates and possibly the number of bioluminescent flashes that could be potentially stimulated naturally in the environment. Results also indicate that the seasonal variability in potential bioluminescent intensity broadly follows that of total dinoflagellate abundance which may allow total dinoflagellate abundance to also be used as a proxy for stimulated bioluminescent intensity. However, such an association must be used with care as the composition and physiological state of the bioluminescent community could weaken the strength of any such association.

Chapter 4 will use the findings from this chapter to inform and develop a simple biogeochemical model which can be used to investigate the ecological function of bioluminescence and its impacts upon the wider ecosystem.

Chapter 4: Modelling Dinoflagellates – Model Structure and Data.

4.1 Introduction

Previous modelling studies of bioluminescence have focused upon simulating its distribution over relatively large spatial scales (1000 – 2000 km) or forecasting changes in its spatial distribution on time scales of the order of days. These models have been based upon empirical relationships between bioluminescence and other biogeochemical environmental variables such as chlorophyll (Ondercin et al 1995) or the advancement of the bioluminescent field through advective and diffusive processes (Shulman et al 2010; 2011). As discussed in **Section 1.5**, these models have had limited success in simulating the distribution of the bioluminescence field. The lack of success indicates that the distribution of bioluminescent organisms will not always coincide with that of the phytoplankton dominating the chlorophyll signal or be correlated with physical properties. It is therefore suggested that the ecological and behavioural dynamics of the bioluminescent organisms themselves need to be considered within models for the forecasting of bioluminescence to be improved (Shulman et al., 2011). Field measurements reveal that, although a range of organisms contribute to the bioluminescent field in the upper ocean, dinoflagellates are responsible for the majority of observed bioluminescence (Seliger et al., 1962; Neilson et al., 1995; Latz and Rohr, 2005). Thus, it is appropriate that the inclusion of bioluminescent dinoflagellates into models is prioritised since modelling these organisms will capture a large proportion the bioluminescent field.

Although much has been done over the past century to understand dinoflagellate bioluminescence, there are still many unanswered questions regarding its ecological purpose and potential impact upon the wider ecosystem. For example, although there are several hypotheses regarding how the emission of light could act as a defence/survival strategy (e.g. a burglar alarm or startle response), in situ and laboratory studies have not been able to show conclusively the positive impact that bioluminescence has upon the survival of a bioluminescent individual or a community. If the consideration of the ecological dynamics of the bioluminescent organisms is indeed the next step in improving forecast models of mechanically stimulated bioluminescence, this lack of knowledge may hinder future forecasting attempts.

Accurate modelling of any organism requires specific knowledge regarding their physiological, behavioural and morphological traits. Thus, the development of a model that is able to accurately forecast the temporal and spatial distributions of bioluminescent dinoflagellates requires a clear understanding of several key questions regarding their ability to emit light:

1. What are the ecological benefits of bioluminescence to both the individual and wider phytoplankton community?
2. By what processes might such benefits occur and how might these be modelled?
3. Does bioluminescence enable an ecological niche for these dinoflagellates?

Answers to these questions can be difficult to obtain through in situ observations or laboratory studies. Therefore, the aim of the work presented in the following chapters is to try and address some of these questions through a modelling study. Specifically, the work presented in **Chapter 6** investigates how the ecological function of dinoflagellate bioluminescence as a defence/survival strategy could be modelled given our current knowledge of the mechanisms by which it is hypothesised to occur (**Section 1.6.3**). This is followed by an examination of what impact including the ecological function of bioluminescence may have upon a modelled ecosystem.

Results of the CPR data analysis (**Chapter 3**) indicated that bioluminescent dinoflagellate abundance was positively correlated ($r_s = .848$; $p < .0001$; $n = 75$) with the total dinoflagellate community abundance within the E5 region of the northeast Atlantic. This result, combined with evidence from past studies showing a positive correlation between stimulated bioluminescent intensity and dinoflagellate abundance (Tokarev et al 1999a; Kim et al. 2006), implies that the total dinoflagellate community can be used as a first order proxy for bioluminescent dinoflagellates. Given this, an assumption is made here that in the waters surrounding the PAP observatory the bioluminescent dinoflagellate population can be modelled as a constant fraction of the total dinoflagellate population.

The present chapter sets out the structure of a simple biogeochemical model that includes a dinoflagellate phytoplankton group and the data used for its development and assessment. The model has been developed to simulate the annual cycle of a typical year between 2001 and 2007 within the waters surrounding the PAP observatory (CPR region E5). This period and region have been chosen to correspond

with the data analysed within **Chapter 3** and because there were several datasets available which were adequate for model assessment. The model will be used as a basis for investigating how the ecological function of dinoflagellate bioluminescence may be modelled and for examining its impact upon modelled ecosystem dynamics (**Chapter 6**).

4.2 Modelling Dinoflagellates

The representation of dinoflagellates as a functional group within a model for an open ocean region such as E5, is nontrivial. The majority of dinoflagellate models focus on Harmful Algal Bloom (HAB) species in specific coastal areas (Franks, 1997; Anderson, 1998; Walsh et al., 2001; Olascoaga et al., 2008; Montagnes et al., 2008) or on dinoflagellates as a functional type in regional coastal waters (Cugier et al., 2005; Vanhoutte-Bruiner et al., 2008). In contrast, there have been relatively few marine ecosystem models that have explicitly modelled the abundance or distribution of dinoflagellates within the open ocean. Ecosystem models for open ocean regions have typically been NPZD-type models representing all phytoplankton as a single group (e.g. Fasham et al., 1990; Anderson and Pondaven, 2003; Schartau and Oschlies, 2003a; 2003b). It is only more recently that these models have become more complex containing two or more Phytoplankton Functional Types (PFTs), ranging from those consisting solely of diatoms and non-diatoms (Yool et al., 2011) to those containing several PFTs including organisms such as coccolithophorids, cyanobacteria and nanoflagellates (Merico et al. 2004; Le Quere et al., 2005; Vichi et al. 2007; Follows et al., 2007). These more complex PFT models for open ocean regions regularly overlook dinoflagellates. This is because dinoflagellates are often considered unimportant away from coastal areas (Vichi et al., 2007) or are thought to have “no distinct biogeochemical role” [p. 2020; Le Quere et al., 2005] in contrast to other groups such as calcifiers or nitrogen fixers. This may also be because dinoflagellates, unlike phytoplankton groups such as diatoms, do not have a defining biogeochemical characteristic, such as silicate limitation, that can be easily modelled and used to define them as a functional type. Whilst over the past decade understanding the factors controlling populations of other phytoplankton groups, such as diatoms, has advanced substantially, modelling of dinoflagellates, particularly as a mixed population away from coastal areas, is still in its infancy (Hood et al., 2006).

Despite being under-represented in ecological models, dinoflagellates are nevertheless known to have several traits which distinguish them from other phytoplankton and which can be used to define a PFT (Litchman and Klausmeier, 2008). One well known physiological trait that dinoflagellates typically have is a lower maximal growth rate

than diatoms and other phytoplankton of comparable size (Banse, 1982; Litchman et al., 2007). Another behavioural trait is motility. Many dinoflagellates are capable of directed swimming as a response to changes in chemical stimuli, light and gravity (Heaney and Eppley, 1981; Tyler and Sliger, 1981; Kamykowski et al., 1981). However, the large number (>1500; Gomez et al., 2005) and diversity (Taylor et al., 2008) of dinoflagellate species can still make parameterisation of a functional group encompassing these organisms difficult. For example, results from laboratory studies have shown nitrate uptake rates for dinoflagellates that are both larger and smaller than those for diatoms (Smayda 1997; Litchman et al., 2007; Baek et al., 2008). Also, although dinoflagellates have traditionally been modelled as autotrophs, many species are known to be heterotrophic or mixotrophic (Gains and Elbrachter, 1987; Stoecker, 1999; Ismael, 2003). Indeed, several dinoflagellate species once thought to be solely autotrophic have been recently identified as having the ability to use phagotrophy to supplement limiting nutrients or to increase growth rates through the consumption of a large array of other phytoplankton including diatoms (Jeong et al., 2005; Yoo et al., 2009). Primarily phagotrophic species have also been found to be able to photosynthesise using kleptochloroplasts (chloroplasts taken from ingested phytoplankton) (Skovgaard 1998; Schnepf and Elbrachter, 1999). Nevertheless, several models that describe dinoflagellates as slow-growing autotrophs without a requirement for silicate have been able to correctly capture broad changes in dinoflagellate abundance within the Bering Sea (Merico et al., 2004) and north west European continental shelf (Lewis et al., 2006).

Given that the results of **Chapter 3** indicated that the majority of dinoflagellate cells within E5 region were mixotrophic (**Table B.1**), it may be concluded that dinoflagellates within a model for this region should be represented as such. However, the modelling of mixotrophy as a nutritional strategy is not a straight forward task. Mixotrophic organisms are complex and have many types of mechanisms that can trigger a change in nutrient strategy (Stoecker, 1998). Currently there is a lack of data which can be used to parameterise these processes. In fact, many of the physiological processes are still very poorly, if at all, known. An incorrect description of mixotrophy could lead to erroneous behaviour within the modelled ecosystem and potential confusion in the interpretation of the model results (Flynn and Mitra, 2009). Accurate modelling a mixotrophic feeding strategy was thought to be beyond the scope of the current project. Thus, the model for the E5 region developed in this chapter assumes that all dinoflagellates are autotrophs.

The decision to model dinoflagellates as autotrophs was made upon evidence from the CPR data analysis presented in **Chapter 3**. The aggregation of data into groups of different nutritional strategy showed that combined mixotrophic and photoautotrophic

species accounted for > 90% of the dinoflagellate population on average over the typical year. As mixotrophic dinoflagellate abundance was dominated (> 85%) by species or genera which are considered to be primarily photosynthetic or contain permanent chloroplasts (i.e. Type II mixotrophs) it was thought important that the nutrient uptake by these cells was modelled as it is a primary process affecting the system. Hence, for the purposes of this study, a decision was made not to ignore mixotrophs but instead to assume that they are autotrophs.

Additionally, there are several reasons not to model dinoflagellates as heterotrophic. Firstly, CPR data analysis showed that pure heterotrophs and primarily heterotrophic mixotrophs were a much smaller fraction of the typical dinoflagellate community than photoautotrophs and primarily photosynthetic mixotrophs. Secondly, it is unclear how the parameterisation of heterotrophic dinoflagellates as grazers could be differentiated from that of other zooplankton within a model. Results from **Chapter 3** also indicated that, within the E5 region, dinoflagellates using all nutritional strategies followed very similar seasonal patterns (**Figure 3.8**). This suggests that a model representing dinoflagellates attaining their energy primarily through inorganic nutrient uptake will adequately capture the seasonal variability of the total dinoflagellate community without the need to explicitly model other nutrient strategies.

4.3 Model Structure and Equations

In the development of all ecosystem models it is necessary to make simplifying assumptions in order to reduce complexity to a level which is both intellectually and computationally achievable. An aim to fully simulate a biological system would lead to an impossibly complex model. Model development requires a fine balance to be struck between capturing the characteristics of the system that are dynamically important in terms of the questions the modeller seeks to answer (Fasham, 1993), the necessary computational power and time required for the model to run, and the ability to adequately constrain parameters and assess model performance with the observational data available.

The North Atlantic, including the E5 region, is characterised by a large spring phytoplankton bloom (Ducklow and Harris, 1993). The spring bloom is known to be dominated by diatoms (Barlow et al., 1993; Lochte et al., 1993). Post bloom, other phytoplankton including dinoflagellates, prymnesiophytes and small flagellates (<10 μm) take over the summer phytoplankton population (Barlow et al., 1993; Lochte et al., 1993). This section describes the structure of a simple "NPZ type" model developed for the investigation of dinoflagellate bioluminescence. A zero-dimensional model with

five components representing the interactions between nutrients, phytoplankton and zooplankton was developed and coded in Fortran 90. The model assumes that the biological ecosystem is homogenously distributed within an upper mixed layer which overlies a deep abiotic layer. Organisms are not modelled in the deeper layer as the study is focused upon interactions within the surface waters. The system is composed of two phytoplankton types, diatoms (*P1*) and dinoflagellates (*P2*), two nutrients, nitrate (*N*) and silicate (*Si*), and one predator, metazoan zooplankton (*Z*). A schematic of the model including the flows between state variables is shown in **Figure 4.1**.

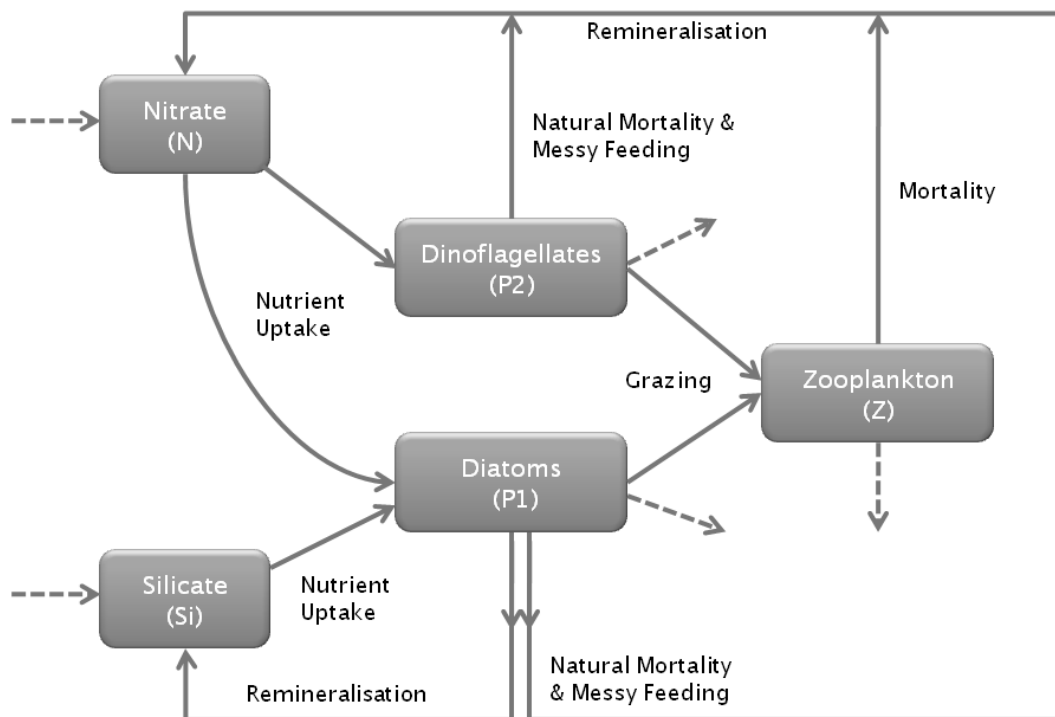


Figure 4.1: Model schematic stating major coupling processes between state variables. Solid arrows indicate flows of nitrogen between model components within the mixed layer. Dashed arrows indicate input and output from the mixed layer.

The model composition shown in **Figure 4.1** was chosen because it provided a simple structure that captured the primary interactions of the ecosystem. A decision was made to include diatoms within the model structure along with dinoflagellate because they are known to dominate the spring bloom in the North Atlantic (Barlow et al., 1993; Lochte et al., 1993). Silicate was included as limiting nutrient for diatoms as it is thought silicate depletion can have a strong effect on phytoplankton succession. The simple model structure shown in **Figure 4.1** was preferred for several reasons. Firstly, findings from more complex models can often be more difficult to interpret and can restrict understanding of the modelled system at a basic level. For the impact of the

ecological function of dinoflagellate bioluminescence upon the dynamics of a system to be accurately assessed it is necessary that the modelled system without these functions is well understood. Secondly, very little observational data was available for other PFTs for the period and location of interest and adding components to the model which could not be constrained would increase uncertainty in the model (Anderson, 2005). Thirdly, the simple structure ensured the computational power and time required to run the model was achievable.

The modelled ecosystem is time dependent with seasonal changes in biology forced by changes in the physical environment. However, physical dynamics within the mixed layer were not explicitly modelled and no horizontal affects, such as advection, were considered. Data has instead been used to define changes in Mixed Layer Depth (MLD), Photosynthetically Active Radiation (PAR) and nutrient concentrations directly below the mixed layer as a function of time (t (days)), and to drive seasonal changes in the ecosystem (data are described in **Section 4.4**). This relatively simple physical forcing of the model has the advantage that it allows for the biological dynamics in the system to be fully understood without being confused by a more complex physical model (Fasham, 1993). The consideration of no horizontal affects leads the model to be appropriate for large uniform areas of open ocean (Evans and Parslow, 1985), such as the CPR E5 region.

Nitrogen is used as the model currency. However, for comparison of silicate and chlorophyll state variables to their equivalent observations a conversion was required. Nitrate is converted to silicate using a fixed N:Si ratio of 1.0666 (Brzezinski, 1985). Conversion from nitrate to chlorophyll uses a C:N ratio of 6.6250 based on the widely used "Redfield" ratio (Redfield, 1934), and a Chl:C ratio of 0.0141, a value corresponding to the midpoint between Chl:C_{\min} and Chl:C_{\max} suggested by Behrenfeld et al. (2005) for the north-east Atlantic.

4.3.1 Mixed Layer Depth

The response of the ecosystem to changes in depth of the mixed layer (M) is modelled following Evans and Parslow (1985). Changes in M as a function of time (t) in days, are calculated as

$$\frac{dM}{dt} = h(t) \quad \text{Eq. 4.1}$$

A positive change in M caused by a deepening in MLD, defined by $h^+(t)$ (**Equation 4.2**), produces entrainment and mixing of nutrients from the deep abiotic layer into the upper mixed layer.

$$h^+(t) = \max(h(t), 0) \quad \text{Eq. 4.2}$$

Such a change also causes a dilution of phytoplankton and zooplankton within the upper mixed layer.

A negative change in M associated with a shoaling of the MLD leads to no changes in nutrient or phytoplankton concentrations as no new water is entrained in to the upper mixed layer. Zooplankton are considered able to maintain their feeding position within the upper mixed layer and therefore their concentration is modelled to increase and decrease when M shoals or deepens, respectively in order to maintain their total stock within the mixed layer (Fasham, 1993).

4.3.2 Phytoplankton Equations

The differential equations for phytoplankton state variables, diatoms ($P1$) and dinoflagellates ($P2$), have a common form following

$$\frac{dP}{dt} = \text{Grow} - \text{Mort} - \text{Graz} - \text{Mix} - \text{Sink} \quad \text{Eq. 4.3}$$

where *Grow* is the gain in phytoplankton due to population growth, *Mort* is the loss due to phytoplankton natural mortality, *Graz* is the loss due to grazing by zooplankton, *Mix* is the loss due to changes in M and *Sink* is the loss due to cells sinking out of the mixed layer.

Within the model, phytoplankton growth is a function of both nutrient limitation and light limitation. The nutrient limited growth of $P2$ is controlled by the availability of nitrate, whereas $P1$ have nutrient limited growth associated with both nitrate and silicate. The *Grow* terms for $P1$ and $P2$ are given by **Equation 4.4** and **4.5**, respectively.

$$\text{Grow}_{P1} = J_1 \left[\min \left(\frac{N}{N+k_{N1}}, \frac{Si}{Si+k_{Si}} \right) \right] P_1 \quad \text{Eq. 4.4}$$

$$\text{Grow}_{P2} = J_2 \frac{N}{N+k_{N2}} P_2 \quad \text{Eq. 4.5}$$

where k_{N1} and k_{Si} are the half saturation constants for nitrate and silicate for $P1$, k_{N2} is the half saturation constant for nitrate for $P2$ and J_1 and J_2 are the light-limited growth rates for $P1$ and $P2$, respectively.

Light limited growth rates (J_1 and J_2) are calculated as a function of the intensity of PAR just above the ocean surface (I_s) and MLD based on the relationship defined in Evans and Parslow (1985). The relationship assumes that the time a cell spends at a given depth is long compared to the photosynthesis reaction time, but short compared to the cell division time. Thus, the total light limited growth rate of a cell averaged over a mixed layer of depth M is given as

$$J(t, M) = \frac{2}{M} \int_0^\tau \int_0^M G_j[I_0(t) \cdot \exp((-k_w - k_c P)z)] dz dt \quad \text{Eq. 4.6}$$

where G_j is a function describing the relationship between photosynthesis and irradiance following a hyperbolic P vs I curve for the specified phytoplankton type j , I_0 is the intensity of PAR just below the surface of the water, k_w is the light attenuation coefficient due to water, k_c is the phytoplankton self-shading parameter, and time (t) is measured in days and is 0 at sunrise and τ at noon.

An analytical integration can be performed if G_j takes the form

$$G_j(I) = \frac{\mu_j \alpha_j I}{\sqrt{\mu_j^2 + \alpha_j^2 I^2}} \quad \text{Eq. 4.7}$$

where μ_j is the maximum growth rate for the specified phytoplankton type j , α_j is the initial gradient of the P-I curve for the specified phytoplankton type and $I_0(t)$ is the local light level whose variation with time of day is assumed triangular for simplicity, as in Steele (1962). The intensity of PAR just below the surface water $I_0(t)$ is given as

$$I_0(t) = (1 - a)I_s(t) \quad \text{Eq. 4.8}$$

where a is the air-sea albedo, set equal to 0.05, and $I_s(t)$ is the intensity of PAR just above the ocean surface.

The mortality term for each phytoplankton type parameterises all losses through non-grazing activity. The *Mort* term for the specified phytoplankton type j is given by **Equation 4.9** following Fasham (1993).

$$Mort_{Pj} = \frac{m_p P_j^2}{k_m + P_j} \quad \text{Eq. 4.9}$$

where m_p is the maximum natural phytoplankton mortality rate and k_m is the half saturation constant for phytoplankton mortality.

The *Graz* term, parameterising the losses through grazing by zooplankton, for the specified phytoplankton type j is given by

$$Graz_{Pj} = g \left(\frac{P_j}{k_z + P_1 + P_2} \right) Z \quad \text{Eq. 4.10}$$

where g is the zooplankton maximum ingestion rate and k_z is the half saturation constant for grazing.

The *Mix* terms for the specified phytoplankton type j is given by

$$Mix_{Pj} = \frac{(m + h^+(t))P_j}{M} \quad \text{Eq. 4.11}$$

where m represents the mixing due to turbulence between the upper mixed layer and the deeper abiotic layer.

Diatoms are known to actively sink from surface waters, as such within the model $P1$ are assumed to sink from the upper mixed layer at an assigned rate. This assigned rate is the *Sink* term in **Equation 4.3** and is given by a constant V_{diatom} . In contrast, dinoflagellates are not considered to actively sink and the model assumes $P2$ remain within the upper mixed layer when there is a shoaling or no change in M . Hence the *Sink* term for $P2$ is set to a constant equal to zero and the term disappears.

4.3.3 Zooplankton

The differential equation for zooplankton (Z) has the form

$$\frac{dZ}{dt} = Grow_Z - Mort_Z - Mix_Z \quad \text{Eq. 4.12}$$

where $Grow_Z$ is the gain in zooplankton due to population growth through grazing upon phytoplankton, $Mort_Z$ is the loss due to zooplankton mortality, and Mix_Z represents changes in zooplankton concentration due to the varying depth (M) of the mixed layer.

Within the model, $Grow_Z$ takes the form of a Holling Type II function to represent the relationship between grazing and prey density. The Holling Type II function effectively assumes that when prey are scarce zooplankton spend the majority of their time searching and find prey at a rate proportional to its abundance. As the number of prey

increases the grazing rate rises increasingly slowly as zooplankton are assumed to spend an increasing amount of time handling and consuming prey. When prey become superabundant a maximum grazing rate is reached which is solely dependent upon how fast the zooplankton can process their prey. The term assumes that zooplankton effectively have equal grazing preference for $P1$ and $P2$ phytoplankton types and is defined by

$$Grow_Z = g\beta \left(\frac{P_1 + P_2}{k_z + P_1 + P_2} \right) Z \quad \text{Eq. 4.13}$$

where g is the zooplankton maximum specific grazing rate, β is the assimilation efficiency and k_z is the half saturation constant for grazing.

Grazed material that is not assimilated by zooplankton for growth is defined as being lost via messy feeding (MF_z) and available for remineralisation back into the nutrient pool. MF_z is given as

$$MF_Z = (1 - \beta)g \left(\frac{P_1 + P_2}{k_z + P_1 + P_2} \right) Z \quad \text{Eq. 4.14}$$

The mortality term for zooplankton is the effective closure term of the model and represents the losses due to both natural mortality and higher predators which are not explicitly modelled. The $Mort_z$ term as a whole follows the hyperbolic form given in Fasham (1993) which leads to a loss rate which is effectively quadratic at small zooplankton concentrations and linear at large zooplankton concentrations and is given by

$$Mort_Z = \frac{\varepsilon Z^2}{k_{mz} + Z} \quad \text{Eq. 4.15}$$

where ε is the zooplankton maximum mortality rate and k_{mz} is the half saturation constant for the zooplankton mortality rate.

The Mix_z term concentrates or dilutes zooplankton with the shoaling or deepening of the MLD, respectively. Mix_z is given as

$$Mix_Z = \frac{Zh(t)}{M} \quad \text{Eq. 4.16}$$

4.3.4 Nitrate

The differential equation for nitrate takes the following form

$$\frac{dN}{dt} = \tau(Mort_Z + Mort_{P1} + Mort_{P2} + MF_Z) - Grow_{P1} - Grow_{P2} + Mix_N \quad \text{Eq. 4.17}$$

as no detritus pool is explicitly modelled a constant fraction τ of the material lost from phytoplankton and zooplankton through mortality and messy feeding is remineralised into the nutrient pool, $Mort_Z$ is the zooplankton mortality term as defined in **Equation 4.15**, $Mort_{P1}$ and $Mort_{P2}$ are the mortality terms for $P1$ and $P2$ as defined in **Equation 4.9**, MF_Z represents the loss of grazed material through messy feeding given in **Equation 4.14**, $Grow_{P1}$ and $Grow_{P2}$ are the $P1$ and $P2$ growth terms defined in **Equations 4.4** and **4.5**, respectively and Mix_N represents the gain in nitrate due to mixing. The remineralisation efficiency τ sets the export rate from the biologically active upper layer into the abiotic deep layer. All material not remineralised (equal to $1-\tau [Mort_Z + Mort_{P1} + Mort_{P2} + MF_Z]$) effectively disappears from the model domain and should be considered exported.

The Mix_N term specifies the increase in nitrate due to a deepening of the MLD and is given as

$$Mix_N = \frac{(m+h^+(t))}{M} (N_0 - N) \quad \text{Eq. 4.18}$$

where N_0 is the nitrate concentration below the mixed layer which is defined by the physical forcing data described in **Section 4.4.3**.

4.3.5 Silicate

The differential equation for silicate takes the following form

$$\frac{dSi}{dt} = [\tau(Mort_{P1} + Graz_{P1}) - Grow_{P1}]/R_{N:Si} + Mix_{Si} \quad \text{Eq. 4.19}$$

where Mix_{Si} represents the gain in silicate due to mixing and $R_{N:Si}$ is the N:Si ratio. Mix_{Si} follows the same form as the mixing term for nitrate given in **Equation 4.19** replacing N and N_0 with Si and S_0 respectively.

Within the model it is assumed that zooplankton do not uptake silicate for growth and therefore all grazed silicate material ($Grow_z + MF_z$) is available for remineralisation back into the system. The FORTRAN 90 code setting out the biological differential equations is given in **Appendix C**.

4.3.6 Model Parameters

A full list of parameters used within the model is given in **Table 4.1**

Table 4.1: List of parameters used in model containing dinoflagellates for the waters surrounding the PAP observatory for a typical year within the period 2001 to 2007.

Parameter	Symbol	Unit
<i>Phytoplankton</i>		
Maximum Growth Rate P1	μ_1	day^{-1}
Maximum Growth Rate P2	μ_2	day^{-1}
Nitrate Half Saturation Constant P1	k_{n1}	mmol m^{-3}
Nitrate Half Saturation Constant P2	k_{n2}	mmol m^{-3}
Silicate Half Saturation Constant P1	k_{Si}	mmol m^{-3}
Initial P-I Slope P1	α_1	$(\text{Wm}^{-2})^{-1}\text{day}^{-1}$
Initial P-I Slope P2	α_2	$(\text{Wm}^{-2})^{-1}\text{day}^{-1}$
Sinking rate P1	V_{diatom}	m day^{-1}
Phytoplankton Maximum Natural Mortality Rate	m_p	day^{-1}
Phytoplankton Mortality Half Saturation Constant	k_{mp}	mmol m^{-3}
<i>Zooplankton</i>		
Zooplankton Maximum Grazing Rate	g	day^{-1}
Zooplankton Half Saturation Constant	k_z	mmol m^{-3}
Zooplankton Gross Growth Efficiency	β	
Zooplankton Maximum Mortality Rate	ϵ	day^{-1}
Zooplankton Mortality Half Saturation Constant	$k_{m\epsilon}$	mmol m^{-3}
<i>Other</i>		
Remineralisation Efficiency	τ	
Across Thermocline Mixing Coefficient	m	m day^{-1}
Light Attenuation Coefficient Due To Self-Shading	k_c	$\text{m}^2(\text{mmol N})^{-1}$
Water Attenuation Coefficient	k_w	m^{-1}

4.4 Physical Forcing Data

Seasonal forcing of the ecosystem model was provided by changes in MLD, PAR and nutrient concentrations below the mixed layer. The following sections describe the methodologies used to create the forcing datasets.

4.4.1 Mixed Layer Depth

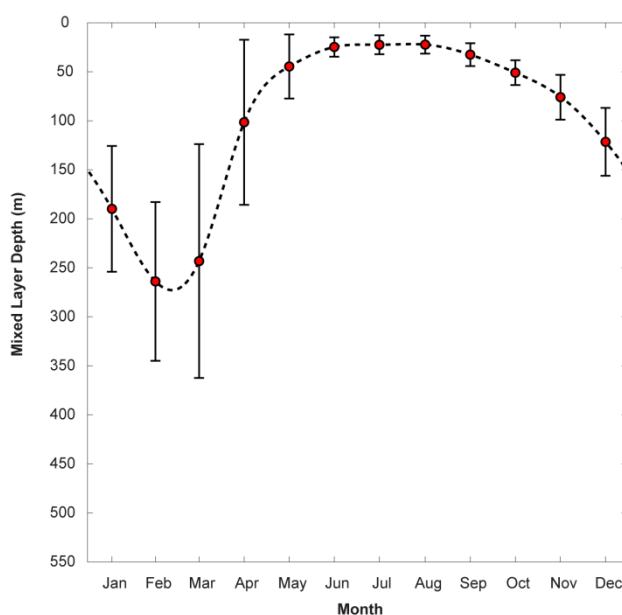


Figure 4.2: Mixed layer depth used for physical forcing of model. Red closed circles show calculated monthly averaged MLD within the E5 region from 2001 to 2007, error bars indicate ± 1 standard deviation from the monthly mean calculated from temporal and spatial variability across the E5 region, dashed line shows interpolated daily changes in MLD using temperature data from Argo profiles.

Argo profile data were sourced from www.coriolis.eu.org. Profiles were extracted from within the CPR E5 region for the period 2001–2007. Mixed layer depths were calculated using temperature data from the extracted profiles². There is no uniform criterion for the estimation of MLD and numerous criteria have been used. A criterion of a 0.2°C temperature difference from that at 10 m below the surface, as suggested by Boyer Montegut et al. (2004), was chosen. This criterion has been shown to provide significantly better approximations to the MLD for North Atlantic Argo profiles than the 0.5° temperature criterion of Monterey and Levitus (1997) (Steinhoff et al., 2010). The

² The use of a temperature criterion assumes that the difference between the iso-thermal layer (ILD) and the MLD is negligible. Density data are not used to define MLD as salinity sensors are not present on all Argo floats.

MLDs obtained from the individual profiles were used to calculate an average climatology (2001 to 2007) in the E5 region for each month of the year. Monthly data were then spline interpolated, using the averaged data as the midpoint values for each month, to obtain daily estimates of MLD (**Figure 4.2**). These interpolated data were used to seasonally force the model.

4.4.2 Photosynthetically Active Radiation

Monthly 9 km resolution PAR data (intensities representative of just above the sea surface) from the Sea-viewing Wide Field-of-view Sensor (SeaWiFS) were downloaded from <http://oceandata.sci.gsfc.nasa.gov/> for the years 2001 to 2007. Pixel data were extracted within the CPR E5 region for the individual months of each year. These data were averaged temporally and spatially to give monthly composites of PAR averaged over the 2001 to 2007 period. As for the MLD data, a spline interpolation was applied to the averaged PAR data to achieve daily values of PAR. These interpolated data were then converted from Einsteins $\text{m}^{-2} \text{d}^{-1}$ to W m^{-2} for use in seasonally forcing of the model. Einsteins $\text{m}^{-2} \text{d}^{-1}$ were converted to Einsteins $\text{m}^{-2} \text{s}^{-1}$ using a conversion factor of 86400 seconds in a day, then Einsteins $\text{m}^{-2} \text{s}^{-1}$ were then converted to W m^{-2} using a conversion factor of $1 \mu\text{Einsteins m}^{-2} \text{s}^{-1} = 0.2174 \text{ W m}^{-2}$ (Kirk, 1994) (**Figure 4.3**).

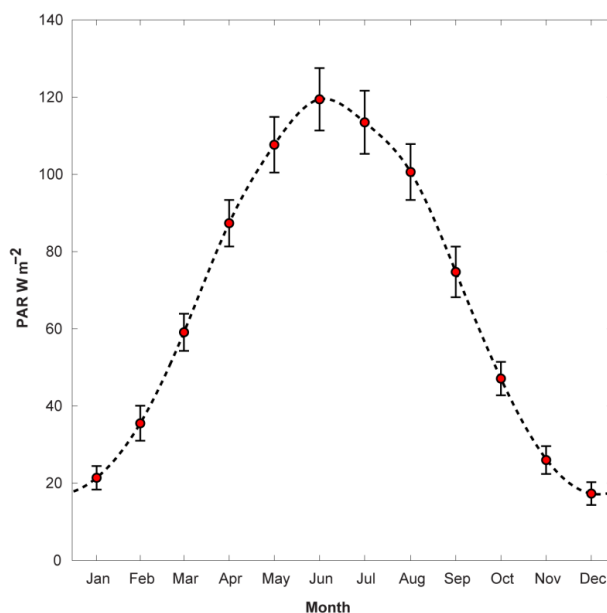


Figure 4.3: Photosynthetically active radiation data used for physical forcing of model. Red closed circles show calculated monthly averaged PAR within the E5 region from 2001 to 2007, error bars show ± 1 standard deviation from the monthly mean calculated from temporal and spatial variability across the E5 region, dashed line shows interpolated daily changes in PAR.

4.4.3 Below Mixed Layer Nutrient Concentrations

Nitrate and silicate monthly climatology data at 1° resolution were sourced from the World Ocean Atlas 2009 (WOA09). Data for the E5 region between 0 and 500 m were downloaded from http://www.nodc.noaa.gov/OC5/WOA09/pr_woa09.html (accessed 16/05/2011; Garcia et al., 2010). For each month nitrate and silicate data were extracted from depth ranges corresponding to the monthly average $MLD \pm 1$ standard deviation as calculated in **Section 4.4.1**. For each month and each nutrient type, data within these depth ranges were averaged to give monthly values for the E5 region between 2001 and 2007. Once more a spline interpolation was applied to the monthly composites to achieve daily changes in the nutrient concentrations below the mixed layer depth (**Figure 4.4**).

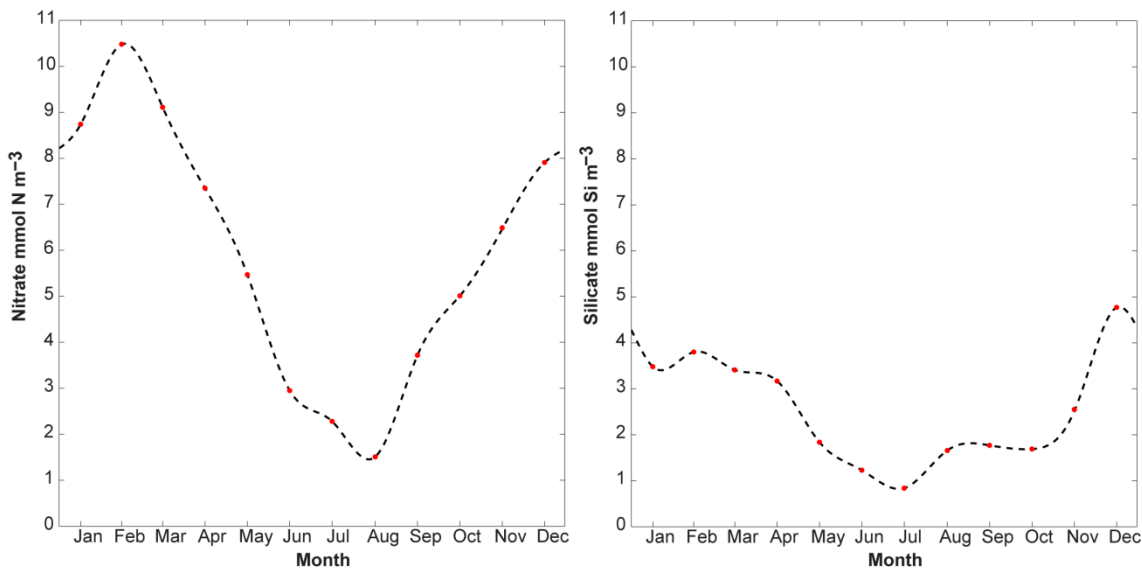


Figure 4.4: Below mixed layer nutrient concentrations. Red closed circles show calculated monthly nitrate and silicate within the E5 region averaged over 2001 to 2007, dashed lines show spline interpolated daily changes in nitrate and silicate.

4.5 Data for Model Assessment

Observational datasets were required for comparison to model output in order for model performance to be assessed. As the simulation of the dinoflagellate population was of primary importance, the assessment of the model's ability to simulate the dynamics of the dinoflagellate population was a priority. However, it is also important for other aspects of the model to be assessed in order to have confidence in the simulation of the ecosystem as a whole. Thus, the model was assessed on its ability to recreate 1) the relative seasonal variation of diatoms and dinoflagellates; 2) the seasonal change in the concentration of total phytoplankton biomass; 3) the seasonal changes in nitrate and silicate concentrations.

The following sections describe the observational data used for assessing model performance. It was necessary to ensure that all datasets had an approximate normal distribution for the purposes of model optimisation which is subsequently described in **Chapter 5**.

4.5.1 Phytoplankton Seasonal Variability

As described in **Chapter 3**, data from the CPR can provide information on the relative changes in abundance of phytoplankton throughout the year. Thus, CPR data of dinoflagellates and diatoms within the E5 region were used to compare observed relative seasonal variation in phytoplankton to model output. Data for diatoms (all species summed) and dinoflagellates³ (all species summed excluding cysts) were obtained for the E5 region between the years 2001 and 2007 from SAHFOS. The reader is referred to **Section 3.2.1** for a full description of the CPR methodology.

Data for diatoms and dinoflagellates were $\log_{10}(x+1)$ transformed and averaged for each month of each year as in Head and Pepin (2010). Climatological monthly averages over the 2001 to 2007 period were calculated following the methodology described in **Chapter 3 (Equation 4.20; Cochran, 1977)** and are shown in **Table 4.2**.

$$\bar{x}_j = \frac{\sum_{i=1}^n w_{ij} x_{ij}}{\sum_{i=1}^n w_{ij}} \quad \text{Eq. 4.20}$$

where x_{ij} is the average value of month j for year i and w_{ij} is the number of samples used to calculate x_{ij} and n is the number of years, here 7.

As stated previously in **Chapter 3**, a weighted average was used to better represent the seasonal pattern over the seven year period and to ensure that years with a high sampling frequency have a larger influence on the mean than those with a low sampling frequency.

³ Data from all dinoflagellate genera were summed as analysis in Chapter 3 indicated that the seasonal variability of the mixotrophic + autotrophic genera was extremely close to that of the total dinoflagellate population sampled (i.e. mixotrophs + autotrophs + heterotrophs). The small difference that occurs in April/May lies well within the standard deviation of the mixotroph + autotroph count data (not shown). Thus, for simplicity and convenience the seasonal variability of the total dinoflagellates sampled from the CPR is used for model analysis.

The uncertainties associated with the climatological averages were calculated using a weighted standard deviation (**Equation 4.21**, Galassi et al., 2009) and are also shown in **Table 4.2**.

$$\sigma_j = \sqrt{\frac{\sum_{i=1}^n w_{ij}}{[(\sum_{i=1}^n w_{ij})^2 - \sum_{i=1}^n w_{ij}^2]}} \sum_{i=1}^n w_{ij} (x_{ij} - \bar{x}_j)^2 \quad \text{Eq. 4.21}$$

where x_{ij} is the average value of month j for year i , w_{ij} is the number of samples used to calculate x_{ij} and \bar{x}_j is the weighted climatological average for month j .

Unfortunately, because CPR data is not systematically spatially sampled (**Section 3.2.2**) the calculation of the uncertainties associated with the climatological abundances are potentially underestimated as spatial variance is not fully considered. The lack of an estimate for spatial variance in the data is discussed further in **Section 4.5.4**.

Table 4.2: Monthly average dinoflagellate and diatom abundance, $\log(x+1)$ transformed, for the E5 region from 2001 to 2007 and their corresponding standard deviations.

Month	Dinoflagellates		Diatoms	
	Average	Standard Deviation	Average	Standard Deviation
Jan	0.4237	0.6472	0.9219	1.1284
Feb	0.2433	0.5733	0.7192	0.8630
Mar	0.1593	0.1504	1.2974	0.8587
Apr	1.3877	1.0633	3.7230	1.5075
May	1.7504	1.1521	3.4969	2.1880
Jun	1.6642	1.5689	2.0052	1.7368
Jul	3.7430	0.8224	2.3368	1.4373
Aug	2.5135	1.2150	0.9828	0.5978
Sep	1.4982	1.3696	0.9812	0.5833
Oct	1.2766	1.1156	0.9598	0.6586
Nov	0.6300	0.6304	0.5707	0.5790
Dec	0.4556	0.3115	0.6239	0.4992

Statistically assessing whether the data used to calculate the monthly climatologies were normally distributed was hampered by small sample sizes (~7 samples per month). Approximately 100 data points are required for a semi accurate evaluation of a distribution from a histogram, whilst ≥ 50 points are required to assess a distribution using a Kolomogorov–Smirnov test. A Shapiro–Wilk test is thought to be a more appropriate test of normal distribution when a sample size is below 50 points. Hence this test was used to assess whether data conformed to a normal distribution. Results indicated that both diatom and dinoflagellate data used to calculate monthly climatologies were consistent with normal distribution at the $p < 0.05$ significance level.

As stated in **Section 3.2.1** the CPR data is only semi-quantitative and thus does not provide information that can be directly compared to the model output of biomass. However, the CPR does capture a consistent fraction of the plankton population and therefore the seasonal variations observed are thought to be an accurate representation of those occurring in situ (Richardson, 2006). To overcome the lack of comparability between observational data and model output, the monthly climatologies of diatom and dinoflagellate abundance (**Table 4.2**) were standardised to zero mean and unit standard deviation z-scores (z_j) following **Equation 4.22** (Cheadel et al., 2003).

$$z_j = \frac{\bar{x}_j - \mu}{\sigma_\mu} \quad \text{Eq. 4.22}$$

where \bar{x}_j is the average value for month j , μ is the average of all months over the year and σ_μ is the standard deviation associated with μ .

As in **Chapter 3** z-scores show the relative changes in abundance for the phytoplankton groups over a year. Lewis et al (2006) have previously shown that by standardising the corresponding model output to z-scores in the same way, a comparison can be made between the variation simulated in a model and that observed in situ by the CPR.

The uncertainty associated with z_j due to the standard deviation of the CPR data (**Table 4.2**) was calculated following **Equation 4.23**.

$$\sigma_{j_z} = \frac{\sigma_j}{\sigma_\mu} \quad \text{Eq. 4.23}$$

where σ_j is the weighted standard deviation given in **Equation 4.22** and σ_μ is the standard deviation used in the calculation of z_j in **Equation 4.23**. Derivation of this relationship can be found in **Appendix D**.

Calculated z-scores and their associated uncertainty for averaged diatom and dinoflagellate abundance within the E5 region between 2001 and 2007 are shown in **Figure 4.5**.

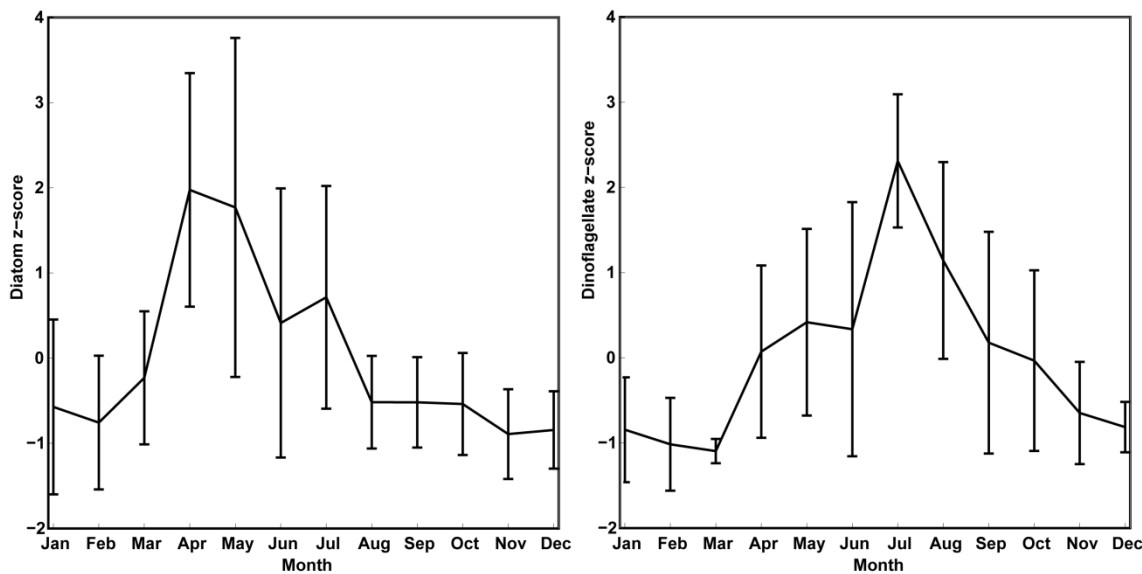


Figure 4.5: Diatom and dinoflagellate z-scores calculated from climatologically averaged CPR abundances within the E5 region from 2001 to 2007 and their associated uncertainties.

4.5.2 Chlorophyll

CPR data only provides information on relative changes in abundance (**Section 3.2.1**). Thus, in order to assess how well the model simulates the absolute phytoplankton abundance it was necessary to find a dataset comparable to modelled phytoplankton biomass. Chlorophyll data can provide such information if converted to carbon units or vice versa. Surface water chlorophyll concentration is regularly measured on a global scale via sensors onboard several satellites. Chlorophyll data were used for comparison to the total modelled phytoplankton biomass (i.e. diatoms + dinoflagellates). Although several methodologies have recently been developed that allow the identification of different phytoplankton groups based on satellite detected ocean colour data (Alvain et al., 2008), it was not possible to acquire data which reliably distinguished between dinoflagellates and diatoms. Thus, unfortunately no comparison between modelled and observed biomass for the individual phytoplankton types could be made.

Level 3 SeaWiFS chlorophyll data originally downloaded from NASA/GSFC at <http://oceandata.sci.gsfc.nasa.gov/> at a resolution of 9 km with units mg m^{-3} were obtained from the National Oceanography Centre 'GADGET' archive. The data had undergone additional processing within the 'GADGET' archive to interpolate data to 0.5° resolution using a Gaussian smoother and had been \log_{10} transformed. Monthly data were extracted for the years 2001 to 2007 within the CPR E5 region⁴. Pixel data were averaged temporally to achieve average monthly composites.

⁴ SeaWiFS chlorophyll data for December 2007 was not available for this location due to a sensor error.

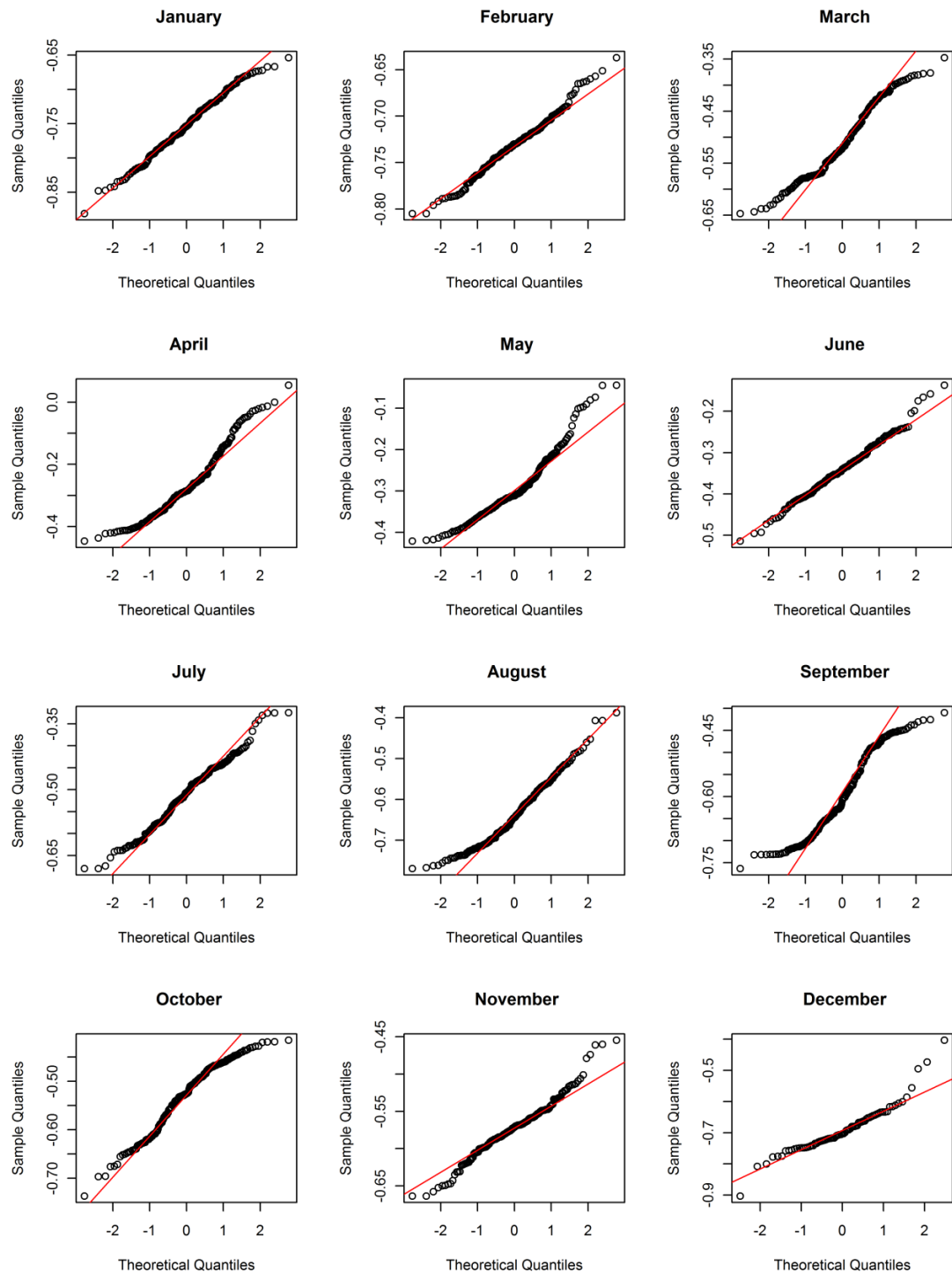


Figure 4.6: Q-Q plots indicating averaged \log_{10} transformed monthly chlorophyll data approximates to a normal distribution, red line indicates perfect normal distribution.

Kolmogorov–Smirnov tests indicated that monthly composite log transformed data broadly conformed to a normal distribution at the $p < .05$ significance level. Quantile – Quantile (Q–Q) plots were created to look closer at the distribution of each month (**Figure 4.6**). A normal distribution is followed if the data points lie along the straight line shown in red. An arching of the data points about the red line indicates the distribution of data may be skewed. An S-shape in the data points indicates that the distribution has heavy tails compared to that of the normal distribution. **Figure 4.6** indicates that data from months later in the year, September to December, diverged most from that of a normal distribution. This is potentially due to a reduced number of data points in these months because of increased cloud cover. The majority of months are seen to conform well to a normal distribution.

Monthly composite pixel data were averaged over the spatial extent of E5 to provide an average measure of chlorophyll for the region between 2001 and 2007 (**Figure 4.7; Table 4.3**). It should be noted that chlorophyll data for the E5 region in December is systematically affected by cloud cover above 47°N, which could potentially affect the reliability of the averaged measurement. The standard deviations (σ_{jchl}) associated with the monthly E5 chlorophyll values were calculated incorporating both the temporal and spatial variance in the data as set out in **Equation 4.24** (**Figure 4.7; Table 4.3**).

$$\sigma_{jchl} = \sqrt{\sigma_{jchl\ spatial}^2 + \sigma_{jchl\ temporal}^2} \quad \text{Eq. 4.24}$$

where $\sigma_{jchl\ spatial}^2$ is given by

$$\sigma_{jchl\ spatial}^2 = \frac{1}{n} \sum_{i=1}^n (x_{ij} - \bar{x}_j)^2 \quad \text{Eq. 4.25}$$

and $\sigma_{jchl\ temporal}^2$ is given by

$$\sigma_{jchl\ temporal}^2 = \frac{1}{n} \sum_{i=1}^n \sigma_{ij}^2 \quad \text{Eq. 4.26}$$

where \bar{x}_j is the mean of the composite pixels over the E5 area for month j , x_{ij} is the composite value of pixel i in month j , n is the number of pixels i in month j , σ_{ij} is the standard deviation related to pixel i in month j associated with the temporal averaging to monthly composites.

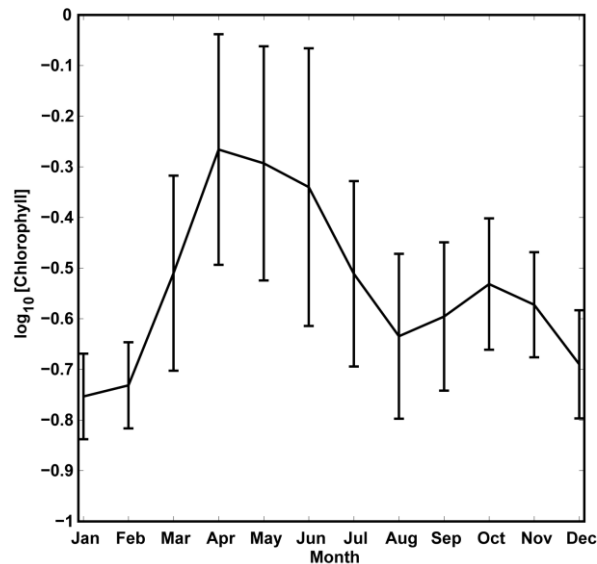


Figure 4.7: Monthly climatologically averaged chlorophyll data within the E5 region from 2001 to 2007 and their associated uncertainties.

It should be noted that the satellite chlorophyll data will undoubtedly include the chlorophyll signal from phytoplankton other than diatoms and dinoflagellates. In situ observations within the Northeast Atlantic have previously shown that phytoplankton in the size fraction $<5 \mu\text{m}$ can contribute significantly to primary production, particularly in the summer months (Lochte et al., 1993). Calculations from HPLC pigment measurements have also indicated that small prymnesiophytes may be responsible for up to 55% of measured chlorophyll between May and June (Barlow et al., 1993). Thus, by constraining and assessing model simulations of total phytoplankton biomass with satellite derived chlorophyll concentrations, simulated individual biomass for both diatoms and dinoflagellate may be over estimated.

Table 4.3: Monthly averaged chlorophyll data within the E5 region from 2001 to 2007 and their corresponding standard deviations

Month	Average $\log_{10}[\text{Chlorophyll}]$	Total Standard Deviation
Jan	-0.7534	0.0844
Feb	-0.7314	0.0851
Mar	-0.5099	0.1927
Apr	-0.2657	0.2277
May	-0.2930	0.2312
Jun	-0.3400	0.2742
Jul	-0.5111	0.1831
Aug	-0.6345	0.1628
Sep	-0.5956	0.1465
Oct	-0.5315	0.1298
Nov	-0.5723	0.1038
Dec	-0.6900	0.1068

4.5.3 Nutrients

Global nitrate and silicate monthly climatology data at 1° resolution were sourced from the World Ocean Atlas 2009 (WOA09). Objectively analysed data, which consists of objectively interpolated mean fields at standard depth levels for the World's Oceans, were downloaded from <http://www.nodc.noaa.gov/OC5/WOA09/woa09data.html> (accessed 15/03/2010; Garcia et al., 2010). Data were extracted from within the E5 region at a depth of 10 m. Nutrient concentrations at this depth level were used as they correspond closely to the depth at which the CPR instrument is towed (~ 7 m) and were always within the mixed layer.

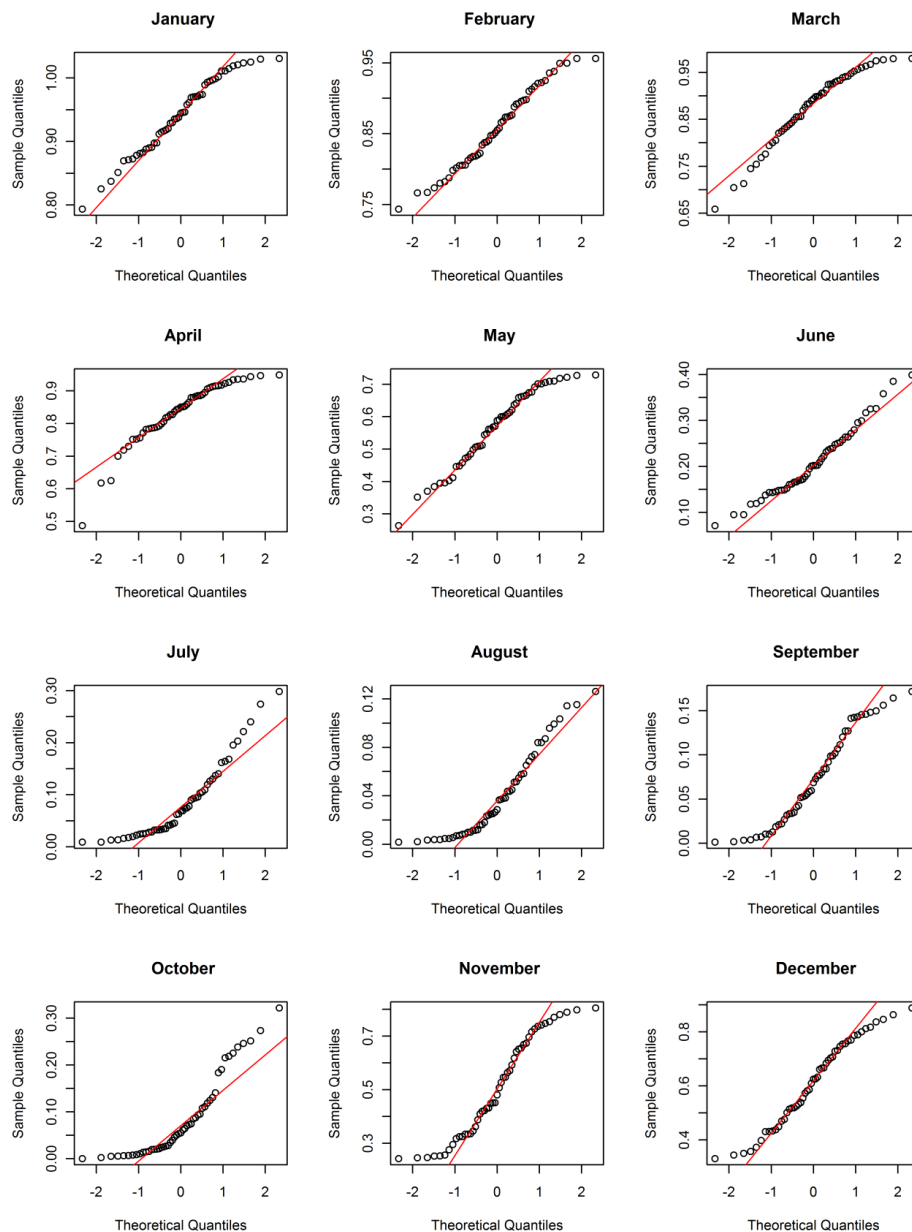


Figure 4.8: Q-Q plots indicating that $\log_{10}(x+1)$ transformed nitrate data approximates to a normal distribution, red line indicates perfect normal distribution.

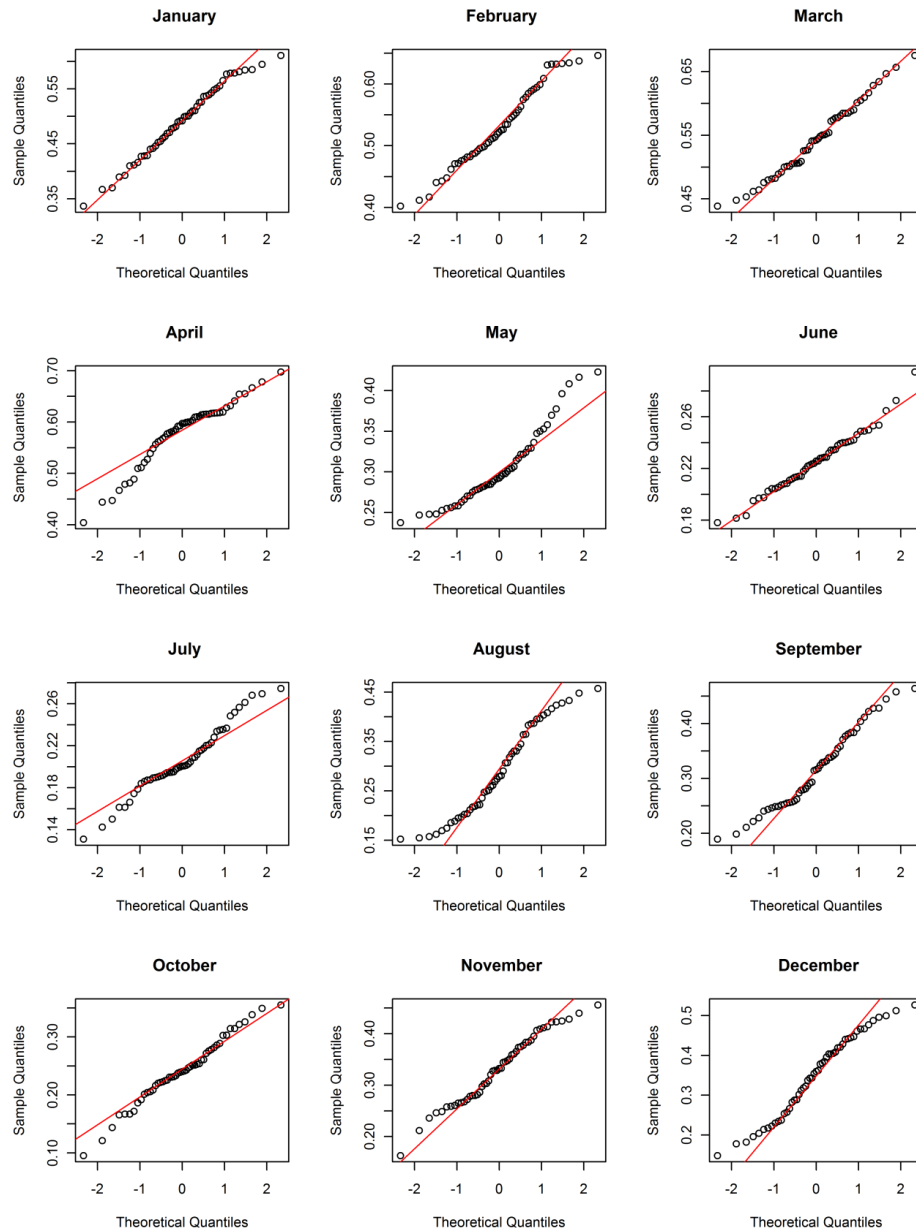


Figure 4.9: Q-Q plots indicating that $\log_{10}(x+1)$ transformed silicate data approximates to a normal distribution, red line indicates perfect normal distribution.

Nitrate and silicate data were $\log_{10}(x + 1)$ transformed. As with the chlorophyll data, Kolomogorov-Smirnov tests confirmed that transformed data were consistent with normal distributions at the $p < .05$ significance level. Q-Q plots showed that the nitrate data in some months, particularly July, August and October, had a distribution with heavier tails than would strictly be found for a perfect normal distribution (**Figure 4.8**). The same was also true of silicate data in the months of May, August and December (**Figure 4.9**). A comparison of nitrate and silicate Q-Q plots suggests that silicate data conforms more strictly to a normal distribution in more months than nitrate data. On

the whole, deviations from a normal distribution in the monthly nutrient data were considered to be small and thus, normal distributions were assumed.

Gridded climatological data were averaged over the spatial extent of E5 to provide an average measure of nitrate and silicate for the region in each month (**Figure 4.10**). Uncertainty associated with the data was accounted for by the calculation of the standard deviation across the 1° pixels within the E5 region (**Figure 4.10**). However, uncertainty may be underestimated as there was no information available from the WOA09 regarding temporal variance associated with the climatological data. The lack of an estimate for temporal variation is discussed further in **Section 4.5.4**.

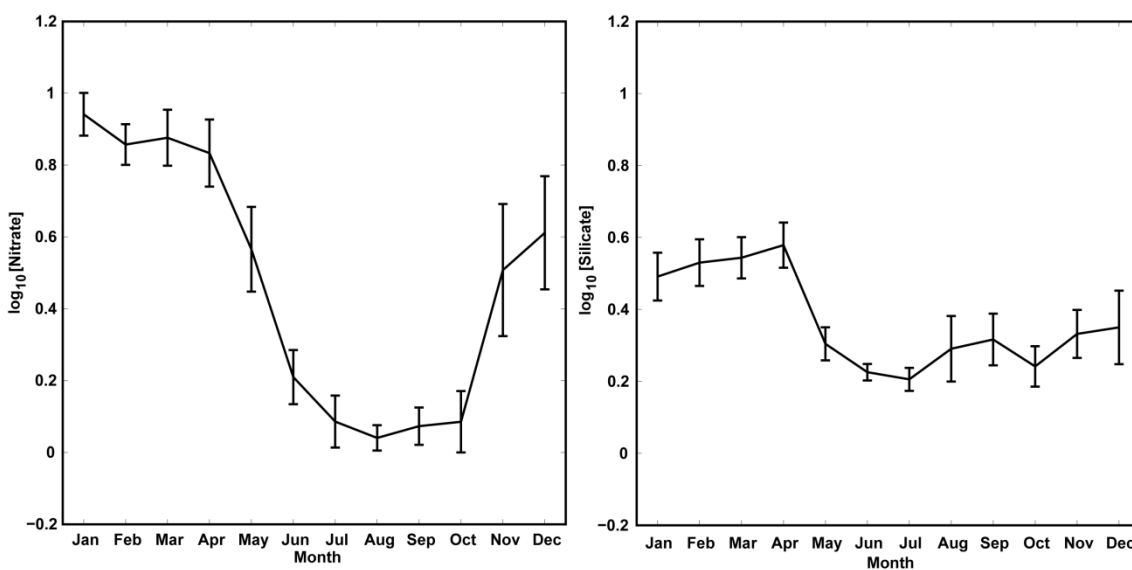


Figure 4.10: Nitrate and silicate monthly climatologically averaged values within the E5 region from 2001 to 2007 and their associated uncertainties.

4.5.4 Estimating Missing Variance

4.5.4.1 CPR Phytoplankton Data

It was not possible to calculate the spatial variance associated with the climatological dinoflagellate and diatom seasonal variability calculated from the CPR data. Thus, the z-score uncertainties shown in **Figure 4.5** do not account for any spatial variance in the data and therefore potentially underestimate the uncertainty in the calculated z-scores. To address this underestimation, an estimate of the spatial variance in each month was calculated based upon the spatial/temporal variance ratios from the SeaWiFS chlorophyll dataset. This estimation assumes that the spatial/temporal variance ratio associated with the averaged SeaWiFS data will be the same for the CPR

data. Spatial variances associated with the CPR z-scores were estimated using **Equation 4.27**.

$$\sigma_{j_z \text{ spatial}}^2 = \sigma_{j_z}^2 \left(\frac{\sigma_{j_{Chl \text{ spatial}}}^2}{\sigma_{j_{Chl \text{ temporal}}}^2} \right) \quad \text{Eq. 4.27}$$

where $\sigma_{j_z}^2$ is the underestimated z-score variance with no account of spatial variance, $\sigma_{j_{Chl \text{ spatial}}}^2$ is the spatial variance associated with the SeaWiFS chlorophyll data as calculated using **Equation 4.25** and $\sigma_{j_{Chl \text{ temporal}}}^2$ is the temporal variance associated with the SeaWiFS chlorophyll data as calculated using **Equation 4.26**.

Uncertainties associated with z-scores were subsequently recalculated following **Equation 4.28**.

$$\sigma_{j_z \text{ estimated}} = \sqrt{\sigma_{j_z \text{ spatial}}^2 + \sigma_{j_z}^2} \quad \text{Eq. 4.28}$$

Table 4.4 shows the z-scores for dinoflagellates and diatoms with corresponding originally calculated temporal uncertainties and revised estimated (temporal + spatial) uncertainties. The revised z-score uncertainties are subsequently used for model assessment.

Table 4.4: z-scores for averaged diatom and dinoflagellate abundance within the E5 region between 2001 and 2007 together with originally calculated temporal uncertainties and revised estimated uncertainties including a spatial variance.

Month	Dinoflagellates			Diatoms		
	z-score	Temporal	Estimated	z-score	Temporal	Estimated
		Uncertainty	Uncertainty		Uncertainty	Uncertainty
Jan	-0.8447	0.6153	0.7253	-0.5727	1.0263	1.2098
Feb	-1.0162	0.5450	0.5873	-0.7570	0.7849	0.8459
Mar	-1.0960	0.1430	0.1536	-0.2311	0.7810	0.8387
Apr	0.0719	1.0109	1.1517	1.9749	1.3711	1.5621
May	0.4167	1.0953	1.1647	1.7693	1.9900	2.1160
Jun	0.3348	1.4916	1.5364	0.4126	1.5796	1.6271
Jul	2.3111	0.7819	0.8598	0.7142	1.3072	1.4375
Aug	1.1422	1.1551	1.3323	-0.5173	0.5437	0.6271
Sep	0.1769	1.3021	1.7019	-0.5187	0.5305	0.6934
Oct	-0.0337	1.0606	1.2608	-0.5383	0.5990	0.7121
Nov	-0.6485	0.5994	0.6419	-0.8921	0.5266	0.5640
Dec	-0.8143	0.2962	0.4094	-0.8438	0.4540	0.6276

4.5.4.2 World Ocean Atlas Nutrient Data

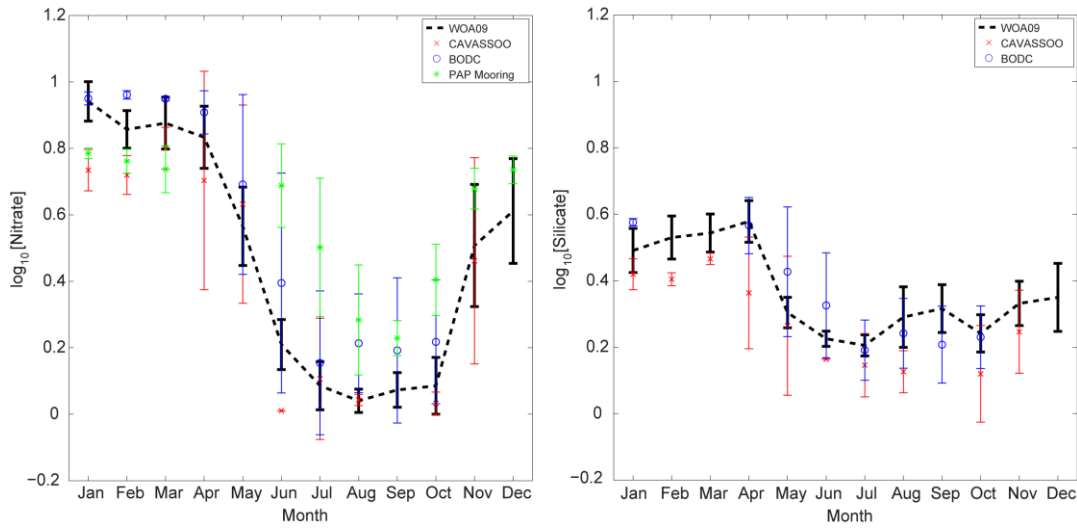


Figure 4.11: Comparison of uncertainties in nutrient data from the WOA09 (black) without temporal variance estimation to that from CAVASSOO (red), BODC (blue) and the PAP mooring (green) for nitrate and silicate.

The WOA09 nutrient data had a similar issue to that of the CPR z-score data. However, in the nutrient datasets it was not possible to calculate the temporal variances due to no estimation being available from the WOA09. Nutrient data within the E5 region from the PAP observatory mooring, Carbon VARIability Studies by Ships Of Opportunity project (CAVASSOO) and the British Oceanographic Data Centre (BODC) showed that the standard deviations shown in **Figure 4.10** for the WOA09 climatological data were substantially underestimated (**Figure 4.11**). Therefore, the method of estimating spatial variances applied to the CPR z-scores was adapted to estimate temporal variances, by using the temporal/spatial ratios from the SeaWiFS chlorophyll data applied to the WOA09 nutrient data. Temporal variances associated with the WOA09 nutrient climatologies were estimated using **Equation 4.29**.

$$\sigma_{j_N \text{ temporal}}^2 = \sigma_{j_N}^2 \left(\frac{\sigma_{j_{Chl \text{ temporal}}}^2}{\sigma_{j_{Chl \text{ spatial}}}^2} \right) \quad \text{Eq. 4.29}$$

where $\sigma_{j_N}^2$ is the underestimated nutrient variance with no account of temporal variance.

The uncertainty on the nutrient data were then recalculated using **Equation 4.30**.

$$\sigma_{j_N \text{ estimated}} = \sqrt{\sigma_{j_N \text{ temporal}}^2 + \sigma_{j_N}^2} \quad \text{Eq. 4.30}$$

Figure 4.12 demonstrates the increases in the standard deviation around the monthly averages and indicates that the new estimates give an improved approximation to those calculated from the PAP mooring, CAVASSOO and BODC datasets. **Table 4.5** shows the nitrate and silicate concentrations with corresponding original calculated spatial uncertainties compared to the revised estimated (spatial + temporal) uncertainties. The revised estimated nitrate and silicate uncertainties are subsequently used for model assessment.

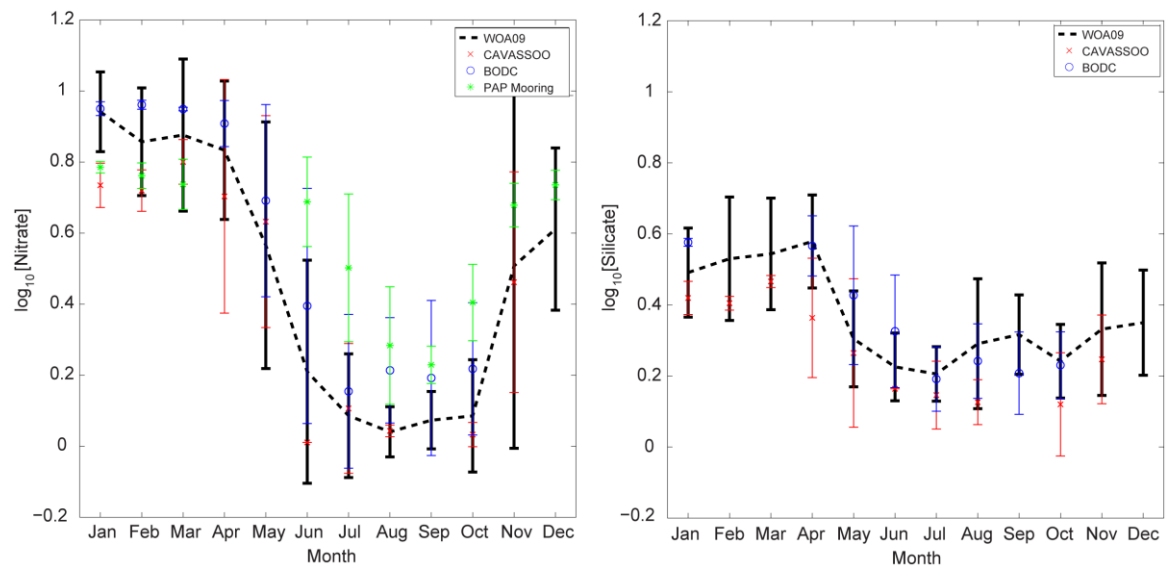


Figure 4.12: Comparison of nutrient data from the WOA09 (black) with temporal variance estimation to that from CAVASSOO (red), BODC (blue) and the PAP mooring (green) for nitrate and silicate.

Table 4.5: Monthly averaged nutrient concentrations within the E5 region from 2001 to 2007 and original spatial uncertainties and revised estimated uncertainties including temporal variance.

Month	log ₁₀ [Nitrate]			log ₁₀ [Silicate]		
	Average	Spatial Uncertainty	Estimated Uncertainty	Average	Spatial Uncertainty	Estimated Uncertainty
Jan	0.9415	0.0594	0.1122	0.4910	0.0664	0.1254
Feb	0.8572	0.0565	0.1516	0.5299	0.0648	0.1738
Mar	0.8761	0.0780	0.2141	0.5435	0.0573	0.1573
Apr	0.8334	0.0934	0.1949	0.5785	0.0627	0.1309
May	0.5657	0.1180	0.3471	0.3042	0.0459	0.1350
Jun	0.2098	0.0753	0.3140	0.2254	0.0229	0.0955
Jul	0.0860	0.0724	0.1740	0.2055	0.0319	0.0767
Aug	0.0405	0.0352	0.0706	0.2905	0.0911	0.1828
Sep	0.0732	0.0520	0.0808	0.3163	0.0720	0.1118
Oct	0.0854	0.0855	0.1581	0.2414	0.0561	0.1038
Nov	0.5077	0.1838	0.5135	0.3317	0.0668	0.1866
Dec	0.6115	0.1577	0.2284	0.3499	0.1022	0.1480

4.6 Summary

Within this chapter a model has been described which forms the basis of an investigation into how the ecological function of dinoflagellate bioluminescence can be modelled and its potential impacts upon a modelled ecosystem. Given the findings of **Chapter 3**, it is assumed that within the waters surrounding the PAP observatory the seasonal variations of the dinoflagellate community as a whole can be used as a proxy for those of the bioluminescent dinoflagellate community and that, on average, bioluminescent dinoflagellates make up a constant fraction of the total dinoflagellate population over a typical year. These assumptions have led to the development of a simple zero-dimensional biogeochemical model which includes a dinoflagellate PFT. The model is intended to simulate seasonal changes in the ecosystem surrounding the PAP observatory for a typical year between 2001 and 2007. Within this model dinoflagellates are assumed to be photoautotrophic and this assumption has been justified in **Section 4.2**.

Datasets for MLD, PAR and below mixed layer nitrate and silicate concentrations, which are used for forcing seasonal changes in the biological ecosystem, have been described. The chapter also described datasets to be used to assess model performance. Data has been identified which allows comparison between model output and real observations across four out of the five state variables. These include mixed layer nitrate and silicate concentrations, the relative seasonal variation of diatoms and dinoflagellates and the seasonal change in total phytoplankton biomass.

Chapter 5 will describe the parameterisation of the model through the use of a micro-genetic algorithm (μ GA). The modelled system will be assessed and the monthly datasets that have been set out in **Section 4.5** will be used to quantify model performance.

Chapter 5: Modelling Dinoflagellates – Model Parameterisation and Assessment

5.1 Introduction

The structure of an ecosystem model including a dinoflagellate phytoplankton functional type (PFT) was described in **Chapter 4**. This model forms the basis for a study into how the ecological function of dinoflagellate bioluminescence might be modelled and the resulting impacts upon the modelled ecosystem (**Chapter 6**). However, first the ecosystem needs to be assessed without terms representing dinoflagellate bioluminescence in order that their impacts can be clearly identified later.

In this chapter, the selection of model parameters, using a stochastic optimisation technique and several synthetic datasets, is described. The sensitivity of the model to the parameterisation is then evaluated. A baseline model run, containing no representation of dinoflagellate bioluminescence, is presented and the dynamics of this modelled ecosystem are examined. Model performance is assessed through comparison of model output to the observational datasets previously set out in **Chapter 4**.

5.2 Methods

5.2.1 Model Simulations

The differential equations for the model, set out in **Chapter 4**, were solved using a fourth-order Runge-Kutta algorithm (for more information on this method the reader is referred to Press et al., 1996). The model was run using a time step of 0.01 days and model spin up was carried out for a period of 9 years to ensure a repeating seasonal cycle had been reached. Simulated data for the tenth year of model runtime were taken as model output. Model output was confirmed to be independent of initial conditions by running the model with fixed parameterisation from a range of different initial conditions and analysing the sum of differences squared between tenth year model runs.

5.2.2 Cost Function

To assess model performance a cost function was constructed. The cost function provides a non-dimensional value which quantifies the misfit between model output and observational data and is therefore indicative of the "goodness of fit" (Allen et al., 2007). It is defined as the sum of weighted least square misfits between model output and observations (Schartau and Oschlies, 2003a). The closer the cost function is to zero the better the model is said to perform.

The model was assessed on its ability to recreate the relative seasonal variation of diatoms and dinoflagellates and the seasonal changes in chlorophyll, nitrate and silicate concentrations. All observational datasets, for use in model assessment (**Chapter 4**), were log transformed to ensure an approximate normal distribution before averaging into monthly values. Approximation to a normal distribution was necessary because the cost function makes the assumption that observational errors are Gaussian. Model output for chlorophyll, nitrate and silicate state variables were also log transformed and averaged to monthly values for comparison with the corresponding observations, given in **Tables 4.3** and **4.5** respectively. The same processes were carried out for model diatom and dinoflagellate state variables. However, in addition to this, the monthly averages were standardised into z-scores (as in **Equation 4.22**) to be compared with corresponding CPR abundance z-scores given in **Table 4.4**.

The cost function is the sum of the misfits between model output and observations over the 5 different data types. The individual misfit of each data type was calculated as

$$CF_j = \frac{1}{N} \sum_{n=1}^{12} \frac{(y_{jn} - o_{jn})^2}{\sigma_{jn}^2} \quad \text{Eq. 5.1}$$

where j represents each of the 5 different data types (nitrate, silicate, chlorophyll, diatom z-score, dinoflagellate z-score), y_{jn} is the averaged model output in month n of data type j , o_{jn} is the averaged observation in month n of data type j , σ_{jn} is the estimated uncertainty associated with o_{jn} and $N = 12$ (the total number of observations within each data type over the year).

The cost function was therefore defined as

$$CF = \sum_{j=1}^5 CF_j \quad \text{Eq. 5.2}$$

The cost function can be highly sensitive to the uncertainty estimate (σ_{j_n}) on the observed data (o_{j_n}). A large uncertainty estimate associated with an observation will lead to a lower cost than if there was a smaller uncertainty estimate associated with the same observation. This should be kept mind when using the cost function to assess model performance.

5.2.3 Micro-Genetic Algorithm

Parameterisation of biological models is notoriously problematic. Many parameter values are poorly constrained and often difficult or impossible to determine (Franks, 2009). Difficulties are compounded by the aggregation of phytoplankton species within models which is required to minimise complexity. For example, although growth rates can be obtained for individual species within culture, it is difficult to obtain a growth rate representative of a heterogeneous phytoplankton community in the ocean. Parameter optimisation techniques allow parameter values, including those which it might never be possible to measure, to be estimated by utilising the assumed structure and interactions represented by the model. There are several optimisation techniques available to modellers, including annealing algorithms, genetic algorithms and variational adjoint techniques (Friedrichs, 2001; Schartau and Oschlies, 2003a; Kidston et al. 2011). All of these techniques allow a set of parameter values (a parameter vector) to be found which minimises the misfit (cost function) between model output and a set of observations. In this way it is possible to use abundance and environmental data to infer process rates, for instance related to zooplankton grazing and phytoplankton growth. The advantage of estimating model parameters in this way is that assigned values are based on the behaviour of all components in the observed ecosystem interacting (Ward et al. 2010).

Within this study model parameter values (**Table 4.1**) were estimated through the use of a micro-genetic algorithm (μ GA) following a similar procedure to Schartau and Oschlies (2003a). The μ GA is an automated stochastic optimisation technique that operates on a Darwinian principal of "survival of the fittest" and is crudely based on the mechanics of genetics (Carroll, 1996; Goldberg, 1989). A flow diagram illustrating the general processes carried out by the algorithm is given in **Figure 5.1** and is described below.

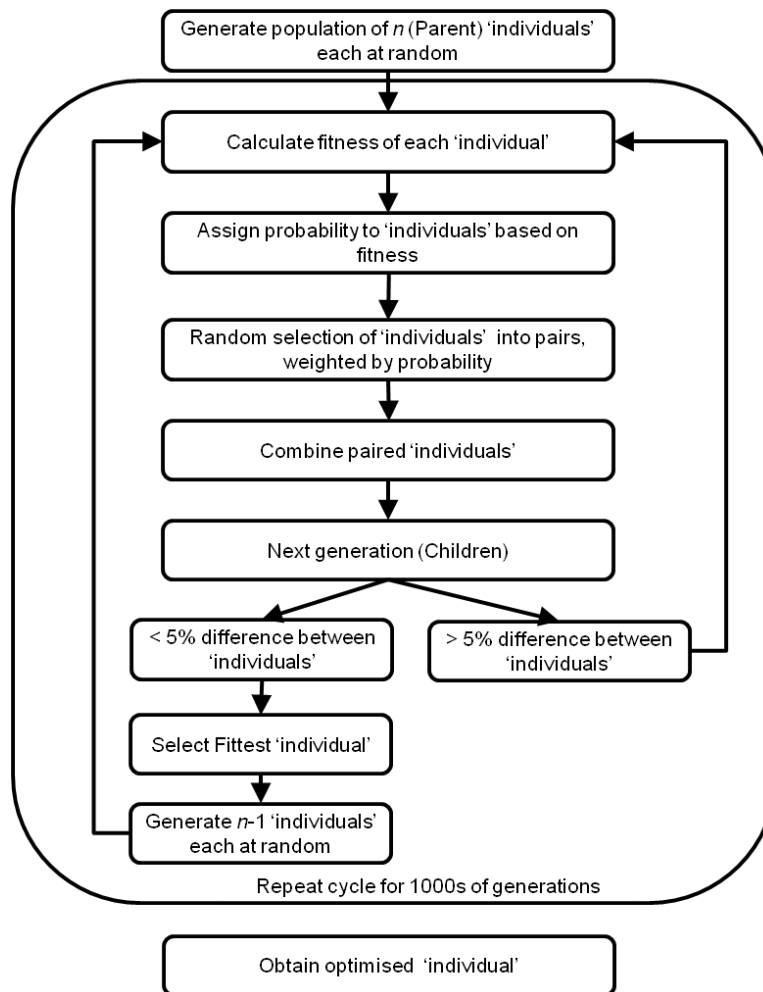


Figure 5.1: Flow diagram illustrating the general optimisation process of a μ GA. 'Individuals' are representative of a parameter vector made up of a set of parameter values.

The algorithm starts by generating a population of n random parameter vectors (parents) each containing N parameters. Each parameter value is randomly chosen from within a parameter specific predefined range. The model is run independently using each parameter vector and each vector is assigned a misfit value (referred to as cost from here on) using a cost function. Parameter vectors are then randomly combined into $n-1$ pairs, weighted according to cost. Parameter vectors with low costs have a higher probability of being selected. Each parameter vector is then encoded into a single string of binary digits (0's and 1's) equivalent to their set of numeric values. This is achieved by converting each parameter value into a 6 bit binary number. Therefore, the parameter vector becomes a binary number $6N$ digits long. Within each pairing, a single point is randomly selected along the length of the binary string. All digits before the selected point are taken from one parameter vector and all the digits after and including the selected point are taken from the other parameter vector. The two sections are then combined to make a new parameter vector (child). This process is analogous to genetic cross over. It ensures that new points within the parameter

space are evaluated whilst retaining some information that describes the best parameters. The parameter vector with the lowest cost is retained in full and this along with the $n-1$ children parameter vectors comprise the n parent vectors for the next generation. This process is repeated for many iterations. At any point, if all parameter vectors within a single generation show less than 5% difference between each other only the best individual parameter vector is retained and a new random population of $n-1$ parameter sets is generated. A predefined number of iterations are carried out to achieve acceptable convergence and exploration of the parameter space. A detailed review of genetic algorithms can be found in Goldberg (1989) and further information regarding the μ GA technique is given by Ward et al. (2010).

5.2.4 Parameter Optimisation

Parameter estimates were obtained using the μ GA technique described in the previous section. The cost function defined in **Equation 5.2** was used to assign a cost to parameter vectors within the optimisation process. To ensure parameter estimates gained from the μ GA were not unrealistic, upper and lower limits were set for each parameter. These limits defined the range in which the optimiser could search. Explanations of model parameters are given in **Section 4.3**. All parameters in the model were optimised with the exception of the water attenuation coefficient of downwelling irradiance (k_w) which was held constant because it is a well-defined optical property of seawater. A decision was taken to optimise the coefficient representing the attenuation of light due to self shading (k_c) as its value was not thought to be sufficiently well known to fix. However, it should be noted that the value of k_c effectively parameterises attenuation of light in the water column due to suspended matter including chlorophyll containing phytoplankton. As such the value of k_c could be considered to be linked to the Chl:C ratio. As a fixed Chl:C ratio has been used to compare model simulations to observations, in future, a case could be made for fixing k_c to a constant value. Possible ranges for the 18 optimised parameters were determined from the literature. Where no literature values could be found a deliberately broad range was set to ensure potential values were not excluded. Fixed values and upper and lower bounds to be considered by the μ GA for each parameter are shown in **Table 5.1**. Due to the use of 6-bit precision in the coding procedure, $2^6 = 64$ discrete values within each predefined range could be assigned to a parameter.

The μ GA requires some parameters of its own to be set. These include the population size and number of generations. These parameters affect how efficiently the optimisation converges on a solution. The μ GA population size (n) in this study was set equal to the number of optimised parameters, in this case $n = 18$, as previous studies using an μ GA for the optimisations of a similar NPZD type model had shown matching

n to the number of parameters to be a good choice in test experiments (Schartau, 2001). Schartau and Oschlies (2003a) used a μ GA to optimise 13 parameters in an NPZD and found good convergence of the cost function using 2000 generations. However, as 18 parameters are optimised in this study, optimisations have been run for a more generous 5000 generations as in Ward et al. (2010).

Table 5.1: Parameter ranges defined from the literature for use within the parameter optimisation process. A description of model parameters is given in Table 4.1 (p.77).

Symbol	Unit	Parameter Range		Reference
		Min	Max	
<i>Optimised Parameters</i>				
<i>Phytoplankton</i>				
μ_1	day^{-1}	0.4	5.9	Reviewed in Sarthou et al (2005); Smayda (1997)
μ_2	day^{-1}	0.09	2.7	Chang and Carpenter (1994); Juhl (2005); Jeong and Latz (1994); Tang (1996); Hensen et al. (2000); Hensen and Nielson (1997); Baek et al. (2007); Beak et al. (2008); Smayda (1997)
k_{n1}	mmol m^{-3}	0.1	5.1	Sarthou et al (2005)
k_{n2}	mmol m^{-3}	0.01	2	Ignatades et al. (2007); Qasim et al (1973); Baek et al (2008); Kudela et al (2008); Kudela et al (2010); Seeyave et al (2009); Kudela and Cochlan (2000)
k_{Si}	mmol m^{-3}	0.2	4	Sarthou et al (2005)
α_1	$(\text{Wm}^{-2})^{-1}\text{day}^{-1}$	0.001	0.1	Sarthou et al (2005); Popova and Srokosz (2009); Maranon and Holligan (1999); Denman and Pena (1999); Fasham (1993).
α_2	$(\text{Wm}^{-2})^{-1}\text{day}^{-1}$	0.001	0.1	Popova and Srokosz (2009); Maranon and Holligan (1999); Denman and Pena (1993); Fasham (1993).
V_{diatom}	m day^{-1}	0.1	2.5	Sarthou et al (2005)
m_p	day^{-1}	0.01	0.5	Fasham (1993); Losa (2004); Merico et al (2004); Sarthou et al (2005)
k_{mp}	mmol m^{-3}	0	1	
<i>Zooplankton</i>				
g	day^{-1}	0.4	3	Losa (2004); Fasham (1993); Petzoldt et al (2009); Odate and Imai (2003); Obayashi and Tonove (2002)
k_z	mmol m^{-3}	0.01	3	Losa (2004); Sarmiento et al (1993); Fasham (1993)
β		0.1	1	Evans and Parslow (1985); Fasham (1993)
ϵ	day^{-1}	0.01	0.5	Losa (2004); Samiento et al (1993); Fasham (1993); Edvardsen et al (2002)
$k_{m\epsilon}$	mmol m^{-3}	0	0.55	
<i>Other</i>				
τ		0.001	1	
m	m day^{-1}	0	0.01	Upper limit taken from Fasham (1993)
k_c	$\text{m}^2(\text{mmol N})^{-1}$	0.01	0.2	Fasham (1993)
<i>Fixed Parameters</i>				
Symbol	Unit	Value		Reference
k_w	m^{-1}	0.04		Fasham (1993); Schartau and Oschlies (2003a)

The use of a μ GA can have some limitations. For example, as with other optimisation techniques, it can be sensitive to the initial parameter values used at the beginning of the optimisation (Ward et al., 2010). Another limitation is that convergence on the global minimum of the cost function (i.e. the optimal solution) within the set number of iterations cannot be guaranteed (Ward et al., 2010). These issues were addressed through the use of the multiple optimisation procedure, shown in **Figure 5.2**. Multiple optimisations (ten) were carried out with different sets of randomly generated initial parameters. This maximised the search over parameter space. The parameter vector with the lowest cost across these multiple optimisations was then used as the starting point (i.e. the initial parameter vector) for a further set of optimisations (five). This multiple step process increased the likelihood that the μ GA converged on a solution. It also increased confidence that the final selected parameter vector was the optimum in the parameter space explored. However, it must be noted that there is no guarantee that this was the case.

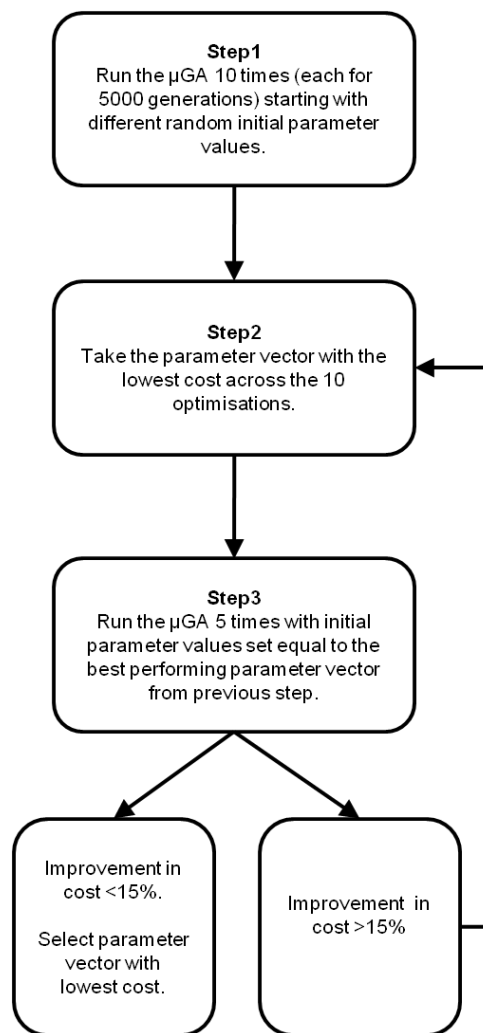


Figure 5.2: Parameter optimisation procedure to increase confidence in solutions gained using the μ GA.

Within steps one and three, ten and five optimisation runs were chosen, respectively, because this was the maximum number of runs that could be carried out in a sensible timeframe (3–4 days) given computational limitations. Steps two and three were repeated if the minimum cost reached at the end of step three was greater than 15% different to that previously found at the end of step one. This level of improvement was felt to warrant the extra computational power and time required to run additional optimisations and the above method performed is seen to perform well in the Twin experiment presented in **Section 5.3.1**.

5.2.5 Twin Experiment

Twin experiments are often used as a first step in model parameterisation through data assimilation techniques. They provide a method to test the ability of the optimisation technique, in this case the μ GA, to recover parameters and reproduced assimilated data which are known to be consistent with the forward model. A twin experiment was carried out to assess the ability of the μ GA to 1) find a parameter vector that recreates a given dataset and 2) recover a known set of optimal parameter values. The experiment required an idealised dataset generated by the model itself. The idealised dataset was produced by running the model using parameter values optimised to the observational data presented in **Chapter 4 (Table 5.2)**. The model output was processed into monthly averages as described in **Section 5.2.2**.

Table 5.2: Parameter values which created the model generated data used in the twin experiment.

Parameter	Unit	Parameter Value
<i>Phytoplankton</i>		
μ_1	day^{-1}	3.5429
μ_2	day^{-1}	0.7529
k_{n1}	mmol m^{-3}	2.4016
k_{n2}	mmol m^{-3}	0.0732
k_{Si}	mmol m^{-3}	2.3714
α_1	$(\text{Wm}^{-2})^{-1}\text{day}^{-1}$	0.0984
α_2	$(\text{Wm}^{-2})^{-1}\text{day}^{-1}$	0.0953
V_{diatom}	m day^{-1}	0.3286
m_p	day^{-1}	0.4456
k_{mp}	mmol m^{-3}	0.6987
<i>Zooplankton</i>		
g	day^{-1}	1.7206
k_z	mmol m^{-3}	2.7627
β		0.8571
ϵ	day^{-1}	0.3911
k_{me}	mmol m^{-3}	0.2537
<i>Other</i>		
τ		0.7146
m	m day^{-1}	0.0000
k_c	$\text{m}^2(\text{mmol N})^{-1}$	0.0281
k_w	m^{-1}	0.04

To conduct the twin experiment, parameter optimisation was performed treating the idealised dataset (**Table 5.3**) as "real" observational data in the cost function. As these data were generated by the model itself it is known that the model can reproduce them. Therefore, the ability of the optimisation process to recreate a given dataset can be assessed. As the parameter vector used to create the idealised data is also fully known the ability of the optimisation process set out in **Section 5.2.3** and **2.2.4** to recover the parameter vector can also be explored.

For the twin experiment the uncertainties associated with the idealised data to be used in the cost function (σ_{jn}) were set equal to those associated with the observations presented in **Chapter 4**. Model parameters were optimised to the idealised data through the process described in **Section 5.2.4**. The model was then run using the optimised parameter obtained and monthly averaged model output was compared to the idealised dataset. The optimised parameter vector was also compared to the parameter vector known to have created the idealised data. This experiment tested the ability of the optimiser both to reproduce the assimilated data and to recover a known set of parameters with the same constraints on the data that would be used for fitting the model to observational data.

Table 5.3: Idealised dataset generated by the model for use in the twin experiment.

Month	Nitrate	Silicate	Chlorophyll	Diatom z-scores	Dinoflagellate z-score
Jan	0.8068	0.6002	-0.7793	-0.5946	-1.2388
Feb	0.8640	0.6113	-0.6664	-0.2452	-1.1026
Mar	0.8549	0.5996	-0.5222	0.3854	-0.9340
Apr	0.8045	0.5480	-0.3086	1.5731	-0.4250
May	0.6780	0.3971	-0.2093	2.2075	0.0245
Jun	0.4814	0.2334	-0.2151	0.9217	1.3874
Jul	0.1613	0.1756	-0.2882	-0.2741	1.7208
Aug	0.0297	0.1917	-0.5782	-0.8041	-0.0397
Sep	0.1144	0.2834	-0.4040	-0.8365	1.1873
Oct	0.3171	0.3437	-0.4533	-0.8236	0.7994
Nov	0.5170	0.3957	-0.6192	-0.7788	-0.2967
Dec	0.6986	0.5249	-0.7765	-0.7309	-1.0825

5.2.6 Model Calibration

Calibration of the model was undertaken with the aim of finding the parameter set that most accurately represented the seasonal variation in the observations. It is good practice to calibrate a model with a different dataset to the one used for model assessment otherwise the predictive skill of the model cannot be fully evaluated in an unbiased manner. This procedure is often limited by the availability of adequate data (Janssen and Heuberger, 1995). A common practice to overcome such limitations is to

split datasets and use one part for model calibration and another for model assessment (cross-validation). However, the observational dataset to be used in this study was considered too small to be split and still retain an accurate description of the average seasonal variability of each observed variable. Therefore, calibration of the model was instead carried out using several sets of synthetic data.

Synthetic data were generated by estimating the statistical distribution of chlorophyll, nutrient and phytoplankton observations in each month. It was found that log transforming the data gave Gaussian distributions, well described by using calculated averages and associated standard deviations. A number of data points, equal to the number of real observations, were randomly chosen from Gaussian distributions with these properties. The synthetic data were then averaged in the same way as their corresponding real observations (**Chapter 4**) to produce a synthetic dataset. Synthetic phytoplankton averages were once again standardised into z-scores for comparison to model output. An example of synthetic dinoflagellate abundance data is shown in **Figure 5.3** and indicates that synthetic data retains the broad seasonal trend present in the observational data.

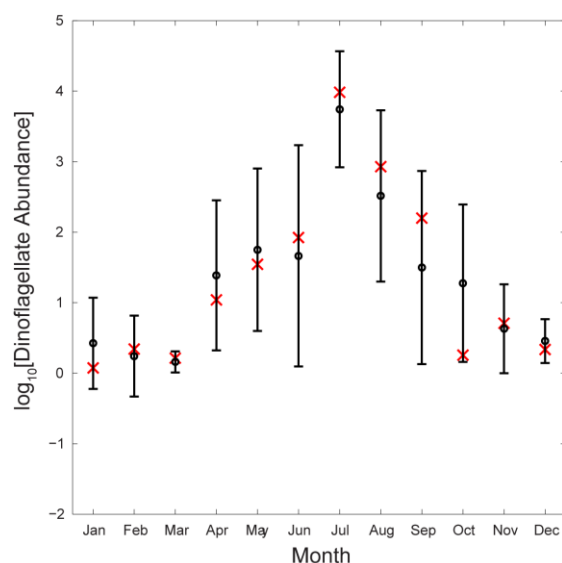


Figure 5.3: Example of averaged synthetic dinoflagellate abundance data (red x) in comparison to averaged true observational data (black o) and associated uncertainty.

The synthetic datasets were comparable to those that would be obtained through data splitting. This is because the datasets created from splitting data should also share the distribution of the full observational dataset. Both these methods assume that the distribution of the full observational dataset is representative of some “true” distribution which would be found if an infinite number of observations were taken. An advantage of using synthetic data generation is that it allows an infinite number of

datasets for model calibration to be obtained, without decreasing the size of the dataset used for model assessment.

To calibrate the model, four synthetic datasets were generated. The model was optimised to each of the synthetic datasets in turn following the procedure set out in **Section 5.2.4**. Thus, four optimised parameter vectors were obtained, one for each synthetic dataset. The model was then run using each of the optimised parameter vectors in turn. Model output from each run was compared to all four synthetic datasets and the cost function quantifying the misfit between model output and each synthetic dataset (**Section 5.2.2**) to give a cost matrix. The parameter vector that led to the lowest total cost over all four synthetic datasets was considered to be the best performing. This parameter vector was taken forward to be used in the assessment of the baseline model against real observations.

The method of cross comparing parameter sets tuned to different synthetic datasets allowed a final parameter set to be produced that best recreated the broad scale variability in the system. Thus, parameterisation of the model was achieved with limited over-fitting to small scale variances caused by uncertainty in the observed data (i.e. measurement noise) whilst ensuring that the broad scale seasonal variation was reproduced.

The number of synthetic datasets chosen for the calibration method was limited by time. Each 5000 generation run of the μ GA optimiser took the order of 18 hours of computation. A minimum of 15 runs were required to complete the optimisation procedure for each set of synthetic data. Thus, the optimisation of model parameters to four synthetic datasets required a minimum of 1080 hours of computational time. This time was reduced substantially by running optimisations in parallel using a Condor High Throughput Computing (HTC) environment that enabled numerous processes to run on a pool of otherwise idle machines (Thain et al., 2005). Despite the reduction in computational time achieved by using the Condor HTC environment, calibration to four synthetic datasets was the largest number that could be achieved in the time frame of this study.

5.2.7 Sensitivity Analysis

Model sensitivity to each of the optimised parameters was assessed. The model was run using each of the four parameter vectors in turn, as determined by the model calibration process (**Section 5.2.6**). Perturbations were carried out on individual parameters for each parameter vector in turn whilst all other parameters were held at their optimised value. Perturbations of each parameter were made over the range of 64

values that were available for selection by the μ GA between the limits set in **Table 5.1**. Changes in cost between model output and real observations were evaluated for each perturbation of the parameter under investigation. Large increases or abrupt changes in cost indicate the model was sensitive to the parameter. A change in cost over 50 indicates the model has reached a state where the two phytoplankton groups no longer co-exist.

5.3 Results

5.3.1 Twin Experiment

Table 5.4: Model twin experiment: comparison of parameter vector used to generate assimilated data and parameter vector gained through optimisation.

Parameter	Unit	Parameter Value to generate data	Parameter value from optimisation	Percentage difference
<i>Phytoplankton</i>				
μ_1	day^{-1}	3.5429	1.3603	>50
μ_2	day^{-1}	0.7529	0.5043	<40
k_{n1}	mmol m^{-3}	2.4016	1.1317	>50
k_{n2}	mmol m^{-3}	0.0732	0.2627	>50
k_{Si}	mmol m^{-3}	2.3714	2.1302	<20
α_1	$(\text{Wm}^{-2})^{-1}\text{day}^{-1}$	0.0984	0.0859	<20
α_2	$(\text{Wm}^{-2})^{-1}\text{day}^{-1}$	0.0953	0.0434	>50
V_{diatom}	m day^{-1}	0.3286	0.7476	>50
m_p	day^{-1}	0.4456	0.1656	>50
k_{mp}	mmol m^{-3}	0.6987	0.9524	<40
<i>Zooplankton</i>				
g	day^{-1}	1.7206	1.4317	<20
k_z	mmol m^{-3}	2.7627	2.6678	<10
β		0.8571	0.8857	<10
ϵ	day^{-1}	0.3911	0.3056	<30
$k_{m\epsilon}$	mmol m^{-3}	0.2537	0.1230	>50
<i>Other</i>				
τ		0.7146	0.4291	<40
m	m day^{-1}	0.0000	0.0000	0
k_c	$\text{m}^2(\text{mmol N})^{-1}$	0.0281	0.0703	>50

The parameter set gained from the optimisation process provided a model output that compared very well with the assimilated data (**Figure 5.4**). This was confirmed in the low model to data cost of 0.1730. However, large differences in individual parameter values were seen between the optimised parameter vector and that used to generate the assimilated data (**Table 5.4**). Only the across thermocline mixing coefficient (m) had the same value in both parameter vectors. Optimised parameters with values close to those used to create the assimilated data were the zooplankton half saturation constant (k_z) and zooplankton gross growth efficiency (β) which were both within a $\pm 10\%$ margin. Silicate half saturation constant (k_{Si}) and the initial P-I slope for diatoms

(α_1) were found to be within a $\pm 20\%$ margin. However, eight of the 18 optimised parameters had values that were outside the $\pm 50\%$ margin of the parameter value used to generate the assimilated data.

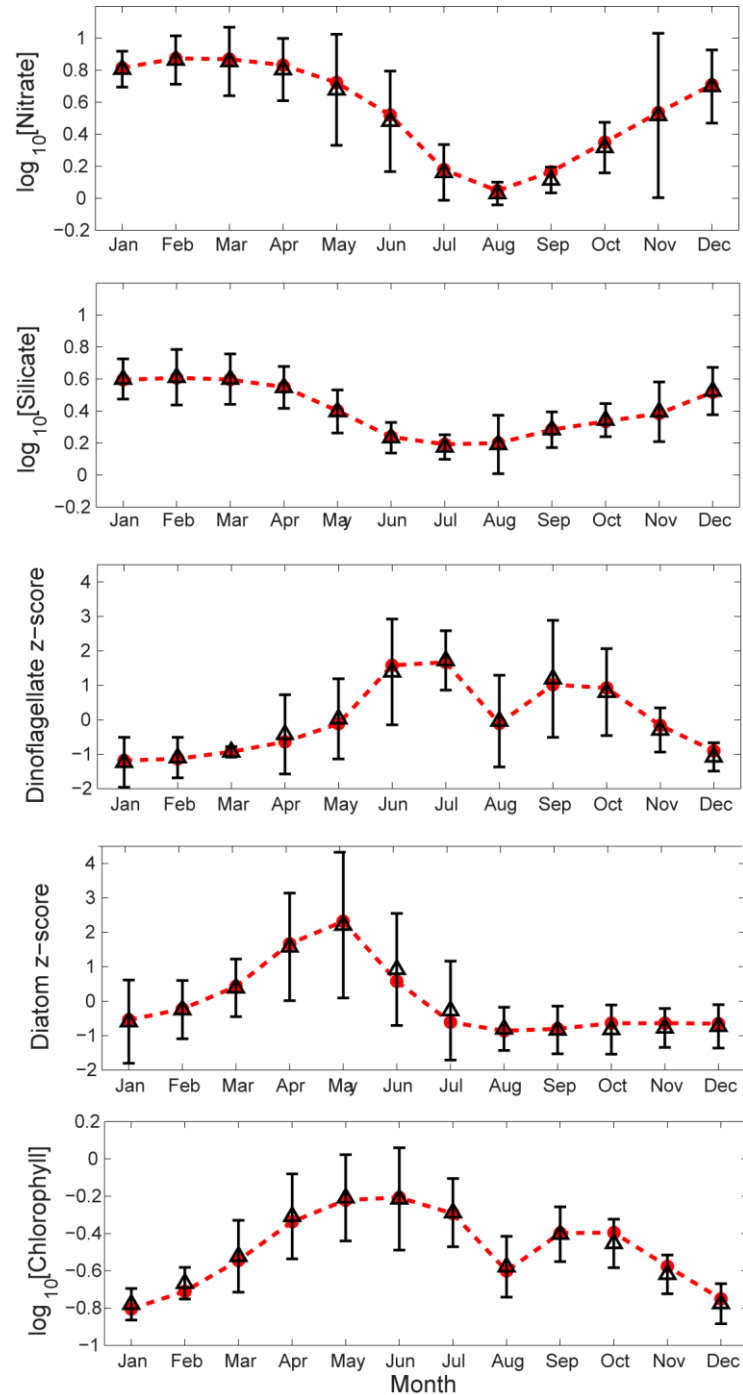


Figure 5.4: Model twin experiment: comparison of monthly averaged model output created by optimised parameter set (dashed line) and assimilated data (triangles) created by a known set of parameters. Error bars indicate uncertainties in assimilated data used in the cost function. Data has been \log_{10} transformed in order to approximate a normal distribution for use in the cost function which assumes data have Gaussian uncertainty distributions.

5.3.2 Model Calibration

Parameter optimisation was carried out on four synthetic datasets. The best performing parameter vectors for each synthetic dataset are given in **Table 5.5**. Model output obtained using each optimised parameter vector was then compared to each of the four synthetic datasets in turn to produce a cost matrix (**Table 5.6**). The parameter vector optimised to synthetic data 1 (Parameter vector 1) was found to have the lowest total cost over all four synthetic datasets; indicating that this set of parameters best replicated the general seasonal variation in the system. Therefore, parameter vector 1 (**Table 5.5**) was taken forward to be used in both sensitivity analysis and model assessment.

Table 5.5: Parameter vectors obtained from model optimisation to the four synthetic data sets. Parameter vector 1 is the optimal set of parameters found through the calibration process.

Parameter	Parameter Vector 1	Parameter Vector 2	Parameter vector 3	Parameter vector 4
<i>Phytoplankton</i>				
μ_1	1.4476	2.5825	3.1937	1.5349
μ_2	0.4629	0.5457	0.9186	0.5871
k_{n1}	0.3381	4.7032	2.6397	0.3381
k_{n2}	0.0732	0.1679	0.5154	0.3890
k_{si}	2.3714	2.4921	1.8889	1.5873
α_1	0.0969	0.1000	0.1000	0.0827
α_2	0.0607	0.1000	0.0874	0.0529
V_{diatom}	0.8238	1.1667	0.1000	1.8905
m_p	0.2511	0.4378	0.3522	0.2667
k_{mp}	0.6829	0.7463	1.0000	0.9049
<i>Zooplankton</i>				
g	1.4317	2.5460	1.1016	2.7937
k_z	1.7186	2.4779	1.8135	1.7186
β	0.8857	0.6000	0.8571	0.5714
ε	0.4922	0.3756	0.3056	0.3600
k_{me}	0.1666	0.0446	0.2276	0.0097
<i>Other</i>				
τ	0.5084	0.6353	0.6036	0.4133
m	0.0097	0.0000	0.0000	0.0008
k_c	0.0311	0.0462	0.0733	0.0914

Table 5.5 indicates that optimum values of several parameters were highly variable across the four optimised parameter vectors. Parameters with very large differences were the nitrate half saturation constants for both diatoms (k_{n1}) and dinoflagellates (k_{n2}) and the diatom sinking rate ($V_{diatoms}$). Maximum growth rate for diatoms (μ_1) and dinoflagellates (μ_2), zooplankton maximum grazing rate (g), zooplankton mortality half saturation constant (k_z), across thermocline mixing coefficient (m) and the light attenuation coefficient due to self-shading (k_c) were also found to be particularly variable. Parameters that varied little between the four parameter sets were the initial P-I slope for diatoms (α_1), silicate half saturation constant (k_{si}), zooplankton half

saturation constant (k_z), zooplankton maximum mortality rate (ϵ) and nutrient remineralisation efficiency (τ). Despite the variability in many of the parameters, some consistent trends in parameterisation were evident. For example, μ_1 was always greater than μ_2 , α_2 was never larger than α_1 and k_{n2} was always less than one. These trends will be discussed further in **Section 5.4**.

Table 5.6: Matrix of model costs gained through calibration of model parameters across four synthetic datasets. Diagonal values shown in bold indicate that assimilated data was used in the optimisation process to find the respective parameter vector.

	Parameter Vector 1	Parameter Vector 2	Parameter Vector 3	Parameter Vector 4
Synthetic Dataset 1	1.7273	1.9115	1.9724	1.8486
Synthetic Dataset 2	2.0733	2.0489	2.3421	2.2454
Synthetic Dataset 3	1.7209	1.8451	1.8899	1.7544
Synthetic Dataset 4	1.8827	2.0408	2.1119	1.9944
Total	7.4042	7.8463	8.3163	7.8428

5.3.3 Model Sensitivity

The sensitivity analysis carried out using the best performing parameter vector (parameter vector 1 in **Table 5.5**) shows that the model cost is most sensitive to the parameters for maximum growth rate of dinoflagellates (μ_2), initial P-I slope for diatoms (α_1), initial P-I slope for dinoflagellates (α_2), phytoplankton mortality half saturation constant (k_{mp}), zooplankton maximum mortality rate (ϵ) and zooplankton half saturation constant (k_z) (**Figure 5.5**). Conversely, model cost was shown to be affected very little by the values taken for the across thermocline mixing coefficient (m), sinking rate for diatoms (V_{Diatom}), zooplankton gross growth efficiency (β) and the silicate half saturation constant (k_{Si}).

Results indicate that the model cost when using the best performing parameterisation was particularly sensitivity to the dinoflagellate maximum growth rate when perturbed above a value of 1.52 day^{-1} which prevented co-existence between the two phytoplankton groups. This was in contrast to the diatom maximum growth rate which had little influence upon the cost achieved unless the very lowest value in the parameter range was chosen. Model cost was also seen to be sensitive to the initial P-I slope of both phytoplankton groups. A value of less than $0.02 \text{ (W m}^{-2}\text{)}^{-1} \text{ day}^{-1}$ for the initial P-I slope of diatoms prevented coexistence between phytoplankton groups and values less than $0.02 \text{ (W m}^{-2}\text{)}^{-1} \text{ day}^{-1}$ for the P-I slope of dinoflagellates also caused a steep increase in cost. Results also suggested that for the current parameterisation the model becomes unstable at zooplankton mortality rates less than 0.05 day^{-1} as this led to the phytoplankton being grazed to near extinction within the system. The model cost was equally affected by the zooplankton half saturation constant which affects

zooplankton grazing. A zooplankton half saturation constant of less than 1.3 mmol m^{-3} led to a steep increase in cost.

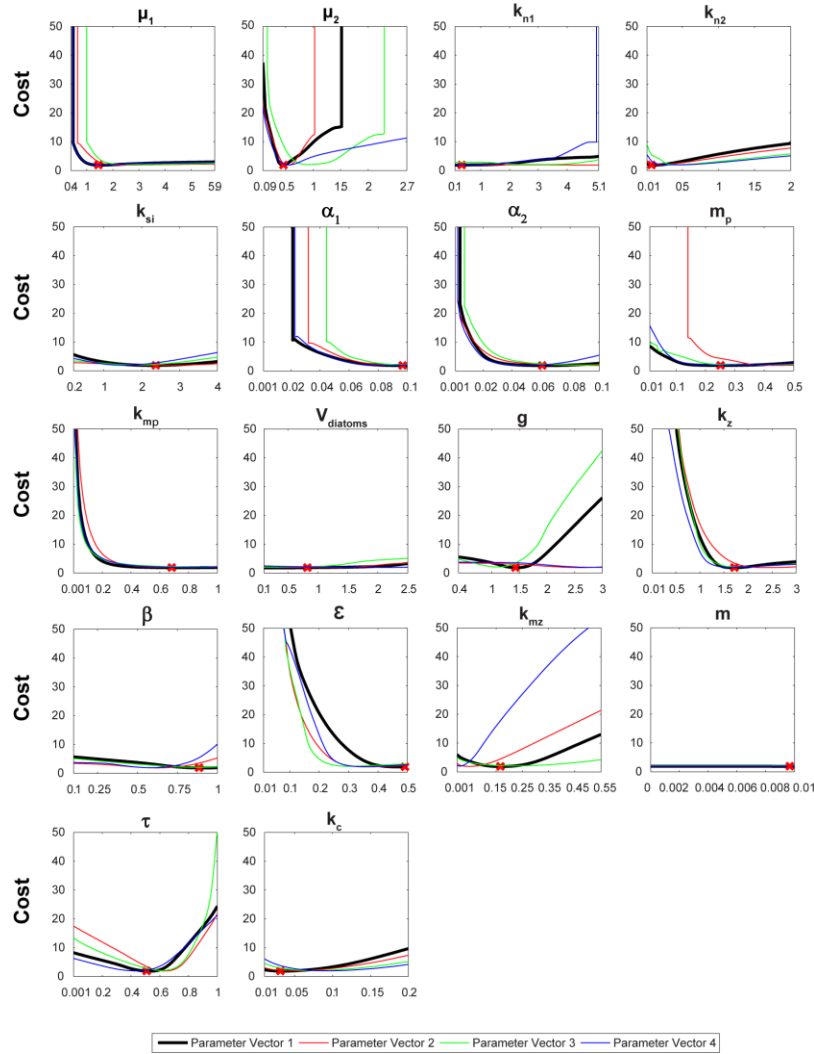


Figure 5.5: Model Cost sensitivity to perturbations in individual parameters for each of the parameter vectors obtained through optimisation. Parameters were varied individually whilst all others were held at their optimised values. Red dot indicates optimised parameter value for the best performing parameter vector, solid lines shows changes in cost between model output and real observations as the parameter varied. A cost value over 50 indicates no co-existence of phytoplankton groups.

Sensitivity analyses performed for parameter vectors two, three and four similarly show the model to be most sensitive to μ_2 , α_1 , α_2 , k_{mp} , ϵ and k_z and least sensitive to m , V_{Diatom} , β and k_{si} . However, as might be expected, the value at which coexistence of the phytoplankton types cease varies between parameter vectors for the most sensitive parameters. It is also interesting to note that there is some variation in how sensitive the model is to zooplankton maximum grazing rate (g), zooplankton mortality half saturation constant (k_{mz}) and phytoplankton mortality rate (m_p) between the four different parameter vectors.

5.3.4 Model Assessment

The model was run using the best performing parameter vector, parameter vector 1 (**Table 5.5**). Monthly averaged model output was compared to observations. The cost function, which quantifies the misfit between model simulations and observational data, was calculated as 1.8637. The contribution of the individual data types to the cost function (CF_j ; **Equation 5.1**) are shown in **Table 5.7**. These individual components can be used to assess the model's ability to simulate the observational data presented in **Chapter 4**. Assessment can be made using performance criteria that are subjectively scaled by the number of standard deviations that model simulations are away from the observations (Allen et al., 2007). Here, model assessment is made using the performance criteria suggested by Radach and Moll (2006) for a cost function as defined in **Equation 5.1**. These criteria are: $CF_j < 1$ is considered very good, 1 – 2 is good, 2 – 3 is reasonable and > 3 is poor. These criteria are refined from those originally proposed by OSPAR et al. (1998).

Table 5.7: Breakdown of calculated misfit between model output and observations

Model Output to Observational Data Misfit					
Nitrate	Silicate	Diatoms	Dinoflagellates	Chlorophyll	Total Cost
0.4788	0.2877	0.3027	0.4158	0.3788	1.8637

5.3.4.1 Nutrients

The model is able to successfully recreate the typically nutrient seasonal cycles observed in the region surrounding the PAP observatory (**Figure 5.6**). The breakdown in the cost function indicates that model simulated silicate concentrations are closer to their corresponding observations than those for nitrate (**Table 5.7**). However, using the criteria suggested by Radach and Moll (2006) to assess model performance, the model's ability to simulate both nitrate and silicate concentrations is classified as very good ($CF = < 1$).

Simulated nitrate concentrations are higher than average observations through May to December. However, concentrations in all months, with the exception of October, are within the uncertainty estimates on the observational data. Simulated silicate concentrations in the summer months of June and July are well matched to their corresponding observations. Model simulated silicate concentrations are higher than average observations through October to March but still fall within the estimated uncertainty, with the exception of the December concentration which lies just outside the uncertainty range.

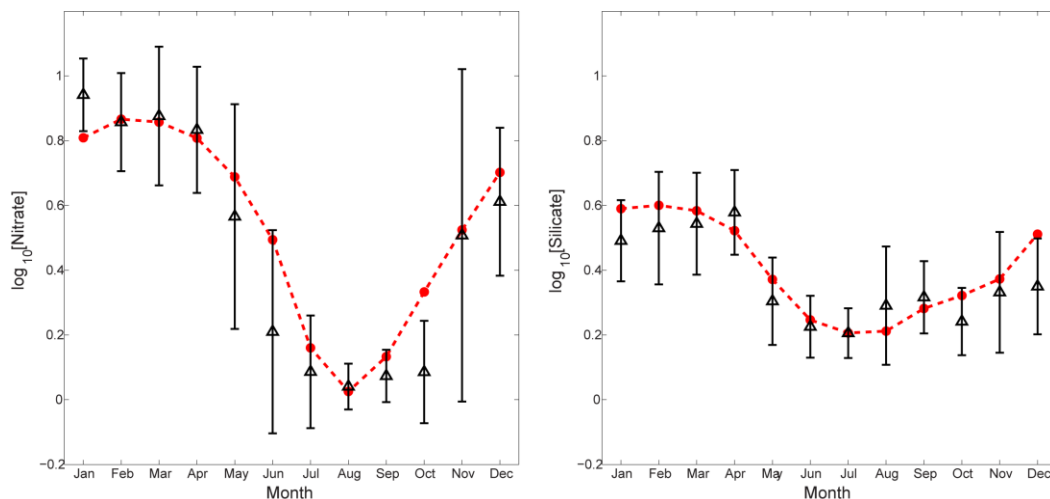


Figure 5.6: Comparison of model simulated nitrate and silicate (red dashed lines) against observations taken from the WOA09 dataset (black triangles). Data has been log transformed in order to approximate to a normal distribution for use in the cost function which assumes Gaussian uncertainty estimates.

5.3.4.2 Phytoplankton

Figure 5.7 shows that the model is able to accurately replicate the timing of the main peak in seasonal variability for both diatoms (April/May) and dinoflagellates (June/July). The individual contributions to the cost function indicate the model simulates the seasonal variation about the annual mean in diatoms slightly more accurately than in dinoflagellates. However, as with the nutrients, the ability of the model to simulate the seasonal pattern of both diatoms and dinoflagellates is classified as very good (Radach and Moll, 2006).

Model simulation of the seasonal variation in dinoflagellates shows two peaks, one in mid-summer and a second in autumn. The summer peak corresponds well to the pattern in the observational data, whereas the autumnal peak is not so obvious with the observational data instead suggesting a slow continuous decline in dinoflagellates into winter. All simulated dinoflagellate z-scores fall within the uncertainty estimates on the observational data with the exception of the August value which lies outside the lower uncertainty boundary and is responsible for the two peak pattern observed. Model simulation of the seasonal pattern in diatoms correctly shows a peak in early spring. However, comparison to observations indicates that the modelled spring diatom bloom may decline too quickly as the simulated z-score for the month of July is just outside the lower bound of the uncertainty estimate on the observational data. The model simulated diatom z-scores also show a slight increase in autumn as seen in the dinoflagellate z-scores. The two peak patterns in both simulations are however dependent upon only one data point.

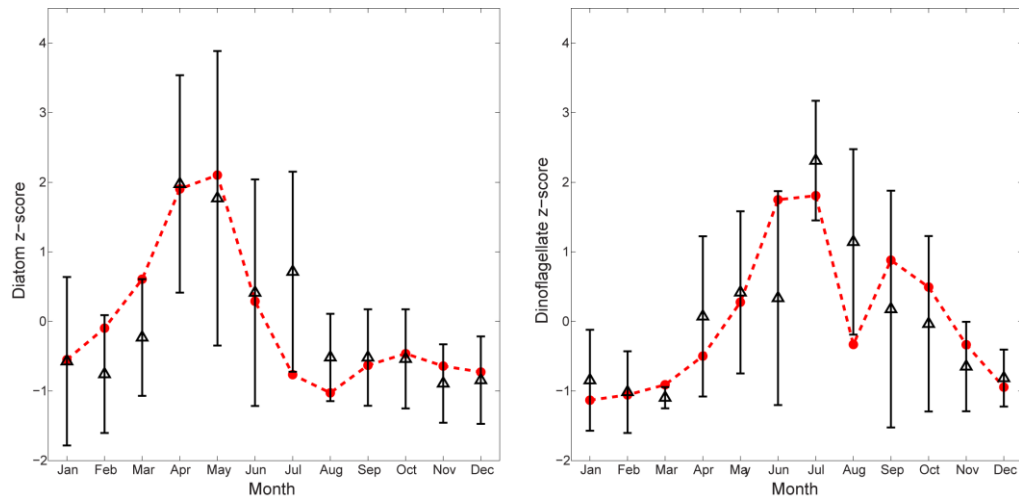


Figure 5.7: Comparison of model simulated z-scores of diatoms and dinoflagellates (red dashed lines) against observations taken from the CPR (black triangles). See Chapter 4 for details of calculation of z-score and associated uncertainties.

5.3.4.3 Chlorophyll

Figure 5.8 shows model simulations of total chlorophyll compared to observations derived from satellite remotely sensed data. Seasonal changes in modelled chlorophyll generally agree well with the observations. Assessment of the model performance using individual contributions to the cost (Table 5.7) also indicates that the model's ability to recreate the seasonal changes in chlorophyll are very good (Radach and Moll, 2006).

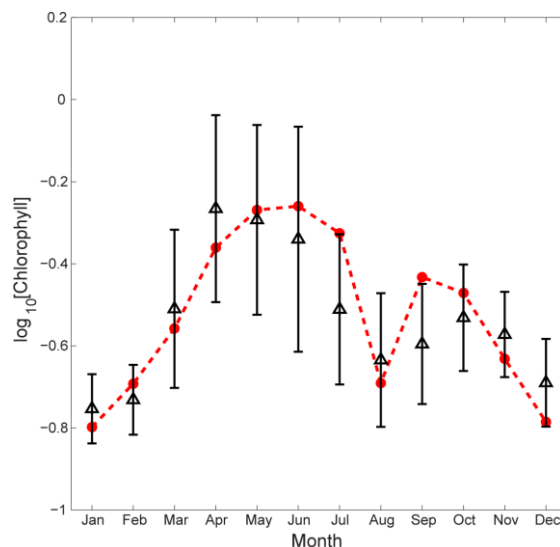


Figure 5.8: Comparison of model simulated chlorophyll (red dashed lines) against SeaWiFS satellite remotely sensed data (black triangles). Data has been log transformed in order to approximate to a normal distribution for use in the cost function which assumes Gaussian uncertainty estimates.

Modelled chlorophyll has a broad primary peak over the spring and summer months spanning both diatom and dinoflagellate blooms. Maximum chlorophyll concentration is seen to occur in June. A secondary peak in chlorophyll occurs in autumn (September). This pattern is not exactly comparable with that in the observations. The modelled primary peak lags the chlorophyll peak in the observations by two months. However, there are only small differences in average observed chlorophyll concentrations between April and June and large associated uncertainties. The secondary autumnal peak in the modelled chlorophyll precedes that in the observations by one month.

5.3.5 Model System Dynamics

Model simulations for each state variable and changes in Photosynthetically Active Radiation (PAR) and Mixed Layer Depth (MLD) used for forcing seasonal changes are shown in **Figure 5.9**.

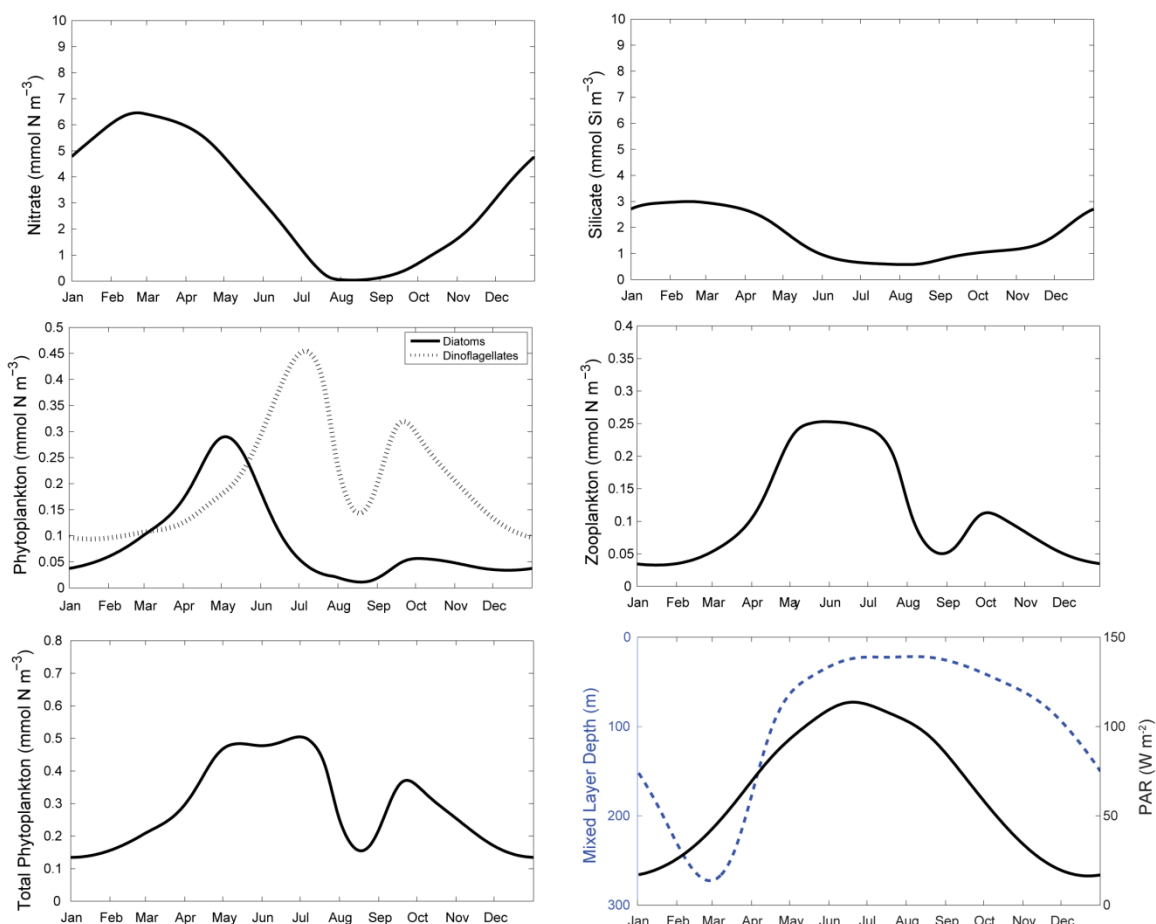


Figure 5.9: Model simulations of seasonal changes in nitrate, silicate, diatom and dinoflagellate biomass, zooplankton biomass and total phytoplankton biomass are shown (reading left to right) for a typical year (2001–2007) in the waters surrounding the Porcupine Abyssal Plain observatory. The bottom right plot shows mixed layer depth (blue dashed line) and photosynthetically active radiation (black solid line) used to force seasonal changes.

As the MLD shoals and PAR increases in early spring (April), diatoms are able to take early advantage of the improving environmental conditions due to their high initial P-I slope and increase in biomass (**Figure 5.9**). This growth of diatoms leads to a draw down in both nitrate and silicate. Dinoflagellates with their lower initial P-I slope, start to increase as the diatoms peak and begin to decline due to increasing silicate limitation. The low nitrate half saturation constant assigned to dinoflagellates allow them to uptake nitrate more efficiently at lower concentrations.

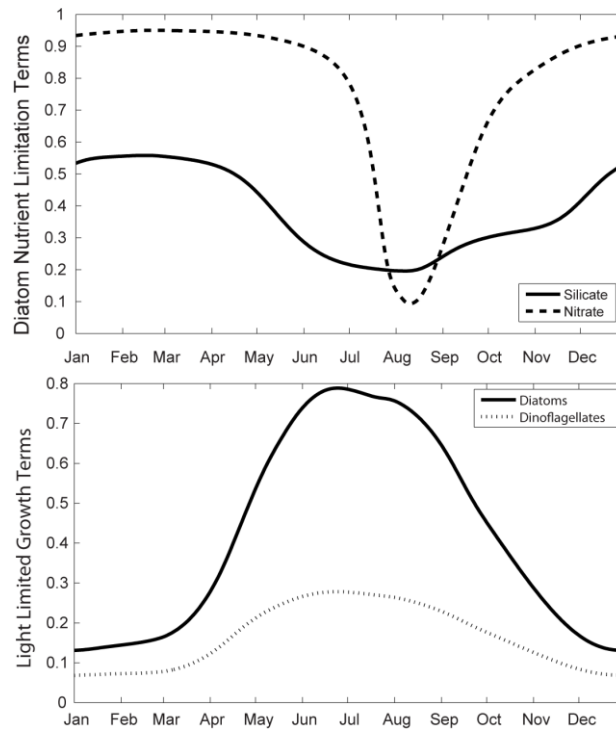


Figure 5.10: Top plot shows nutrient limitation terms for diatoms indicating silicate regulates diatom nutrient limited growth in all months except August. Bottom plot shows that diatom light limited growth (defined in Equation 4.6) is greater than dinoflagellate light limited growth.

The light limited growth term for diatoms (**Equation 4.6**) is seen to be much greater than for dinoflagellates (**Figure 5.10**). Thus, based on light limitation alone diatom growth rates would be higher than dinoflagellate growth rates throughout the year. However, specific diatom growth rates are lower than that of dinoflagellates between June and December (**Figure 5.11**). This is a result of the high silicate half saturation constant for the diatoms, set by the optimiser ($2.3714 \text{ mmol m}^{-3}$), causing diatom growth rates to remain much lower than the assigned maximum rate (μ_1) of 1.4476 day^{-1} over the whole year. Silicate was seen to be the limiting nutrient for diatom growth throughout all months of the year, with the exception of August (**Figure 5.10**). Specific diatom growth rates are only greater than that of dinoflagellates between Feb

and May when their higher initial P-I slope gives them the advantage at lower levels of irradiance (**Figure 5.11**) and allows them to bloom earlier than dinoflagellates.

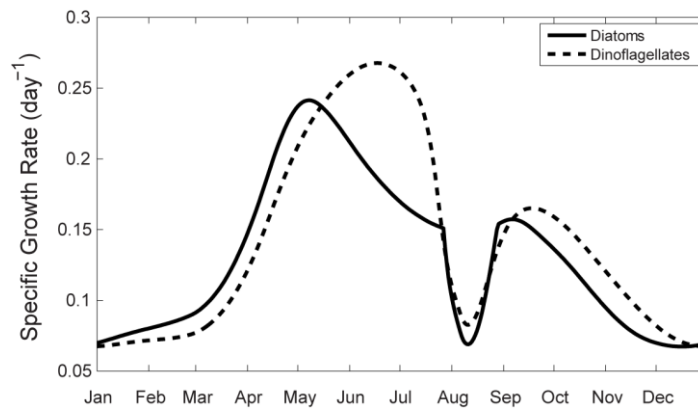


Figure 5.11: Seasonal changes of phytoplankton specific growth rates (Phytoplankton growth rates are defined in Equation 4.4 and 4.5).

Nitrate is drawn down to low levels in August and this is reflected in the dinoflagellate population which begin to decline as their growth rate becomes nutrient limited (**Figure 5.9**). However, as the MLD deepens in September, nutrient levels increase due to mixing. This increase in nutrients causes an autumnal increase in both phytoplankton types. Dinoflagellates gain a greater advantage from the increase in nutrient concentration as their stock biomass in September is much higher than that of diatoms which, because of silicate limitation during late summer had decreased to a very low level.

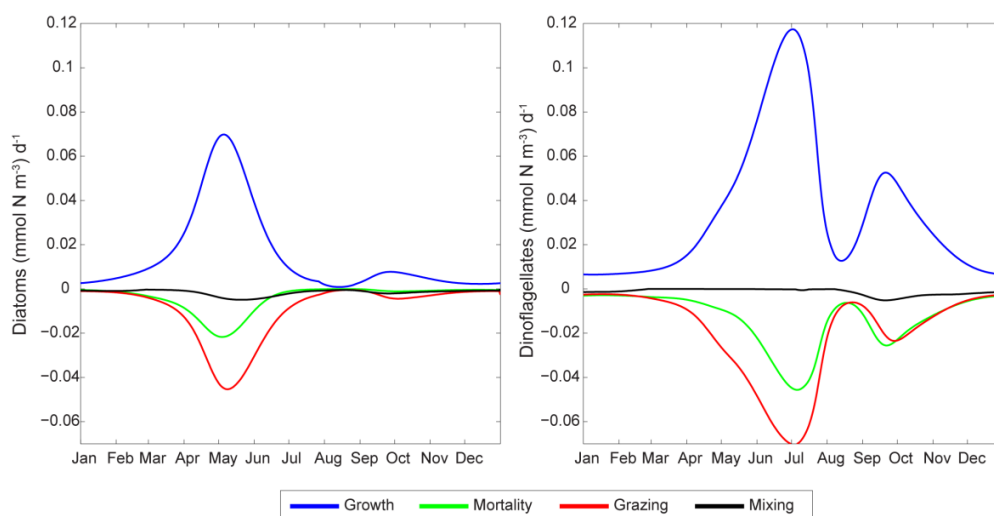


Figure 5.12: Fluxes for diatom and dinoflagellate state variables indicating zooplankton grazing is the dominant source of loss to phytoplankton.

More generally, it is interesting to note that dinoflagellate biomass stays relatively high throughout the year in comparison to diatoms (**Figure 5.9**). Although diatoms dominate the phytoplankton in April and May, dinoflagellates dominate at all other times of the year and the magnitude of the summer peak in dinoflagellate biomass is larger than that of the spring diatom peak. **Figure 5.12** shows that losses in biomass of both phytoplankton groups are dominated by zooplankton grazing rather than natural mortality, indicating that zooplankton are the primary control upon phytoplankton biomass.

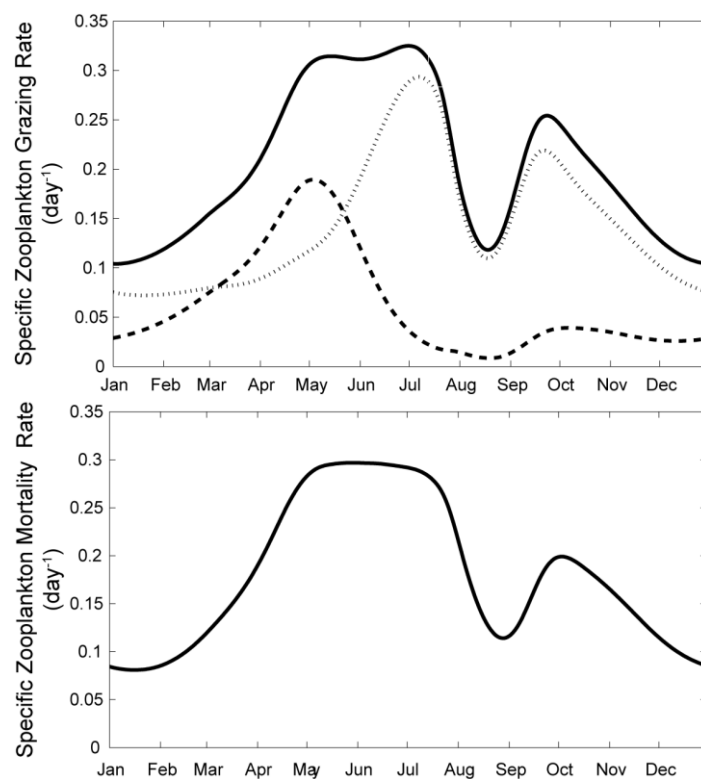


Figure 5.13: Top plot shows seasonal changes in zooplankton specific grazing rate indicating the total grazing rate on phytoplankton (solid line) and individual grazing rates on diatom (dashed line) and dinoflagellates (dotted line). Bottom plot shows seasonal changes in specific zooplankton mortality rate.

Seasonal changes in zooplankton track changes in phytoplankton (**Figure 5.8**). Zooplankton are seen to respond to the increase in phytoplankton in early spring (April) and retain a relatively constant biomass over the summer months. They then decline in August, as phytoplankton stock falls, before increasing once again in October followed by another decline into winter. Although the maximum grazing rate of zooplankton (g) was assigned a value of 1.4317 day^{-1} by the optimiser, the grazing

rate does not reach above 0.35 day^{-1} due to a high zooplankton half saturation constant of $1.7186 \text{ mmol m}^{-3}$ (**Figure 5.12**). Zooplankton grazing contributes significantly to the decline of dinoflagellates during August when zooplankton grazing rate exceeds the dinoflagellate growth rate. A high gross growth efficiency coefficient (β) of 0.8857 means much of the phytoplankton biomass grazed is available for zooplankton growth which leads to increased grazing pressure. Zooplankton specific mortality rate does not saturate at its maximum assigned value of 0.4922 day^{-1} but is relatively high, being greater than 60% of the total grazing rate in all months (**Figure 5.12**).

5.4 Discussion

A simple “NPZ type” model including a dinoflagellate phytoplankton functional type (PFT) has been calibrated and assessed against a set of observational data for the waters surrounding the PAP observatory. A μ GA was used to optimise model parameters to data.

The twin experiment indicated that the optimisation process could successfully recreate the assimilated data created from the known parameter vector ($CF = 0.1730$). However, the parameter vector obtained through the optimisation procedure was substantially different to that known to have generated the assimilated data. The variability in parameter values demonstrated by the twin experiment are consistent with results from other studies using the μ GA optimisation technique. Ward et al. (2010) found when using the μ GA to optimise 10 parameters that their values could vary across a wide range without having a significant effect upon the model fit to assimilated data. Such variability in parameter values could potentially impact upon the spatial and temporal transferability of the model using any one parameter solution (Ward et al., 2010).

Results from the twin experiment point to the model being underdetermined. Underdetermination can occur when model parameters are not fully constrained by the assimilated data. This can lead to non-unique solutions of the parameter vector. The results of the twin experiment suggest more observational data is required to fully constrain model parameters but that the current model structure is sufficient to recreate the broad seasonal changes in the system. Underdetermination is common in marine ecosystem models as data to constrain model parameters are often sparse (Matear, 1995; Fennel et al. 2001; Ward et al., 2010). Model parameters may be better constrained in future through the assimilation of zooplankton data. Lawson et al. (1995) demonstrated that recovery of biological rates using an adjoint optimisation

technique could be improved by the assimilation of zooplankton data, even if data was of reduced frequency of that available for phytoplankton. In future, further twin experiments could be conducted to investigate whether the assimilation of zooplankton data would improve the recovery of parameter values. Zooplankton data generated by the model itself could be incorporated into the twin experiment and the ability of the optimiser to recover parameter values could be compared to the results reported here.

Calibration of the model to four synthetic datasets produced four independently optimised parameter vectors. These show a large amount of variability in values for several parameters. This variability arises from the underdetermination of the system and represents the uncertainty in the parameter values that arise from potential limitations of the optimiser, potential deficiencies in the model structure and uncertainties in, or the lack of, observational data used in the cost function (Schartau and Oschlies, 2003a).

Furthermore, the ranges from which the optimisation procedure could assign parameter values used in this study were deliberately broad to ensure potential values were not excluded (Table 5.1). The use of these broad ranges could, to some extent, also explain the variability observed in model solutions in both the twin experiment and across the four vectors obtained through model calibration to synthetic data. For example, estimated ranges for phytoplankton maximum growth rate and half saturation constants were taken from both in situ and laboratory studies. Unfortunately, in situ data for phytoplankton growth is often spatially sparse and heavily skewed towards coastal waters (Furnas, 1990). As phytoplankton growth is dependent upon the rate of metabolic processes, temperature at any location or time of year can impact measured rates (Eppley, 1972). In this study values for phytoplankton growth rate and half saturation constants used to construct parameter ranges were not corrected for potential temperature effects. Thus, the ranges given for these parameters were almost certainly larger than average for the region of temperate open ocean North Atlantic being modelled. In future, it may be favourable to further restrict parameter ranges and fix values for parameters to which the model is insensitive, to better constrain the solution obtained by the optimisation procedure.

In this study the number of synthetic datasets the model was optimised to was limited by time constraints and the computational power available (**Section 5.2.6**). However, time permitting, optimisation of the model to more synthetic datasets may allow, in future, for the uncertainty associated with individual parameter values to be calculated and explored. Efron & Tibshirani (1986) suggest that between 50 and 200

bootstrapped samples (in this case synthetic datasets) would be required for adequate estimation of parameter uncertainty.

Despite the variability seen in the parameter values, several trends in the optimised parameter vectors are observed. Dinoflagellate maximum growth rate (μ_2) is always lower than diatom maximum growth rate (μ_1). This trend agrees with the known physiological traits of dinoflagellates which are observed to have lower maximum growth rates than other phytoplankton types of similar size (Banse, 1982; Litchman et al., 2007). However, it must be noted that the parameter value range for maximum growth rates of dinoflagellates is smaller than that of diatoms. Thus, there may be some bias in the optimisation process that will more readily lead to dinoflagellate maximum growth rate being set lower than diatom growth rate. Another observed trend is that the initial P-I slope of diatoms (α_1) is never lower than that of dinoflagellates (α_2). Again this trend is in agreement with the fact that diatoms are known to be generally better adapted to low-light characteristics (Le Quere et al., 2005; Litchman et al., 2007).

The results of the sensitivity analysis suggest that the model is particularly sensitive to the maximum growth rate assigned to dinoflagellates, with values at the high and low end of the parameter range preventing co-existence of the two phytoplankton groups. The model is also sensitive to the zooplankton mortality rate (ϵ). This is not surprising as it represents the model closure term. Edwards and Yool (2000) have shown that both the form of the closure term and the values of its parameters can have important influences on the dynamics of ecosystem models. Performing the sensitivity analysis across all four parameter vectors obtained from the optimiser indicates that similar patterns in cost are shown for the most and least sensitive parameters. However, this analysis also highlights that the model can have varying degrees of sensitivity to some parameters (zooplankton maximum grazing rate, zooplankton mortality half saturation constant and phytoplankton mortality) dependent on the parameter vector. The sensitivity of baseline model simulations to the uncertainty in the forcing data (shown in **Section 4.4**) was investigated by running the model forced by interannual, rather than climatological, variations in MLD and PAR (**Appendix E**). Baseline model simulations withstand interannual variations in forcing and results show that the model produces similar seasonal patterns to the climatological average when forced by interannual data over the 2001 to 2007 period (**Figure E.1**). Results also indicate that there is very little variability between the four optimised parameter vectors in terms of their ability to fit the interannual variations in the observational data (**Table E.2**). Thus, there is no evidence to suggest that the sensitivity of the model to changes in forcing differs significantly between the four optimised parameter vectors.

The initial P-I slope for diatoms (α_1) was found to vary little across the four parameter vectors gained from the optimisation to the synthetic datasets and sensitivity analysis indicated that the model is particularly sensitive to its parameterisation. The optimised value of α_1 within the four parameter vectors is towards the high end of the range available to the optimiser and the maximum value in the range ($0.1 \text{ (Wm}^{-2})^{-1} \text{ day}^{-1}$) is chosen twice. These results suggest that the upper limit in the optimisation range may be restrictive. The values assigned by the optimiser to the initial P-I slope for both diatoms and dinoflagellates are much larger than those that have been traditionally chosen for phytoplankton in modelling studies (e.g. $\alpha = 0.025 \text{ (Wm}^{-2})^{-1} \text{ day}^{-1}$ in Fasham, 1993). However, more recent studies have also found a tendency towards higher values of the initial P-I slope parameter (e.g. $\alpha = 0.256 \text{ (Wm}^{-2})^{-1} \text{ day}^{-1}$ in Schartau and Oschlies, 2003a).

Examination of the modelled ecosystem indicates that nutrient limitation is an important controlling factor of phytoplankton succession from diatoms to dinoflagellates. Although diatoms are first to take advantage of the improved environmental conditions in spring their growth rate becomes limited by declining silicate availability which allows dinoflagellates to become dominant in the summer months. The decline of dinoflagellates in August was due to a combination of nitrate depletion slowing growth rate and increased grazing by zooplankton. Grazing by zooplankton plays an important role in controlling the magnitude of the peak concentration reached in both diatoms and dinoflagellates.

Assessment of model performance indicates a very good fit between monthly averaged model simulations and monthly climatology observations for all 5 data types. The model was able to recreate both the seasonal peak in dinoflagellates (discussed and analysed in **Chapter 3**) and the seasonal peak of diatoms shown in the CPR data. Simulated nitrate concentrations were found to be slightly higher than those observed but still predominately within the uncertainty estimate and the overall seasonal pattern conformed well. Model simulations showed an autumnal increase in dinoflagellates that was not obviously present in the CPR data. However, it is possible that the model is over estimating the input of nitrate due to a deepening of the MLD in autumn and therefore allowing an increase in the simulated phytoplankton abundance that is not present in the observational data. This hypothesis is supported by the flux data which indicates that there is a large input of nitrate into surface due to a deepening of the mixed layer from the end of August into September (data not shown). This leads to simulated nitrate concentrations that are higher than observations in September and October (**Figure 5.5**). However, an autumnal increase in phytoplankton biomass is

present in the chlorophyll observations. Thus, it is also possible that during calibration there has been a trade off in the fit between different data types. For example, although the CPR data do not indicate an increase in the dinoflagellate population from August to September, this increase is required to minimise the cost between simulated and observed chlorophyll, where an increase is present, and also to draw down the nitrate concentration to an acceptable level.

Comparison of simulated and observed chlorophyll concentrations indicates a two month lag by the model in the timing of peak chlorophyll. This lag is a consequence of the summer peak in dinoflagellate biomass being greater than that of the diatom biomass peak in spring. This result suggests that the model may be either underestimating the peak in diatom biomass or overestimating peak dinoflagellate biomass. Unfortunately, observational data are not available to directly compare with simulated biomass estimates of the individual phytoplankton groups. However, data shown in Taylor (1993) taken around 47°N 20°W during May to August 1989 as part of the Joint Global Ocean Flux Study indicate that calculated biomass estimates for the summer dinoflagellate population (~50 mg C m⁻³ in mid July) were slightly higher than those for the late spring diatom population (~45 mg C m⁻³ in mid May). This may suggest that the result of the model simulation is not completely unreasonable. It is also possible that the model simulations cannot match the exact observational pattern in chlorophyll due to limitations of the model structure which does not consider other phytoplankton such as fast growing phytoflagellates or coccolithophores which may contribute to the chlorophyll signal in early spring and early summer, respectively. However, at present there is very little observational data available for these phytoplankton groups for the period and location of interest. Further discussion of the potential limitations of the model structure and the impact that the fixed C:Chl ratio may have upon the models ability to recreate patterns in observed chlorophyll are given in **Section 6.6** and **Section 7.2**.

It is difficult to assess how well the model simulates both the timing and magnitude of the seasonal changes in zooplankton biomass due to a lack of comparable in situ data. However, there have been a few studies within the northeast Atlantic that provide some spring/summer mesozooplankton biomass estimates. Dam et al. (1993) measured the biomass of zooplankton of size 0.2 to 2 mm within the North Atlantic at 47°N, 20°W between April and May 1989. They calculated a maximum zooplankton biomass averaged between day and night tows of 12.65 mg C m⁻³, approximately equivalent to 0.16 mmol N m⁻³ using a C:N ratio equal to 6.625. In the same year Lenz et al. (1993) measured the standing stock in the upper 100 m of zooplankton of the same size range. Measurements were made along a transect running from 46°N, 19°W to 46°N, 17°W between 7th – 21st May and mean standing stock was given as 1561 mg C m⁻²,

equivalent to $0.2 \text{ mmol N m}^{-3}$. Night time zooplankton dry weight (DW) ($>0.2 \text{ mm}$) taken at the PAP observatory in early August 2009 averaged 8.9 mg DW m^{-3} (Giering, unpublished). Assuming 50% of the dry weight to be carbon (Walve and Larsson, 1999) and a C:N ratio of 6.625, this is approximately equivalent to $0.05 \text{ mmol N m}^{-3}$. Model simulation gave peak zooplankton biomass (May/June) slightly higher than the upper range of the in situ estimates at $0.25 \text{ mmol N m}^{-3}$. Model simulation of zooplankton biomass for August were also slightly higher than observations averaging $0.07 \text{ mmol N m}^{-3}$. These comparisons indicate that the model may be slightly overestimating zooplankton biomass.

5.5 Summary

A simple zero-dimensional model including an explicit dinoflagellate group has been shown to successfully simulate the seasonal changes in the ecosystem surrounding the PAP observatory for a typical year between 2001 and 2007. The seasonal succession from diatoms to dinoflagellates within the modelled ecosystem is primarily controlled by the limitation of silicate. Grazing by zooplankton is an important mechanism for the decline of dinoflagellates in late summer in combination with reduced growth due to nitrate depletion. The model's ability to simulate the seasonal variation of diatoms and dinoflagellates about their annual average, seasonal changes in nitrate and silicate, and the seasonal change in chlorophyll concentration is graded as very good, being within one standard deviation of the available observational data.

Chapter 6, will now develop mathematical terms representing the potential effects that dinoflagellate bioluminescence may have upon zooplankton. These terms will be implemented in the model described in **Chapter 4** and their impacts upon model parameterisation, model performance and ecosystem dynamics will be assessed in comparison to the results shown here in **Chapter 5**.

Chapter 6: Modelling the Ecological Function of Dinoflagellate Bioluminescence.

6.1 Introduction

The ability to emit light is wide spread among marine organisms (Young, 1983; Widder 2010) and for bioluminescence to persist in the marine environment it must confer some competitive advantage (Buck, 1978). Numerous functions have been suggested that may confer a competitive advantage upon different organisms. These include luminescing to i) attract prey, ii) for intraspecies communication such as attracting a mate, and iii) to avoid predation by means of counter-illumination or startling predators. Although many suggested functions exist, there is often little evidence to support them. In many cases, functions have been inferred from an organism's morphological and physiological characteristics rather than from observational evidence (Herring, 2007). Opportunities to observe bioluminescent behaviour directly in situ are rare (Widder 2010).

The ecological advantage of a bioluminescent lure to attract prey in organisms such as deep sea angler fish is obvious. The advantage provided by bioluminescence in single celled organisms such as dinoflagellates is less so. As such, some authors have suggested that there is no selective advantage to bioluminescence in dinoflagellates and it may be only a by-product of another cellular function (Sverdrup et al., 1942; Nicol, 1967). However, as pointed out by Tett and Kelly (1973), it is unlikely that the control mechanisms for bioluminescence, such as circadian regulation and light inhibition, would survive unless bioluminescence has some ecological value. It is now generally accepted that bioluminescence can provide an ecological advantage to dinoflagellates by acting as a survival strategy.

As discussed in **Chapter 1**, two hypotheses have been put forward as to the mechanism by which bioluminescence provides a survival benefit to dinoflagellates. The first is known as the 'burglar alarm' hypothesis. This was proposed by Burkenroad (1943) who suggested, "A peridinium sieved by a copepod might by its spark of light facilitate capture of the copepod by a herring... There might thus be a net advantage to the luminescent plankton from facilitation of the capture of primary predators...". Feeding activity by copepods on bioluminescent dinoflagellates is known to produce a

bright spot of light lasting several seconds (Esaías and Curl, 1972). The peak wavelength of bioluminescent emissions (~475 nm) is also known to coincide with that required for maximum transmittance through water and the maximum visual sensitivity in many marine organisms (Tett and Kelly, 1973). Combined, this suggests that grazers feeding upon bioluminescent dinoflagellates may be highly visible to their predators. It has even been suggested that bioluminescence can act posthumously, not only indicating the location of a predator during capture, but also after ingestion as the bioluminescence could be seen through the stomach of transparent predators (Porter and Porter, 1979).

The burglar alarm hypothesis is more directly supported by the findings of Abrahams and Townsend (1993) which show that mortality rates of copepods increased by up to 70%, from 19.5 ± 5.4 deaths per hour to 33.4 ± 10.3 deaths per hour, in the presence of bioluminescence. The increased mortality rate of zooplankton should increase the survival of the bioluminescent dinoflagellates. However, assuming that predator contact is required for bioluminescence to be stimulated (Latz et al., 2004a), the burglar alarm response may not directly benefit the bioluminescent individual that is being grazed upon as it may not assist escape. Instead, the emission of bioluminescence acts to reduce grazing upon the remaining bioluminescent dinoflagellate population. As noted by Burkenroad (1943), if an ecological advantage is gained in this way the function will not only benefit the bioluminescent dinoflagellate community but also, potentially, all zooplankton prey within the surrounding region including non-luminescent phytoplankton. It is unclear if this partly altruistic behaviour would survive because there would be no selective pressure for preserving the bioluminescent response (Buck, 1978).

The second hypothesis for how bioluminescence gives an ecological advantage to dinoflagellates is known as the 'startle response' hypothesis. This suggests that bioluminescent emission during close contact with a predator startles the predator and either causes it to change course away from the bioluminescent individual (Buskey et al., 1983) or suspends its filter feeding providing the bioluminescent individual time to escape (Esaías and Curl, 1972). Experimental studies have shown that in the presence of dinoflagellate bioluminescence the ingestion rates of copepods can reduce by 30 to 70% (Esaías and Curl, 1972; White 1979). Later studies showed that in the presence of bioluminescent dinoflagellates the swimming characteristics of copepods changed, causing copepods to increase the number of high-speed swimming bursts and decrease the amount of slow-speed swimming, which is characteristic of their grazing behaviour (Buskey et al., 1983; Buskey et al., 1985). It was inferred that the high-speed swimming activity represented a startle response by the copepods and led to a reduction in copepod grazing rate. As with the burglar alarm hypothesis, should

dinoflagellate bioluminescence lead to a reduction in predator grazing rate via high-speed swimming bursts, then the potential to benefit all prey species including non-luminescent phytoplankton may exist. This is because when zooplankton are swimming at high speeds they are not only unable to graze on bioluminescent phytoplankton but also unable to graze on other phytoplankton within the region.

It is important to note that the hypothesised ecological advantages of dinoflagellate bioluminescence are not mutually exclusive. Indeed, there may be multiple mechanisms by which bioluminescence provides a survival benefit to dinoflagellates. Buskey et al. (1987) showed that the photophobic response to dinoflagellate bioluminescence observed in marine copepods was not present in fresh water copepod species. As bioluminescent dinoflagellates are not known to occur in fresh water systems the results of their study suggest that the photophobic behaviour demonstrated in marine copepods evolved in response to selective pressures. It has been speculated that copepods developed this photophobic behaviour in order to decrease the probability of being grazed upon if they encounter a bioluminescent prey. Dinoflagellate bioluminescence may have multiple functions and act to both startle zooplankton, thereby reducing zooplankton grazing efficiency, and alert higher trophic predators to the position of zooplankton, thereby increasing zooplankton mortality. The extent to which either the startle response or burglar alarm mechanisms may impact upon an ecosystem, both separately or combined, is unknown. This is due to the inability and difficulty of observing these processes under in situ or experimental conditions.

This chapter investigates how the ecological function of bioluminescence might be incorporated into a simple biogeochemical model based on the mechanisms set out above. The chapter then examines what impact terms (mathematical equations) representing the ecological function of bioluminescence have on the dynamics of a modelled system and its ability to simulate the typical seasonal change in the dinoflagellate population and the represented ecosystem as a whole. Several terms are formulated which are representative of the potential advantages provided to the phytoplankton community by dinoflagellate bioluminescence. These terms are incorporated into the simple dinoflagellate model described in **Chapter 4** and their impacts upon model performance, parameterisation and the dynamics of the modelled ecosystem are explored.

6.2 Development of Bioluminescent Terms

The following sections investigate how zooplankton grazing and mortality within the model described in **Chapter 4** may be modified to take into account the hypothesised mechanisms through which bioluminescence provides an ecological advantage to dinoflagellates.

6.2.1 Determining Parameters To Represent Bioluminescence Effect

6.2.1.1 Startle Response

A startle response in a predator to a bioluminescent flash decreases the rate at which the predator grazes on bioluminescent prey. However, it will also decrease the rate at which the predator grazes upon all prey including non-luminescent phytoplankton as it disrupts feeding behaviour more generally. Under this assumption, the startle response is best considered to affect the model terms representing the loss of phytoplankton through zooplankton grazing (**Equation 4.10**). As zooplankton (Z) are considered to graze upon diatoms (P_1) and dinoflagellates (P_2) with equal preference, the zooplankton grazing terms can be combined into a total grazing impact given by

$$Graz_p = g \left(\frac{P_1 + P_2}{k_z + P_1 + P_2} \right) Z \quad \text{Eq. 6.1}$$

where g is the zooplankton maximum grazing rate and k_z is the half saturation constant for grazing. For fixed population sizes the $Graz_p$ term can be decreased in two ways, by either decreasing g or increasing k_z .

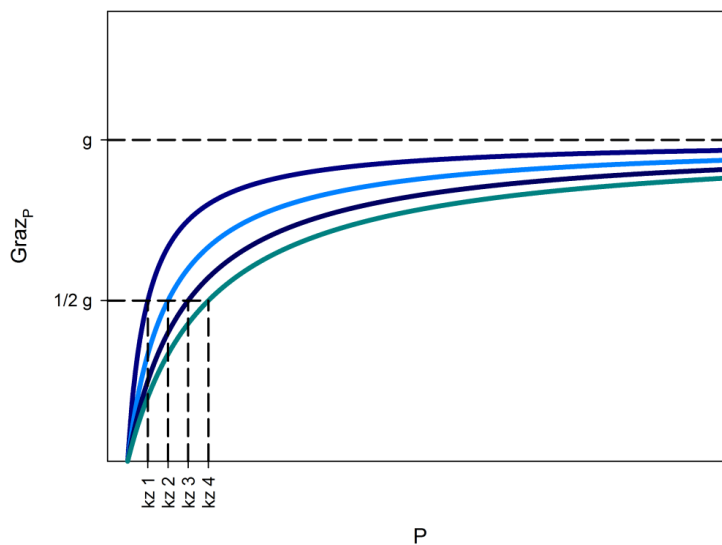


Figure 6.1: Illustration of changes to the zooplankton grazing term when varying the grazing half saturation constant (k_z).

Increasing k_z reduces the gradient of the slope in the Michaelis–Menten curve (**Figure 6.1**). This increases the abundance of phytoplankton (P) required to achieve the maximum grazing rate g .

Decreasing g reduces the maximum grazing rate which can be reached by the term (**Figure 6.2**).

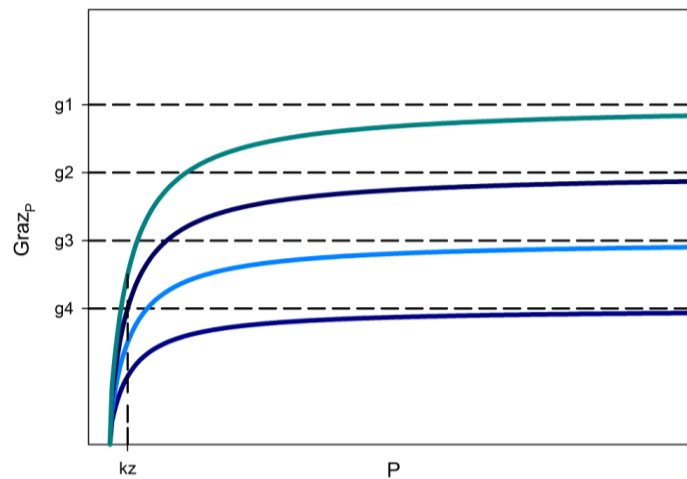


Figure 6.2: Illustration of changes to the zooplankton grazing term when varying the maximum grazing parameter (g).

Varying k_z to parameterise the effect of the startle response implies that if dinoflagellates were present in a large enough abundance, zooplankton could still obtain the same maximum grazing rate as when no bioluminescence was present. However, the results of Esaias and Curl, (1972) showed a consistently lower predator ingestion rate for samples with a higher potential for bioluminescence, regardless of culture concentration. Thus, the most appropriate way of altering the grazing term within the model to reflect a startle response to bioluminescence is through the variation of g .

6.2.1.2 Burglar Alarm

Bioluminescent emission acting as a burglar alarm will illuminate the location of predators to their own higher trophic predators. This would increase the mortality rate of predators of bioluminescent dinoflagellates. However, as the model assumes that zooplankton graze indiscriminately on all phytoplankton types, any increased mortality of zooplankton will benefit all zooplankton prey in the modelled system including non-luminescent phytoplankton. The burglar alarm response is therefore best

considered to affect the zooplankton mortality term within the model rather than the grazing term (**Equation 6.2**).

$$Mort_Z = \frac{\varepsilon Z^2}{k_{m\varepsilon} + Z} \quad \text{Eq. 6.2}$$

where ε is the zooplankton maximum mortality rate and $k_{m\varepsilon}$ is the half saturation constant for the zooplankton mortality rate.

As in the case of the grazing term ($Graz_p$) there are two ways in which $Mort_Z$ can be increased for a fixed population size, an increase in ε or a decrease in $k_{m\varepsilon}$. The mortality term in the model is assumed to include both natural and predator driven mortality losses. Therefore, it is argued that the most appropriate way to alter the mortality term is through the variation of ε , as this parameter directly constrains the rate at which zooplankton are lost through predation.

Representing the potential ecological functions of dinoflagellate bioluminescence by adjusting $Mort_Z$ and $Graz_p$ through the variation of the maximum rate parameters, g and ε , enables the terms' original hyperbolic and Hollings Type II forms to be preserved, respectively (**Section 4.3.3**). This has the advantage that the terms will still account for decreases in grazing and mortality rate at low phytoplankton and zooplankton concentrations respectively, due to the reduced likelihood of encountering predators.

6.2.2 Formulation of Bioluminescent Terms

In the formulation of bioluminescent terms it is assumed that, for the region surrounding the PAP observatory, bioluminescent dinoflagellates can be modelled as a constant fraction of the total dinoflagellate population, as demonstrated in **Chapter 3**.

6.2.2.1 Startle Response

To represent the startle response hypothesis in the model a term was required that reduced zooplankton grazing as a function of bioluminescent dinoflagellate abundance. Two different scenarios were considered.

1. Increased bioluminescent dinoflagellate abundance leads directly to increased bioluminescent emissions and reduces the zooplankton grazing rate.

2. An increased proportion of bioluminescent dinoflagellates in the total phytoplankton population (diatoms + dinoflagellates) increases the likelihood of zooplankton encountering a bioluminescent individual whilst grazing and reduces the zooplankton grazing rate.

In the first scenario zooplankton grazing rate is a direct function of bioluminescent dinoflagellate abundance. In the second scenario zooplankton grazing rate is a function of the ratio between bioluminescent dinoflagellate abundance and the total phytoplankton abundance.

Scenario One

As described in **Section 6.2.1**, the zooplankton grazing term ($Graz_p$) is most appropriately adjusted through the variation of the zooplankton maximum grazing rate (g). Therefore, assuming scenario one, g will reduce as bioluminescent dinoflagellate abundance (P_{BL}) increases. This can be achieved through **Equation 6.3**.

$$g = \left[g_{NBL} \left(1 - \left(\frac{P_{BL}}{k_g + P_{BL}} \right) \right) \right] \quad \text{Eq. 6.3}$$

where g is the now variable zooplankton maximum grazing rate, dependent on the abundance of P_{BL} , g_{NBL} is the maximum zooplankton grazing rate that would occur in an environment with no bioluminescent dinoflagellates and k_g is a half saturation constant that determines at what concentration of P_{BL} , g is half of g_{NBL} . This formulation will provide a relationship where g asymptotically approaches zero as P_{BL} increases (**Figure 6.3**).

The results of **Chapter 3** indicate that P_{BL} can be considered to represent some constant fraction, λ , of P_2 , therefore **Equation 6.3** can be rewritten as

$$g = \left[g_{NBL} \left(1 - \left(\frac{\lambda P_2}{k_g + \lambda P_2} \right) \right) \right] \quad \text{Eq. 6.4}$$

Equation 6.4 can be simplified further because λ may be combined with the half saturation constant k_g into a single parameter. This can be shown by dividing $\frac{\lambda P_2}{k_g + \lambda P_2}$ by

λ . The simplification gives

$$g = \left[g_{NBL} \left(1 - \left(\frac{P_2}{k_g + P_2} \right) \right) \right] \quad \text{Eq. 6.5}$$

where k_g now represents k_g/λ .

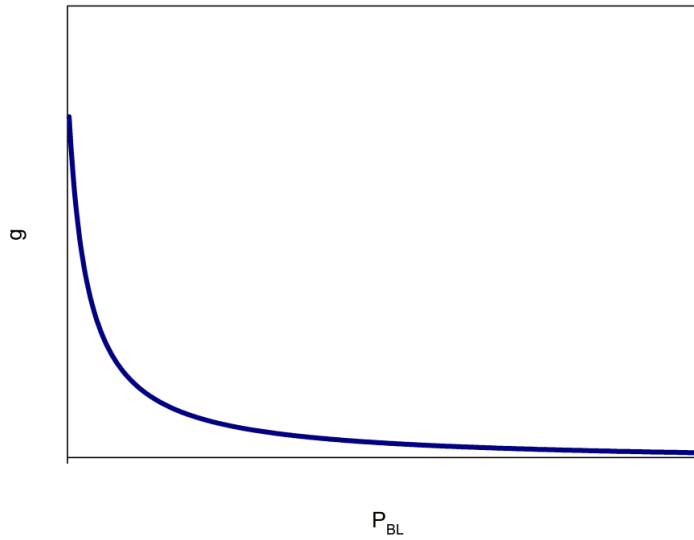


Figure 6.3: Illustration of the relationship between zooplankton maximum grazing rate (g) and bioluminescent dinoflagellates (P_{BL}) given by Equation 6.3

Scenario Two

In scenario two, g will reduce as bioluminescent dinoflagellate abundance (P_{BL}) increases as a proportion of the total phytoplankton abundance ($P_1 + P_2$). Assuming that g is at its highest value when no prey are bioluminescent (i.e. when $\frac{P_{BL}}{P_1 + P_2} = 0$) and lowest when all prey are bioluminescent (i.e. when $\frac{P_{BL}}{P_1 + P_2} = 1$), the relationship can be given by

$$g = (g_{BL} - g_{NBL}) \left(\frac{P_{BL}}{P_1 + P_2} \right) + g_{NBL} \quad \text{Eq. 6.6}$$

where g is the now variable zooplankton maximum grazing rate dependent on the proportion of P_{BL} in the phytoplankton community, g_{NBL} is the zooplankton grazing rate that would occur in an environment where no prey were bioluminescent and g_{BL} is the grazing rate which would occur in an environment where all zooplankton prey were

bioluminescent. This formulation will provide a relationship where g linearly decreases as $\frac{P_{BL}}{P_1+P_2}$ increases.

Again, because **Chapter 3** results indicate that P_{BL} can be considered to represent some constant fraction, λ , of P_2 , **Equation 6.6** can be rewritten as

$$g = (g_{BL} - g_{NBL}) \left(\frac{\lambda P_2}{P_1 + P_2} \right) + g_{NBL} \quad \text{Eq. 6.7}$$

The terms defined by **Equations 6.5** and **6.7** were taken forward to represent a startle response function for dinoflagellate bioluminescence within the model described in **Chapter 4**.

6.2.2.2 Burglar Alarm

To represent the burglar alarm hypothesis in the model a term is required that increases zooplankton mortality as a function of bioluminescent dinoflagellate abundance. As discussed previously in **Section 6.2.2.1** there are two different scenarios for how variations in bioluminescent dinoflagellates may impact upon zooplankton mortality rate.

Scenario One

As described in **Section 6.2.1**, zooplankton mortality rate ($Mort_z$) is most appropriately adjusted through the variation of the zooplankton maximum mortality rate (ϵ). Therefore, considering a scenario where zooplankton mortality is a direct function of bioluminescent dinoflagellate abundance, ϵ will increase as bioluminescent dinoflagellate abundance (P_{BL}) increases. This can be achieved through **Equations 6.8**.

$$\epsilon = \epsilon_{BL} \left(\frac{P_{BL}}{k_\epsilon + P_{BL}} \right) \quad \text{Eq. 6.8}$$

where ϵ is the variable zooplankton maximum mortality rate now dependent on the abundance of P_{BL} , ϵ_{BL} is the maximum zooplankton mortality rate which would occur if all prey were bioluminescent, and k_ϵ is the half saturation constant that determines at what concentration of P_{BL} , ϵ is half of ϵ_{BL} . This formulation will provide a relationship where ϵ asymptotically approaches ϵ_{BL} as P_{BL} increases (**Figure 6.4**).

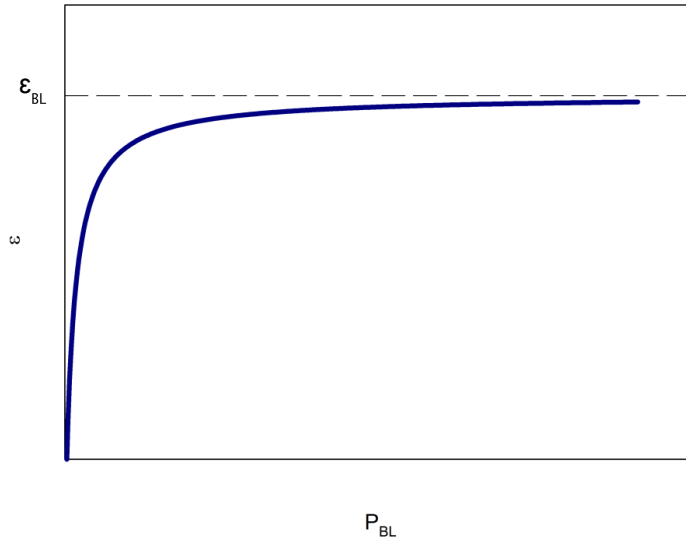


Figure 6.4: Illustration of the relationship between zooplankton maximum mortality rate (ϵ) and bioluminescent dinoflagellates (P_{BL}) given by Equation 6.8

As with **Equation 6.3** in **Section 6.2.2.1**, using the assumption that P_{BL} is some constant fraction, λ , of P_2 and simplifying so that λ is represented within the half saturation constant k_ϵ , **Equation 6.8** is reduced to

$$\epsilon = \epsilon_{BL} \left(\frac{P_2}{k_\epsilon + P_2} \right) \quad \text{Eq. 6.9}$$

Scenario Two

Scenario two considers the formulation of a bioluminescent term where zooplankton mortality rate is a function of the ratio between bioluminescent dinoflagellate abundance and the total phytoplankton abundance. In this scenario, ϵ will increase as bioluminescent dinoflagellate abundance (P_{BL}) increases as a proportion of the total phytoplankton abundance ($P_1 + P_2$). This can be achieved with a term similar to that proposed to represent the startle response in **Equation 6.6** given as

$$\epsilon = (\epsilon_{BL} - \epsilon_{NBL}) \left(\frac{P_{BL}}{P_1 + P_2} \right) + \epsilon_{NBL} \quad \text{Eq. 6.10}$$

where ϵ is the variable zooplankton maximum mortality rate dependent on the abundance of P_{BL} , ϵ_{BL} is the zooplankton mortality rate that would occur in an environment where all zooplankton prey were bioluminescent, ϵ_{NBL} is the zooplankton mortality rate that would occur with no bioluminescent dinoflagellates in an

environment. This term would provide a zooplankton maximum mortality rate (ε) that linearly increases as $\frac{P_{BL}}{P_1+P_2}$ increases.

As P_{BL} can be assumed as some constant fraction, λ , of P_2 , **Equation 6.10** can be rewritten as

$$\varepsilon = (\varepsilon_{BL} - \varepsilon_{NBL}) \left(\frac{\lambda P_2}{P_1 + P_2} \right) + \varepsilon_{NBL} \quad \text{Eq. 6.11}$$

The terms defined by **Equations 6.9** and **6.11** were taken forward to represent a burglar alarm function of dinoflagellate bioluminescence within the model described in **Chapter 4**.

Table 6.1: List of parameters used in bioluminescent terms representative of the startle response and the burglar alarm hypothesis.

Parameter	Symbol	Unit
<i>Startle Response</i>		
Zooplankton maximum grazing rate with no bioluminescent prey	g_{NBL}	day^{-1}
Zooplankton maximum grazing rate with all bioluminescent prey	g_{BL}	day^{-1}
Zooplankton maximum grazing rate half saturation constant	k_g	mmol m^{-3}
<i>Burglar Alarm</i>		
Zooplankton maximum mortality rate with no bioluminescent prey	ε_{NBL}	day^{-1}
Zooplankton maximum mortality with all bioluminescent prey	ε_{BL}	day^{-1}
Zooplankton maximum mortality rate half saturation constant	k_ε	mmol m^{-3}
<i>Other</i>		
Fraction of P_2 considered bioluminescent	λ	

In total four terms have been developed; two representative of the startle response hypothesis and two representative of the burglar alarm hypothesis. These terms require the addition of several parameters to the model which are listed in **Table 6.1**. It must be noted that the terms developed in this section make several assumptions regarding the ecological function of dinoflagellate bioluminescence. Bioluminescence is assumed to be an altruistic behaviour which is able to benefit not only the

surrounding dinoflagellate population but all surrounding phytoplankton. There is still much debate over whether genes for bioluminescence could have survived if an advantage to the bioluminescent individual does not exist. An alternate approach to the terms developed here might be to restrict the benefit of bioluminescence to solely the dinoflagellate population or to separate bioluminescent dinoflagellates from non-bioluminescent dinoflagellates within the model and restrict the benefit of bioluminescence further to only bioluminescent dinoflagellates. The terms developed also assume that there is no cost to individuals associated with bioluminescence. As discussed in **Section 1.6.3**, very little is currently known about the cost associated with bioluminescence but it may be possible in future to incorporate hypothesised costs, such as reduced growth rate of bioluminescent species, into bioluminescent terms to examine what impact they may have upon the dinoflagellate population.

6.3 Preliminary Analysis

Before detailed analysis of the effects that bioluminescence has upon model performance, parameterisation and ecosystem dynamics a preliminary analysis was carried out. The preliminary analysis aimed to examine the value of parameters in the bioluminescent terms, the impact of the terms upon model stability and their ability to provide an advantage to the dinoflagellate population. This was to ensure that bioluminescent terms behaved as expected and did not cause any adverse effects upon the model (e.g. prevented coexistence of phytoplankton groups). The four terms formulated to represent both the burglar alarm and startle response hypotheses were each incorporated, in turn, into the model described in **Chapter 4**. Unless otherwise stated, the model was run using the best performing parameter values as described in **Chapter 5 (Table 5.5)**.

6.3.1 Parameterisation

For the startle response scenario one term given in **Equation 6.5** (henceforth referred to as SR1) the value of g_{NBL} was set to 1.4317 day^{-1} . This is equal to the zooplankton maximum grazing rate g in the best performing model in **Chapter 5** which contains no bioluminescent term. As a value for k_g could not be measured directly or gained from the literature, a suitable value was considered to be in the range of $0.01 \text{ mmol N m}^{-3}$ to twice the maximum value reached by the controlling term in the function, in this case P_2 . Given that the maximum concentration of P_2 in the best performing model in **Chapter 5** was approximately $0.4 \text{ mmol N m}^{-3}$, the maximum value of k_g was set equal to $0.8 \text{ mmol N m}^{-3}$.

For the startle response scenario two bioluminescent term given in **Equation 6.7** (henceforth referred to as SR2) the value of g_{NBL} was again set to 1.4317 day^{-1} . Experimental evidence suggests that zooplankton grazing rates are reduced by up to 70% in the presence of prey which are all bioluminescent (Esaias and Curl, 1972; White 1979). Therefore, g_{BL} was assumed to be a 70% reduction of g_{NBL} . Bioluminescent dinoflagellates accounted for between 19 and 67% of the total dinoflagellate abundance within the PAP region over a typical year (**Chapter 3**). Therefore, a suitable value for λ was considered to be within this range.

For the burglar alarm scenario one term given in **Equation 6.9** (henceforth referred to as BA1) the value of ϵ_{BL} was set equal to a 70% increase in the maximum mortality rate where no prey were bioluminescent. This was because experimental evidence suggests that zooplankton mortality rates increase by up to 70% in the presence of prey that are all bioluminescent (Abrahams and Townsend, 1993). It was assumed here that the value of ϵ in the best performing model in **Chapter 5** (0.4922 day^{-1}) was the maximum mortality rate when no prey were bioluminescent. Therefore, ϵ_{BL} was set equal to 0.8367 day^{-1} . A value for k_{ϵ} could not be measured directly or gained from the literature. Thus, a suitable value was considered to be within the range of $0.01 \text{ mmol N m}^{-3}$ to $0.8 \text{ mmol N m}^{-3}$, as for k_g .

Finally, for the burglar alarm scenario two term given in **Equation 6.11** (henceforth referred to as BA2) the value of ϵ_{NBL} was set to 0.4922 day^{-1} equal to the zooplankton maximum mortality rate ϵ in the best performing model without bioluminescence. The value of ϵ_{BL} was set equal to a 70% increase of ϵ_{NBL} , as in the BA1 term, and a suitable value for λ was again considered to be between 19 and 67%.

6.3.2 Sensitivity analysis

There are insufficient data to precisely constrain the values of the newly introduced k_g , k_{ϵ} and λ parameters, therefore each of these parameters has been assigned a range in which their value may lie. To investigate how sensitive the model output was to the specific value assigned to these parameters within these ranges a sensitivity analysis was carried out on each parameter in turn following the method described in **Section 5.2.7**. Results indicate that the model cost is not significantly affected by the value chosen for k_g or λ in the SR1, SR2 or BA2 bioluminescent terms, respectively (**Figure 6.5**). However, the model is very sensitive to the value assigned to k_{ϵ} in the BA1 bioluminescent term. For the present parameterisation, the model becomes unstable, through a lack of phytoplankton coexistence, very quickly as k_{ϵ} increased over $0.085 \text{ mmol N m}^{-3}$ (**Figure 6.5**). Below a value of $0.085 \text{ mmol N m}^{-3}$ there is no significant difference in model cost. These results are perhaps contrary to what might be expected

as they suggest that the greatest likelihood of instability from the BA1 term may be caused by the zooplankton mortality rate being too low rather than too high. It is not surprising that the model is highly sensitive to the parameterisation of the BA1 term. As seen in **Section 5.3.3**, the best performing model without bioluminescence became unstable when ϵ was set to values of less than 0.1 day^{-1} . Results suggest that when k_ϵ is greater than $0.085 \text{ mmol N m}^{-3}$ the maximum zooplankton mortality rate ϵ becomes so low that phytoplankton are grazed to extinction.

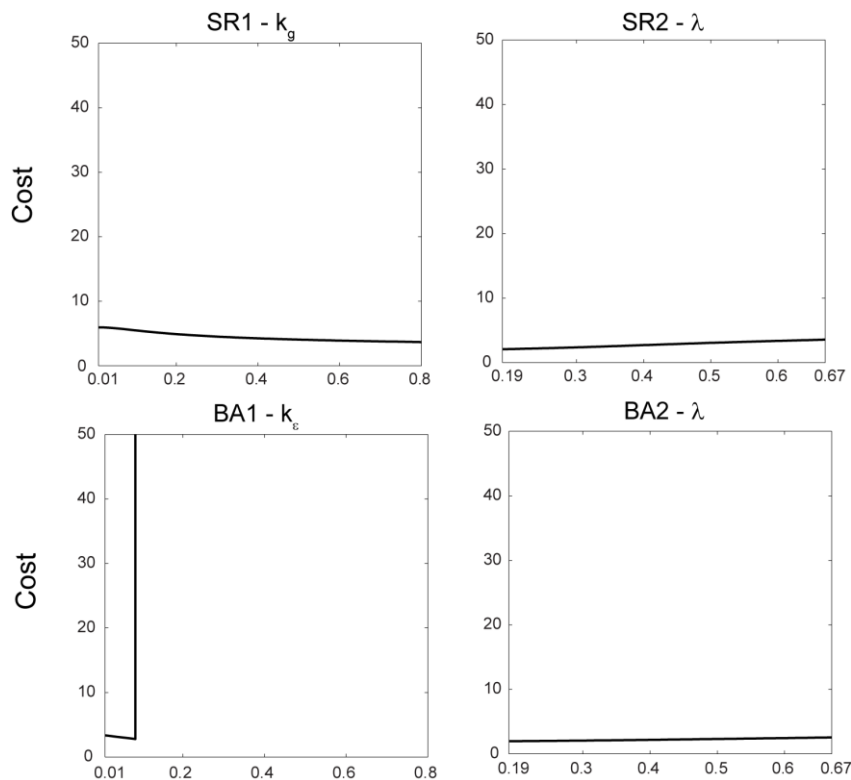


Figure 6.5: Model sensitivity to perturbations in (from left to right) k_g in SR1 scenario, λ in the SR2 scenario, k_ϵ in the BA1 scenario and λ in the BA2 scenario. Plots indicate changes in cost between model output and real observations.

6.3.3 Effects on Baseline Model Output

To examine the impact of the bioluminescent terms on the baseline model k_g , λ and k_ϵ were assigned values based on the results of the sensitivity analysis (**Section 6.3.2**). As the sensitivity analysis indicated that the model was relatively insensitive to the value of k_g and λ , k_g was set to $0.4 \text{ mmol N m}^{-3}$ representing the mid value in the assumed range and λ was set to 37% representing the average over a typical year (**Section 3.3.3**). The value of k_ϵ was set to $0.04 \text{ mmol N m}^{-3}$ representing the mid value in the reduced range over which phytoplankton were able to coexist. Outputs from the model including the bioluminescent terms were compared to that of the baseline model without a bioluminescent term (**Figure 6.6**). Results indicate that all of the proposed

bioluminescent terms benefit dinoflagellates by increasing their peak biomass and allowing them to bloom earlier in the summer. The SR1 term is the most beneficial providing an approximate 300% increase in peak dinoflagellate biomass. This corresponds with a significant decrease in zooplankton biomass over the year. All terms also provide a benefit to diatoms through a small increase in their biomass, again with the SR1 having the largest effect.

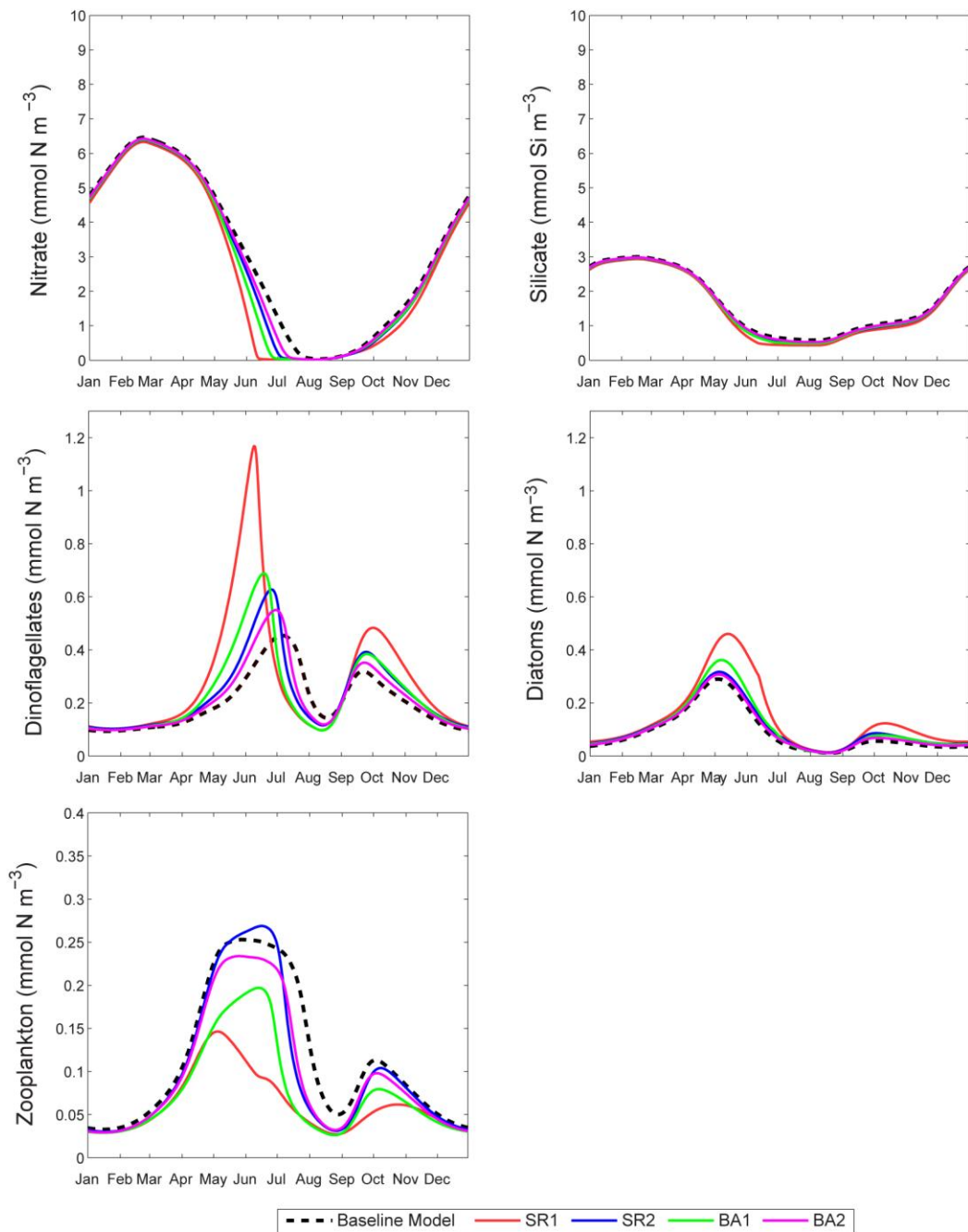


Figure 6.6: Comparison of model output with the inclusion of SR1, SR2, BA1 and BA2 bioluminescent terms (solid lines) with baseline model output without a bioluminescent term (dashed line).

In general, scenario two terms (SR2 and BA2) are seen to reduce zooplankton biomass to a lesser extent than scenario one terms (SR1 and BA1). Thus, these terms show a correspondingly smaller impact on the biomass of both phytoplankton types. The SR2 term actually provide a small increase in peak zooplankton biomass. Nutrient concentrations are relatively unchanged for all of the bioluminescent terms especially for silicate. However, all bioluminescent terms show a quicker draw down of nitrate during late spring and summer months, which is brought about by the more rapidly increasing phytoplankton.

Overall, preliminary analysis demonstrates that each of the bioluminescent terms developed in **Section 6.2.2** can be incorporated into the simple dinoflagellate model described in **Chapter 4** without causing model instability. Furthermore, it has been shown that each of the bioluminescent terms can provide an ecological advantage to the dinoflagellate community.

6.4 Methods for Detailed Analysis

Table 6.2: Summary of models including bioluminescent terms and additional parameters required for optimisation within the calibration process.

Models	Additional Parameters for Optimisation
Baseline model + SR1 term	k_g
Baseline model + SR2 term	λ
Baseline model + BA1 term	k_ϵ
Baseline model + BA2 term	λ
Baseline model + SR1 + BA1 terms	k_g and k_ϵ
Baseline model + SR2 + BA2 terms	λ

A detailed analysis was carried out to investigate how the bioluminescent terms developed in **Section 6.2** impacted upon model performance, parameterisation and system dynamics. To best understand the impact of the bioluminescent terms on the model it was important that they were included within the calibration process. As such, each bioluminescent term was incorporated, in turn, into the model described in **Chapter 4** and model parameters were optimised to the four synthetic datasets as described in **Section 5.2.6**. In addition to the 18 parameters originally optimised in the calibration of the baseline model without bioluminescence (**Table 5.1**), parameters k_g , k_ϵ and λ were optimised in the calibration of the models including their respective terms. The optimisation process was able to select values for these parameters within the ranges set out in **Section 6.3.1**. The values of ϵ_{NBL} and g_{NBL} were equal to ϵ and g in

the baseline model and optimised using the ranges set in **Table 5.1**. A decision was made not to include ε_{BL} and g_{BL} in the calibration procedure at this time to keep the number of optimised parameters to a minimum and concentrate on examining the more extreme effects bioluminescence may have upon the ecosystem. As in the preliminary analysis, the values of ε_{BL} and g_{BL} were set to a 70% increase and a 70% reduction of ε_{NBL} and g_{NBL} , respectively based on experimental literature values.

In addition to models containing individual bioluminescent term, calibration of two models jointly incorporating SR and BA terms for the two scenarios were carried out. Startle response and burglar alarm terms were combined because, as stated in **Section 6.1**, it is possible that the two survival mechanisms co-occur. Therefore, in total, six models incorporating one or more bioluminescent terms were calibrated to synthetic datasets and compared to the baseline model described in **Chapter 5**. A summary of all the models run and additional optimised parameters is given in **Table 6.2**.

6.4.1 Assessment of Model Parameterisation

Differences in the parameterisation of the models containing bioluminescent terms and the baseline model without bioluminescence were assessed. Four parameter vectors were gained for each model from the calibration procedure which corresponded to each of the four synthetic datasets. Each set of four parameter vectors for models containing bioluminescent terms (**Table 6.2**) were compared to those obtained for the baseline model without bioluminescence (**Table 5.5**). Student t-tests were used to indicate whether the distribution of values for a particular parameter (e.g. dinoflagellate maximum growth rate, μ_2) across a set of four parameter vectors was significantly different for models with bioluminescent terms compared to the baseline model. This statistical approach is used as an alternative to directly comparing differences between the parameter values in the best performing vectors. This is because, as indicated in **Chapter 5**, large variations in parameter values could occur between parameter vectors for the same model due to a lack of data to constrain parameters and the limitations of the optimisation procedure. By comparing the distribution of parameter values across each set of four vectors, trends in parameterisation between models could be identified more robustly.

6.4.2 Assessment of Model Performance

The performance of models including terms representing the ecological function of dinoflagellate bioluminescence compared to the baseline model was assessed in two ways. Firstly, the models were assessed on how well they were able to simulate the synthetic datasets used in the calibration procedure. A cost matrix was produced for

each model listed in **Table 6.2** following the procedure described in **Section 5.2.6**. Analysis of variance (ANOVA) was then used to compare the distribution of costs within the cost matrices from models containing bioluminescent terms and that of the baseline model (**Table 5.6**). This method provided a way of indicating if any model containing a bioluminescent term was significantly better or worse at simulating the synthetic calibration data than the baseline model. A post hoc Tukey test was carried out to identify which models differed significantly from each other. Statistical significance was considered at the $p < .05$ level.

Secondly, the models were assessed on how well they were able to simulate real observations (**Section 4.5**). The baseline model and the models including bioluminescent terms were each run, in turn, using all four of their respective parameter vectors. The output of each run was compared to the observational data and the cost function calculated. Student t-tests were carried out to investigate whether there were any significant differences in total model costs or individual cost components between models containing bioluminescent terms and the baseline model. As described in **Section 6.4.1**, the use of statistical tests to indicate changes in cost over each set of four parameter vectors is preferential to solely analysing differences between the costs from the best performing parameter vectors. This is because variations in parameter values could be due to the underdetermined nature of the model or the limitations of the optimisation method (**Section 5.2.4**). A comparison of the distribution of cost values across each set of four vectors allows consistent differences in cost between models to be identified.

For the purposes of student t-tests carried out in the analysis of model parameterisation (**Section 6.4.1**) and model performance (**this Section**) the level of statistical significance was considered at the $p < .10$ level. This was due to the small size of the data sample used in each test ($n=4$). An investigation into the power of the statistical significance at such a small sample size was carried out. For a subset of models (3 of 6) the sample size was doubled ($n=8$) by calibrating the models to an additional four synthetic datasets. Student t-tests were then re-run. Results of the investigation indicated that some differences observed at the 90% ($p = .10$) confidence interval within the $n=4$ sample became significant at the 95% ($p = .05$) confidence interval upon increasing the sample size. However, differences initially at the 80% confidence interval did not increase in significance. Thus, a lowering of the statistical confidence band to $p < .10$ was thought sufficient to overcome issues of small sample size for this analysis. All statistical analysis was carried out in Sigma Plot 11.0.

6.4.3 Assessment of Model Ecosystem Dynamics

The impacts of the bioluminescent terms upon the dynamics of the system were assessed. The best performing parameter vector for each model in **Table 6.2** was identified. This was achieved using a cost matrix as for the baseline model (**Section 5.3.2**). Each model was run, in turn, using its respective best performing parameter vector (**Section 6.4.2**). Outputs for state variables, specific rates and mass fluxes for each model were compared to those from the baseline model. This enabled an investigation into how the dynamics of the ecosystem had changed due to the inclusion of terms representing the effects that dinoflagellate bioluminescence may have upon zooplankton.

6.5 Results

There are several considerations to keep in mind whilst interpreting results. The models including bioluminescent terms contain within them the baseline model. It has been found that more complex models will often provide increased fit to data because of their increased number of parameters (Burnham and Anderson, 2002). Therefore, the models including bioluminescent terms may be expected to provide a smaller model cost than the baseline model purely because of the increase in parameters. However, the models including bioluminescent terms are being calibrated to and compared against the same data as that used for the baseline model analysis. As the baseline model already matched these data well, it might be expected that significant changes in the variables for which there are data will not occur. Instead changes are more likely in variables which are not constrained by data, such as zooplankton biomass. Furthermore, improvements in the fit of some variables to data could be balanced by a worsening of the fit between other variables and data. This implies that the models including bioluminescent terms may not provide significant improvements in model cost but may still significantly impact upon the dynamics of the system by changing the manner in which fluxes balance to allow the model to fit the observations.

First the impact of including the bioluminescent terms on model parameterisation is analysed. This is followed by an investigation of whether the inclusion of the bioluminescent terms improves simulations indicated by reduced model cost. Finally, the impacts of the bioluminescent terms upon the dynamics of the system are investigated.

6.5.1 Assessment of Model Parameterisation

Results of the statistical analysis on parameters from models containing bioluminescent terms and the baseline model are shown in **Table 6.3**. Results indicate that there are several significant differences in parameter values between the baseline model and models containing bioluminescent terms. Models incorporating scenario one terms (SR1, BA1, combined SR1 & BA1) are seen to have more differences in parameterisation compared to the baseline model than models incorporating scenario two terms (SR2, BA2, combined SR2 & BA2). However, results also show that trends in parameterisation found for the baseline model are also present in the models including bioluminescent terms. For example, average values of μ_1 are consistently greater than μ_2 , average values of α_2 are never larger than α_1 and average values of k_{n2} are less than k_{n1} across all models.

Table 6.3: Results of student t-tests are shown comparing the parameter vectors from models incorporating bioluminescent terms and the baseline model (n=4). Average parameter values over the four parameter vectors gained through calibration to synthetic datasets are given. ** indicates a significantly difference at the $p < .05$ confidence interval and * denotes significant difference at $p < .10$ confidence interval.

Parameters	Baseline	SR1	SR2	BA1	BA2	SR1 & BA1	SR2 & BA2
<i>Phytoplankton</i>							
μ_1	2.190	2.168	2.517	1.928	2.910	1.382	2.408
μ_2	0.629	0.349**	0.494	0.494	0.908	0.639	0.587
k_{n1}	2.005	1.568	1.608	1.826	0.735	2.838	2.203
k_{n2}	0.286	0.0337**	0.152	0.184	0.192	0.0811	0.192
k_{Si}	2.085	3.110**	2.583	2.522	2.402	3.125**	2.160
α_1	0.0949	0.0961	0.0980	0.0937	0.1000	0.0969	0.0969
α_2	0.0753	0.0792	0.0937	0.0870	0.0780	0.0383	0.0855
V_{diatom}	0.995	1.243	1.052	0.748	0.938	0.481	0.776
m_p	0.327	0.393	0.370	0.321	0.342	0.397	0.358
k_{mp}	0.834	0.849	0.719*	0.659	0.726	0.834	0.707
<i>Zooplankton</i>							
g_{NBL}	1.968	1.690	1.091*	0.782**	1.370	0.617**	1.545
k_z	1.932	2.573**	2.336	2.442	2.585*	2.585*	1.825
β	0.729	0.532	0.711	0.514	0.800	0.286**	0.889
ϵ_{NBL}	0.383	0.208	0.232*	0.257*	0.288	0.356	0.273
$k_{m\epsilon}$	0.112	0.221	0.241	0.332*	0.249	0.262	0.0620
<i>Other</i>							
τ	0.540	0.457	0.540	0.417	0.631	0.417	0.508
m	0.00263	0.00433	0.000913	0.00389	0.00218	0.00246	0.00365
k_c	0.0605	0.0628	0.0718	0.0681	0.0567	0.0545	0.0907

For those models including individual SR and BA terms, many of the observed changes in parameterisation act to counteract the effect of the bioluminescent terms. For example, the model incorporating the SR1 term has a dinoflagellate maximum growth rate (μ_2) which is significantly lower (~45%) than that of the baseline model and a silicate half saturation constant for diatoms (k_{si}) that is significantly higher. A reduction in μ_2 and an increase in k_{si} have the effect of reducing dinoflagellate and diatom growth rates, respectively. This balances the decreased grazing pressure on dinoflagellates brought about by the SR1 term itself. Such changes in parameterisation are perhaps unsurprising because the models including bioluminescent terms are still required to fit the same data as the baseline model. Therefore, simulated cycles in variables that are compared to data need to be very similar between models.

For those models including the combined BA and SR terms, interpretation of the significant differences in parameters is more complex. There are no significant differences in the parameter values for the model incorporating both the SR2 and BA2 terms compared to the baseline model. This is in contrast to the model including both the SR1 and BA1 terms, which has several significantly different parameter values compared to the baseline model. Some of these parameter changes are consistent with those found for the models incorporating the terms separately. However, others are not. All of the significant changes in the parameterisation of the model including both the SR1 and BA1 terms have the effect of limiting zooplankton growth. However, it is not obvious why this should be the case.

It is interesting to note that many of the significant changes in parameterisation, across all the models incorporating bioluminescent terms, have affected zooplankton parameters, such as the half saturation constant for zooplankton (k_z). This may be because there is a comparative lack of data to constrain zooplankton output from the models. The lack of data may allow the optimisation procedure to change zooplankton parameter values without having as large an effect on cost as might be had if parameters directly associated with other variables such as phytoplankton were varied.

6.5.2 Assessment of Model Performance

A statistical analysis was carried out to assess whether there were any significant differences in the cost matrices of models incorporating bioluminescent terms and the cost matrix of the baseline model. ANOVA results indicate that there are significant differences between cost matrices ($F(6,105) = 13.332$, $p < 0.001$). Post hoc analysis reveals that the cost matrix of the model including the SR1 and BA1 terms combined has a mean cost significantly higher than that for the baseline model ($p < 0.001$). There is no evidence to suggest that incorporating any bioluminescent terms into the

baseline model significantly improves the model's ability to simulate the synthetic datasets during the calibration process.

A secondary analysis compared each model's ability to simulate observational data across all four calibrated parameter vectors using student t-tests. Results, shown for specific variables in **Table 6.4**, indicate that the incorporation of the BA2 term significantly increases the models ability to simulate the typical seasonal change in nitrate concentration. This is in contrast to the incorporation of the BA1 term where the ability of the model to simulate changes in nitrate is significantly decreased. The ability to simulate the typical seasonal change in chlorophyll is significantly decreased in models including the SR1 term, BA2 term and the SR1 and BA1 terms combined. The analysis also shows that overall the model including both the SR1 and BA1 terms is significantly worse at simulating the observational data than the baseline model. This is in agreement with the results of the cost matrix analysis. The inclusion of the bioluminescent terms does not provide a significant improvement in the model's ability to simulate either the seasonal changes in the dinoflagellate population or the represented ecosystem as a whole.

Table 6.4: Results of Student t-tests are shown comparing the cost functions for models incorporating bioluminescent terms with those from the baseline model (n=4). Average model costs, indicating the misfit of model simulations to observational data, across the four parameter vectors gained through calibration to synthetic data are given. . ** indicates a significantly difference at the $p < .05$ confidence interval and * denotes significant difference at $p < .10$ confidence interval.

Components of Cost Function	Baseline Model	SR1	SR2	BA1	BA2	SR1 & BA1	SR2 & BA2
Average Cost							
Nitrate	0.580	0.576	0.584	0.722*	0.457**	0.553	0.528
Silicate	0.350	0.413	0.384	0.401	0.312	0.366	0.385
Diatoms	0.237	0.202	0.170	0.226	0.271	0.289	0.222
Dinoflagellates	0.462	0.390	0.413	0.365	0.502	0.528	0.420
Chlorophyll	0.321	0.488**	0.485	0.404	0.523**	0.754**	0.429
Total	1.950	2.069	2.036	2.117	2.065	2.490**	1.983

Results suggest that the inclusion of bioluminescent terms can bring about improvements in the simulation of some state variables. However, these improvements are cancelled out by the worsening of other variables (e.g. for the BA2 term). As discussed earlier, it may be unsurprising that significant improvements in total cost do not occur due to the baseline model's initial ability to simulate the data well. The bioluminescent terms may be having a larger effect upon the zooplankton state variable which is not constrained by data in the calibration procedure or considered in

the performance analysis. This is supported by the results of **Section 6.5.1** which indicate that significant differences in the parameterisation of models predominantly affect zooplankton parameters.

6.5.3 Assessment of Model Ecosystem Dynamics

The inclusion of bioluminescent terms did not appreciably improve the fit of model simulations to the data. However, it is not clear whether the inclusion of bioluminescent terms make the model fit the data for different reasons. An examination of the effect the bioluminescent terms have upon the dynamics of the modelled system is therefore carried out.

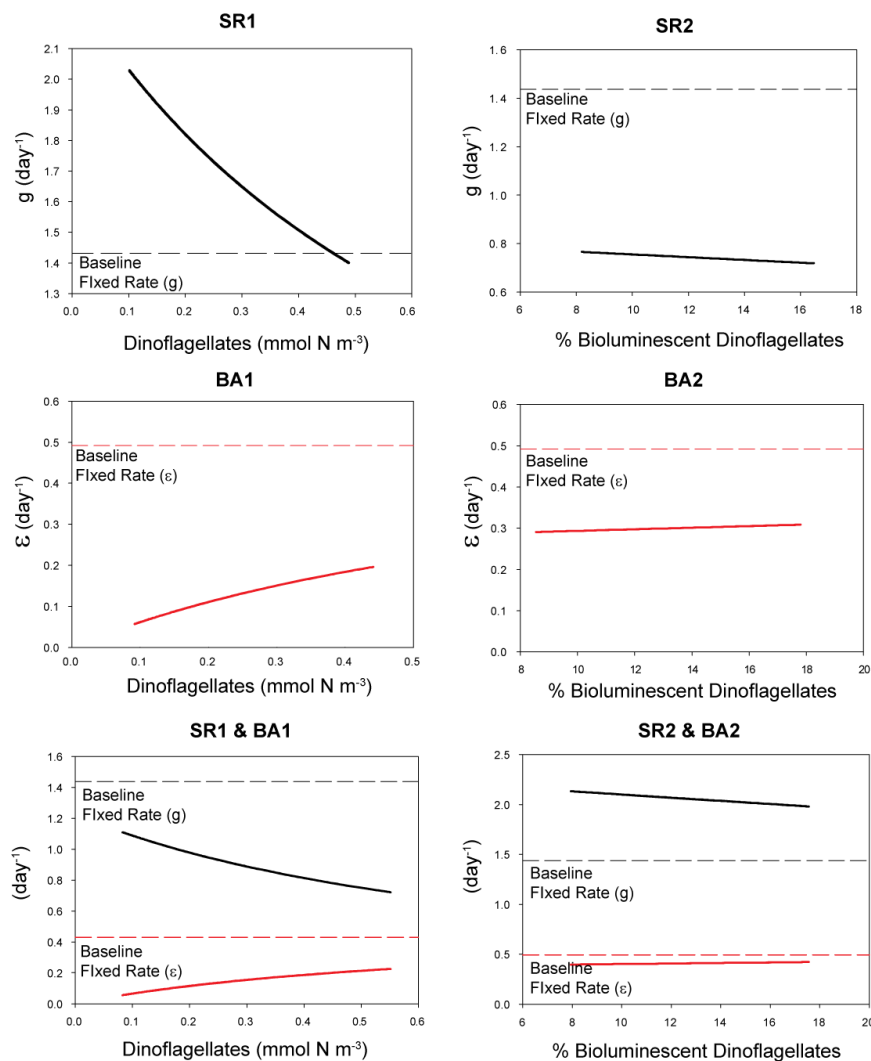


Figure 6.7: Variations in maximum zooplankton grazing rate g (shown in black) and maximum zooplankton mortality rate ϵ (shown in red) caused by the bioluminescent terms in models run using the best performing parameter vector.

The best performing parameter vectors for the baseline model and models containing bioluminescent terms are shown in **Table 6.5**. The variations in g and ϵ , that occur when the models including bioluminescent terms are run using their respective best performing parameter vector are shown in **Figure 6.7**. These variations arise from changes in P_1 and P_2 over the annual cycle as defined in **Section 6.2**. Some general patterns are present. Variations of g and ϵ caused by scenario two terms have a smaller range than those caused by scenario one terms, by approximately one order of magnitude. For example, the model including the SR1 term enables g to vary between 1.400 and 2.028 day^{-1} , giving a range of 0.628 day^{-1} . This can be compared to the model including the SR2 term where g varies between 0.719 and 0.766 day^{-1} , giving a range of only 0.047 day^{-1} , over tenfold lower. The model incorporating the SR1 term has values of g that never fall considerably below the fixed rate used within the baseline model whereas, the model including the SR2 term, has values of g that are approximately 50% lower.

Table 6.5: Comparison of the best performing parameter vector gained through calibration to synthetic data of the baseline model and models including bioluminescent terms.

Parameter	Baseline Model	SR1	SR2	BA1	BA2	SR1 & BA1	SR2 & BA2
<i>Phytoplankton</i>							
μ_1	1.4476	1.9714	1.7095	3.1937	3.8921	1.7968	2.4952
μ_2	0.4629	0.3800	0.3386	0.6700	0.6286	0.4214	0.7114
k_{n1}	0.3381	0.2587	0.2587	0.1000	0.4175	2.4016	0.6556
k_{n2}	0.0732	0.0732	0.1048	0.1048	0.0416	0.0100	0.1048
k_{Si}	2.3714	2.8540	3.2159	2.1302	3.3365	2.1302	1.9492
α_1	0.0969	0.1000	0.0969	0.0984	0.1000	0.0874	0.0984
α_2	0.0607	0.0859	0.0859	0.0811	0.0906	0.0969	0.0953
V_{diatom}	0.8238	2.3476	0.9000	2.5000	0.8238	0.4048	0.6333
m_p	0.2511	0.4922	0.3522	0.4300	0.4611	0.5000	0.4767
k_{mp}	0.6829	0.9524	0.7780	0.7621	0.6670	0.6511	0.7304
λ	N/A	N/A	0.1900	N/A	0.1976	N/A	0.1976
<i>Zooplankton</i>							
$g_{\text{NBL}} (g)$	1.4317	2.2984	0.8127	1.8444	1.4730	1.2254	2.2571
k_z	1.7186	2.9051	2.8102	2.7627	2.7152	3.0000	2.6203
β	0.8857	0.5714	0.9571	0.9000	0.9571	0.1571	0.9571
$\epsilon_{\text{NBL}} (\epsilon)$	0.4922	0.1733	0.3289	0.3289	0.2744	0.2900	0.3756
$k_{m\epsilon}$	0.1666	0.0184	0.4367	0.0446	0.1491	0.4367	0.1317
k_g	N/A	0.7624	N/A	N/A	N/A	0.7875	N/A
k_ϵ	N/A	N/A	N/A	0.0010	N/A	0.6605	N/A
<i>Other</i>							
τ	0.5084	0.5243	0.4609	0.6670	0.6353	0.5877	0.6353
m	0.0097	0.0075	0.0005	0.0003	0.0060	0.0030	0.0033
k_c	0.0311	0.0583	0.0522	0.0733	0.0341	0.0583	0.0432

Figure 6.7 also shows that models including BA terms have values for ϵ that are always lower than the fixed rate used in the baseline model. Using the BA1 term, the largest value achieved by ϵ is 60% lower than the fixed rate used for ϵ in the baseline model whilst the lowest value is 88% lower. The opposite pattern is observed for the SR and BA terms combined. The model incorporating both the SR1 and BA1 terms has values of g that are approximately 23 – 50 % lower than the fixed rate used in the baseline model whilst the model incorporating both the SR2 and BA2 terms has values of g approximately 37 – 48 % higher.

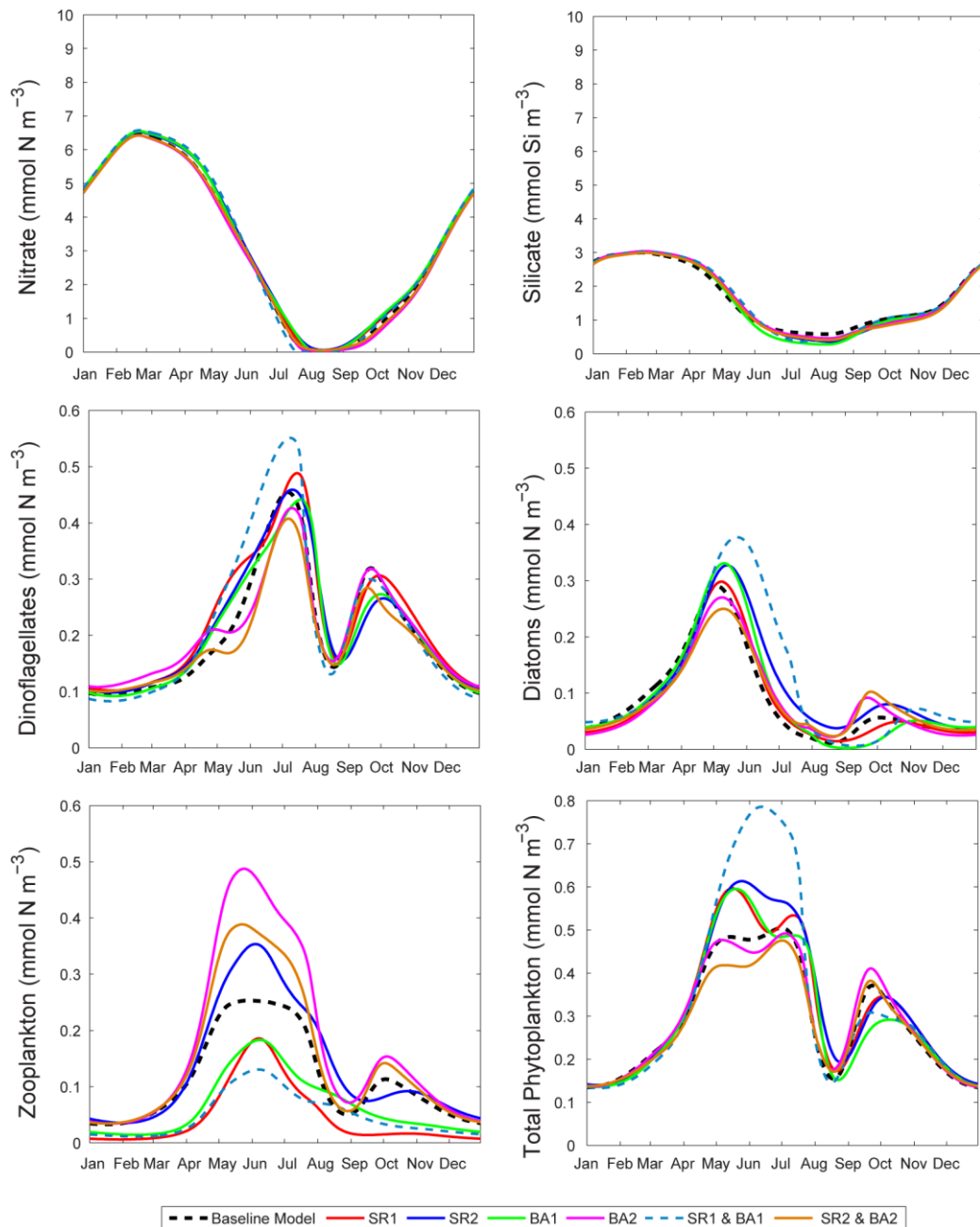


Figure 6.8: Comparison of output from models including SR1, SR2, BA1, BA2, SR1 and BA1 and SR2 and BA2 bioluminescent terms with that from the baseline model without a bioluminescent term. Models were run with their respective best performing parameter vectors.

A comparison of model simulations for each state variable is made in **Figure 6.8**. Results indicate that there is very little difference in the simulations of nitrate and silicate between the baseline model and those models including bioluminescent terms. As described earlier, this is expected as models have been calibrated against data which constrains both the magnitude and seasonal variations in nitrate and silicate.

The models including the SR1 term and the SR1 and BA1 terms combined are shown to increase the magnitude and breadth of the summer dinoflagellate biomass peak in comparison to the baseline model. The SR2 term and BA1 term have a marginal impact upon the magnitude of the summer dinoflagellate peak but still increase its breadth, in particular the population increases faster in spring. In contrast, the models including the BA2 term and both the SR2 and BA2 terms combined decrease both the magnitude and breadth of the summer dinoflagellate peak. The bioluminescent terms are also seen to impact upon the timing of the peak dinoflagellate population with the output from models containing both the SR1 and BA1 terms indicating a delay in peak dinoflagellate biomass of approximately 9 and 14 days, respectively.

Several of the models also increase the magnitude and breadth of the spring diatom biomass peak. These include the models incorporating the SR2 term, the BA1 term and the SR1 and BA1 terms combined. Increases in the breadth of the spring peak are not due to a faster increase in the population at the start of spring, as seen for dinoflagellates, but instead due to a larger post bloom population. As with the dinoflagellate population, the models including the BA2 term and the SR2 and BA2 terms combined bring about a decrease in the magnitude of the diatom peak.

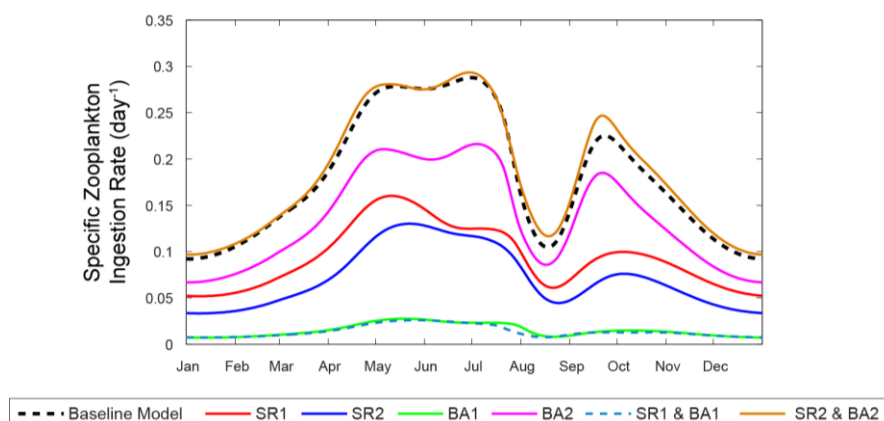


Figure 6.9: Comparisons of zooplankton specific ingestion rates for models including bioluminescent terms and the baseline model without a bioluminescent term.

Model simulations of dinoflagellate and diatom state variables are much more changeable between models than those observed for nutrient state variables. This may be due to the phytoplankton groups being somewhat less constrained by the data used in the optimisation procedure. Although the data used in the cost function constrains the seasonal pattern of each phytoplankton group the absolute magnitude of the seasonal variations for the individual groups is not constrained and is free to vary. Only the summed total biomass of the two phytoplankton groups is constrained by chlorophyll data. However, **Figure 6.8** also indicates that there is a substantial amount of variation of the total phytoplankton biomass between models from April to July. Therefore, the differences between models in both individual and combined phytoplankton biomasses may be instead related to large uncertainties associated with the average chlorophyll estimates throughout the late spring and summer (**Figure 4.7**).

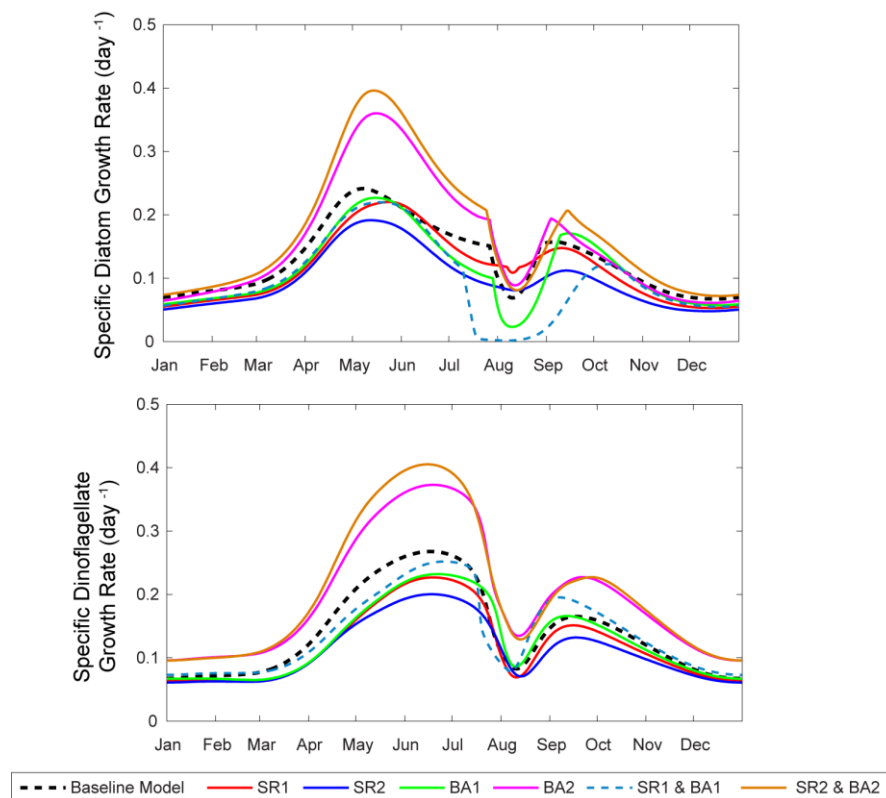


Figure 6.10: Comparisons of phytoplankton specific growth rates for models including bioluminescent terms and the baseline model without a bioluminescent term.

Differences in both the simulated dinoflagellate and diatom biomasses may be explained by analysing the effects that the bioluminescent terms have upon the simulated zooplankton biomass. Unsurprisingly, the state variable which is most changeable between models is zooplankton due to it being unconstrained in the

optimisation procedure. In comparison to baseline model values, zooplankton biomass is reduced in models incorporating the SR1 term, the BA1 term and the SR1 and BA1 terms combined (**Figure 6.8**). These reductions in zooplankton abundance in the models including scenario one terms are related to decreases in zooplankton ingestion rates which slows zooplankton growth (**Figure 6.9**).

Conversely, the models including scenario two terms are seen to lead to increased zooplankton abundance in the modelled system (**Figure 6.8**). For the models incorporating the BA2 term and the SR2 and BA2 terms combined, this increase in zooplankton biomass can be related to increases in diatom and dinoflagellate growth rate (**Figure 6.10**). Increased growth rates lead to a greater supply of phytoplankton between April and August, that is available for grazing. This can clearly be seen in the fluxes in and out of the phytoplankton and zooplankton pools for these two models shown in **Figure 6.11**. The comparative increase in zooplankton biomass in the model containing the SR2 term cannot be explained by an increased supply of phytoplankton. Instead, the parameterisation of the SR2 model leads to a considerable reduction in zooplankton mortality rate (**Figure 6.12**), brought about by a high value for k_{me} , which may explain the increase in zooplankton abundance during the summer months. This is an example where the intercomparison of model dynamics becomes complicated due to the different values for parameters used in each model.

Interestingly, the seasonal zooplankton ingestion rates for the model including the SR2 and BA2 terms combined are very similar to the model without bioluminescent terms (**Figure 6.9**). This is surprising as zooplankton ingestion rates for the models including the SR2 and BA2 terms individually are both lower than the baseline model. This is different to the zooplankton ingestion rates for the model combining the SR1 and BA1 terms which are very similar to those from the model including the BA1 term on its own, suggesting the BA1 term is the dominant term. The similarity between the baseline model and the model including the SR2 and BA2 terms combined may be partly explained by the fact that no significant differences were found between the average parameterisations of the two models (**Table 6.3**). This is in comparison to the parameterisations of the models including the SR2 and BA2 individually which were found to have significantly different values for maximum zooplankton grazing rate (g_{NBL}) and zooplankton grazing half saturation constant, respectively.

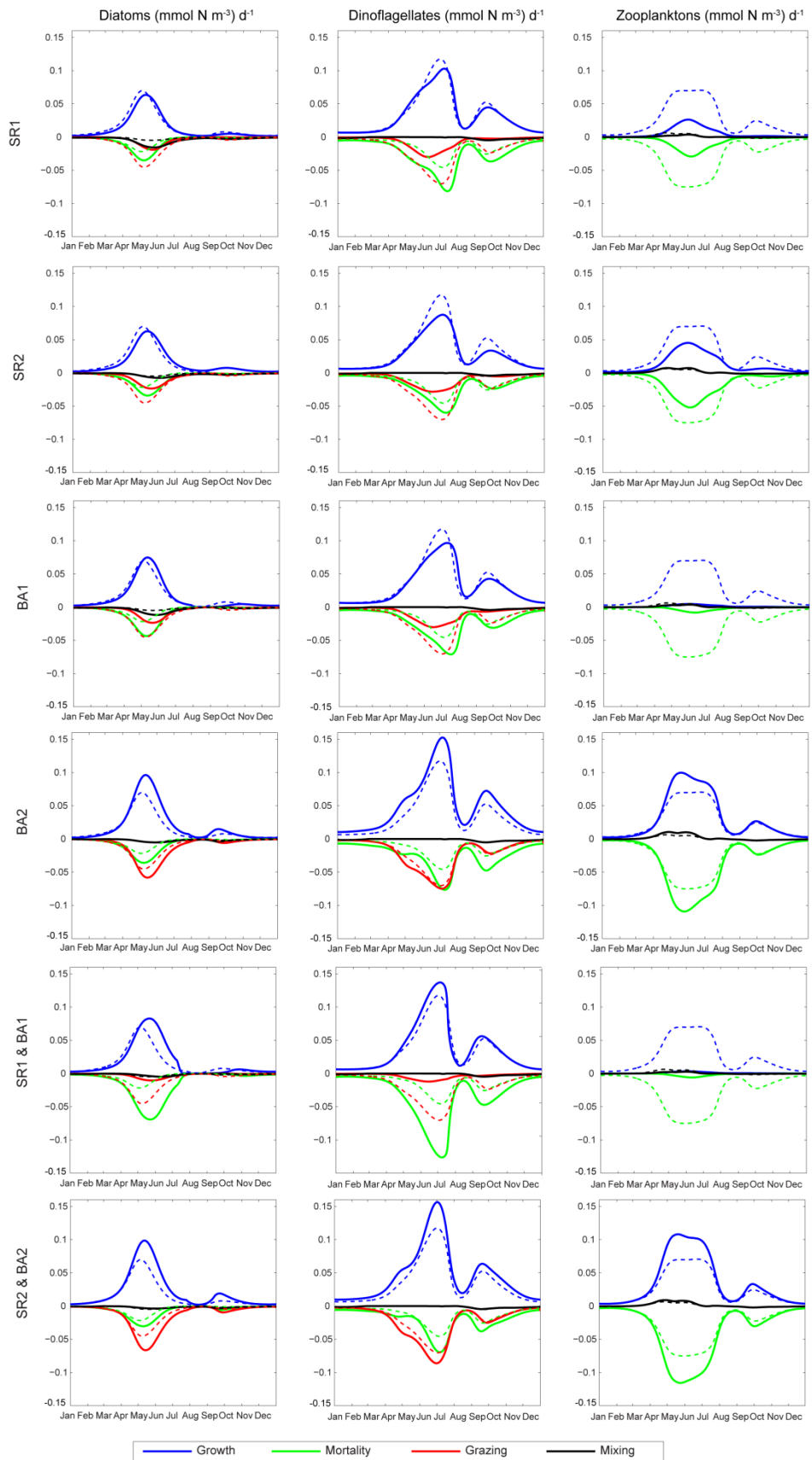


Figure 6.11: Comparison of phytoplankton and zooplankton fluxes for models including bioluminescent terms (solid lines) and the baseline model without a bioluminescent term (dashed lines).

It is notable that the inclusion of several of the bioluminescent terms to the model causes a significant change in the dynamics of the ecosystem. For the models including the SR1, SR2, BA1 and the combined SR1 and BA1 terms the dominant source of loss for the phytoplankton groups switches from zooplankton grazing to natural mortality (**Figure 6.11**). For models including the BA2 term and the combined SR2 and BA2 terms, phytoplankton loss through natural mortality increases and becomes more comparable with the losses from zooplankton grazing (**Figure 6.11**).

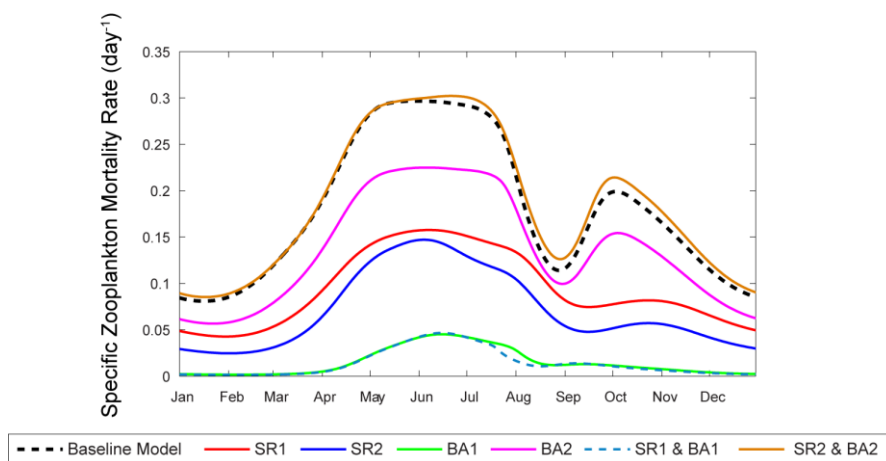


Figure 6.12: Comparisons of zooplankton specific mortality rates for models including bioluminescent terms and the baseline model without a bioluminescent term.

6.6 Discussion

Bioluminescence is hypothesised to provide an ecological benefit to dinoflagellates through a startle response (Esaías and Curl, 1972; Buskey et al., 1983) or a burglar alarm effect (Burkenroad, 1943). Several mathematical terms representative of the proposed mechanisms by which the ecological function of dinoflagellate bioluminescence occurs have been developed. These terms were designed to be easily incorporated into a mechanistic model containing a dinoflagellate phytoplankton group and make use of the current knowledge regarding the impact of bioluminescence on grazers to minimise the requirement for additional parameters. This is the first modelling study to explore what impacts dinoflagellate bioluminescence may have upon an ecosystem and to investigate whether the explicit inclusion of the function of bioluminescence into a mechanistic model can improve performance.

6.6.1 Impact upon Parameterisation and Performance

An investigation into the differences in parameterisation between the models including bioluminescent terms and the baseline model after calibration to synthetic data gave a number of significant findings. Several consistent trends seen in the parameterisation of the baseline model continued to be present in the parameterisation of the models including bioluminescent terms. These included dinoflagellate maximum growth rate (μ_2) always being lower than diatom maximum growth rate (μ_1) and the initial P-I slope of diatoms (α_1) being larger than that for dinoflagellates (α_2). As discussed in **Section 5.4**, these characteristics in parameterisation are in agreement with known physiological differences between diatoms and dinoflagellates (Banse, 1982; Le Quere et al., 2005; Litchman et al., 2007).

Analysis also indicated that significant differences between models including bioluminescent terms and the baseline model occurred primarily in the zooplankton parameters. This suggests that the bioluminescent terms were having the largest impact upon zooplankton within the model. This is perhaps unsurprising given that bioluminescent terms directly affected the zooplankton grazing and mortality and that zooplankton were left unconstrained during model calibration. Therefore, the optimiser had more freedom to change the value of zooplankton related parameters without significantly affecting the cost function. This conclusion was supported by the finding that, with the exception of the model including both the SR1 and BA1 terms, there were no significant differences in the ability of models including bioluminescent terms to simulate nutrient or phytoplankton state variables.

In several models, improvements in the ability to simulate some state variables, such as nitrate, were cancelled out by a worsening of the ability to simulate others. Simulations of chlorophyll were a particular issue for the models including bioluminescent terms with three of the six models having a significantly higher average cost for this state variable. Indeed, the significantly higher overall cost of the model including both the SR1 and BA1 terms was due a worsening of the simulation of chlorophyll. As discussed in **Chapter 5**, the lack of consideration of other phytoplankton groups within the model structure, such as small fast growing phytoflagellates, may limit the ability to simulate the observed pattern in total chlorophyll. The inclusion of the bioluminescent terms may compound this issue by providing a further advantage to summer blooming dinoflagellates to a greater extent than spring blooming diatoms, therefore causing the peak in total chlorophyll concentration to occur further into the summer rather than in spring. Calibration of the model at present does not consider individual biomass estimates for the different phytoplankton groups, only their sum, which limits the ability of the optimisation

procedure constrain phytoplankton parameters, therefore allowing some variation in the chlorophyll state variable between models.

The inclusion of the bioluminescent terms might have been expected to lead to an improvement of model cost simply because of the increased number of parameters alone. The lack of reduction in overall cost for the models including bioluminescent terms compared to the baseline model suggests bioluminescent terms did not allow a better fit to the data. The effect of the additional parameters on model cost was within the range the cost might vary due to the limitations of the optimisation procedure (i.e. within the optimiser noise).

6.6.2 Impact upon Ecosystem Dynamics

Preliminary analysis indicated that all of the bioluminescent terms developed were able to provide an ecological benefit to the modelled dinoflagellate community. Upon re-optimisation of the model, differences in parameterisation, performance and system dynamics were seen between scenario one terms, which were a direct function of dinoflagellate abundance, and scenario two terms, which were a function of the ratio between bioluminescent dinoflagellate and the total phytoplankton abundances. For example, scenario one terms led to much larger variations in maximum grazing and mortality rates and had more significant changes in parameter values. Variations in maximum grazing and mortality rates for the scenario two terms were restricted by a strong correlation between dinoflagellates and total phytoplankton (data not shown).

This meant that the seasonal changes in $\frac{\lambda P_2}{P_1 + P_2}$ were much weaker than for P_1 or P_2 alone.

As suggested from the analyses of parameterisation and performance, the state variable most affected by the inclusion of bioluminescent terms into the model was zooplankton abundance. Both the proposed startle response and burglar alarm mechanisms would be expected to lower zooplankton abundance within the system. Scenario one terms behaved as expected, as they decreased zooplankton abundance in the ecosystem. However, the same was not true for the scenario two terms which, surprisingly, benefited the zooplankton population. This was due to a greater supply of phytoplankton being available to graze (**Figure 6.11**). It is difficult to assess which of the models incorporating the bioluminescent terms provided the most accurate representation of zooplankton biomass due to a lack of comparable in situ data. However, the few studies conducted within the northeast Atlantic give spring/summer mesozooplankton biomass estimates between 0.05 and 0.20 mmol N m⁻³ (Dam et al., 1993; Lenz et al., 1993; Giering, unpublished). The original baseline model simulation

gave peak zooplankton biomass (May/June) slightly higher than the upper range from the in situ estimates of $0.25 \text{ mmol N m}^{-3}$. Results show that models incorporating scenario one bioluminescent terms reduce peak zooplankton biomass to values within the range of the in situ estimates, between 0.13 and $0.19 \text{ mmol N m}^{-3}$. This is compared to peak zooplankton biomass for models including scenario two bioluminescent terms which are up to 2.4 times higher than the in situ estimates (0.353 to $0.487 \text{ mmol N m}^{-3}$).

Given the results above, it may be tentatively suggested that scenario one terms better represent the ecological function of dinoflagellate bioluminescence. The models incorporating these bioluminescent terms showed a notable shift in the simulated phytoplankton dynamics. Phytoplankton losses went from being dominated by grazing in the baseline model, to being dominated by natural mortality. This suggests that mortality due to processes other than predation have a significant control upon phytoplankton abundance. It is difficult to evaluate which situation occurs in reality due to data limitations. Zooplankton grazing has traditionally been thought of as the main loss factor for phytoplankton. This may suggest that the scenario one bioluminescent terms have led to an incorrect representation of phytoplankton dynamics. However, natural mortality, which includes losses due to viruses, has been recognised to have a major role in controlling phytoplankton populations (reviewed in Brussaard, 2004). Previous modelling studies, simulating data from station 'S' off Bermuda, have also found natural mortality to dominate the loss of phytoplankton populations throughout most of the year (Fasham et al., 1990). Thus, scenario one terms cannot be ruled out on this basis as it is feasible that natural mortality dominates phytoplankton losses in the system.

Scenario one terms for the startle response and the burglar alarm have very similar effects upon the modelled ecosystem dynamics. Thus, it is not possible from the results of these analyses to conclude if either hypothesis is more likely to be true than the other.

6.6.3 Limitations

There are several assumptions and limitations within this study that require discussion. Firstly, the ecological function of dinoflagellate bioluminescence remains poorly quantified experimentally and is more a hypothesis than proven fact (**Section 1.6.3**). Within this study it has also been assumed that the mechanisms through which bioluminescence benefits dinoflagellates can provide an advantage to all surrounding phytoplankton including those which are not bioluminescent. There is still much uncertainty whether bioluminescence is such an altruistic behaviour. Furthermore, the

study implicitly assumes at present there is no cost associated with being bioluminescent. For example, bioluminescent organisms within the model do not have additional energy requirements to non-bioluminescent organisms (**Section 1.6.3**). The terms developed for bioluminescence in this study focus upon the more extreme potential effects of bioluminescence. Maximum zooplankton mortality rate (ϵ) and maximum zooplankton grazing rate (g) in the presence of bioluminescence were set to the experimentally observed maximum 70% increase and 70% reduction of their respective values when no bioluminescence was assumed. However, it must be remembered that these values have been gained from very few experimental studies which use concentrations of bioluminescent cells higher than what would be typically found in reality. Thus, these parameters should be considered to be poorly quantified. In future, ϵ_{BL} and g_{BL} parameters could be optimised in the model calibration process.

There is still much uncertainty as to whether the ecological function of bioluminescence occurs in reality, the exact mechanisms by which it takes place, and to what extent they impact upon the surrounding ecosystem. At present it is difficult to validate the formulation of the developed bioluminescent terms without further experimental evidence. However, this study has shown that a simple representation of dinoflagellate bioluminescence leads to shifts in the ecosystem dynamics of a simple NPZ model. These changes could, in future, be tested through collection of appropriate data, particularly related to zooplankton.

The ability to fully evaluate the impact of the bioluminescent terms upon the model simulations was somewhat hindered by a lack of data to constrain the model. This was a particular issue for constraining zooplankton parameters and assessing the model's ability to simulate seasonal changes in zooplankton. The underdetermination of the system, as discussed in **Chapter 5**, leads to non-unique solutions; different parameter sets can give the same quality of fit to data. This creates some uncertainty in determining whether the observed changes within the model system are due to the inclusion of the bioluminescent terms or to the lack of constraint on parameters. This has been dealt with to an extent by statistically analysing changes in parameters using multiple optimisations for each model instead of solely looking at differences between the best performing parameter vectors (**Section 6.4**). However, the lack of zooplankton data will need to be resolved before significant further progress can be made.

Better constraint of model simulated zooplankton might be partly achieved by using zooplankton data collected from the CPR survey. As with phytoplankton, the CPR survey is able to provide semi-quantitative abundance information for a range of zooplankton species (Richardson et al., 2006). Such data could be used to constrain the relative seasonal variations of model simulated zooplankton in a similar manner to

that currently used for diatoms and dinoflagellates. For example, seasonal changes in simulated zooplankton biomass and CPR zooplankton abundance could be compared through standardisation to zero mean values. However, unlike phytoplankton biomass which has its absolute magnitude constrained by chlorophyll data, seasonal changes in the absolute magnitude of zooplankton biomass would remain unconstrained.

As alluded to earlier, the study may also be partially limited by the structure of the baseline model. The simplest structure required to model two phytoplankton groups, diatoms and dinoflagellates, has been used. The lack of consideration for other phytoplankton types, particularly fast growing small flagellates and prymnesiophytes, may limit the model's ability to simulate the seasonal pattern in chlorophyll (**Section 4.4.2**). It may also potentially lead to the over estimation of biomass concentration for the two phytoplankton groups currently included. Another limitation at present may be the assumption of a constant Chl:C ratio. In reality this ratio will vary as a function of several variables including irradiance, nitrate and temperature (Geider, 1987). The lack of consideration of a variable Chl:C ratio could, for example, lead to an over estimation of phytoplankton biomass in winter as organisms' intracellular chlorophyll increases due to decreased irradiance. Furthermore, the model at present does not explicitly include bacteria, protozoa or a detrital pool. The addition of these processes to the model structure has the potential to improve the representation of the remineralisation within the model and thus the nutrient concentrations available for uptake by the phytoplankton community. The inclusion of protozooplankton, such as ciliates, may also be particularly important if other phytoplankton types such as small flagellates are represented in the model in future. This is because protozoa are known to be an important intermediates between small phytoplankton (<20 μm) and larger metazooplankton (e.g. copepods) with the ability to remove a significant proportion daily production from pico and nano-phytoplankton (Lochte et al., 1993).

6.6.4 Future Work

Before any embellishments to the model structure are made it is suggested that the present model, both with and without the best performing bioluminescent terms, be further validated. Validation should be carried out through application of the model to other regions (e.g. a different SAHFOS standard area) to assess its ability to simulate the lower trophic dynamics of other oceanographic areas. The model should also be validated against an interannual time series to explore the model's skill in simulating seasonal changes in individual years rather than a typical seasonal cycle. This would allow both the suitability of the model structure and the inclusion of the bioluminescent terms to be more robustly tested.

6.7 Summary

Mathematical terms representing the ecological function of dinoflagellate bioluminescence have been included in a simple biogeochemical model for the first time. Their impact upon model parameterisation, performance and system dynamics has been assessed. Results indicate that the models incorporating the Startle Response scenario one term (SR1) and Burglar Alarm scenario one term (BA1) individually perform best. These terms may lead to improvements in the simulations of zooplankton biomass, based on literature estimates. Ecologically, the consideration of the ecological function of bioluminescence through these terms caused a shift in phytoplankton dynamics. Phytoplankton losses became dominated by natural mortality (including loss due to viruses) compared to losses through zooplankton predation. A greater appreciation of how bioluminescence may effect an ecosystem has been gained through this study. Furthermore, the study has also indicated that bioluminescent terms do not significantly improve the simulation of the seasonal changes in dinoflagellate abundance. This suggests that, at present, bioluminescent terms are not of primary importance in models to simulate seasonal changes in dinoflagellate abundance.

In future the model with and without the best performing bioluminescent terms should be validated in other oceanographic regions and on interannual, rather than averaged, timescales. This will allow further exploration and comparisons of model skill. Future collection of appropriate data to further constrain model parameterisation and verify model output is required, with abundance data for individual phytoplankton groups and zooplankton being a particular focus. More evidence and information is required on the ecological benefit bioluminescence provides to dinoflagellates and the mechanisms by which it is achieved to be able to validate and/or refine the representative terms developed in this study.

Chapter 7 now brings together the findings from the observational and modelling work carried out over the project. Findings are discussed in the broader context of the aims and objectives of the thesis and ideas for future work are explored.

Chapter 7: Discussion

Bioluminescence in the surface ocean can be used to provide information on the distribution of plankton in relation to physical processes and the functional state of marine ecosystems (Kushnir et al., 1997; Piontkovski et al., 2003; Kim et al., 2006). Furthermore, it has operational importance because emissions of light stimulated by turbulence can allow the detection of surface and subsurface vessels at night (Moline et al., 2007). Forecasting the distribution of bioluminescence would be useful both operationally and to allow further scientific study. However, little is known about how the bioluminescent field varies spatially and temporally and previous attempts to forecast it have had limited success (Ondercin et al., 1995; Shulman et al., 2010; 2011).

It has been suggested that accurate and robust forecasting of surface ocean bioluminescence requires consideration within models of the ecological and behavioural dynamics of bioluminescent organisms (Shulman et al., 2011). In situ observations indicate that dinoflagellates are a major source of bioluminescence in the surface ocean and their light emissions often dominate the stimulated bioluminescent field (Seliger et al., 1962; Batchelder and Swift 1989; Lapota et al., 1992; Neilson et al., 1995; Latz and Rohr, 2005). Therefore, this thesis investigated several aspects of dinoflagellate bioluminescence using a combination of observational and modelling studies. The aim was to build a foundation for the future forecasting of surface ocean bioluminescence within the open ocean North Atlantic. The research addressed three key areas where increased knowledge could guide future forecasting attempts (**Chapter 1**). These were:

Daily variations in bioluminescence intensity;

- The research conducted found that bioluminescent intensity stimulated from mixed populations of dinoflagellates in the northeast Atlantic varies by over an order of magnitude between day and night (**Section 2.3**). The periodicity and magnitude of the variations are significantly influenced by diurnal variations in irradiance (**Section 2.3**).

Seasonal variations in dinoflagellates and their bioluminescence;

- The research conducted found that seasonal changes in bioluminescent dinoflagellate abundance and their potential bioluminescent intensity are positively correlated with seasonal changes in total dinoflagellate abundance within the northeast Atlantic (**Section 3.3**). A biogeochemical model was developed that accurately reproduces the typical dinoflagellate seasonality within the same region (**Section 5.3.4**).

Modelling the ecological function of dinoflagellate bioluminescence;

- The research conducted found that the inclusion of dinoflagellate bioluminescence in a biogeochemical model led to a change in modelled ecosystem dynamics causing mortality from sources other than predation to become a significant control of phytoplankton abundance (**Section 6.5**). Parameterisation of bioluminescence did not significantly improve the ability to simulate seasonal changes in dinoflagellates but did potentially improve the simulations of zooplankton (**Section 6.5**).

7.1 Summary of Research Findings

This section summarises and synthesises the findings from each analysis chapter, relating them back to the objectives and overall aim of the thesis as set out in **Section 1.7**. Analyses of observational data conducted in **Chapters 2** and **3** allowed examination of the dominant timescales over which bioluminescence varies. Information gained from these analyses (specifically **Chapter 3**) was subsequently used to develop a biogeochemical model in **Chapters 4** and **5**. Finally, an exploration of how the ecological function of bioluminescence could be incorporated into this model and its effect upon model performance and ecosystem dynamics was conducted in **Chapter 6**. All studies focused upon the open ocean region surrounding the Porcupine Abyssal Plain (PAP) sustained observatory within the northeast Atlantic (49° N 16.3° W).

7.1.1 Objective 1: Investigate controls upon diurnal changes in bioluminescent intensity

In **Chapter 2**, diurnal variations of bioluminescent intensity and its controls were examined from in situ observations. Diurnal changes in irradiance were found to affect bioluminescent intensity through direct exogenous control (photo-inhibition) and by influencing endogenous (circadian) rhythms. A positive linear relationship was found between intensity of daytime irradiance and brightness of stimulated bioluminescence. This indicated that photo-enhancement was taking place (**Section 2.3**). These findings demonstrate that, on short time scales of hours to days, forecasting bioluminescent

intensity will be heavily dependent upon modelling its relationship with the local light conditions. However, this relationship is a function of the taxonomic composition and the cellular condition (e.g. nutrition) of the dinoflagellate community at any one time or location. Therefore, such a relationship is not, on its own, sufficient to forecast the bioluminescent field across large spatial extents, such as the North Atlantic basin, or on longer time scales of weeks to months.

7.1.2 Objective 2: Explore the seasonal dynamics of bioluminescent dinoflagellates, their inferred bioluminescent signal and relationship with the dinoflagellate community as a whole.

In **Chapter 3**, data from the Continuous Plankton Recorder (CPR) survey were used to gain insight into the seasonal dynamics of the dinoflagellate community and its inferred bioluminescence. For a typical year bioluminescent dinoflagellate abundance and their potential bioluminescent signal were found to peak in July. A strong positive correlation ($r_s = .848$; $p < .0001$; $n = 75$) existed between seasonal changes in bioluminescent dinoflagellate abundance and that of the total dinoflagellate community (i.e. bioluminescent + non-bioluminescent dinoflagellates). This indicated that, seasonal changes in abundance of the total dinoflagellate community can be used as a proxy for those of the bioluminescent dinoflagellate population (**Section 3.4**). Estimates of potentially stimulated bioluminescent intensity also mirrored changes in the total dinoflagellate community (**Section 3.3**) suggesting that total dinoflagellate abundance can also be used as a proxy for stimulated bioluminescent intensity. These findings have important implications for the forecasting of surface ocean bioluminescence in the North Atlantic (**Section 3.3**). They suggest that a first order approximation of the bioluminescent field could be gained through successfully modelling dinoflagellates as a group without the need to explicitly model bioluminescent species. This provides a means for forecasting potential changes in the bioluminescent field across broad spatial scales and seasonal timescales.

7.1.3 Objective 3: Develop a simple biological model which allows the investigation of the ecological function of dinoflagellate bioluminescence.

In **Chapter 4**, a simple zero-dimensional 'NPZ type' model was constructed which could be used to investigate the ecological function of dinoflagellate bioluminescence and its impact upon a modelled ecosystem. The association between bioluminescent dinoflagellate abundance and that of the total dinoflagellate community, found in **Chapter 3**, meant the model did not have to explicitly contain bioluminescent dinoflagellate species, only dinoflagellates as an aggregated group. Diatoms were also accounted for in the model as their competition for nutrients can be a major influence

on dinoflagellate seasonality and they are important members of the phytoplankton community in the North Atlantic in regards to the spring bloom.

In **Chapter 5**, the calibration of model parameters and analysis of model performance and system dynamics were carried out without consideration of the ecological function for bioluminescence. This baseline run of the model was necessary to assess and understand the full impact of the ecological function of bioluminescence on the modelled system in **Chapter 6**. Without considering the ecological function of bioluminescence the baseline model performed well when compared to observations, successfully simulating the typical seasonal variation in dinoflagellate abundance (**Section 5.3.4**).

7.1.4 Objective 4: Explore the ecological function of dinoflagellate bioluminescence – how it could be modelled and what its potential affects upon an ecosystem are.

In **Chapter 6**, the impacts of dinoflagellate bioluminescence upon a modelled ecosystem were explored. This is, to the author's knowledge, the first attempt to model the ecological function of dinoflagellate bioluminescence. Several terms representative of the two proposed mechanisms by which dinoflagellate bioluminescence acts as a survival strategy were developed. Inclusion of these terms into a biogeochemical model had several effects on the dynamics of the modelled ecosystem, including phytoplankton losses becoming dominated by natural mortality rather than grazing (**Section 6.5.3**). There was some evidence that consideration of the ecological function of bioluminescence could improve simulations of zooplankton. However, terms representative of dinoflagellate bioluminescence were not able to significantly improve the ability of the model to simulate the seasonal changes in other state variables including dinoflagellates (**Section 6.5.2**). A lack of data to adequately constrain the model system, particularly for zooplankton and individual phytoplankton group biomasses, made it difficult to determine whether the observed changes within the model system were due to the bioluminescent terms or a lack of constraint in parameters. This limitation needs to be addressed in future studies. Further experimental evidence to directly verify the ecological function of dinoflagellate bioluminescence and the exact mechanisms by which it occurs is also required to ensure its ecological effect is being accurately represented in models. Improvement in modelling the dynamics of an ecosystem where bioluminescent dinoflagellates are present will in turn improve forecasting of surface ocean bioluminescence.

7.2 Forecasting Bioluminescence in the North Atlantic

This section provides a broader discussion of how, given the findings of the thesis, the forecasting of surface ocean bioluminescence in the North Atlantic may best progress, with a specific focus on the priorities for future research.

The abundance and distribution of any bioluminescent organism is a physiological and ecological response to the physical, chemical and biological environment (Moline et al., 2007; Haddock et al., 2010). Consequently, variations in environmental conditions will influence how the organisms which dominate the bioluminescent field vary both spatially and temporally. The reason why empirical relationships between bioluminescent intensity and environmental variables such as temperature and chlorophyll do not remain consistent throughout the ocean (Losee et al. 1989; Lapota et al., 1989; Cussatlegras et al., 2001) is due to the complex and ever changing relationships between bioluminescent plankton, their environment and other planktonic organisms. Attempts to forecast the distribution of the bioluminescent field within the North Atlantic using such inconsistent relationships has had very limited success (Ondercin et al., 1995). Modelling the ecological processes of bioluminescent organisms and their reactions to changes in environment could potentially offer a more reliable way to forecast the spatial and temporal distribution of bioluminescence.

7.2.1 Correlations between Bioluminescence and Dinoflagellate Abundance

The abundance of bioluminescent dinoflagellate species and their potential bioluminescent intensity were shown to be positively correlated ($r_s = .848$; $p < .0001$; $n = 75$) with seasonal changes in the total dinoflagellate abundance within the northeast Atlantic (**Section 3.3.3**). These results are comparable with previous findings within the Mediterranean, Black Sea and Southern Sea of Korea (Tokarev et al., 1999a; Kim et al., 2006). The results suggest that within the North Atlantic, a first order approximation of the bioluminescent field could be gained by modelling the dinoflagellate community as an aggregated group. This removes the need to separate bioluminescent species from non-bioluminescent species within models.

The ability to relate broad changes in bioluminescent intensity to changes in the total dinoflagellate abundance is advantageous as modelling a solely bioluminescent dinoflagellate 'functional group' requires information which is currently unknown. For example, specific knowledge of what, if any, ecological niche bioluminescent dinoflagellates hold and how their physiological, behavioural and morphological traits differ from their non-bioluminescent counterparts would be required.

However, before such a forecasting approach to bioluminescence is taken further, analysis is needed to ensure that the positive correlation found holds over the wider North Atlantic. This can be achieved using the full extent of the CPR survey data, which covers extensive regions of the North Atlantic (Richardson et al., 2006) (**Figure 3.2**).

7.2.2 Modelling Dinoflagellates

Assuming a correlation between bioluminescence and dinoflagellate abundance across the North Atlantic, a model able to simulate changes in dinoflagellate abundance may have the capability to reproduce much of the seasonal and large scale spatial variation in the bioluminescent field. However, dinoflagellates have been under represented within ecological models for the open ocean as they are often considered unimportant away from coastal areas (Vichi et al., 2007) with no distinct biogeochemical role (Le Quere et al., 2005) (**Section 4.2**).

Within this thesis an ecological model was developed that is able to successfully simulate the broad seasonal changes in dinoflagellates within the open ocean northeast Atlantic (**Section 5.3**). This model potentially provides a platform for the future forecasting of the bioluminescent field in the North Atlantic. However, further development of the model and consideration of potential limitations is required before it can be used for the purposes of forecasting dinoflagellates.

7.2.2.1 Further Validation

Further validation of the present model is required on an interannual level. For the purposes of forecasting it is important that the model is able to simulate changes in dinoflagellates in individual years rather than over a typical year that averages over several years, as has been achieved at present. For the model to be applied to the wider North Atlantic it is also important that its ability to simulate interannual variations in dinoflagellate abundance is independently assessed in locations other than the region surrounding the PAP observatory. This could be achieved by testing the models ability to simulate seasonal changes in dinoflagellate abundance from other standard areas of the CPR survey which stretch across the North Atlantic (**Figure 3.2**). However, it must be ensured that both the temporal and spatial coverage within other CPR regions is sufficient to accurately represent the seasonal changes of the dinoflagellate population before further validation of the model is carried out.

7.2.2.2 Model Structure

At present the structural simplicity of the model may hamper its predictive skill in other locations. Currently the model lacks terms representing a detrital pool or microbial loop (bacteria), which could restrict accurate simulation of recycled nutrient availability (Anderson, 2010). These terms may be particularly important in oligotrophic regions (such as the subtropical North Atlantic) where nutrient availability is heavily dependent upon recycling in the surface layer. Thus, representing the detrital pool and microbial loop in the model may be important for future application of the model to the wider North Atlantic. Prior to the addition of these terms, it may also be useful to compare between model simulated loss of material from the upper mixed layer and export flux measured within the E5 area. As described in **Section 4.3.4**, at present, material which is not remineralised within the upper layer of the model effectively represents exported material. Thus, a rough comparison between model and observed export flux could be made to further assess the current models ability to simulate recycled nutrient availability.

As discussed in **Sections 5.4** and **6.6**, the model structure may also require the addition of other phytoplankton types, such as small flagellates and their corresponding grazers protozooplankton. The inclusion of small flagellates to the model may improve simulations of chlorophyll and in turn simulations of absolute dinoflagellate biomass, particularly because in situ observations have shown they can make up a significant amount of the pre and post bloom chlorophyll biomass within the North Atlantic (Sieracki et al., 1993; Verity et al., 1993). The inclusion of protozooplankton would be required for accurate representation of nutrient transfer between small phytoplankton and metazooplankton. Furthermore, the inclusion of protozooplankton may also improve simulations of recycled nutrient availability as they are thought to have an important role in the cycling of organic matter in oceanic waters (Verity et al., 1993). These additions may also improve the spatial transferability of the model as there is some evidence to suggest that greater phytoplankton complexity within ecosystem models can generate enhanced portability (Friedrichs et al., 2007). However, it must be remembered that, increasing model complexity will require additional data to constrain any additional parameters. Such data may not be readily available.

7.2.2.3 Mixotrophy

The current model assumes that dinoflagellates are purely photoautotrophic. As indicated in **Section 3.3.2**, the majority of dinoflagellates present in the CPR data for the open ocean northeast Atlantic were classified as mixotrophs, gaining nutrition

through both photosynthesis and phagotrophy (**Appendix B**). Although the modelling of mixotrophy is still very much in its infancy, a more accurate description of dinoflagellate nutritional intake and growth in future models may potentially lead to improvements in the ability to model them as a group. However, it must be remembered that increasing model complexity does not guarantee increased predictive power (Fulton et al., 2004; Cordoleani et al., 2011).

Inclusion of mixotrophy in models increases the number of paths by which nutrients can pass through a system to the highest trophic levels compared to traditional models. This has been found to have important effects on the trophic dynamics and stability of modelled ecosystems (Stickney, 2000; Jost et al., 2004). Mixotrophic behaviour may also mean that bioluminescence has a greater ecological effect upon an ecosystem than previously considered. Increased survival of dinoflagellates could not only come via a startle response or burglar alarm effect, but also by reducing the abundance of predators competing for their prey. For example, if mixotrophic dinoflagellates share a prey species with a metazoan zooplankton such as copepods, increased copepod mortality or decreased copepod grazing due to encounters with bioluminescence will decrease dinoflagellate–copepod competition for food.

7.2.2.4 Physical Limitations

The present model represents the biological ecosystem as homogeneously distributed within an upper mixed layer which overlies a deep abiotic layer. Physical dynamics within the mixed layer are not explicitly modelled and no horizontal effects, such as advection, are currently considered. Physical processes determine the structure and distribution of pelagic ecosystems as they are the controlling factor in the availability of nutrients and light, and cause the advection and diffusion of plankton vertically and horizontally. If the forecasting of dinoflagellates on finer horizontal or vertical spatial resolutions is desired in future, the biological model developed will need to be coupled with a more detailed physical model that accurately represents changes in the physical environment at the required spatial scale. This will, for example, allow the spatial patchiness of plankton at the mesoscale to be resolved. Finer horizontal or vertical spatial resolution may be achieved by implementing the model into a 3-D ocean general circulation modelling (GCM) framework such as NEMO (Nucleus for European Models of the Ocean; Madec, 2008). Incorporation into such a GCM will require investigation of the impact of the more complex physical environment upon the model simulations.

7.2.2.5 Data Limitations

A major limitation for the further development of the current dinoflagellate model is a lack of observational data to constrain model parameters and to validate simulations. Additions to the model structure will need to weigh up the benefit to predictive skill against the cost of increasing the number of parameters that require constraining. The increase in parameter numbers can be significant, approximating to the square of the number of model compartments (Denman, 2003). Apart from the lack of zooplankton data which has been discussed in **Sections 5.4** and **6.6**, the lack of availability of abundance data for individual phytoplankton groups is known to hinder the calibration and validation of multiple phytoplankton functional type (PFT) models (Hofmann, 2010). However, the development of methods to identify PFTs from satellite derived data are continually advancing and may provide data, in the near future, which can be used for robust model testing of the horizontal distributions of specific phytoplankton types such as dinoflagellates (Aiken et al., 2007; Alvain et al., 2008; Raitsos et al., 2008).

Although satellite and CPR survey data can provide information on the horizontal distribution of phytoplankton biomass it cannot provide any information on their vertical distribution. Data indicating the vertical distribution of plankton is spatially and temporally sparse, especially for individual PFTs. This is because vertical profiles of chlorophyll, which indicate total phytoplankton biomass, or HPLC (High-Performance Liquid Chromatography) pigments, which allow the identification of PFTs, are collected from direct in situ measurements that are themselves spatially and temporally sparse.

7.2.3 What it is Feasible to Forecast?

Given a model which simulates the distribution of a dinoflagellate phytoplankton group, the question of how it may be used to forecast bioluminescence arises. In the first instance model simulations could be used to provide a straight forward probability map of when and where high intensities of stimulated bioluminescence are likely to occur. For example, an increase in integrated mixed layer dinoflagellate biomass above the annual average would be associated with increased presence of bioluminescent cells. This in turn, would be associated with a higher than average probability of stimulating bioluminescence in that particular area at that particular time of year; a relative probability scale in relation to the magnitude of any increase above an average could be subjectively set.

Forecasting the intensity of the potentially stimulated bioluminescence will be more challenging. One approach to forecasting bioluminescent intensity would be to

combine a successful dinoflagellate model with a bioluminescent algorithm such as that used in the modelling attempt of Ondercin et al. (1995). A simple term was used by Ondercin et al (1995) which estimated bioluminescent intensity within the mixed layer as a function of simulated chlorophyll concentration and instantaneous solar irradiance at the sea surface. Such an algorithm could be easily altered to become a function of simulated dinoflagellate biomass rather than chlorophyll. The results of **Chapter 2** indicate that such an algorithm should incorporate a relationship between bioluminescent intensity and irradiance which accounts for both photo-inhibition and photo-enhancement. As discussed in **Section 2.4**, the intensity of bioluminescent emissions can also be dependent on the nutritional and physiological state of the population (Buskey et al., 1994; Latz and Jeong, 1996). Therefore, a more complex algorithm could also calculate bioluminescent intensity as a function of nutrient concentration. For the accurate forecasting of bioluminescent intensity the relationships between dinoflagellate abundance, irradiance, nutrient concentration and bioluminescent intensity will need to be further defined through in situ observations and laboratory experiments.

The forecasting of the board seasonal patterns in the bioluminescent field within the North Atlantic, even if at coarse spatial resolutions, would be a significant step forward from what can currently be achieved. From an operational perspective, the forecasting of where and when bioluminescence is likely to occur, even if the intensity itself cannot be estimated, will provide valuable information that can be used to inform decision making. Scientifically, this information could be used to target field studies. For example, knowing when and where dinoflagellates, and therefore bioluminescent dinoflagellates, are likely to be in high abundance could be used to target the collection of North Atlantic bioluminescent species to be held in culture. Species which are common in the North Atlantic but not commonly held in culture such as bioluminescent *Ceratium* spp. or *Protoperidinium* spp. could be targeted for collection. Such cultures are required in laboratory experiments to determine the relationships between dinoflagellate abundance, irradiance, nutrient concentration and bioluminescent intensity. Cultures are also required to gain specific information on physiological rates of bioluminescent species and to gain further experimental evidence of the ecological function of their light emitting ability and its mechanisms.

7.2.4 Future Work for Forecasting Bioluminescence

One major limitation to the forecasting of bioluminescence in the North Atlantic at present is the lack of bioluminescence data available. Spatial and seasonal time series datasets of bioluminescent intensity are required for the calibration and validation of future modelling attempts. These can be gained through bathyphotometers mounted

on fixed moorings or towed platforms. Measurements of irradiance and stimulated bioluminescence should also be made on laboratory cultures and in mixed populations to both further determine and parameterise the relationship between them. Results obtained can be used to develop an algorithm for bioluminescence which can be combined with a model that forecasts dinoflagellate abundance in the North Atlantic. The uncertainty surrounding the ecological function of dinoflagellate bioluminescence, and the mechanisms by which it occurs, limits the current ability to investigate its ecological impact through modelling studies. Further laboratory studies are required to quantify the survival benefit bioluminescence provides to bioluminescent dinoflagellates and surrounding phytoplankton.

7.3 Conclusion

Forecasting the bioluminescent field across the World's surface ocean is an enormous challenge. This thesis has provided insight into how the forecasting of bioluminescence within the open ocean could be met in future. The thesis has demonstrated that within the North Atlantic modelling the dinoflagellate population could provide a potentially fruitful way to forecast the bioluminescent field. To this end, a model has been developed that provides a platform for forecasting the bioluminescent field in the future. Furthermore, gaps in current knowledge and data necessary to further develop forecasting capability have been identified. Overall, the thesis reveals how understanding bioluminescent organisms' physiology, ecology and ability to emit light will allow the forecasting capability of surface ocean bioluminescence to evolve and improve.

Appendix A: Bioluminescent Dinoflagellate Species

Table A.1 lists 68 dinoflagellate species identified as bioluminescent within the literature reviewed throughout the thesis. Only species which have been confirmed to be bioluminescent through use in laboratory studies or measurement of flash kinetics have been included. The list does not include species whose bioluminescence has been disputed, such as *Ceratium tripos*, or species where bioluminescence has been presumed due to correlation in their presence and a bioluminescent event, such as *Alexandrium margalefii*.

Table A.7.1: List of 68 dinoflagellate species identified as bioluminescent within the literature reviewed throughout the thesis.

Species	Reference
<i>Alexandrium affine</i>	Liu et al. (2004)
<i>Alexandrium fundyense</i>	Baker et al. (2008)
<i>Alexandrium monilatum</i>	Latz et al. (2008); Sweeney (1963)
<i>Alexandrium ostenfeldii</i>	Kremp et al. (2008)
<i>Alexandrium tamarense</i>	Buskey et al. (1983)
<i>Alexandrium acatenella</i>	Esaias et al. (1973)
<i>Alexandrium cf. catenella</i>	Sweeney (1963); Esaias and Curl (1972); Baker et al. (2008)
<i>Ceratium breve</i>	Lapota and Losee (1984)
<i>Ceratium furca</i>	Sweeney (1963); Lapota and Losee (1984)
<i>Ceratium fusus</i>	Kelly (1968); Kelly and Katona (1966); Lapota and Losee (1984); Buskey and Swift (1990); Lapota et al., (1992); Sullivan and Swift (1995); Swift et al. (1995); Latz et al. (2004a)
<i>Ceratium gibberum</i>	Lapota and Losee (1984)
<i>Ceratium horridum</i>	Lapota and Losee (1984); Buskey and Swift (1990); Batchelder et al. (1992)
<i>Ceratocorys horrida</i>	Latz and Jeong (1996); Latz et al. (2004a); Latz et al. (2004b)
<i>Fragilidium heterolobum</i>	Sweeney (1963)
<i>Alexandrium acatenella</i>	Esaias and Curl (1972)
<i>Gonyaulax catenata</i>	Tett and Kelly (1974)
<i>Gonyaulax digitale</i>	Kelly and Katona (1966); Kelly (1968); Swift et al. (1995)
<i>Gonyaulax excavata</i>	White (1979)
<i>Gonyaulax grindleyi</i>	Swift et al. (1995)




<i>Gonyaulax hyalina</i>	Sweeney (1963)
<i>Gonyaulax monacantha</i>	Buskey and Swift (1990)
<i>Gonyaulax parva</i>	Swift et al. (1995)
<i>Gonyaulax ploygramma</i>	Buskey and Swift (1990); Swift et al. (1995)
<i>Gonyaulax scrippsae</i>	Buskey and Swift (1990)
<i>Gonyaulax sphaeroides</i>	Sweeney (1963)
<i>Gonyaulax spinifera</i>	Kelly and Katona (1966); Kelly (1968); Swift et al. (1995)
<i>Lingulodinium polyedrum</i>	Sweeney (1963); Biggley et al. (1969); Esaias and Curl (1972); Abrahams and Townsend (1993); Latz and Rohr (1999);); Latz et al. (2004a); Latz et al. (2004b); von Dassow et al. (2005); Maldonado and Latz (2007); Latz et al. (2009)
<i>Noctiluca scintillans</i>	Sweeney (1971); Swift et al. (1973); Buskey and Swift (1990); Buskey et al. (1992)
<i>Polykrikos kofoidii</i>	Buskey et al. (1992)
<i>Polykrikos schwartzii</i>	Tett and Kelly (1971)
<i>Protoceratium reticulatum</i>	Liu et al. (2004)
<i>Protoberidinium antarcticum</i>	Raymond and DeVries (1976)
<i>Protoberidinium brevipes/breve</i>	Swift et al. (1995)
<i>Protoberidinium brochii</i>	Sweeney (1963)
<i>Protoberidinium cerasus</i>	Swift et al. (1995)
<i>Protoberidinium claudicans</i>	Kelly and Katona (1966); Kelly (1968)
<i>Protoberidinium conoides</i>	Swift et al. (1995)
<i>Protoberidinium conicum</i>	Sweeney (1963); Kelly and Katona (1966); Kelly (1968); Swift et al. (1995)
<i>Protoberidinium crassipes</i>	Buskey and Swift (1990); Buskey et al. (1992); Swift et al. (1995)
<i>Protoberidinium curtipes</i>	Lapota et al. (1992); Lapota et al. (1989)
<i>Protoberidinium depressum</i>	Sweeney (1963); Kelly (1968); Lapota and Losee (1984); Lapota et al. (1989); Buskey et al. (1992); Swift et al (1995); Li et al. (1996)
<i>Protoberidinium divergens</i>	Kelly (1968); Buskey et al. (1992); Latz and Jeong (1996)
<i>Protoberidinium excentricum</i>	Buskey et al. (1992)
<i>Protoberidinium exiquipes</i>	Buskey et al. (1992)
<i>Protoberidinium globulus</i>	Kelly (1968); Buskey and Swift (1990); Swift et al. (1995)
<i>Protoberidinium granii</i>	Kelly and Katona (1966); Swift et al. (1995)
<i>Protoberidinium huberi</i>	Buskey et al. (1994)
<i>Protoberidinium leonis</i>	Kelly (1968); Buskey and Swift (1990); Swift et al. (1995); Herren et al. (2004)
<i>Protoberidinium minutum</i>	Swift et al. (1995)
<i>Protoberidinium oceanicum</i>	Kelly and Katona (1966); Kelly (1968); Lapota and Losee (1984); Buskey and Swift (1990)
<i>Protoberidinium ovatum</i>	Swift et al. (1995); Buskey and Swift (1990)
<i>Protoberidinium pallidum</i>	Kelly (1968); Swift et al. (1995); Buskey and Swift (1990)
<i>Protoberidinium pellucidum</i>	Swift et al. (1995)
<i>Protoberidinium pentagonum</i>	Sweeney (1963); Kelly (1968); Buskey et al. (1992); Swift et al. (1995)
<i>Protoberidinium punctulatum</i>	Kelly (1968)


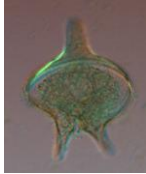


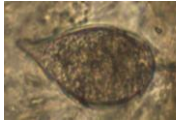
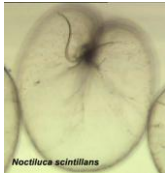
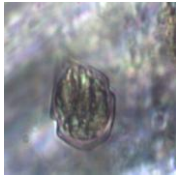
<i>Protoperidinium pyriforme</i>	Swift et al. (1995)
<i>Protoperidinium saltans</i>	Swift et al. (1995)
<i>Protoperidinium sinaicum</i>	Swift et al. (1995)
<i>Protoperidinium sournia</i>	Swift et al. (1995)
<i>Protoperidinium steinii</i>	Buskey and Swift (1990); Swift et al. (1995)
<i>Protoperidinium subinermis</i>	Kelly and Katona (1966); Kelly (1968)
<i>Protoperidinium tubum</i>	Swift et al. (1995)
<i>Pyrocystis acuta</i>	Swift et al. (1973)
<i>Pyrocystis fusiformis</i>	Swift et al. (1973); Sweeny (1982); Mensinger and Case (1992); Fleisher and Case (1995); Latz et al. (2004b)
<i>Pyrocystis lunula</i>	Kelly and Katona (1966); Seliger et al. (1966); Biggley et al. (1969); Swift et al. (1973); Swift and Buskey (1996); Craig et al. (2003)
<i>Pyrocystis noctiluca</i>	Herring (1983); Cussatlegras and Gal (2004); Buskey and Swift (1990)
<i>Pyrodinium bahamense</i>	Biggley et al. (1969)
<i>Pyrophacus steinii</i>	Lapota et al. (2007)

Appendix B: Dinoflagellate Nutritional Strategy

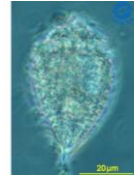
Analysis in **Chapter 3** required the nutritional strategy of each dinoflagellate genera or species present in the CPR data to be identified from the literature. For the purpose of this classification all *Ceratium* species in the CPR data are considered in a single *Ceratium* spp. group and the two categories of *Prorocentrum* (previously shown as *Prorocentrum* spp. and *Prorocentrum* spp. ('*Exuviaella*' type)) are also considered as a single grouping. **Table B.1** presents the results of the literature search along with a brief summary of what is known regarding each dinoflagellate genera or species nutritional status.

Table B.1: Classification of dinoflagellate types into representative nutritional strategies. P = Photoautotrophy; M = Mixotrophy and H = Heterotrophy.

Dinoflagellate genera	Nutritional status	Reference	Comments	Picture of Example Species
<i>Cladopyxis</i> spp.	P	http://www.algaebase.org (accessed 06/07/11)	Not many descriptive papers but reported to have "Numerous chloroplasts".	
<i>Dinophysis</i> spp.	M	Hansen (1991); Minnhagen and Janson (2006); Carvalho et al (2007)	Toxic species primarily thought to be photoautotrophic. However, some species classified as heterotrophic with evidence kleptochloroplasty.	
<i>Gonyaulax</i> spp.	M	Stoecker (1999); Yoo et al (2009)	Primarily thought to be photoautotrophic. Only recently found to be mixotrophic.	

<i>Oxytoxum</i> spp.	P	Dodge and Saunders(1985)	All species reported as photosynthetic.	
<i>Protoperidinium</i> spp.	H	Jeong et al (1997); Olseng et al (2002)	Widely known as a heterotrophic species. There is no evidence as yet of mixotrophy.	
<i>Podolampas</i> spp.	M	Hallegraeff and Jeffrey (1984); Stoecker et al (2009); Naik et al (2011)	One species known to host endosymbionts to photosynthesise. Reports of other species not containing red chloroplast fluorescence and other species classified as photoautotrophic.	
<i>Pronoctiluca pelagica</i>	H	Hallegraeff and Jeffrey (1984); Naik et al (2011)	Widely thought of as heterotrophic no examples of mixotrophy found.	
<i>Prorocentrum</i> spp.	M	Stoecker (1999); Hansen (2011); Naik et al (2011)	Seen to contain permanent chloroplasts. But also contain food vacuoles.	
<i>Cystodinium</i> spp.	P	Schnepf and ElbräChte (1999)	Species seen to contain chloroplasts. Freshwater species are also known to be photoautotrophic.	No Picture
<i>Noctiluca scintillans</i>	H	Stoecker (1999); Hansen (2011);	Widely known as heterotrophic but can contain endosymbionts in the green Noctiluca strain which is mainly found in tropical regions. Other strains have no symbionts.	
<i>Scrippsiella</i> spp.	M	Hallegraeff and Jeffrey (1984); Stoecker (1999) Naik et al (2011)	Known to contain red fluorescent chloroplasts but some studies have suggested cells also have food vacuoles.	

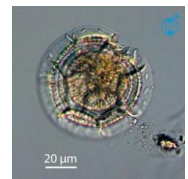
<i>Corythodinium</i> spp.	P	Hallegraeff and Jeffrey (1984); Naik et al (2011)	Known to contain red fluorescent chloroplasts.
------------------------------	---	---------------------------------------------------------	---------------------------------------------------



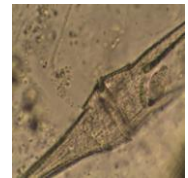
<i>Gyrodinium</i> spp.	M	Stoecker 1999; Hansen 2011; Skovgaard 2000	Contain permanent chloroplasts. Observation of food vacuoles and ingestion.
------------------------	---	--------------------------------------------------	-----------------------------------------------------------------------------------



<i>Goniodoma</i> <i>polyedricum</i>	P	Hallegraeff and Jeffrey (1984); Naik et al (2011)	Known to contain red fluorescent chloroplasts.
----------------------------------------	---	---------------------------------------------------------	---------------------------------------------------



<i>Ceratium</i> spp.	M	Smalley et al (1999); Stoecker (1999); Hansen (2011)	Thought to be primarily photoautotrophic but known to ingest prey.
----------------------	---	------------------------------------------------------------	--------------------------------------------------------------------------



Pictures were sourced from the SAHFOS taxonomy web pages at www.sahfos.ac.uk/taxonomy/phytoplankton/dinoflagellates. Exceptions to this were *Podolampas* spp., *Corythodinium* spp. and *Goniodoma polyedricum* which were sourced from planktonnet.awi.de, *Pronoctiluca pelagica* sourced from www.smhi.se and *Noctiluca scintillans* sourced from tolweb.org/Dinoflagellates.

Appendix C: Model Code

The FORTRAN 90 code of the biological model equations is given below.

```
Module ODE

  Use Growth
  Use accuracy
  Use Parameters
  Use nrtype
  Use Mixedlayer
  Use Terms
  Use Functions

  Implicit None

  Contains

  Subroutine Derivs (x,y,dydx)!x is time

    Real(SP), Dimension (:), Intent(in):: y
    Real(SP), Dimension (:), Intent(out):: dydx
    Real(SP),intent(in) :: x
    Real(SP) :: growth1, growth2, M, M2, yrln, t,p2,p1
    Real(SP) :: h, hplus
    Real :: a1, c1, d1,rnsi

    yrln=365

    t=ceiling(x)

    !Define value for deep nutrient concentrations
    N0=Nit0(t,1)
    Si0=S0(t,1)

    p1=y(2)
    p2=y(3)

    call functional_response(p1,p2,g,eps)
    call MLDepth(t,M,M2)
    call EP85_eqn (x,y,t,yrln,M,growth1,growth2)

    h=(M2-M)/1
    hplus=max(h,0.0)
```



```

! yin(1)=Nitrate, yin(2)=Diatoms, yin(3)=Dinoflagellates,
yin(4)=Zooplankton, yin(5)=Silicate

      a1 = min((y(1)/(y(1)+kn1)), (y(5)/(y(5)+ksi)))
!zooplankton mortality
      zoomort = (eps*(y(4)**2))/(kmz+y(4))
!proportion grazing lost as messy feeding
      c1 = (1-beta)*g
      d1 = (y(2)+y(3))/(kz+y(2)+y(3))
!total messy feeding term
      messyfeed = c1*d1*y(4)
!diatom growth term
      diatgrowth = growth1*a1*y(2)
!Dinoflagellate growth term
      dinogrowth = growth2*(y(1)/(y(1)+kn2))*y(3)
!diatom mortality
      diatmort = (mp*(y(2)**2))/(km+y(2))
!dino mortality
      dinomort = (mp*(y(3)**2))/(km+y(3))
!zooplankton growth term
      zoogrowth = g*beta*d1*y(4)
!grazing loss on diatoms
      diatgraz = g*(y(2)/(kz+y(2)+y(3)))*y(4)
!grazing loss on dinos
      dinograz = g*(y(3)/(kz+y(2)+y(3)))*y(4)
!redfield ratio N:Si
      rnsi = (16/15)
!N remineralisation term
      Nremin=tau*(zoomort+(diatmort+dinomort)+messyfeed)
!Si remineralisation term
      Siremin=tau*(diatmort+diatgraz)

      !Calculation of mixing coeffiecents

      mixcop1=(y(2)*(mix+hplus+Vdia))/M
      mixcop2=(y(3)*(mix+hplus))/M
      mixcoz=(y(4)*h)/M
      mixcon=(N0-y(1))*((mix+hplus)/M)
      mixcosi=(Si0-y(5))*((mix+hplus)/M)

      !Biological Equations

      dydx(1)= Nremin-diatgrowth-dinogrowth
      dydx(2)= diatgrowth-diatmort-diatgraz
      dydx(3)= dinogrowth-dinomort-dinograz
      dydx(4)= zoogrowth-zoomort
      dydx(5)= Siremin-diatgrowth

      !Addition of effects due to mixing and mixed layer
      dydx(1)=dydx(1)+mixcon
      dydx(2)=dydx(2)-mixcop1

```

```
dydx(3)=dydx(3)-mixcop2  
dydx(4)=dydx(4)-mixcoz  
dydx(5)=(dydx(5)/rnsi) + mixcosi  
  
return  
  
End Subroutine Derivs  
  
End Module ODE
```


Appendix D: Derivation of z-score Uncertainty

It was necessary to convert the phytoplankton data from the CPR into non-dimensional z-scores for the purposes of comparing seasonal variation in the data to that simulated by the model. Furthermore, for the purposes of model assessment and parameter optimisation the associated standard deviation on phytoplankton data also needed to be retained and thus converted to the corresponding z-score uncertainty. A derivation of this uncertainty is given below.

The climatological average abundance of phytoplankton for month j over years $i=1$ to n is given by

$$\bar{x}_j = \frac{\sum_{i=1}^n w_{ij} x_{ij}}{\sum_{i=1}^n w_{ij}} \quad \text{Eq. D.1}$$

where x_{ij} is the average value of month j for year i and w_{ij} is the number of samples used to calculate x_{ij} .

The climatological average \bar{x}_j has an associated variance equal to

$$\sigma_j^2 = \frac{\sum_{i=1}^n w_{ij}}{(\sum_{i=1}^n w_{ij})^2 - \sum_{i=1}^n w_{ij}^2} \sum_{i=1}^n w_{ij} (x_{ij} - \bar{x}_j)^2 \quad \text{Eq. D.2}$$

The average abundance over all climatologically averaged months $j=1$ to N is given by

$$\mu = \frac{1}{N} \sum_{j=1}^N \bar{x}_j \quad \text{Eq. D.3}$$

with an associated variance equal to

$$\sigma_\mu^2 = \frac{1}{N} \sum_{j=1}^N (\bar{x}_j - \mu)^2 \quad \text{Eq. D.4}$$

The z-score for a climatologically averaged month \bar{x}_j with respect to the variation over all climatological averaged months μ is given by

$$z_j = \frac{\bar{x}_j - \mu}{\sigma_\mu} \quad \text{Eq. D.5}$$

z-score (z_j) has an associated variance which can be written as

$$\sigma_{j_z}^2 = \frac{\sum_{i=1}^n w_{ij}}{(\sum_{i=1}^n w_{ij})^2 - \sum_{i=1}^n w_{ij}^2} \sum_{i=1}^n w_{ij} (z_{ij} - z_j)^2 \quad \text{Eq. D.6}$$

where z_{ij} is the z-score for any particular month j in year i over the total dataset and is given by

$$z_{ij} = \frac{x_{ij} - \mu}{\sigma} \quad \text{Eq. D.7}$$

Thus $z_{ij} - z_j$ can be calculated as

$$z_{ij} - z_j = \frac{x_{ij} - \mu - \bar{x}_j + \mu}{\sigma_\mu} \quad \Rightarrow \quad z_{ij} - z_j = \frac{x_{ij} - \bar{x}_j}{\sigma_\mu} \quad \text{Eq. D.8}$$

Substituting Equation D.8 into Equation D.6 gives

$$\sigma_{j_z}^2 = \frac{\sum_{i=1}^n w_{ij}}{(\sum_{i=1}^n w_{ij})^2 - \sum_{i=1}^n w_{ij}^2} \sum_{i=1}^n w_{ij} \frac{(x_{ij} - \bar{x}_j)^2}{\sigma_\mu^2} \quad \text{Eq. D.9}$$

Substituting in Equation D.2, Equation D.9 simplifies to

$$\sigma_{j_z}^2 = \frac{\sigma_j^2}{\sigma_\mu^2} \quad \text{Eq. D.10}$$

Using Equation D.10 the effective standard deviation associated with a z-score z_j is calculated as

$$\sigma_{j_z} = \frac{\sigma_j}{\sigma_\mu} \quad \text{Eq. D.11}$$

It is the value of σ_{j_z} that is quoted as the z-score error within **Chapter 4, Section 4.5.1.**

Appendix E: Model Sensitivity to Forcing

To investigate the sensitivity of model simulations to the forcing data, the baseline model was run using the interannual variations in MLD and PAR for the seven years between January 2001 and December 2007 within CPR standard area E5. Monthly values of MLD and PAR were calculated within each year from ARGO float data and SeaWiFS 9 km resolution PAR data respectively, these data were then spline interpolated to daily values (**Figure E.1a**). Model runs for interannual simulations were initialised from the end of the standard 10 year climatological run. The model was run using each of the optimised parameter vectors in **Table 5.5** in turn and model simulations were compared to observational data. Average monthly simulated nitrate and silicate across the seven year period was compared to climatological WOA09 nitrate and silicate data as no interannual estimates existed (**Figure E.1b and E.1c**). Monthly simulated total phytoplankton biomass (in nitrogen units) was converted to chlorophyll and compared to interannual chlorophyll estimates across the E5 region from the SeaWiFS ocean colour sensor (**Figure E.1d**). The relative seasonal changes in monthly simulated diatom and dinoflagellate phytoplankton biomass was compared to the relative seasonal variation in the monthly averaged cells counts from the CPR survey across the E5 region by standardising phytoplankton biomass and CPR cell counts to a zero (**Figure E.1e and E.1f**). Uncertainties associated with SeaWiFS ocean colour chlorophyll measurements and CPR survey cell abundance data used to calculate model cost were calculated as in **Section 4.5** however, without including the uncertainty associated with the climatological averaging. The reader is referred back to **Section 4.5** for further details on the observational data and its processing.

Table E.1: Breakdown of calculated misfit between model output and observational data using interannual MLD and PAR forcing between 2001 and 2007 for the four parameter vectors found through model optimisation.

Parameter Vector	Model Output to Observational Data Misfit					
	Nitrate	Silicate	Diatoms	Dinoflagellates	Chlorophyll	Total Cost
1	0.6461	0.2924	9.4249	3.8028	1.7199	15.8861
2	0.7873	0.4027	7.6396	3.4108	1.6605	13.9009
3	0.7945	0.3715	7.8505	2.9607	1.5482	13.5254
4	0.7219	0.2958	9.3516	4.9763	1.5553	16.9008

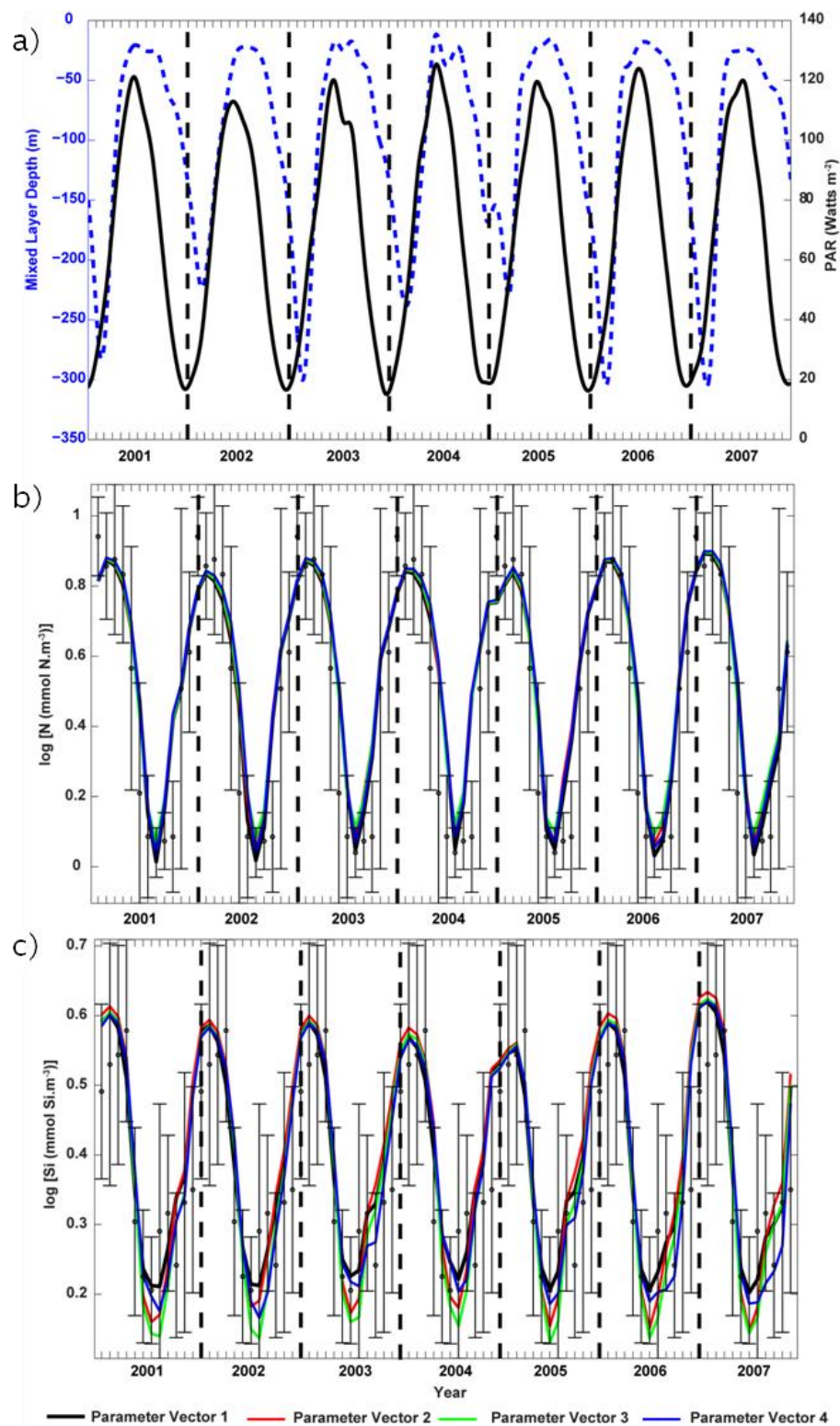
Results indicate that, in general, patterns seen in model simulations are robust and can withstand small changes in forcing (**Figure E.1**). However, using the interannual forcing data causes an increase in the total calculated model to data misfit compared to that which can be achieved using the climatological forcing (equal to 1.8637) (**Table E.1**). The increase in total cost when using the interannual forcing is primarily due to a reduced fit of the relative seasonal variations in diatom and dinoflagellate biomass. On closer investigation the large costs associated with the inability of the model to simulate the relative seasonal variations of diatoms and dinoflagellates over the 2001 to 2007 period can be attributed to just a few months in the years 2004 and 2007 (circled in **Figure E.1e and E.1f**). Using the interannual forcing the model is unable to simulate an increase in both diatoms and dinoflagellates from August to September in 2004. A particularly large cost is associated with the model not simulating this increase as there are only small uncertainties related to the averaged monthly data. The model is also unable to simulate and increase in diatoms from June to July in 2007. Again a large cost is associated with this as the uncertainty related to the monthly values is small. It is worth noting here that only a small number of samples (2 and 5) make up the monthly averages in for September 2004 and July 2007. Thus, it is possible that the uncertainty on these values is substantially underestimated. Removing the three data points in question and recalculating the model to data misfit indicates that model simulations are still classed as very good (<1) or good (1–2) using the performance criteria suggested by Radach and Moll (2006) (**Table E.2**).

Table E.2: Recalculation of misfit between model output and observational data for the four optimised parameter vectors with the comparisons between model diatom and dinoflagellate relative seasonal variations and observational data in September 2004 and diatom relative seasonal variation to observational data in July 2007 removed.

Parameter Vector	Model Output to Observational Data Misfit					Total Cost
	Nitrate	Silicate	Diatoms	Dinoflagellates	Chlorophyll	
1	0.6461	0.2924	0.8757	0.4818	1.7199	4.0159
2	0.7873	0.4027	0.8387	0.5443	1.6605	4.2334
3	0.7945	0.3715	0.8081	0.9089	1.5482	4.4313
4	0.7219	0.2958	0.8877	0.5457	1.5553	4.0062

Figure E.1 indicates that there is little variation in the interannual simulations of the model when using the four different parameter vectors however, some patterns are evident. For example, parameter vector two gives consistently higher peak chlorophyll values over the 2001 to 2007 period. Calculated costs suggest that although parameter vector one was the best at simulating the climatologically averaged data (**Table 5.6**) that parameter vector three is best at simulating interannual variability in the data (**Table E.1**). However, when data from September 2004 and July 2007 are removed the total costs associated with the different parameter vectors are very close

and parameter vector four is narrowly better than the other parameter vectors at simulating the interannual variability in the data.



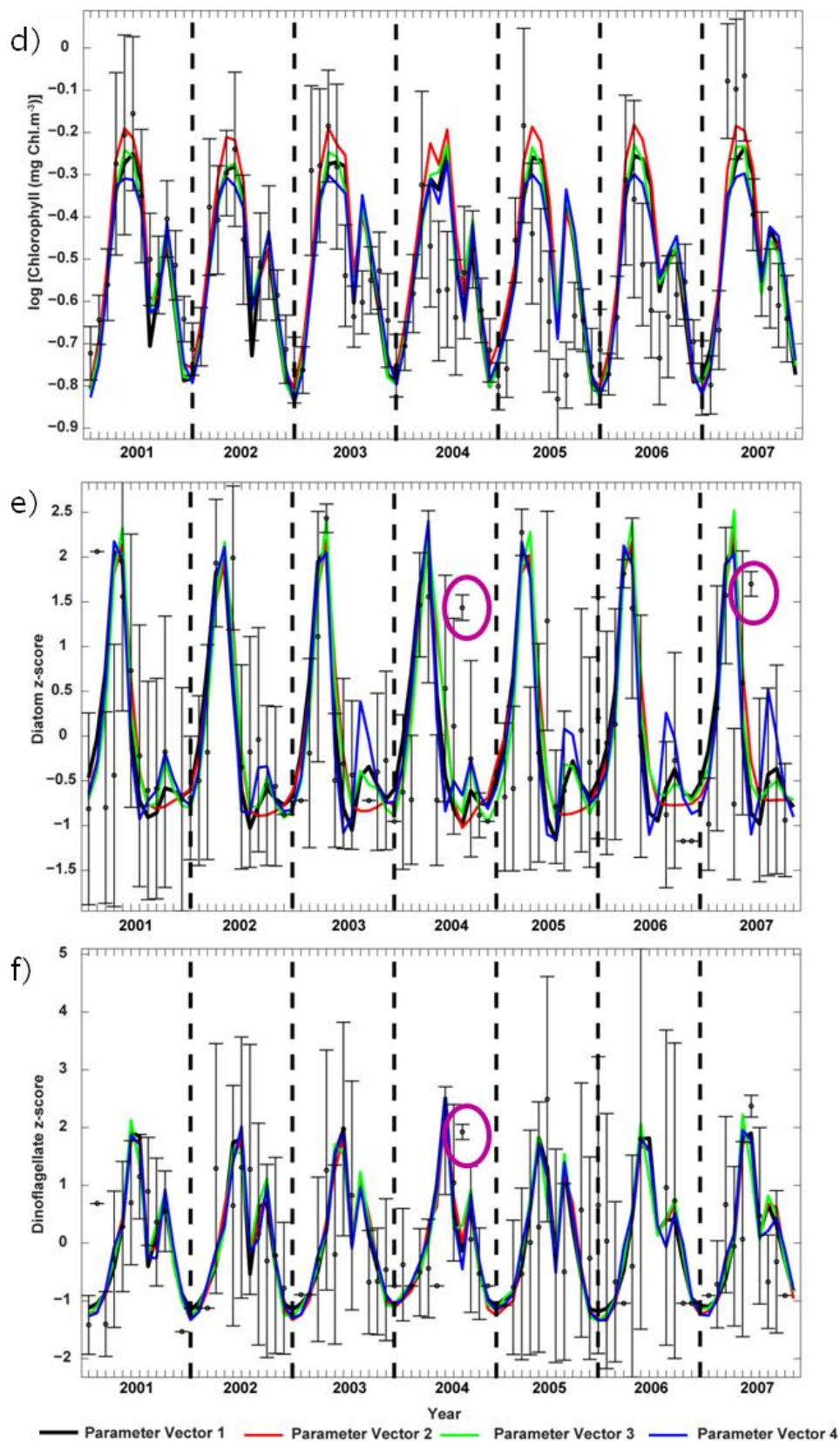


Figure E.1: (a) Interannual variations in MLD and PAR between January 2001 and December 2007. Comparison between interannual model simulations and observational data for (b) nitrate, (c) silicate, (d) chlorophyll, (e) relative seasonal variations in diatoms, (f) relative seasonal variations in dinoflagellates.

References

- Aßmus, J., Melle, W., Tjøstheim, D., Edwards, M. (2009). Seasonal cycles and long term trends of plankton in shelf and oceanic habitats of the Norwegian Sea in relation to environmental variables. *Deep-Sea Research II*, 56: 1895–1909.
- Abrahams, M.V. and Townsend, L.D. (1993). Bioluminescence in dinoflagellates: a test of the burglar alarm hypothesis. *Ecology*, 74: 258–260.
- Aiken, J., Fishwick, J.R., Lavender, S., Barlow, R., Moore, G.F., Sessions, H., Bernard, S., Ras, J., Hardman-Mountford, N.J. (2007). Validation of MERIS reflectance and chlorophyll during the BENCAL cruise october 2002: preliminary validation of new demonstration products for phytoplankton functional types and photosynthetic parameters. *International Journal of Remote Sensing*, 28(3): 497–516
- Aiken, J. and Kelly, J. (1984). A solid state sensor for mapping and profiling stimulated bioluminescence in the marine environment. *Continental Shelf Research*, 3: 445 – 464.
- Allen, J.I., Holt, J.T., Blackford, J., Proctor, R. (2007). Error quantification of a high-resolution coupled hydrodynamic-ecosystem coastal-ocean model: Part 2. Chlorophyll-a, nutrients and SPM. *Journal of Marine Systems*, 68(3–4): 381–404.
- Allen, J.I., Blackford, J., Holt, J., Proctor, R., Ashworth M., Siddorn, J. (2001). A highly spatially resolved ecosystem model for the North West European Continental Shelf. *Sarsia*, 86: 423–440.
- Alvain, S., Moulin, C., Dandonneau, Y., Loisel, H. (2008). Seasonal distribution and succession of dominant phytoplankton groups in the global ocean: a satellite view. *Global Biogeochemical Cycles*, 22: GB3001.
- Anderson, J.T. (1998). The Effects of Seasonal variability on the germination and vertical transport of a cyst forming dinoflagellate, *Gyrodinium sp.*, in Chesapeake Bay. *Ecological Modelling*, 112: 85–109.
- Anderson, T.R. (2005). Plankton functional type modelling: running before we can walk? *Journal of Plankton Research*, 27(11): 1073–1081.
- Anderson, T.R. and Pondaven, P. (2003). Non-Redfield carbon and nitrogen cycling in the Sargasso Sea: pelagic imbalances and export flux. *Deep-Sea Research I*, 50: 573–591.
- Baek, S.H., Shimode, S., Han, M.-S., Kikuchi, T. (2008). Growth of dinoflagellates, *Ceratium furca* and *Ceratium fusus* in Sagami Bay, Japan: the role of nutrients. *Harmful Algae*, 7: 729–739.
- Baek, S.H., Shimode, S., and Kikuchi, T., (2007). Reproductive ecology of the dominant dinoflagellate, *Ceratium fusus* in coastal area of Sagami Bay. *Journal of Oceanography*, 30:35–45
- Baker, A., Robbins, I., Moline, M.A., Iglesias-Rodríguez, M.D. (2008). Oligonucleotide primers for the detection of bioluminescent dinoflagellates reveal novel luciferase

- sequences and information on the molecular evolution of this gene. *Journal of Phycology*, 44.
- Banse, K. (1982). Cell Volumes, Maximal growth rates of unicellular algae and ciliates, and the role of ciliates in the marine pelagial. *Limnology and Oceanography*, 27: 1059–1071.
- Barlow R.G., Mantoura R.F.C., Gough M.A., Fileman T.W. (1993) Pigment signatures of the phytoplankton composition in the Northeastern Atlantic during the 1990 spring bloom. *Deep Sea Research Part II*, 40: 459–477.
- Batchelder, H.P., Swift, E., Keuren, J.R. (1992). Diel patterns of planktonic bioluminescence in the northern Sargasso Sea. *Marine Biology*, 113: 329–339.
- Batchelder, H.P., Swift, E., Van Keuren, J.R. (1990). Pattern of planktonic bioluminescence in the northern Sargasso Sea: seasonal and vertical distribution. *Marine Biology*, 104: 153–164.
- Batchelder, H.P. and Swift, E. (1989). Estimated near-surface mesoplanktonic bioluminescence in the western North Atlantic during July 1986. *Limnology and Oceanography*, 34: 113–128.
- Batten, S. D., Clark, R., Flinkman, J., Hays, G., John, E., John, A. W. G., Jonas, T., Lindley, J. A., Stevens, D. P., Walne, A. (2003). CPR sampling: the technical background, materials and methods, consistency and comparability. *Progress in Oceanography*, 58(2–4): 193–215.
- Behrenfeld, M.J., Boss, E., Siegel, D.A., Shea, D.M. (2005). Carbon-based ocean productivity and phytoplankton physiology from space. *Global Biogeochemical Cycles*, 19(1): GB1006.
- Biggley W.H., Swift E., Buchanan R.J, Seliger H.H. (1969). Stimulable and spontaneous bioluminescence in the marine dinoflagellates, *Pyrodinium bahamense*, *Gonyaulax polyedra*, and *Pyrocystis lunula*. *Journal of General Physiology*, 54: 96–122.
- Bivens, J.R., Geiger, M.L., Bird, J.L. (2002). Interpreting bathyphotometer signals. *Oceans '02 MTS/IEEE*, 3: 1705–1710.
- Bivens, J.R., Geiger, M.L., Bird J.L., Lapota, D. (2001). Advances in bioluminescence instrumentation. *IEEE*, 3: 1895–1898.
- Brussaard, C. (2004). Viral Control of Phytoplankton populations—a review. *The Journal of Eukaryotic Microbiology*, 51(2): 125–138.
- Brzezinski, M.A. (1985). The Si:C:N ratio of marine diatoms: interspecific variability and the effect of some environmental variables. *Journal of Phycology*, 21(3): 347–357.
- Buck, J.B., (1978). Function and Evolutions of Bioluminescence. In: Herring, P.J. (Ed) *Bioluminescence in Action*, London Academic press, 419–460.
- Burkenroad, M.D. (1943). A possible function of bioluminescence. *Journal of Maine Science*, 5: 161–164
- Burnham, K.P., and Anderson, D.R. (2002). Model selection and multimodel inference a practical information – theoretical approach (second ed.). Springer, p. 487.
- Buskey, E.J. (1995). Growth and bioluminescence of *Noctiluca scintillans* on varying algal diets. *Journal of Plankton Research*, 17 (I): 29–40.

- Buskey, E.J., Coulter, C.J., Brown, S.L. (1994). Feeding, growth and bioluminescence of the heterotrophic dinoflagellate *Protoperidinium huberi*. *Marine Biology*, 121: 373–380.
- Buskey, E.J., Strom, S., Coulter, C. (1992). Bioluminescence of heterotrophic dinoflagellates from Texas coastal waters. *Journal of Experimental Marine Biology and Ecology*, 159: 37–49.
- Buskey, E.J., and Swift, E. (1990). An encounter model to predict natural planktonic bioluminescence. *Limnology and Oceanography*, 35(7): 1469–1485.
- Buskey, E.J., Mann, C.G., Swift, E. (1987). Photophobic responses of calanoid copepods: possible adaptive value. *Journal of Plankton Research*, 9(5): 857–870.
- Buskey, E.J. and Swift, E. (1985). Behavioral responses of oceanic zooplankton to simulated bioluminescence. *Biological Bulletin*, 168:263–275.
- Buskey, E.J. and Swift, E. (1983). Behavioral responses of the coastal copepod *Acartia Hudsonica* (Pinhey) to simulated dinoflagellate bioluminescence. *Journal of Experimental Marine Biology and Ecology*, 72: 43–58.
- Buskey, E., Mills, L., Swift, E. (1983). The effects of dinoflagellate bioluminescence on the swimming behavior of a marine copepod. *Limnology and Oceanography*, 28: 575–579.
- Carroll, D.L., (1996). Chemical laser modelling with genetic algorithms. *AIAA Journal* 34 (2): 338–346.
- Carvalho, W.F., Minnhagen, S., Graneli, E. (2008). *Dinophysis norvegica* (Dinophyceae), more a predator than a producer? *Harmful Algae*, 7: 174–183.
- Case, J.F., Widder, E.A., Bernstein, S., Ferer, K., Young, D., Latz, M.I., Geiger, M., Lapota, D. (1993) Assessment of marine bioluminescence. *Naval Research Review*, 45: 31 – 41.
- CEDIT (2008). New Taxa. Centre of Excellence for Dinophyte Taxonomy, <http://www.dinophyta.org/> – viewed 28/11/2008.
- Chang, J. and Carpenter E.J. (1994). Active growth of the oceanic dinoflagellate *Ceratium teres* in the Caribbean and Sargasso Seas estimated by cell cycle analysis. *Journal of Phycology*, 30: 375–381.
- Cheadle, C., Vawter, M.P., Freed, W.J., Becker, K.G. (2003). Analysis of microarray data using z-score transformation. *Journal of Molecular Diagnostics* 5, 73–81.
- Cochran, W. G. (1977). *Sampling techniques* (3rd Ed). New York.
- Colebrook, J.M. (1960). Continuous Plankton Records: methods of analysis, 1950–59. *Bulletins of Marine Ecology*, V(41): 51–64.
- Cordoleani, F., Nerini, D., Gauduchon, M., Morozov, A., Poggiale, J.C. (2011). Structural sensitivity of biological models revisited. *Journal of Theoretical Biology*, 283: 82–91.
- Craig, J.M., Klerks, P.L., Heimann, K., Waits, J.L. (2003). Effects of salinity, pH and temperature on the re-establishment of bioluminescence and copper or SDS toxicity in the marine dinoflagellate *Pyrocystis lunula* using bioluminescence as an endpoint. *Environmental Pollution*, 125(2): 267–275.

- Cugier, P., Ménésguen, A., Guillaud, J.F. (2005). Three-dimensional (3D) ecological modelling of the Bay of Seine (English Channel, France). *Journal of Sea Research*, 54: 104–124.
- Cussatlegras, A.S. and Le Gal, P. (2004). Bioluminescence of the dinoflagellate *Pyrocystis Noctiluca* induced by laminar and turbulent couette flow. *Journal of Experimental Marine Biology and Ecology*, 310: 227–246.
- Cussatlegras, A.S., Geistdoerfer, P., Prieur, L. (2001). Planktonic bioluminescence measurements in the frontal zone of Almeria–Oran (Mediterranean Sea). *Oceanologica Acta*, 24: 239–250.
- Dam, H.G., Miller, C.A., Jonasdottir, S.H. (1993). The trophic role of mesozooplankton at 47°N, 20°W during the North Atlantic Bloom Experiment. *Deep-Sea Research Part II*, 40(1–2): 197–212.
- de Boyer Montégut, C., Madec, G., Fischer, A.S., Lazar, A., Iudicone, D. (2004). Mixed layer depth over the global ocean: An examination of profile data and a profile-based climatology. *Journal of Geophysical Research*, 109(C12): C12003.
- Denman, K.L. (2003). Modelling planktonic ecosystems: parameterizing complexity. *Progress in Oceanography*, 57(3–4): 429–452.
- Denman K.L., and Pena, M.A. (1999). A coupled 1-D biological/physical model of the northeast subarctic north Pacific Ocean with iron limitation. *Deep-Sea Research Part II*, 46(11–12): 2877–2908.
- Dickey, T.D., Granata, T., Marra, J., Langdon, C., Wiggert, J., Chai, Z., Hamilton, M., Vasquez, J., Stramska, M., Bidigare, R., Siegel, D. (1993). Seasonal variability of bio-optical and physical properties in the Sargasso Sea. *Journal of Geophysical Research*, 98: 865–898.
- Dickey, T., Marra, J., Granata, T., Langdon, C., Hamilton, M., Wiggert, J., Siegel, D., Bratkovich, A. (1991). Concurrent high resolution bio-optical and physical time series observations in the Sargasso Sea during the spring of 1987. *Journal of Geophysical Research*, 96.
- Dodge J.D (1993). Armoured dinoflagellates in the NE Atlantic during the BOFS cruises, 1988–90. *Journal of Plankton Research* 15: 465–483.
- Dodge, J.D. and Saunders R.D. (1985). A partial revision of the genus *Oxytoxum* (Dinophyceae) with the aid of scanning electron microscopy. *Botanica Marina*, 28(3): 99–122.
- Ducklow H.W, and Harris R.P. (1993). Introduction to the JGOFS North Atlantic bloom experiment. *Deep-Sea Research Part II* 40: 1–8
- Edwardsen, A., Zhou, M., Tande, K. S. and Zhu, Y. (2002). Zooplankton population dynamics: measuring in situ growth and mortality rates using an Optical Plankton Counter. *Marine Ecological Progress Series*, 227: 205–219.
- Edwards, M., Johns, D.G., Leterme, S.C., Svendsen, E., Richardson, A.J. (2006). Regional climate change and harmful algal blooms in the northeast Atlantic. *Limnology and Oceanography*, 51(2): 820–829
- Edwards, M., Richardson, A. J. (2004). Impact of climate change on marine pelagic phenology and trophic mismatch. *Nature*, 430(7002): 881–884.
- Edwards, A.M. and A. Yool (2000). The role of higher predation in plankton population models. *Journal of Plankton Research*, 22(6): 1085–1112.

- Efron, B., Tibshirani, R. (1986) Bootstrap Methods for Standard Errors, Confidence Intervals, and Other Measures of Statistical Accuracy. *Statistical Science* 1: 54–75.
- Eppley, R.W. (1972). Temperature and phytoplankton growth in the sea. *Fishery Bulletin*, 70(4): 1063–1085.
- Esaias W.E., Curl H.C., Seliger H.H. (1973). Action spectrum for a low intensity, rapid photoinhibition of mechanically stimuable bioluminescence in the marine dinoflagellates *Gonyaulax catenella*, *G. acatenella*, and *G. tamarensis*. *Journal of Cellular Physiology* 82(3): 363–372.
- Esaias, W.E. and Curl, H.C., Jr. (1972). Effect of Dinoflagellate Bioluminescence on Copepod Ingestion Rates. *Limnology and Oceanography*, 17: 901–906.
- Evans, G.T. and Parslow, J.S. (1985). A model of annual plankton cycles. *Biological Oceanography*, 3(3): 327–347.
- Fasham, M.J.R. (1993). Modelling the marine biota. *NATO ASI Series*, I(15): 457–504.
- Fasham, M.J.R., Ducklow, H.W., McKelvie, S.M. (1990). A nitrogen-based model of plankton dynamics in the oceanic mixed layer. *Journal of Marine Research*, 48: 591–639.
- Fennel, K., Losch, M., Schröter, J., Wenzel, M. (2001). Testing a marine ecosystem model: sensitivity analysis and parameter optimization. *Journal of Marine Systems*, 28(1–2): 45–63.
- Filimonov, V.A. and Sadovskaya, G.M. (1986). Photoinhibition of phytoplankton bioluminescence. *Oceanology/Oceanology/Okeanologiya*, 26: 621–622.
- Fleisher, K.J. and Case, J.F. (1995). Cephalopod predation facilitated by dinoflagellate luminescence. *Biological Bulletin*, 189: 263–271.
- Flynn, K.J. and Mitra, A. (2009). Building the "perfect beast": modelling mixotrophic plankton. *Journal of Plankton Research*, 31(9): 965–992.
- Follows, M.J., Dutkiewicz, S., Grant, S., Chisholm, S.W. (2007). Emergent biogeography of microbial communities in a model ocean. *Science*, 315: 1843
- Franks, P.J.S. (2009). Planktonic ecosystem models: perplexing parameterizations and a failure to fail. *Journal of Plankton Research*, 31 (11):1299–130.
- Franks, P.J.S. (1997). Models of harmful algal blooms. *Limnology and Oceanography*, 42: 1273–1282.
- Friedrichs, M.A., Dusenberry, J.A., Anderson, L.A., Armstrong, R.A., Chai, F., Christian, J.R., Doney, S.C., Dunne, J., Fujii, M., Hood, R., McGillicuddy, D.J., Moore, J.K., Schertau, M., Spitz, Y.H., Wiggert, J.D. (2007). Assessment of skill and portability in regional marine biogeochemical models: Role of multiple planktonic groups. *Journal of Geophysical Research*, 112(C8): C08001.
- Friedrichs, M.A. (2001). A data assimilative marine ecosystem model of the central equatorial Pacific: Numerical twin experiments. *Journal of Marine Research*, 59, 859–894.
- Fulton, E.A., Parslow, J.S., Smith, A.D.M., Johnson, C.R. (2004). Biogeochemical marine ecosystem models II: the effect of physiological detail on model performance. *Ecological Modelling*, 173(4): 371–406.

- Furnas, M.J. (1990). In situ growth rates of marine phytoplankton: approaches to measurement, community and species growth rates. *Journal of Plankton Research*, 12(6): 1117–1151.
- Gaines, G. and Elbrachter, M. (1987). Heterotrophic nutrition. In: Taylor, F J. R. (Ed.) *The biology of dinoflagellates*. Blackwell, Oxford: 224–268
- Galassi, M., Davies, J., Theiler, J., Gough, B., Jungman, G., Alken, P., Booth, M., Rossi, F. (2009). GNU Scientific Library Reference Manual (v1.12), GNU Scientific Library.
- Garcia, H.E., Locarnini, R.A., Boyer, T.P., Antonov, J.I, Zweng, .M.M., Baranova, O.K., Johnson, D.R. (2010). *World Ocean Atlas 2009, Volume 4: Nutrients (phosphate, nitrate, and silicate)*. S. Levitus, Ed., NOAA Atlas NESDIS 71, U.S. Government Printing Office, Washington, D.C., 398 pp.
- Gayoso, A.M. (2001). Observations on *Alexandrium tamarense* (Lebour) Balech and Other Dinoflagellate Populations in Golfo Nuevo, Patagonia (Argentina), *Journal of Plankton Research*, 23(5): 463–468.
- Geider, R.J. (1987). Light and temperature dependence of the carbon to chlorophyll a ratio in microalgae and cyanobacteria: implications for physiology and growth of phytoplankton. *New Phytologist*, 106(1): 1–34.
- Goldberg, D. (1989). *Genetic algorithms in search, optimization, and machine learning*, Addison–Wesley Professional.
- Gomez, F. (2005). A list of free–living dinoflagellate species in the world's oceans. *Acta Botanica Croatica*, 64: 129–212.
- Greenblatt, P.R., Feng, D.F., Zirino, A., Losee, J.R. (1984). Observations of Planktonic Bioluminescence in the Euphotic Zone of the California Current. *Marine Biology*, 84: 75–82.
- Haddock, S.H.D., Moline, M.A., Case, J.F. (2010). Bioluminescence in the sea. *Annual Review of Marine Science*, 2: 443–493.
- Hallegraeff, G.M., and Jeffery, S.W. (1984). Tropical phytoplankton species and pigments of continental shelf waters of North and North–West Australia. *Marine Ecology Progress Series*, 20: 59–74.
- Hamman, J.P., Biggley, W.H., Seliger, H.H. (1981a). Action spectrum for the photoinhibition of bioluminescence in the marine dinoflagellate *dissodinium lunula*. *Photochemistry and Photobiology* 33(5): 741–747.
- Hamman, J.P., Biggley, W.H., Seliger, H.H. (1981b). Photoinhibition of stimutable bioluminescence in marine dinoflagellates. *Photochemistry and Photobiology* 33(6): 904–914.
- Hamman, J.P and Seliger, H.H. (1982). The chemical mimicking of the mechanical stimulation, photoinhibition, and recovery from photoinhibition of bioluminescence in the marine dinoflagellate, *Gonyaulax polyedra*. *Journal of Cellular Physiology*, 111: 315–319.
- Hansen, P.J. (2011). The role of photosynthesis and food uptake for the growth of marine mixotrophic dinoflagellates. *Journal of Eukaryotic Microbiology*, 58(3): 203–214.
- Hansen, P.J., Skovgaard, A., Ronnie, N. G., Stoecker, D. K., (2000). Physiology of the mixotrophic dinoflagellate *Fragilidium subglobosum*. II. Effects of time scale and prey

- concentration on photosynthetic performance. Marine Ecology Progress Series, 201: 137–146.
- Hansen, P.J. and Nielsen, T.G. (1997). Mixotrophic feeding of *Fragilidium subglobosum* (Dinophyceae) on three species of *Ceratium*: effects of prey concentration, prey species and light intensity. Marine Ecology Progress Series, 147: 187–196.
- Hansen, P.J. (1991). *Dinophysis* – a planktonic dinoflagellate genus which can act both as a prey and a predator of a ciliate. Marine Ecological Progress Series, 69: 201–204.
- Hardy, A.C. (1939). Ecological investigations with the continuous plankton recorder: object, plan and methods. Hull Bulletins of Marine Ecology, 1, 1–57.
- Harvey, E.N. (1957). A history of luminescence from the earliest times until 1900. Memoirs of the American Philosophical Society, Philadelphia, 44, p.692.
- Hastings, J.W. (1996). Chemistries and colors of bioluminescent reactions: a review. Gene, 173: 5–11.
- Hastings, J.W. (1959). Unicellular clocks. Annual Review of Microbiology 13(1): 297–312.
- Hastings J.W., and Sweeney, B.M. (1958). A persistent diurnal rhythm of luminescence in *Gonyaulax polyedra*. Biological Bulletin 115(3): 440–458.
- Hastings, J.W. and Sweeney, B.M. (1957). On the mechanism of temperature independence in a biological clock. PNAS 43: 804–811
- Havskum, H., Hansen, P.J., Berdalet, E. (2005). Effect of turbulence on sedimentation and net population growth of the dinoflagellate *Ceratium tripos* and interactions with its predator, *fragilidium subglobosum*. Limnology and Oceanography, 50(5): 1543–1551.
- Hays, G.C., Warner, A.J., John, A.W.G., Harbour, D.S., Holligan, P.M. (1995). Coccolithophores and the Continuous Plankton Recorder Survey. Journal of the Marine Biological Association of the UK, 75(02): 503–506.
- Head, E. and Pepin, P. (2010). Monitoring changes in phytoplankton abundance and composition in the Northwest Atlantic: a comparison of results obtained by continuous plankton recorder sampling and colour satellite imagery. Journal of Plankton Research, 32 (12): 1649–1660
- Heaney, S.I. and Eppley, R.W. (1981). Light, temperature and nitrogen as interacting factors affecting diel vertical migrations of dinoflagellates in culture. Journal of Plankton Research, 3(2): 331–344.
- Herren C.M., Haddock, S.H.D., Johnson, C., Orrico, C.M., Moline, M.A., Case, J.F. (2005). A multi-platform bathyphotometer for fine-scale, coastal bioluminescence research. Limnology and Oceanography: Methods, 3: 247–262.
- Herren C.M., Alldredge, A.L., Case, J.F. (2004). Coastal bioluminescent marine snow: fine structure of bioluminescence distribution. Continental Shelf Research, 24:413–429.
- Herring, P. J. (2007). REVIEW. Sex with the lights on? A review of bioluminescent sexual dimorphism in the sea. Journal of the Marine Biological Association of the United Kingdom, 87(04): 829–842.

- Herring, P.J. and Widder, E.A. (2001). Bioluminescence in the plankton and nekton. *In Steele, J.H., Thorpe, S.A., Turekian, K.K. (Ed). Encyclopedia of Ocean Science*, 1: 308 – 317. Academic Press, San Diego.
- Herring P.J. (1983). The spectral characteristics of luminous marine organisms. *Proceedings of the Royal Society of London, Series B, Biological Sciences*, 220 (1219): 183 – 217.
- Hofmann, E.E. (2010). Plankton functional group models – an assessment. *Progress in Oceanography*, 84: 16–19.
- Hood, R.R., Laws, E.A., Armstrong, R.A., Bates, N.R., Brown, C.W., Carlson, C.A., Chai, F., Doney, S.C., Falkowski, P.G., Feely, R.A., Friedrichs, M.A.M., Landry, M.R., Keith Moore, J., Nelson, D.M., Richardson, T.L., Salihoglu, B., Schartau, M., Toole, D.A., Wiggert, J.D. (2006). Pelagic functional group modeling: progress, challenges and prospects. *Deep-Sea Research Part II: Topical Studies In Oceanography*, 53: 459–512.
- Ignatiades, L., Gotsis-Skretas, O., Metaxatos, A. (2007). Field and culture studies on the ecophysiology of the toxic dinoflagellate *Alexandrium minutum* (Halim) present in Greek coastal waters. *Harmful Algae*, 6(2): 153–165.
- Ismael, A.A. (2003). Succession of heterotrophic and mixotrophic dinoflagellates as well as autotrophic microplankton in the harbour of Alexandria, Egypt. *Journal of Plankton Research*, 25: 193–202.
- Janssen, P.H.M and Heuberger, P.S.C. (1995). Calibration of process-oriented models. *Ecological Modelling*, 83: 55–66.
- Jeong, H. J., Yoo, Y. D., Park, J. Y., Song, J. Y., Kim, S. T., Lee, S. H., Kim, K. Y., Yih, W. H. (2005). Feeding by phototrophic red-tide dinoflagellates: five species newly revealed and six species previously known to be mixotrophic. *Aquatic Microbial Ecology*, 40:133–155.
- Jeong, H.J., Shim, J.H., Kim, J.S., Park, J.Y., Lee, C.W., Lee, Y. (1999). The feeding by the thecate mixotrophic dinoflagellate *Fragilidium* cf. *mexicanum* on red tide and toxic dinoflagellate. *Marine Ecological Progress Series*, 176:263–277.
- Jeong, H.J., Lee C.W., Yih, W.H., Kim, J.S. (1997). *Fragilidium* cf. *mexicanum*, a thecate mixotrophic dinoflagellate, which is prey for and a predator on co-occurring thecate heterotrophic dinoflagellate *Protoperdinium* cf. *divergens*. *Marine Ecological Progress Series*, 151:299–305
- Jeong, H.J., Latz, M.I., (1994). Growth and grazing rates of the heterotrophic dinoflagellate, *Protoperdinium*, on red tide dinoflagellates. *Marine Ecology Progress Series* 106: 173–185.
- Jost, C., Lawrence, C.A., Campolongo, F., Van De Bund, W., Hill, S., and Deangelis, D.L. (2004). The Effects Of Mixotrophy On The Stability And Dynamics Of A Simple Planktonic Food Web Model. *Theoretical Population Biology*, 66: 37–51
- Juhl, A.R. (2005). Growth rates and elemental composition of *Alexandrium monilatum*, a red-tide dinoflagellate. *Harmful Algae*, 4(2): 287–295.
- Juhl, A.R., Latz, M.I. (2002). Mechanisms of fluid shear-induced inhibition of population growth in a red-tide dinoflagellate. *Journal of Phycology*, 38(4): 683–694.
- Kamykowski, D. (1981). Laboratory experiments on the diurnal vertical migration of marine dinoflagellates through temperature gradients. *Marine Biology*, 62(1): 57–64.

- Kelly, M.G. (1968). The occurrence of dinoflagellate luminescence at Woods Hole. *Biological Bulletin* 135(2): 279–295.
- Kelly, M.G. and Katona, S. (1966). An endogenous diurnal rhythm of bioluminescence in a natural population of dinoflagellates. *Biological Bulletin*, 131: 115–126.
- Kidston, M., Matear, R., Baird, M.E. (2011). Parameter optimisation of a marine ecosystem model at two contrasting stations in the Sub-Antarctic Zone. *Deep-Sea Research Part II*, 58: 2301–2315.
- Kim, G., Lee Y-W., Joung D-J., Kim K-R., Kim K. (2006). Real-time monitoring of nutrient concentrations and red-tide outbreaks in the Southern Sea of Korea. *Geophysical Research Letters*, 33:L13607
- Kirk J.T.O. (1994). *Light and photosynthesis in aquatic ecosystems*. Cambridge University Press, Cambridge, 410 pp.
- Knaust, R., Urbig, T., Li, L., Taylor, W., Hastings, J.W. (1998). The circadian rhythm of bioluminescence in *Pyrocystis* is not due to differences in the amount of luciferase: a comparative study of the three bioluminescent marine dinoflagellates. *Journal of Phycology*, 34: 167–172.
- Kremp, A., Lindholm, T., Dreßler, N., Erler, K., Gerds, G., Eirtovaara, S., Leskinen, E. (2009). Bloom forming *Alexandrium ostenfeldii* (Dinophyceae) in shallow waters of the Åland Archipelago, Northern Baltic Sea. *Harmful Algae*, 8:318–328.
- Kudela, R.M., Seeyave, S., Cochlan, W.P., (2010). The role of nutrients in regulation and promotion of harmful algal blooms in upwelling systems. *Progress in Oceanography* 55: 122–135.
- Kudela, R.M., Lane, J.Q., Cochlan, W.P. (2008). The potential role of anthropogenically derived nitrogen in the growth of harmful algae in California, USA. *Harmful Algae*, 8(1): 103–110.
- Kudela, R.M., Cochlan, W.P. (2000). Nitrogen and carbon uptake kinetics and the influence of irradiance for a red tide bloom off southern California. *Aquatic Microbial Ecology*, 21: 31–47.
- Kushnir, V.M., Tokarev, Y.N., Williams, R., Piontkovski, S.A., Evstigneev, P.V. (1997). Spatial heterogeneity of the bioluminescence field of the tropical Atlantic ocean and its relationship with internal waves. *Marine Ecology Progress Series*, 160: 1–11.
- Lampitt, R.S., Salter, I., de Cuevas, B. A., Hartman, S., Larkin, K. E., Pebody, C. A. (2010). Long-term variability of downward particle flux in the deep northeast Atlantic: Causes and trends. *Deep-Sea Research Part II: Topical Studies in Oceanography*, 57(15): 1346–1361.
- Lapota D., Osorio, A.R., Liao, C., Bjorndal, B. (2007). The use of bioluminescent dinoflagellates as an environmental risk assessment tool. *Marine Pollution Bulletin*, 54: 1857–1867.
- Lapota D., Paden S., Duckworth D., Rosenberg, D.E., Case, J.F. (1994). Coastal and oceanic bioluminescent trends in the Southern California Bight using MOORDEX bathyphotometers. In: Campbell AK, Kricka LJ, Stanley PE (Eds) *Bioluminescence And Chemiluminescence*. John Wiley and Sons, Chichester: 127–131
- Lapota, D., Moskowitz, G.J., Rosenberger, D.E., Grovhoug, J.G. (1993). The use of stimutable bioluminescence from marine dinoflagellates as a means of detecting toxicity in the marine-environment. *Environmental Toxicology and Risk Assessment: 2nd Volume*, 1216: 3–18.

- Lapota, D., Young, D.K., Bernstein, S.A., Geiger, M.L., Huddell, H.D. and Case, J.S. (1992). Diel bioluminescence in heterotrophic and photosynthetic marine dinoflagellates in an Arctic fjord. *Journal of the Marine Biological Association of the UK*, 72 (4): 733–744.
- Lapota, D., Geiger, M.L., Stiffey, A.V., Rosenberger, D.E., Young, D.K. (1989). Correlations of planktonic bioluminescence with other oceanographic parameters from a Norwegian Fjord. *Marine Ecology Progress Series*, 55, 217 – 227.
- Lapota, D., Galt, C., Losee, J.R., Huddell, H.D., Orzech, K., Nealson, K.H. (1988). Observations and measurements of planktonic bioluminescence in and around a milky sea. *Journal of Experimental Marine Biology and Ecology*, 119: 55–81.
- Lapota, D. and Losee, J.R. (1984). Observations of bioluminescence in marine plankton from the Sea of Cortez. *Journal of Experimental Marine Biology and Ecology*, 77, 209:240.
- Latz, M.I., Jeffery, A., Sarkar S., Rohr, J. (2009). Effect of fully characterized unsteady flow on population growth of the dinoflagellate *Lingulodinium polyedrum*. *Limnology and Oceanography*, 54 (4): 1243–1256.
- Latz, M.I., Bovard, M., VanDelinder, V., Segre, E., Rohr, J., Groisman, A. (2008). Bioluminescent response of individual dinoflagellate cells to hydrodynamic stress measured with millisecond resolution in a microfluidic device. *Journal of Experimental Biology*, 211: 2865–2875.
- Latz, M.I. and Rohr, J. (2005). Glowing with the flow. *Opt. Photon. News*, 16(10): 40–45.
- Latz, M.I., Nauen, J.C., Rohr, J. (2004a). Bioluminescence response of four species of dinoflagellates to fully developed pipe flow. *Journal of Plankton Research*, 26: 1529–1546.
- Latz, M.I., Juhl, A.R., Ahmed, A.M., Elghobashi, S.E., Rohr, J. (2004b) Hydrodynamic stimulation of dinoflagellate bioluminescence: a computational and experimental study. *Journal Of Experimental Biology*, 207: 1941–1951.
- Latz, M.I. and Rohr J. (1999). Luminescent response of the red tide dinoflagellate *Lingulodinium Polyedrum* to laminar and turbulent flow. *Limnology and Oceanography*, 44: 1423–1435.
- Latz, M.I. and Jeong, H.J. (1996). Effect of red tide dinoflagellate diet on the bioluminescence of the heterotrophic dinoflagellate, *Protoperdinium* Spp. *Marine Ecology Progress Series*, 132: 275–285.
- Latz, M.I., Frank, T.M., Case, J.F. (1988). Spectral composition of bioluminescence of epipelagic organisms from the Sargasso Sea. *Marine Biology*, 98, 441–446.
- Lenz, J., Morales, A., Gunkel, J. (1993). Mesozooplankton standing stock during the North Atlantic spring bloom study in 1989 and its potential grazing pressure on phytoplankton: a comparison between low, medium and high latitudes. *Deep-Sea Research Part II*, 40(1–2): 559–572.
- Le Quere, C., Harrison S.P., Prentice I.C., Buitenhuis E.T., Aumont O., et al. (2005). Ecosystem dynamics based on plankton functional types for global ocean biogeochemistry models. *Global Change Biology*, 11: 2016–2040.

- Leterme, S.C., Edwards, M., Seuront, L., Attrill, M.J., Reid, P.C., John, A.W.G. (2005). Decadal basin-scale changes in diatoms, dinoflagellates, and phytoplankton color across the north Atlantic. *Limnology and Oceanography*, 50(4): 1244–1253.
- Lewis, K., Allen, J.I., Richardson, A.J., Holt, J.T. (2006). Error quantification of a high resolution coupled hydrodynamic–ecosystem coastal–ocean model: part3, validation with Continuous Plankton Recorder Data. *Journal Of Marine Systems*, 63: 209–224.
- Li, Y., Swift, E., Buskey, E.J. (1996). Photoinhibition of mechanically stimuable bioluminescence in the heterotrophic dinoflagellate *Protoperidinium Depressum* (Pyrrophyta). *Journal of Phycology*, 32: 974–982.
- Lieberman, S.H., Lapota, D., Losee, J., Zirino, A. (1987). Planktonic bioluminescence in the surface waters of the Gulf of California. *Biological Oceanography*, 4: 25–46.
- Litchman, E. and Klausmeier, C.A. (2008). Trait-based community ecology of phytoplankton. *Annual Review of Ecology, Evolution and Systematics*, 39: 615–639.
- Litchman, E., Klausmeier, C.A., Schofield, O.M., Falkowski, P.G. (2007). The role of functional traits and trade-offs in structuring phytoplankton communities: scaling from cellular to ecosystem level. *Ecology Letters*, 10: 1170–1181.
- Liu, L., Wilson, T.R.S., Hastings, J.W. (2004). Molecular evolution of dinoflagellate luciferases, enzymes with three catalytic domains in a single polypeptide. *Proceedings Of The National Academy Of Sciences Of The United States Of America*, 101: 16555–16560.
- Lochte, K., Ducklow, H.W., Fasham, M.J.R., Stienen, C. (1993). Plankton succession and the carbon cycling at 47 N 20 W during the JGOFS North Atlantic bloom experiment. *Deep-Sea Research II*, 40: 91–114.
- Losa, S., Kivman, G., Ryabchenko, V., (2004). Weak constraint parameter estimation for a simple ocean ecosystem model: what can we learn about the model and data?, *Journal of Marine Systems*, 45: 1–20.
- Losee, J., Richter, K., Lieberman, S., Lapota, D. (1989). Bioluminescence: spatial statistics in the north atlantic. *Deep-Sea Research*, 36: 783–801.
- Lynch, R.V. (1981). Analysis of fleet reports of bioluminescence in the Indian Ocean. U.S. Naval Research Laboratory, Report, 8526.
- Lynch R.V. (1978). The occurrence and distribution of surface bioluminescence in the oceans during 1966 Through 1977. U.S. Naval Research Laboratory, Report, 8210.
- Madec, G., (2008). NEMO ocean engine. Note du P^ole de mod^élisation, Institut Pierre–Simon Laplace (IPSL), France, No 27, ISSN No 1288–1619.
- Maldonado, E.M. and Latz, M.I. (2007). Shear–stress dependence of dinoflagellate bioluminescence. *Biological Bulletin*, 212: 242–249.
- Margalef, R. (1978). Life–forms of phytoplankton as survival alternatives in an unstable environment. *Oceanologica Acta* 1:493–509.
- Margalef, R. (1957). Fitoplancton de las costa de Puerto Rico. *Investigacion Pesquera*, 6 (I): 39–52.
- Marañón, E. and Holligan, P.M. (1999). Photosynthetic parameters of phytoplankton from 50°N to 50°S in the Atlantic Ocean. *Marine Ecology Progress Series*, 176: 191–203.

- Marra, J. (1995). Bioluminescence and optical variability in the ocean: an overview of the Marine Light-Mixed Layers Program. *Journal of Geophysical Research*, 100.
- Matear, R.J. (1995). Parameter optimization and analysis of ecosystem models using simulated annealing: A case study at Station P. *Journal of Marine Research*, 53(4): 571–607.
- McDuffey, A. and Bird, J.L. (2002). The underway survey system at the Naval Oceanographic Office. *Oceans '02 MTS/IEEE*, Vol. 3: 1722–1725.
- McQuatters-Gollop, A., Raitos, D.E., Edwards, M., Attrill, M.J. (2007). Spatial patterns of diatom and dinoflagellate seasonal cycles in the NE Atlantic Ocean. *Marine Ecology Progress Series*, 339: 301–306.
- Merico, A., Tyrrell, T., Lessard, E.J., Oguz, T., Stabeno, P.J., Zeeman, S.I., Whitledge, T.E. (2004). Modelling Phytoplankton Succession on the Bering Sea Shelf: Role Of Climate Influences and Trophic Interactions in Generating *Emiliania Huxleyi* Blooms 1997–2000. *Deep-Sea Research Part I: Oceanographic Research Papers*, 51: 1803–1826.
- Mesinger, A.F. and Case, J.F. (1992). Dinoflagellate luminescence increases susceptibility of zooplankton to teleost predation. *Marine Biology*, 112, 207–210.
- Minnhagen, S., and Janson, S. (2006). Genetic analyses of *Dinophysis* spp. support kleptoplastidy. *FEMS Microbial Ecology*, 57: 47–54.
- Moline, M.A., Blackwell, S.M., Case, J.F., Haddock, S.H.D., Herren, C.M., Orrico, C.M., Terrill, E. (2009). Bioluminescence to reveal structure and interaction of coastal planktonic communities. *Deep-Sea Research Part II*, 56: 232–245.
- Moline, M.A., Oliver, M.J., Mobley, C.D., Sundman, L., Bensky, T., Bergmann, T., Bissett, W.P., Case, J., Raymond, E.H., Schofield, O.M.E. (2007). Bioluminescence in a complex coastal environment: 1. temporal dynamics of nighttime water-leaving radiance. *Journal of Geophysical Research*, 112.
- Moline M.A., Heine E., Case J., Herren C., Schofield O (2001). Spatial and temporal variability of bioluminescence potential in coastal regions. In: Case J.F., Herring P.J., Haddock S.H.D., Kricka L.J. and Stanley P.E. (eds.) *Bioluminescence and Chemiluminescence 2000*. World Scientific Publishing Company, Singapore, 123–126.
- Montagnes, D.J.S., Chambouvet, A., Guillou, L., Fenton, A. (2008). Responsibility of microzooplankton and parasite pressure for the demise of toxic dinoflagellate blooms. *Aquatic Microbial Ecology*, 53: 211–225.
- Monterey, G. and Levitus, S. (1997). Seasonal variability of the mixed layer depth for the world ocean, in: *NOAA Atlas NESDIS 14*, US Gov. Printing Office, Wash., DC.
- Naik, R.K., Hedge, S., Anil, A.C. (2011). Dinoflagellate community structure from the stratified environment of the Bay of Bengal, with special emphasis on harmful algal bloom species. *Environmental Monitoring Assessment*, DOI 10.1007/s10661-010-1855-z.
- Nakamura, Y., Suzuki, S., Hiromi, J. (1995). Population dynamics of heterotrophic dinoflagellates during a *Gymnodinium mikimotoi* red tide in the Seto Inland Sea. *Marine Ecology Progress Series*, 125: 269–277.
- NAVOCEANO (2009)
<https://oceanography.navy.mil/legacy/web/biolum/blwebpge.htm>, viewed – 22/01/2009.

- Neilson, D.J., Latz, M.I., Case, J.F. (1995). temporal variability in the vertical structure of bioluminescence in the North Atlantic Ocean. *Journal Of Geophysical Research*, 100.
- Neilson, D.J., Case, J.F., Bernstein, S., Widder, E.A. (1992). Patterns of bioluminescence in the north atlantic based on moored and profiling bathyphotometers. *EOS* 73:262.
- Nicol, J.A.C. (1960). *The biology of Marine Animals*. Sir Isaac Pitman and Sons, Ltd. London: p.707
- Nicol J.A.C. (1958). Observations on luminescence in *Noctiluca*. *Journal of the Marine Biological Association of the United Kingdom* 37(03): 535–549.
- Nicolas, M.T., Nicolas, G., Johnson, C.H., Bassot, J.M., Hastings, J.W. (1987). Characterization of the bioluminescent organelles in *Gonyaulax Polyedra* (Dinoflagellates) after fast-freeze fixation and antiluciferase immunogold staining. *Journal of Cell Biology*, 105: 723–735
- Obayashi, Y. and Tanoue, E. (2002). Growth and mortality rates of phytoplankton in the northwestern North Pacific estimated by the dilution method and HPLC pigment analysis. *Journal of Experimental Marine Biology and Ecology*, 280: 33–52.
- Odate, T. and K. Imai (2003). Seasonal variation in chlorophyll-specific growth and microzooplankton grazing of phytoplankton in Japanese coastal water. *Journal of Plankton Research*, 25(12): 1497–1505.
- Olascoaga, M. J., Beron-Vera, F. J., Brand, L. E., Kocak, H. (2008). Tracing the early development of harmful algal blooms on the West Florida Shelf with the aid of lagrangian coherent structures. *Journal of Geophysical Research*, 113 (C12014).
- Olseng, C.D., Naustvoll, L.J., Paasche, E. (2002). Grazing by the heterotrophic dinoflagellate *Protooperidinium steinii* on a *Ceratium* bloom. *Marine Ecology Progress Series*, 225:161–167.
- Ondercin, D.G., Atkinson, C.A., Kiefer, D.A. (1995). The distribution of bioluminescence and chlorophyll during the late summer in the North-Atlantic – maps and a predictive model. *Journal of Geophysical Research-Oceans*, 100: 6575–6590.
- OSPAR Commission, (1998). Report of the Modelling Workshop on Eutrophication Issues. 5–8 November 1996. Den Haag, The Netherlands. OSPAR Report, 86 pp.
- Painter, S., Marcinko, C., Valiadi, M., Allen, J., Iglesias-Rodriguez, D. (2011). Dinoflagellate bioluminescence: a review. National Oceanography Centre Research and Consultancy Report No.5. Unpublished manuscript.
- Petzoldt, T., Rudolf, L., Rinke, K., Benndorf, J. (2009). Effects of zooplankton diel vertical migration on a phytoplankton community: A scenario analysis of the underlying mechanisms. *Ecological Modelling*, 220(9–10): 1358–1368.
- Piontkovski, S.A., Tokarev, Yu.N., Levin, L.A. (2006). A Comparison of Bioluminescence and Chlorophyll Fields of the World Ocean. *Bioluminescence and Chemiluminescence – Chistry, Biology and Applications*: 261 – 264.
- Piontkovski, S.A., Landry, M.R., Finenko, Z.Z., Kovalev, A.V., Williams, R., Gallienne, C.P., Mishonov, A.V., Skryabin, V.A., Tokarev, Y.N., Nikolsy, V.N. (2003). Plankton Communities of the South Atlantic Anticyclonic Gyre. *Oceanologica Acta*, 23 (3): 255–268.
- Piontkovski, S.A., Tokarev, Y.N., Bitukov, E.P., Williams, R., Kiefer, D.A. (1997). The bioluminescent field of the Atlantic Ocean. *Marine Ecology Progress Series*, 156: 33–41.

- Plueddemann, A.J., Weller, R.A., Stramska, M., Dickey, T.D., Marra, J. (1995). Vertical structure of the upper ocean during the Marine Light-Mixed Layers experiment. *Journal of Geophysical Research*, 100.
- Popova, E.E. and Srokosz, M.A. (2009). Modelling the ecosystem dynamics at the Iceland–Faeroes Front: biophysical interactions. *Journal of Marine Systems*, 77: 182–196.
- Porter, K.G. and Porter, J.W. (1979). Bioluminescence in marine plankton: a coevolved antipredation system. *The American Naturalist*, 114(3): 458–461.
- Poupin, J., Cussatlegras, A., Geistdoerfer, P. (1999). *Plancton marin bioluminescent. Rapport Scientifique Du Loen*, Brest, France: 64 pp.
- Press, W.H., Teukolsky, S.A., Vetterling, W.T., Flannery, B.P. (1996). *Numerical recipes in Fortran 77 The art of scientific and parallel computing* (Second Ed). Cambridge University Press.
- Prezelin BB, Meeson BW, Sweeney, BM (1977). Characterisation of photosynthetic rhythms in marine dinoflagellates: pigmentation, photosynthetic capacity and respiration. *Plant Physiology* 60: 384–387
- Qasim, S.Z., Bhattathiri, P.M.A., Devassy, V.P. (1973). Growth kinetics and nutrient requirements of two tropical marine phytoplankters. *Marine Biology*, 21(4): 299–304.
- Radach, G., Moll, A., (2006). Review of three-dimensional ecological modelling related to the North Sea shelf system. Part II: model validation and data needs. *Oceanography and Marine Biology*, 44: 1–60 (An Annual Review).
- Raitsos, D.E., Lavender, S.J., Maravelias, C.D., Haralabous, J., Richardson, A.J., Reid, P.C. (2008). Identifying four phytoplankton functional types from space: an ecological approach. *Limnology and Oceanography*, 53(2): 605–613.
- Raymond, J.A., and DeVries, A.L. (1976). Bioluminescence in McMurdo Sound, Antarctica. *Limnology and Oceanography*, 21(4):599–602.
- Redfield, AC, (1934). On the proportions of organic derivatives in sea water and their relation to the composition of plankton. In Daniel J.R. (Ed) *James Johnstone Memorial Volume*, pp. 176–192. Liverpool University Press.
- Rees, J., de Wergifosse, B., Noiset, O., Dubuisson, M., Janssens, B., Thompson, E. (1998). The Origins of Marine Bioluminescence: Turning Oxygen Defence Mechanisms into Deep-Sea Communication Tools. *Journal of Experimental Biology*, 201: 1211–1221.
- Reid, P.C., Holiday, N.P., Smyth, T.J. (2001). Pulses in the eastern margin current and warmer water off the north west European shelf linked to North Sea ecosystem changes. *Marine Ecological Progress Series*, 215: 283–287.
- Richardson, A.J., Walne, A., John, A.W.G., Jonas, T., Lindley, J.A., Simms, D.W., Stevens, D., Witt, M. (2006). Using Continuous Plankton Recorder Data. *Progress in Oceanography*, 68: 27–74.
- Robinson, G.A., (1970). Continuous Plankton Records: variation in the seasonal cycle of phytoplankton in the North Atlantic. *Bulletins of Marine Ecology*, 6: 333–345.
- Roenneberg, T., Foster, R.G. (1997). Twilight times: light and the circadian system. *Photochemistry and Photobiology* 66(5): 549–561.

- Roenneberg, T., Mittag, M. (1996). The circadian program of algae. *Seminars in Cell and Developmental Biology* 7, 753–763.
- Roenneberg, T., Rehman, J. (1996). Nitrate, a nonphotic signal for the circadian system. *The FASEB Journal* 10(12): 1443–1447.
- Sadovskaya, G.M., and Filimonov, V.S. (1985). Factors determining the diurnal dynamics of phytoplankton bioluminescence. *Oceanology| Oceanology| Okeanologiya*, 25: 642–646.
- Sarmiento, J.L., Slater, R.D., Fasham, M.J.R., Ducklow, H.W., Toggweiler, J.R., Evans, G.T. (1993). A seasonal three-dimensional ecosystem model of nitrogen cycling in the north atlantic euphotic zone. *Global Biogeochemical Cycles*, 7(2): 417–450
- Sarthou, G., Timmermans K.R., Blain, S., Tréguer, P. (2005). Growth physiology and fate of diatoms in the ocean: a review. *Journal of Sea Research*, 53(1–2): 25–42.
- Schartau, M. and Oschlies, A. (2003a). Simultaneous data-based optimization of a 1d-ecosystem model at three locations in the North Atlantic Ocean: Part 1. method and parameter estimates. *Journal of Marine Research*, 61(6): 765–793.
- Schartau, M. and Oschlies, A. (2003b). Simultaneous data-based optimization of a 1d-ecosystem model at three locations in the North Atlantic Ocean: Part 2. standing stocks and nitrogen fluxes. *Journal of Marine Research*, 61(6): 794–820.
- Schartau, M., Oschlies, A., Willebrand, J. (2001). Parameter estimates of a zero-dimensional ecosystem model applying the adjoint method. *Deep-Sea Research Part II: Topical Studies in Oceanography*, 48(8–9): 1769–1800.
- Schmidt, R.J., Gooch, V.D., Loeblich, A.R., Hastings, J.W. (1978). Comparative study of luminescent and nonluminescent strains of *Gonyaulax Excavata* (Pyrrhophyta). *Journal of Phycology*, 14: 5–9.
- Schnepf, E. and Elbrächter, M., (1999). *Dinophyte* Chloroplasts and Phylogeny—A Review. *Grana*, 38: 81–97.
- Seeyave, S., Probyn, T.A., Pitcher, G.C., Lucas, M.I., Purdie, D.A. (2009). Nitrogen nutrition in assemblages dominated by *Pseudo-nitzschia* spp., *Alexandrium catenella* and *Dinophysis acuminata* off the west coast of South Africa. *Marine Ecological Progress Series*. 379: 91 – 107.
- Seliger, H.H., Fastie, W.G., Taylor, W.R., McElroy, W.D. (1962). Bioluminescence of marine dinoflagellates: i. an underwater photometer for day and night measurements. *Journal of General Physiology*, 45, 1003–1017.
- Seo, K.S. and Fritz, L. (2000). Cell ultrastructural changes correlate with circadian rhythms in *Pyrocystis Lunula* (Pyrrhophyta). *Journal of Phycology*, 36: 351–358.
- Sher, E.B. and Sher B.F. (2007). Heterotrophic Dinoflagellates: a significant component of microzooplankton biomass and major grazers of diatoms in the sea. *Marine Ecology Progress Series*, 352: 187–197.
- Shulman, I., Moline, M.A., Penta, B., Anderson, S., Oliver, M., Haddock, S.H.D. (2011). Observed and modeled bio-optical, bioluminescent and physical properties during a coastal upwelling event in Monterey Bay, California. *Journal of Geophysical Research*, 116 (C01018).
- Shulman, I., McGillicuddy, D.J., Moline, M.A., Haddock, S.H.D., Kindle, J.C., Nechaev, D., Phelps, M.W. (2005). Bioluminescence intensity modeling and sampling strategy optimization. *Journal Of Atmospheric And Oceanic Technology*, 22: 1267–1281.

- Shulman, I., Haddock, S.H.D., Mcgillicuddy, D.J., Paduan, J.D., Bissett, W.P. (2003). Numerical modeling of bioluminescence distributions in the coastal ocean. *Journal of Atmospheric And Oceanic Technology*, 20: 1060–1068.
- Skovgaard, A. (2000). A phagotrophically derivable growth factor in the plastidic dinoflagellate *Gyrodinium Resplendens* (Dinophyceae). *Journal of Phycology*, 36: 1069–1078.
- Skovgaard, A. (1998). Role of chloroplast retention in a marine dinoflagellate. *Aquatic Microbial Ecology*, 15: 293–301
- Smalley, G.W., Coats, D.W., Adam, E.J. (1999). A new method using fluorescent microspheres to determine grazing on ciliates by mixotrophic dinoflagellate *Ceratium furca*. *Aquatic Microbial Ecology*, 17: 167–179.
- Smayda, T.J. (1997). Harmful algal blooms: their ecophyiology and general relevance to phytoplankton blooms in the sea. *Limnology and Oceanography*, 42: 1137–1153.
- Smith J.M. (1964) Group selection and kin selection. *Nature*, 201: 1145–1147.
- Smith, R.C., Marra, J., Perry, M. J., Baker, K. S., Swift, E., Buskey, E., Kiefer, D. A. (1989). Estimation of a photon budget for the upper ocean in the Sargasso Sea. *Limnology and Oceanography*, 34: 1673–1693.
- Smythe–Wright, D., Boswell, S.M., Kim, Y., Kemp, A.E. (2010). Spatio–temporal changes in the distribution of phytopigments and phytoplanktonic groups at the PAP. *Deep–Sea Research Part II* 57(15): 1324–1335.
- Soli, G., (1966). Bioluminescent cycle of photosynthetic dinoflagellates. *Limnology and Oceanography*, 11(3): 355–363.
- Staples, R.F. (1966). The distribution and characteristics of surface bioluminescence in the oceans. U.S. Naval Oceanographic Office Publ. TR–184: 54 P.
- Steele, J.H. (1962). Environmental control of photosynthesis in the sea. *Limnology and Oceanography* 7: 137 – 150.
- Steinhoff, T., Friedrich, T., Hartman, S.E., Oschlies, A., Wallace, D.W.R., Körtzinger, A. (2010). Estimating mixed layer nitrate in the North Atlantic Ocean. *Biogeosciences*, 7(3): 795 – 807.
- Stickney, H.L., Hood, R.R., and Stoecker, D.K. (2000) The impact of mixotrophy on planktonic marine ecosystems. *Ecological Modelling*, 125: 203–230.
- Stoecker, D.K., Johnson, M.D., de Vargas, C., Not, F. (2009). Acquired phototrophy in aquatic protists. *Aquatic Microbial Ecology*, 57: 279–310.
- Stoecker, D.K. (1999). Mixotrophy among dinoflagellates. *Journal of Eukaryotic Microbiology*, 46: 397–401.
- Stoecker, D.K. (1998). Conceptual models of mixotrophy in planktonic protists and some ecological and evolutionary implications. *European Journal of Protistology*, 34(3): 281–290.
- Stramska, M., Dickey, T.D., Plueddemann, A., Weller, R., Langdon, C., Marra, J. (1995). Bio–Optical variability associated with phytoplankton dynamics in the North Atlantic Ocean during spring and summer of 1991. *Journal of Geophysical Research*, 100.

- Sullivan, J.M. and Swift, E. (2003). Effects of small-scale turbulence on net growth rate and size of ten species of marine dinoflagellates. *Journal of Phycology*, 39, 83–94.
- Sullivan, J.M. and Swift, E. (1995). Photoenhancement of bioluminescence capacity in natural and laboratory populations of the autotrophic dinoflagellate *Ceratium fusus* (Ehrenb.) Dujardin. *Journal of Geophysical Research*, 100(C4): 6565–6574.
- Sullivan, J.M. and Swift, E. (1994). Photoinhibition of mechanically stimutable bioluminescence in the photosynthetic dinoflagellate *Ceratium fusus* (Pyrrophyta). *Journal of Phycology* 33: 627–633.
- Sverdrup, H.U., Johnson, M.W., Flemming R.H. (1942). The oceans their physics, chemistry, and general biology. Prentice-Hall, Inc, New York
- Sweeney B.M. (1987). Bioluminescence and circadian rhythms. In: Taylor FJR (ed.) The biology of dinoflagellates. Blackwell Scientific Publications, Great Britain: 269–281.
- Sweeney, B.M. (1981a). Interaction of the circadian cycle with the cell cycle in *Pyrocystis fusiformis*. *Plant Physiology*, 70: 272 – 276
- Sweeney, B.M. (1981b). Variations In The Bioluminescence Per Cell in Dinoflagellates, p.90–94. In: Nealson KH (ed) Bioluminescence current perspectives. Burgess Publishing.
- Sweeney BM (1981c). The circadian rhythms in bioluminescence, photosynthesis and organellar movements in the large dinoflagellate, *Pyrocystis fusiformis*. In: Schweiger HG (ed.) International Cell Biology 1980–1981. Springer-Verlag, Berlin: 807–814.
- Sweeney, B.M. (1971). Laboratory Studies of a green *Noctiluca* from New Guinea. *Journal of Phycology*, 7(1): 53–58.
- Sweeney, B.M. (1963). Bioluminescent dinoflagellates. *Biological Bulletin* (Woods Hole, Mass.), 125: 177–181.
- Sweeney, B.M., Haxo, F.T., Hastings, J.W. (1959). Action spectra for two effects of light on luminescence in *Gonyaulax polyhedra*. *Journal of General Physiology* 43: 285 – 299.
- Swift, E., Sullivan, J.M., Batchelder, H.P., Van Keuren, J., Vaillancourt, R.D., Bidigare, R.R. (1995). Bioluminescent organisms and bioluminescence measurements in the North Atlantic Ocean near latitude 59.5 °N, longitude 21 ° W. *Journal Of Geophysical Research-Oceans*, 100.
- Swift, E., Lessard, E.J., Biggley, W.H. (1985). Organisms associated with stimulated epipelagic bioluminescence in the Sargasso Sea and the Gulf Stream. *Journal Of Plankton Research*, 7: 831–848.
- Swift, E., Biggley, W.H., Verity, P.G., Brown, D.T. (1983). Zooplankton are major sources of epipelagic bioluminescence in the southern Sargasso Sea. *Bulletin of Maine Science*, 33: 855–863
- Swift, E., Meunier, V.A., Biggley, W.H., Hoarau, J., Barras, H. (1981). Factors affecting bioluminescent capacity in oceanic dinoflagellates, p.95–106. In: Nealson KH (Ed.) Bioluminescence current perspectives. Burgess Publishing.
- Swift, E., Biggley, W.H., Seliger, H.H. (1973). Species of oceanic dinoflagellates in the Genera *Dissodinium* and *Pyrocystis*: Interclonal and interspecies comparisons of teh color and photon yield of bioluminescence. *Journal of Phycology*, 9:420–426.
- Tang, E. (1996). Why do dinoflagellates have lower growth rates? *Journal of Phycology*, 32: 80–84.

- Taylor, F., Hoppenrath, M., Saldarriaga, J. (2008). Dinoflagellate diversity and distribution. *biodiversity and conservation*, 17: 407–418.
- Taylor, A.H., Harbour, D.S., Harris, R.P., Burkill, P.H., Edwards, E.S. (1993). Seasonal succession in the pelagic ecosystem of the North Atlantic and the utilization of nitrogen. *Journal of Plankton Research*, 15(8):875–891.
- Tett, P.B., and Kelly, M.G. (1973). Marine bioluminescence. *Oceanography and Marine Biology Annual Review*, 11: 89–173.
- Tett, P.B., (1971). The relation between dinoflagellates and the bioluminescence of sea water. *Journal of the Marine Biological Association of the U.K.*, 51: 183–206.
- Thain, D., Tannenbaum, T., Livny, M. (2005). Distributed computing in practice: the Condor experience. *Concurrency and Computation: Practice and Experience*, 17(2–4): 323–356.
- Thomas, W.H. and Gibson, C.H. (1990). Quantified small-scale turbulence inhibits a red tide dinoflagellate, *Gonyaulax polyedra* Stein. *Deep-Sea Research*, 37:1583–93.
- Thomas, W.H. and Gibson, C.H. (1992). Effects of quantified smallscale turbulence on the dinoflagellate, *Gymnodinium sanguineum (splendens)*—contrasts with *Gonyaulax (Lingulodinium) polyedra*, and the fishery implication. *Deep-Sea Research*, 39:1429–37.
- Tokarev, Y.N., Melnikov, V.V., Burmistrova, N.V., Belokopytov, V.N., Temnykh, A.V. (2008). Climate impact on long-term changeability of the Black Sea bioluminescence field and plankton community characteristics. *In: Mancheva, S. (Ed), 2008. BS-HOT Collected Reprints Published On CD. Pp. 1–439.*
- Tokarev, Y.N., Bityukov, E.P., Williams, R., Vasilenko, V.I., Piontkovski, S.A., Sokolov, B.G. (1999a). The bioluminescence field as an indicator of the spatial structure and physiological state of the planktonic community at the Mediterranean sea basin. *In: Malanotte-Rizzoli P, Eremeev VN (Eds) The eastern Mediterranean as a laboratory basin for the assessment of contrasting ecosystems. The Netherlands: 407–416.*
- Tokarev, Y.N., Williams, R., Piontkovski, S.A. (1999b). Identification of small-scale structure of plankton communities of the Black and Ionian Seas by their bioluminescence characteristics. *Hydrobiologia* 393: 163–167.
- Tomas, C.R. (1997). *Identifying marine phytoplankton*. Academic Press, New York, pp. 858.
- Tyler, M.A. and Seliger, H.H. (1981). Selection for red tide organism: physiological responses to the physical environment. *Limnology and Oceanography*, 26(2): 310–324.
- Utyushev, R.N., Levin, L.A., Gitelson, J.I. (1999). Diurnal rhythm of the bioluminescent field in the ocean epipelagic zone. *Marine Biology*, 134: 439–448.
- Vanhoutte-Brunier, A., Fernand, L., Ménesguen, A., Lyons, S., Gohin, F., Cugier, P. (2008). Modelling the *Karenia Mikimotoi* bloom that occurred in the western English Channel during summer 2003. *Ecological Modelling*, 210: 351–376.
- Verity, P.G., Stoecker, D.K., Sieracki, M.E., Nelson, J.R., (1993). Grazing and the mortality of microzooplankton during the 1989 North Atlantic spring bloom at 47 N 18 W. *Deep-Sea Research II*, 40 (9): 1793–1814.

- Vichi, M., Pinardi, N., Masina, S. (2007). A generalized model of pelagic biogeochemistry for the global ocean ecosystem. Part I: theory. *Journal of Marine Systems*, 64: 89–109.
- Vicker, M.G., Becker, J., Gebauer, G., Schill, W., Rensing, L. (1988). Circadian rhythms of cell cycle processes in the marine dinoflagellate *Gonyaulax Polyedra*. *Chronobiology International* 5: 5–17.
- Von Dassow, P., Bearon, R.N., Latz, M.I. (2005). Bioluminescent response of the dinoflagellate *Lingulodinium Polyedrum* to developing flow: tuning of sensitivity and the role of desensitization in controlling a defensive behavior of a planktonic cell. *Limnology and Oceanography*, 50: 607 – 619.
- Walsh, J.J., Penta, B., Dieterle, D.A., Bissett, W.P. (2001). Predictive ecological modeling of harmful algal blooms. Research Triangle Pk, Nc: Crc Press Llc: 1369–1383
- Walve, J. and Larsson, U. (1999). Carbon, nitrogen and phosphorus stoichiometry of crustacean zooplankton in the Baltic Sea: implications for nutrient recycling. *Journal of Plankton Research* 21(12): 2309–2321.
- Ward, B.A., Friedrichs, M.A., Anderson, T.R., Oschlies, A. (2010). Parameter optimisation techniques and the problem of underdetermination in marine biogeochemical models. *Journal of Marine Systems*, 81(1–2): 34–43.
- Warner, A.J., Hays, G.C. (1994). Sampling by the Continuous Plankton Recorder Survey. *Progress in Oceanography*, 34: 237–256.
- Watson, M. and Herring, P.J. (1992). A new database for observations of bioluminescence. *Marine Observer*, 62: 182–183.
- White, H.H. (1979). Effects of dinoflagellate bioluminescence on the ingestion rates of herbivorous zooplankton. *Journal of Experimental Biology and Ecology*, 36: 217–224.
- Widder, E.A. (2010). Bioluminescence in the ocean: origins of biological, chemical and ecological diversity. *Science*, 328: 704.
- Widder, E.A. , Frey, C.L., Borne, L.J. (2003). HIDEEX generation II: a new and improved instrument for measuring marine bioluminescence. *Marine Technology Society of The IEEE (Oceans'03)*, 4.
- Widder, E.A. (2002a). SPLAT CAM: Mapping plankton distributions with bioluminescent road-kill. *Oceans '02 MTS/IEEE*, 3: 1711–1715.
- Widder, E.A. (2002b). Bioluminescence and the pelagic visual environment, *Marine and Freshwater Behaviour and Physiology*, 35(1–2): 1–26.
- Wilson, T.R.S. and Hastings, J.W. (1998). Bioluminescence. *Annual Review Of Cell And Developmental Biology*, 14: 197–230.
- Yentsch, C.S. and Laird, J.C. (1968). Seasonal sequences of bioluminescence and the occurrence of endogenous rhythm in oceanic waters of Woods Hole, Massachusetts. *Journal of Marine Research*, 26: 127 – 133.
- Yentsch, C.S., Backus, R.H., Wing, A.S. (1964). Factors affecting the vertical distribution of bioluminescence in the euphotic zone. *Limnology and Oceanography* 9: 519–524.
- Yoo, Y.D., Jeong, H.J., Kim, M.S., Kang, N.S., Song, J.Y., Shin, W., Kim, K.Y., Lee, K. (2009). Feeding by phototrophic red-tide dinoflagellates on the ubiquitous marine diatom *Skeletonema costatum*. *Journal of Eukaryotic Microbiology*, 56, 413–420.

Yool, A., Popova, E.E., Anderson, T.R. (2011). MEDUSA: a new intermediate complexity plankton ecosystem model for the global domain. *Geoscientific Model Development*, 4, 381–417.

Young, R.E. (1983). Oceanic bioluminescence: an overview of general functions. *Bulletin of Marine Science*, 33(4): 829–845.